NASA CR-120988
FR-4976

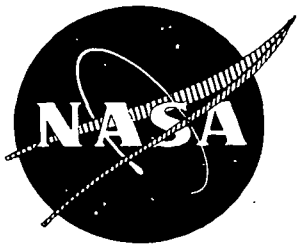

THERMAL SKIN® FABRICATION TECHNOLOGY

FINAL REPORT

by: T. B. Milam

PRATT & WHITNEY AIRCRAFT
DIVISION OF UNITED AIRCRAFT CORPORATION
FLORIDA RESEARCH AND DEVELOPMENT CENTER

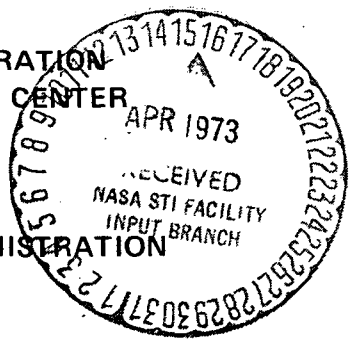

Prepared for
NATIONAL AERONAUTICS AND SPACE ADMINISTRATION

NASA Lewis Research Center
Contract NAS 3-13312

1. Report No.	2. Government Accession No.	3. Recipient's Catalog No.
NASA CR-120988		

4. Title and Subtitle	5. Report Date
THERMAL SKIN® FABRICATION TECHNOLOGY - FINAL REPORT	27 October 1972
	6. Performing Organization Code
7. Author(s)	8. Performing Organization Report No.
T. B. Milam	FR-4976
	10. Work Unit No.
9. Performing Organization Name and Address	
Pratt & Whitney Aircraft Florida Research and Development Center Box 2691 West Palm Beach, Florida 33402	11. Contract or Grant No. NAS3-13312
	13. Type of Report and Period Covered
12. Sponsoring Agency Name and Address	Final Contractor Report
NASA-Lewis Research Center 21000 Brookpark Road Cleveland, Ohio 44135	14. Sponsoring Agency Code

15. Supplementary Notes

16. Abstract

Advanced fabrication techniques applicable to THERMAL SKIN® structures were investigated, including (1) chemical machining, (2) braze bonding, (3) diffusion bonding, and (4) electron beam welding. Materials investigated were nickel and nickel alloys.

Sample THERMAL SKIN panels were manufactured using the advanced fabrication techniques studied and were structurally tested.

Results of the program included (1) development of improved chemical machining processes for nickel and several nickel alloys, (2) identification of design geometry limits, (3) identification of diffusion bonding requirements, (4) development of a unique diffusion bonding tool, (5) identification of electron beam welding limits, and (6) identification of structural properties of THERMAL SKIN material.

17. Key Words (Suggested by Author(s))	18. Distribution Statement
THERMAL SKIN® Chemical Machining Braze Bonding Diffusion Bonding Nickel Nickel Alloys Electron Beam Welding	Unclassified - Unlimited

19. Security Classif. (of this report)	20. Security Classif. (of this page)	21. No. of Pages	22. Price*
Unclassified	Unclassified	185	$3.00

* For sale by the National Technical Information Service, Springfield, Virginia 22151

FOREWORD

The "Thermal Skin® Chamber Fabrication Technology Program", Contract NAS3-13312, was conducted at the Florida Research and Development Center of Pratt & Whitney Aircraft, Division of United Aircraft Corporation.

Contributions to the technical effort were made by the following FRDC personnel: T. E. Bailey, J. P. Mitchell, T. B. Milam, J. F. Keel, B. A. Manty, C. L. Kistler, and S. C. Beck.

The contract was administered by the Lewis Research Center of the National Aeronautics and Space Administration, Cleveland, Ohio. The NASA Project Manager was R. A. Duscha of the Liquid Rocket Technology Branch, Chemical Rocket Division.

CONTENTS

CONTENTS (CONTINUED)

CONTENTS (CONTINUED)

ILLUSTRATIONS

ILLUSTRATIONS

ILLUSTRATIONS

ILLUSTRATIONS

ILLUSTRATIONS

TABLES

TABLES

SUMMARY

A 32-month program beginning 2 July 1969 and ending 29 February 1972 was conducted by P&WA, FRDC to investigate and advance fabrication processes to facilitate manufacture of Thermal Skin® type rocket combustion chambers. Advancing the fabrication technology would allow higher performance rocket engines to be built and would relax undesirable design constraints.

Areas investigated were 1) chemical machining, 2) diffusion bonding and 3) electron beam welding; structural tests were performed using small scale samples.

The chemical machining investigations yielded a powderless etching process which reduces the side etch to 50% in nickel and in certain nickel alloys. The process was identified after investigating many combinations of etchants, maskants, and materials.

Under the chemical machining effort, candidate materials for chamber construction were identified and ranked according to desirability. Pure nickel (Nickel 200) was selected for the chamber hot wall, and candidate outer structural wall materials were investigated for chemical machining characteristics using the etching process developed for nickel.

After investigating many etchants and etchant additives to reduce side etch, commercially available ferric chloride etchant with thiourea added to suppress side etch was selected as the optimum etchant. Inconel-600 and Inconel X-750 were found to be the most desirable structural wall materials that could be etched with the ferric chloride-thiourea etchant.

Spray type etching proved to be more desirable than splash etching because stricter process controls on variables such as etchant velocity and atomization were possible.

Plated silver in combination with conventional photosensitive resists gave more uniform dimensions than could be obtained when photosensitive resists were used alone.

Electrochemical machining and a special form of depth stepping using positive working photoresist as a banking agent were investigated but were found to require more extensive development then the scope of the program permitted.

The etching procedures developed were used to prepare structural test specimens and, at the same time, the etching procedures were further improved and adapted to production-like requirements. Fifty-one panels were etched and dimensionally inspected during the process.

No material degradation such as intergranular attack was caused by the etching process and no significant passage deformation was seen during bend testing. Pressure tests of the cooling passages showed that parent metal strengths were retained, but that silver braze bonding was damaged by conventional welding on the chamber structural wall. This later fact gave rise to the subsequent investigation of diffusion bonding for joining two etched plates to form a Thermal Skin panel.

Overall structural tests indicated that predicted strengths based on material design strength data were attained.

Thermal cycle life tests were performed on sample panels indicating short cyclic life (as few as four cycles) at near-thermal-design limits. The test simulation was suspect and additional investigation was needed, but was beyond the scope of the program.

Test samples were also fabricated by P&WA etching vendors using specifications based on etching procedures developed during the chemical

machining study. These samples proved to be dimensionally superior to any previous chemical machining results, which gave added credibility to the process, and were used for diffusion bonding and electron beam welding investigations.

Under the diffusion bonding effort a large number of panels were bonded using various combinations of time, temperature, bonding load, and diffusion aids. Nickel plated samples bonded at 1700°F (1200°K) and using a bonding load equivalent to the nickel yield strength at 1700°F (1200°K), and for 180 min duration, proved to have the highest strength.

Investigation of a unique bonding tool which would provide uniform pressure loading and would eliminate the need for highly specialized bonding equipment was attempted, but it was not possible to fully develop the concept during the program.

Alternative methods for bonding Thermal Skin panels, (1) "auto-vac" bonding and (2) electroless nickel brazing, were also investigated in a cursory manner. Neither method proved to be acceptable without additional development effort.

Electron beam seam welding for joining performed Thermal Skin panels was demonstrated to be superior to heliarc fusion welding because the narrower fusion zone obtained allows coolant passages at seams to be located in closer proximity. The results showed that equipment drift caused inconsistent results, but that by resorting to pre-weld test samples, edge margins between a passage wall and a weld seam as small as 0.050-in. (0.127 cm) could be attained without passage deformation.

Thermal Skin® thrust chambers have a cooled heat-exchanger type wall containing many micro-size internal coolant passages. They are built up from grooved flat plates that are bonded together, formed, and seam welded (figure 1).

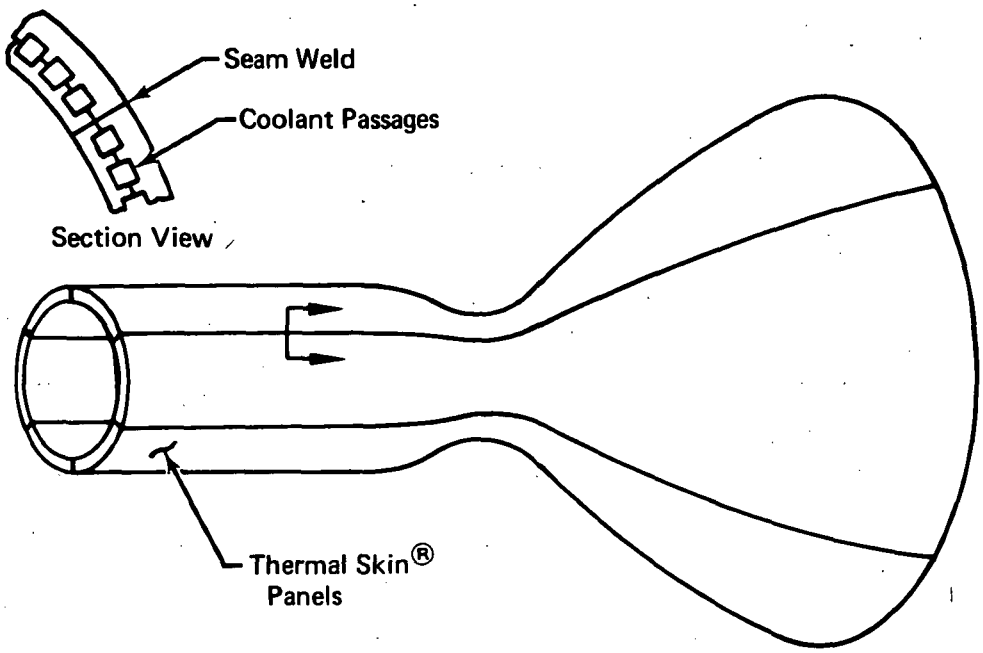

Figure 1. Thermal Skin® Thrust Chamber Construction FD 47893A

Such chambers are particularly attractive for applications where tubular walls are impractical because of a requirement for very small coolant passages to obtain proper heat transfer characteristics. The coolant capability of the Thermal Skin chamber falls between that of the tubular chamber and the transpiration cooled or film cooled combustion chamber. Moderately high heat fluxes can be accomodated with Thermal Skin chamber construction, but for extremely high heat fluxes, such as found in SSME and OOS engines, other fabrication techniques that provide closer dimensional control may be required. A good example of an application for the Thermal Skin chamber was in the Space Storable Regenerative Cooling Investigation, Contract NAS3-11190 (Reference 6).

Advantages of Thermal Skin chambers include light weight and low cost. Light weight is achieved because high strength alloys can be used for the outer "structural wall" layer, while a high thermal conductivity material is used for the combustion side wall. The competing chamber fabrication technique, electroforming, does not provide for an integral high strength alloy wall.

Low cost of the Thermal Skin Chamber is realized through chemical machining utilizing photographic techniques to form the coolant passages. Chemical machining is relatively inexpensive and provides unlimited latitude in coolant passage width (and therefore area) variation in order to match the required coolant coefficients to local heat loads.

Chemical machining is limited to constant depth passages or passages having distinct steps in depth. The possible passage depth-to-width ratio is also limited by the process, and the minimum passage spacing is restricted to that required for seam welding individual chamber sections together. That is, adequate edge margin at the seams is required to prevent damage to adjacent passages during welding, and there is no advantage to having narrow passage spacing in one area if the spacing at the seams must be wide. For braze bonded chambers, welding operations, such as those for attaching coolant manifolds to the outer chamber wall can easily damage the braze bond.

The objectives of this program were to improve Thermal Skin chamber fabrication techniques or to apply new techniques to overcome or alleviate limitations.

Improvements in chemical machining techniques to obtain greater passage depth-to-width ratios and better passage shape for the materials of interest, nickel and nickel alloys, were sought through efforts to develop a powder-less, or self-banking, technique similar to that available for copper.

Substituting diffusion bonding for brazing of plates into panels was attempted to improve strength and prevent bond damage in subsequent weld operations.

Electron beam welding, because of its deep penetration and narrow weld bead, could reduce the required edge margin and permit closer passage spacing at the seams between segments, and so it was investigated.

The fabrication technology program was conducted in five phases. Basic chemical machining technology was identified and then applied to fabricating Thermal Skin samples to characterize etched passages. Strength evaluation tests were performed using etched and brazed panels, and diffusion bonding was investigated as an alternative to braze bonding. During the last phase of the program, electron beam seam welding was investigated. The program phases are discussed in order in the following sections.

CONCLUSIONS

1. Chemical machining using plated silver resist on Nickel 200 or Inconel 600 can yield etched passage dimensional uniformity within ±0.001 in. (±0.00254 cm). Thiourea added to commercially available ferric chloride etchant reduces side etch as much as 50% of the depth of etch on a side.
2. The chemical machining process does not degrade the strength of Nickel 200, Inconel 600, or Inconel X-750 through intergranular attack.
3. Silver brazed Thermal Skin walls can easily be damaged by the heat of fusion welding on the structural wall.
4. Diffusion bonding can provide bonds resistant to higher temperatures than those obtained with silver brazing and therefore less likely to be damaged by subsequent fusion welding.
5. Electron beam seam welding can produce a narrower fusion zone than heliarc fusion welding and can allow the coolant passages to be located within 0.050 in. (0.127 cm) of the welded seam.

CHEMICAL MACHINING

A. DESCRIPTION OF CHEMICAL MACHINING

Chemical machining is a controlled metal removal process where an acid (or strong base) dissolves, or etches, the work piece. Areas not to be etched are protected from chemical attack by a maskant, typically a photosensitive paint called photoresist. Photographic masters (5 to 10X pattern photographically reduced to actual size for increased accuracy) are used to print the desired etch pattern in the photoresist similar to contact printing a photograph using a negative. The work piece is then exposed to the etchant where selective metal removal occurs.

Industrial chemical machining equipment is available and ranges in sophistication from a simple hand-operated spray nozzle to completely automated continuous line systems. Spray and splash etchers are commonly used and are depicted in figure 2. Etching is accomplished in a similar manner in both etchers: the etchant is impinged on the plate, which is moved in some manner to provide uniform etching. In splash etching, the work piece is rotated while the etchant is thrown against the plate by paddle wheels. In spray etching, the etchant is sprayed through atomizing nozzles onto the plate.

Selection of the etchant depends on the material to be etched; etchants that will react with the material being etched to form soluble compounds are usually selected. For example, ferric chloride is recommended for use with nickel alloys (Reference 1). It reacts with nickel to form nickel chloride and ferrous chloride, both of which are soluble in the etchant:

$$Ni + 2\ FeCl_3 \longrightarrow 2\ FeCl_2 + NiCl_2$$

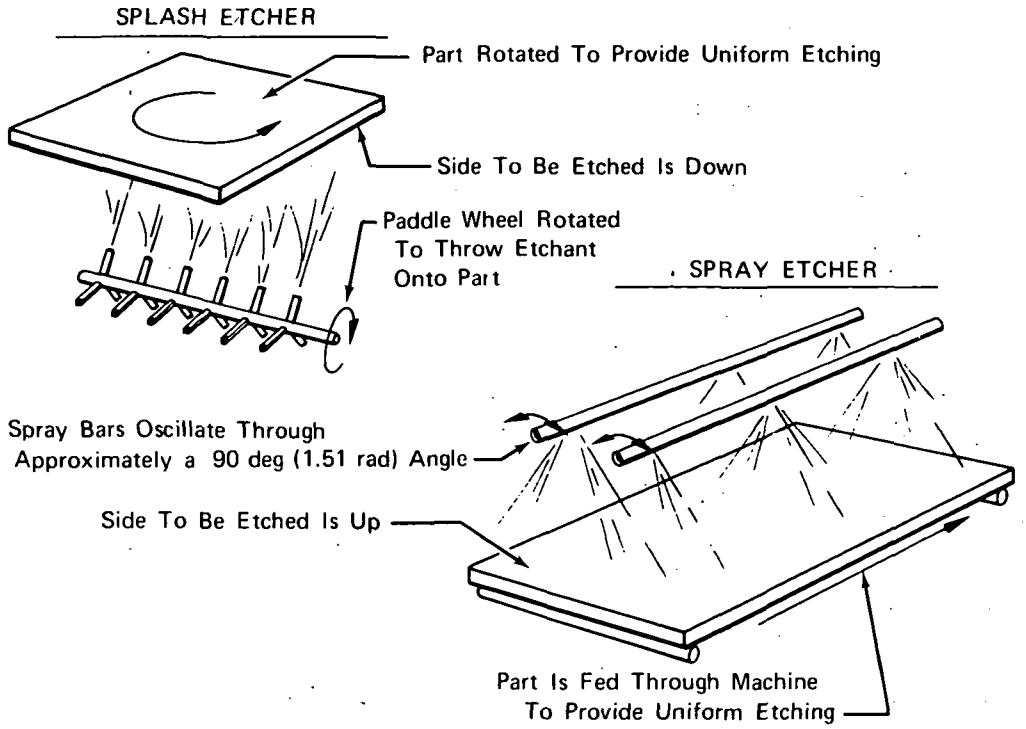

Figure 2. Splash and Spray Type Etchers FD 56981

Three etching techniques in general use are 1) conventional, 2) powder banking, and 3) powderless. Representative cross sections obtained with these methods are shown in figure 3.

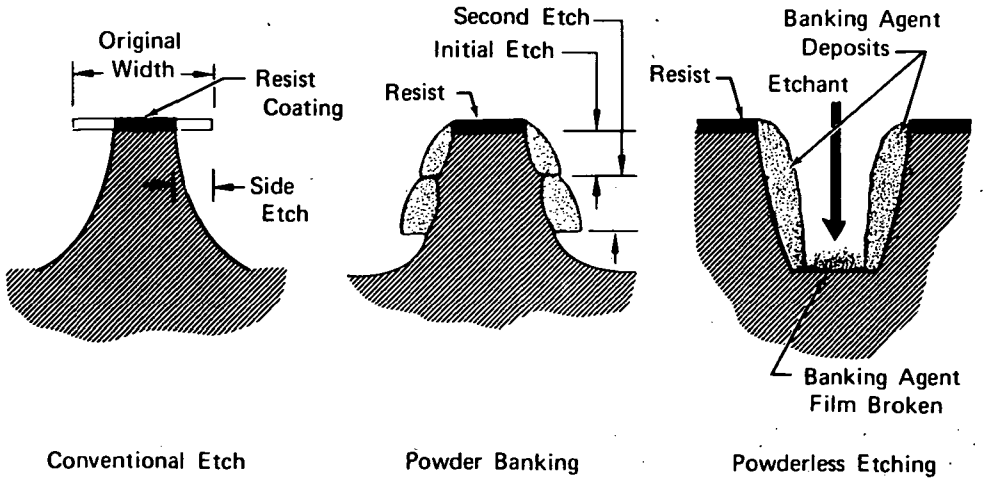

Figure 3. Section Views Depicting Three Etching Techniques FD 56982

In conventional etching no side wall protection is provided and side etch is significant (usually 100%* for nickel, Reference 1). To compensate for side etch, the etching master is made with narrower line widths so that undercutting will bring the etched pattern to correct dimensions when the desired depth is reached.

In powder banking an etchant-resistant material such as a fusible resinous powder is applied to the side walls at intervals during the etching operation to prevent further side etch. The powder is fused at elevated temperature into a protective coating, and then the plate is returned to the etching bath. Etching is continued until the resin deposit itself has been undercut. Then the plate is removed from the etcher and another powder bank is applied. The process often is repeated several times until the proper depth has been achieved. This technique, sometimes referred to as "depth stepping," insures the correct dimensions at the plate surface but results in a stepped side wall.

Although the powder banking process can provide acceptable passages, preparation of the banking compound and its application to the sidewalls involve more art than science. A more repeatable and a more readily controlled process would be preferred.

In the powderless process a substance is added to the etchant that forms an adhering film on the etched surface; it is theorized that direct impingement of etchant breaks up the film at the bottom of the passage, while the film on the sidewalls remains intact to retard chemi-

---

* A 100% side etch corresponds to a completely nondirectional etch: i.e., the etching rate is equal in all directions.

cal attack. Many such processes are patented (Appendix A). A powderless process for copper, in which sidewall protection is achieved by a gelantinous film formed through an organic complexing agent, was developed by the Photoengraver's Research Institute (Reference 3). Powderless etching processes for magnesium and zinc have been developed by the Dow Chemical Company (Reference 4) and use two-phase systems in which a wetting agent (incorporated into the acid etching solution) causes adherence of an oily substance that forms the protective film.

In this investigation, particular attention was given to developing a powderless etching technique for nickel and nickel alloys.

B. SUMMARY

Chemical machining research was conducted to develop and improve methods that would reduce side etch, undercutting, and coolant passage dimensional variations for nickel and nickel alloys. Goals were to obtain (1) maximum channel depth-to-width ratio, (2) minimum land widths and hot-wall thicknesses, and (3) maximum area factor (figure 4).

Nickel alloys including Inconel 600, Inconel 625, Inconel X-750, Inconel 718, Inconel 706, and WASPALOY^{TM} were evaluated along with the pure nickels, Nickel 200, Nickel 201, and Nickel 270. A wide variety of operating conditions and solutions were investigated with special emphasis on the effects of etchant composition on undercutting. Different etching techniques were evaluated.

The experimental program consisted of first selecting candidate materials based on their desirability as chamber materials. Then various side etch inhibitors and maskants for the powderless etching process were evaluated using laboratory techniques. Promising combinations were later

evaluated in splash-type etching equipment where etchant velocity, etchant temperature, starting passage width, surface finish, intergranular attack, and cycle variations were investigated.

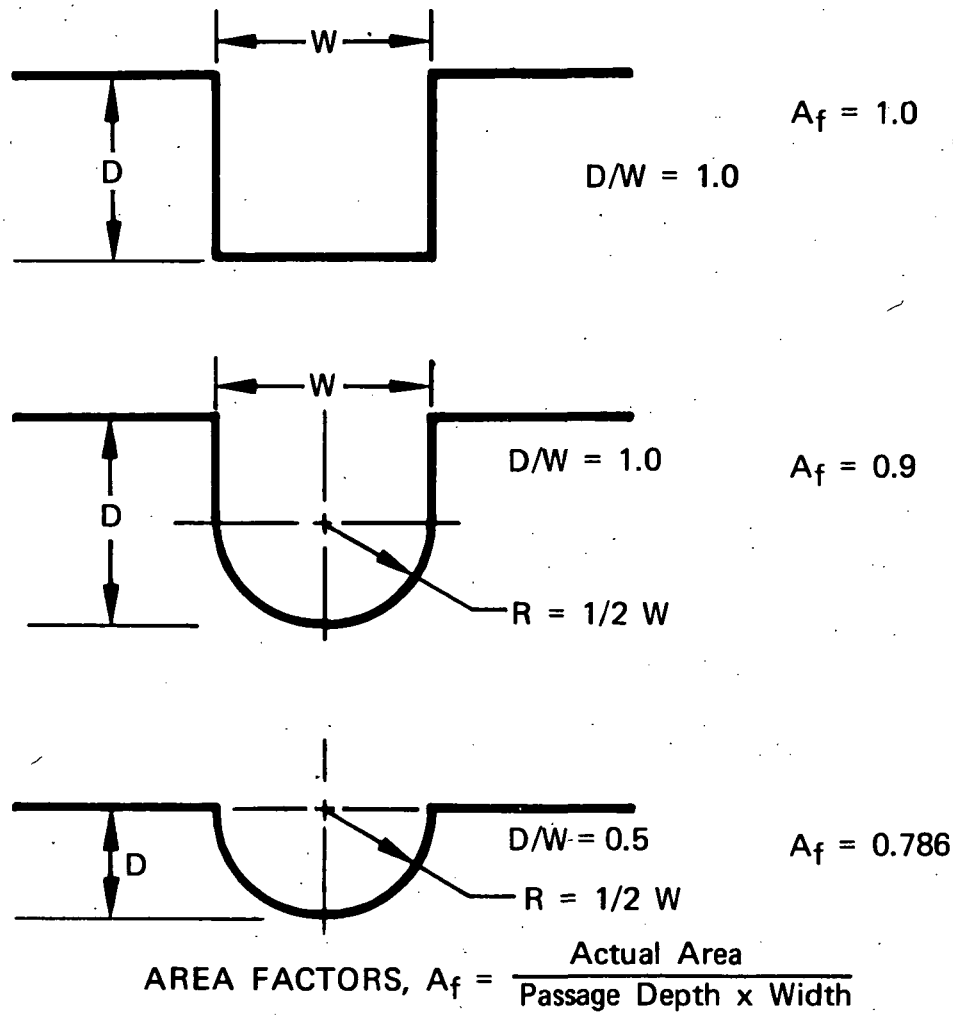

Figure 4. Area Factor and Depth-to-Width Relationships FD 56980

During the laboratory-scale experimental program photoresist banking, spray-type etching, and electrochemical machining were studied. Photo-engraver's Research Institute, a leading developer of powderless etching of copper, was contacted and contracted to investigate nickel using techniques established for copper. The results are discussed in the following pages.

C. EXPERIMENTAL PROGRAM

1. Selection of Materials

Selection of alloys for study was based on their potential for use in rocket chamber construction. Commercially pure nickel (Nickel 200) was used as the base material because of its established requirement as the hot wall material. An analytical study was conducted to evaluate candidate backplate materials, taking into account material strength and fabrication characteristics. The results are summarized in Table I. The optimum backplate material provides the lightest chamber weight while meeting strength and thermal cycle requirements, and can be etched, brazed (or diffusion-bonded), formed, welded, and machined.

The candidate alloys were immersed in 42° Be'* ferric chloride etchant and were compared by weight loss to determine which could possibly be machined using etching procedures developed for Nickel 200. Results are shown in Table II. It was observed that the greater the molybdenum or titanium content in alloys, the slower the milling rate in ferric chloride etchant. Additional etching tests were performed before final selection of a back plate material was made and are discussed in paragraph 8.

2. Selection of Side Etch Inhibitors

Side etch inhibitor candidates were chosen on the basis of their capability to inhibit the dissolution of nickel in ferric chloride etchant. Inhibitors investigated performed as complexing agents, oil additives, and/or corrosion inhibitors. Complexing agents are organic compounds forming insoluble complexes with nickel salts. Oil additives form suspensions when added to the acid etchant and by the addition of

---

* °Be' = ° Beume': a hydrometer scale related to specific gravity.

Table I. Thermal Skin® Structural Wall Material Ranking

	MATERIAL	0.2% YIELD ksi	DENSITY, lb/in.^{3}	Ti, %	MO, %	αX10^6, in./in.°F	WELDABILITY	BRAZEABILITY	FORMABILITY	RELATIVE CHAMBER WEIGHT	COMMENTS
1.	Inconel-706	124	0.292	2.0	1.0	8.5	Good	Good	Good	0.85	High strength low density
2.	Inconel-718	122	0.297	0.9	3.0	8.0	Good	Good	Good	0.87	High strength low density
3.	Inconel X-750	102	0.298	2.5	0	8.0	Difficult	Good	Good	0.92	High strength low density
4.	WASPALOY$_{TM}$	100	0.298	3.0	4.0	7.9	Difficult	Good	Good	0.92	High strength low density
5.	Nimonic-75	27	0.302	0.4	0	7.9	Good	Good	Good	-	Low strength
6.	Inconel-600	22	0.305	0	0	8.2	Good	Good	Good	1.00	Low strength
7.	Haynes-188	45	0.333	0	0	7.8	Good	Good	Good	1.02	Strength increase is offset by increased density.
8.	Haynes-25	35	0.329	0	0	8.0	Good	Good	Good	1.03	Strength increase is offset by increased density.
9.	Nickel-200	9	0.321	0	0	9.0	Good	Good	Good	1.12	Low strength
10.	Inconel-625	42	0.305	0	9.0	7.8	Good	Good	Good	0.97	High moly content
11.	Hastelloy X	35	0.299	0	9.0	8.3	Good	Good	Good	-	High moly content
12.	TD Nickel	25	0.322	0	0	7.8	Very difficult	Experi-mental	Good	-	0.2% yield drops to 9000 psi at welds
13.	Hastelloy C	55	0.322	0	16.0	7.5	Good	No data available	Good	-	High moly content
14.	Hastelloy N	27	0.317	0.2	16.5	7.1	Good	Good	Good	-	High moly content

Note: 1. Material properties at 1017°F
2. α = Thermal coefficient of expansion.

Table II
Relative Dissolution Rate of Metals
in 42° Be' Ferric Chloride

Alloy	Relative Dissolution	Alloy Composition
Inconel 600	110.0	Ni, 15.5 Cr, 0.15C, 8.0 Fe
TD-Ni	109.0	Ni, 2.2 ThO_2
Nickel 200	100.0	99.0 Ni
Nickel 201	100.0	99.0 Ni
Nickel 270	99.7	99.97 Ni
Inconel X-750	88.7	Ni, 15.5 Cr, 0.08C, 7.0 Fe, 2.5 Ti, 0.7 Al
Waspaloy	85.2	Ni, 19.5 Cr, 13.5 Co, 0.08C, 3.0 Ti, 1.4 Al, 4.0 Mo
Inconel 706	65.1	Ni, 16.0 Cr, 37.0 Fe, 1.75 Ti, 2.9 Cb + Ta
Inconel 718	61.9	Ni, 18.5 Cr, 0.10C, 18.0 Fe, 0.9 Ti, 0.6 Al, 3.0 Mo, 5.0 Cb + Ta
Hastelloy X	0	Ni, 22.0 Cr, 1.5 Co, 9.0 Mo, 0.20 C, 18.5 Fe, 0.6 W
Inconel 625	0	Ni, 21.5 Cr, 9.0 Mo, 3.65 Cb + Ta

a wetting agent, adhere to the etched surfaces. Corrosion inhibitors are similar chemically to either of the other side etch inhibitors but form a one-phase solution and do not form an insoluble complex.

Preliminary screening tests of candidate etchant solutions were conducted by measuring the milling rate of nickel in quiescent solutions. If the etching rate was not retarded by a candidate side etch inhibitor, it was assumed that the inhibitor would not be effective in a production type etcher. Table III lists the results obtained with various additives during the immersion tests. Figure 5 shows the effect of increasing thiourea concentration on the dissolution rate of nickel in a quiescent solution. As expected, increasing concentration reduced the etch rate. These results were used as a guide in selecting additives for additional investigation in a splash-type etcher.

3. Maskants

Maskants investigated were photosensitive compounds that undergo physical change by exposure to strong light. Candidate maskants were applied to the work piece by either spraying, dipping, or spin coating on suitably cleaned surfaces. After exposure to high intensity light through a photographic master the unexposed maskant (therefore, not polymerized) was removed with a solvent. The exposed areas were resistant to the solvent and remained intact. Alternatively, photoresists can be positive working and decomposed by light so that the exposed areas are removed during developing. Commercially available Shiply AZ340, Kodak KAR, Kodak KMER, Kodak KTFR, Hunt Waycoat SC, Hunt Waycoat PF, and Chemco Vyna Top photoresists were evaluated.

TABLE III IMMERSION TEST RESULTS FOR NICKEL 200

Etchant	Additive	Relative Dissolution Rate*
1) Laboratory Prepared $FeCl_3$ (500 g/l)	a) 6.7 g/l quinoline	97.6
	b) 6.7 g/l sodium diethylditiocarbonate	95.2
	c) 6.7 g/l sodium oxalate	87.4
	d) 6.7 g/l dimethylglyoxime, disodium salt, octahydrate	86.5
2) Laboratory Prepared $FeCl_3$ (500 g/l) plus 100 ml/l hydrochloric acid	a) 6 g/l polyvinylpynolidinone	93.4
	b) 30 g/l indole	64.9
	c) 10 g/l thiourea	60.6
	d) 30 g/l semicarbazide hydrochloride	45.9
	e) coated sample with oximide	100.0
	f) coated sample with diethloxalate	100.0
	g) coated sample with dithiooxamide	100.0
	h) coated sample with diethylbenzene	100.0
	i) coated sample with hexynol	84.9
3) Commercial 42^o Be' $FeCl_3$ (Rapid Circuit Etch, Hunt Chemical Company)	a) 100 ml/l nitric acid	156.8
	b) 1 ml/l phosphoric acid	109.0
	c) 100 ml/l phosphoric acid	40.0
	d) 1 ml/l acetic acid	100.0
	e) 100 ml/l acetic acid	31.0
	f) 5 g/l copper chloride	99.0
	g) 5 g/l stannous chloride	97.0
	h) 1 ml/l sulfuric acid	95.0
	i) 5 ml/l sulfuric acid	87.5
	j) 100 ml/l surfuric acid	12.4
	k) 2 g/l indole	92.0
	l) 2 g/l hexamethylenetetramine	76.8
	m) 4 g/l hexamethylenetetramine	37.7
	n) 5 g/l lead chloride	74.0
	o) 2 g/l potassium sulfate	73.5
	p) 4 g/l potassium sulfate	46.1
	q) 10 ml/l polyvinylpyrrolidinone (PMC-9323)**	43.5
	r) 10 ml/l polyvinylpyrrolidinone (PMC-9325)**	56.5
	s) 2 g/l zinc sulfate	49.4
4) Commercial 42^o Be' $FeCl_3$ (Rapid Circuit Etch Hunt Chemical Company) plus 100 ml/l hydrochloric acid	a) 100 ml/l phosphoric acid	55.0
	b) 80 ml/l sulfuric acid	30.6

*Relative dissolution rate is based on the dissolution rate of Nickel-200 in the etchant with no additive.

**Specimens first coated with oil then immersed in etchant, PMC-9325 same as Shell Soluble Oil W, code 62103, Emulsion 155B; Shell Oil Company.

PMC-9323 same as Ho-Cut-237; E. F. Houghton Company.

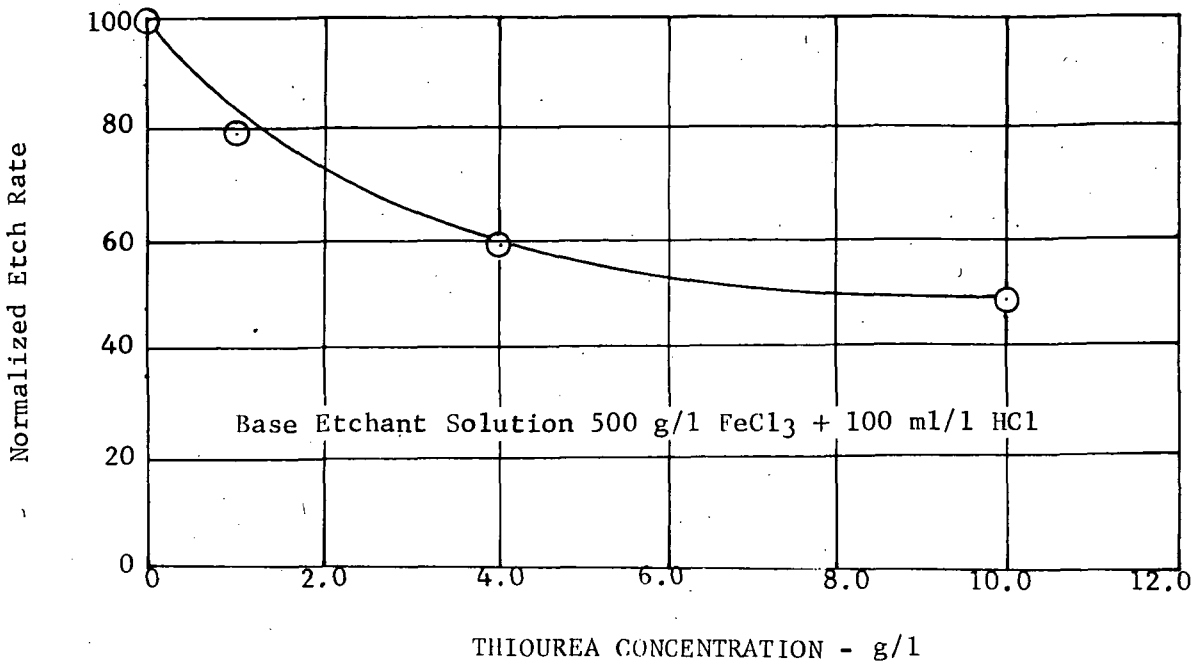

Figure 5. Thiourea Concentration vs Dissoltuion Rate for Nickel-200 Immersed in Etchant FD 56983A

To reduce the possibility of discontinuities caused by the undercut resist breaking off nonuniformly during etching, the work piece was first silver-plated before applying resist. After printing the resist with the desired pattern, the unmasked silver was removed by immersion in a solution of ferric nitrate. Silver was selected to strengthen the resist because it was considerably less soluble in ferric chloride than nickel.

An experimental etching test pattern (figure 6) was used during the maskant evaluation and consisted of a series of parallel lines 0.010 in. (0.0254 cm) and 0.020 in. (0.0508 cm) wide separated by 0.090 in (0.228 cm) and 0.100 in. (0.254 cm) space, respectively. Since the silver was removed by immersion etching, some undercutting of the pattern in the silver occurred and the starting passage widths for etching the nickel were 0.012 in. (0.0305 cm) and 0.022 in. (0.0559 cm), respectively.

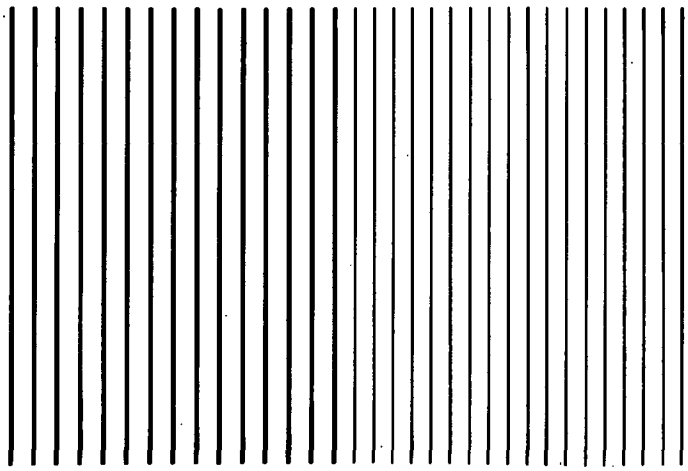

Figure 6. Pattern Used for Chemical Machining Development FC 19303

4. Splash Etching of Nickel 200

A.U. S. Stoneware Bantam Turbinaire splash etcher was used to evaluate candidate etchants and side etch inhibitors. The unit originally impinged etchant onto a vertically oriented stationary work piece. To improve uniformity of etch it was converted to splash the etchant upward against a slowly revolving work piece. The impinging velocity was increased by modifying the pulley drive assembly, and a temperature control was added (figures 7 and 8). Results of etching nickel panels with this splash etcher was summarized in Table IV.

Initial specimens were etched without inhibitors to obtain baseline data on the etchants. The undercut was 90 to 98% for these specimens. A typical cross section of a specimen etched without inhibitors is shown in figure 9.

Side etch inhibitors selected based on the immersion test results were mixed with the ferric chloride solutions and run in the splash etcher. Various concentrations of inhibitors and several operating conditions were evaluated.

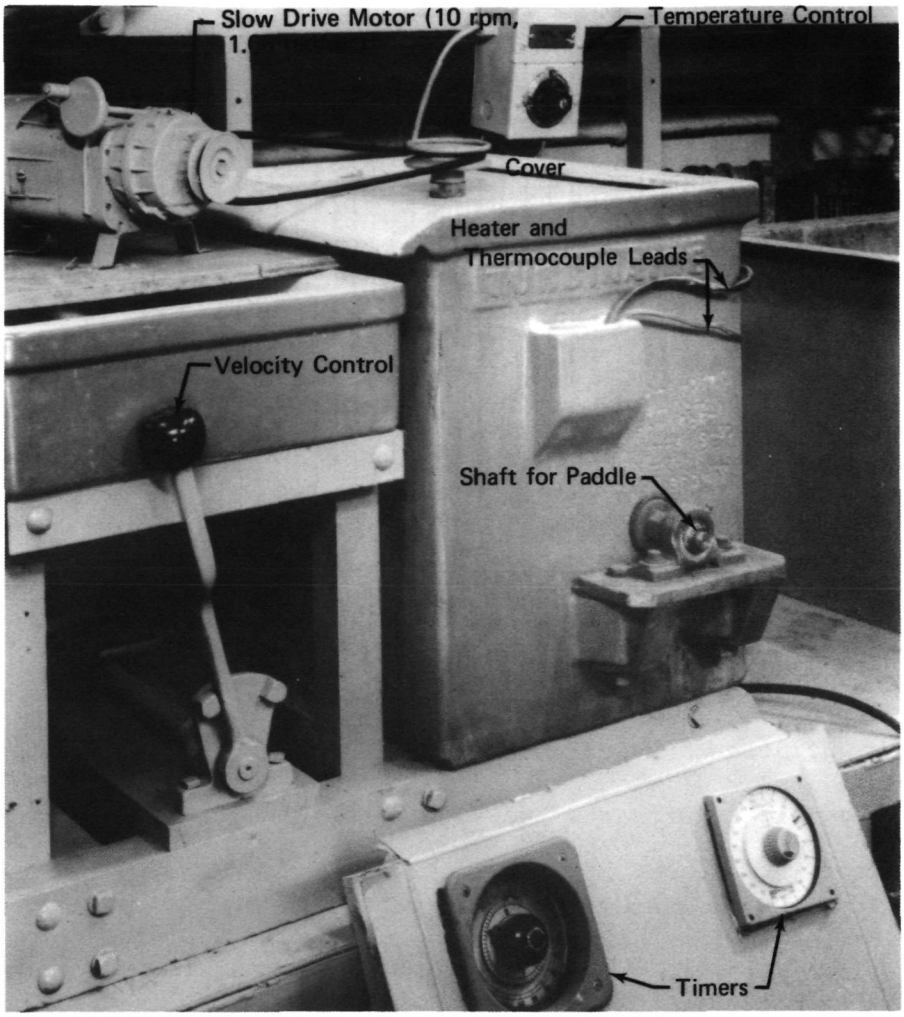

Figure 7. Bantam Turbinaire Splash Etcher FD 56984

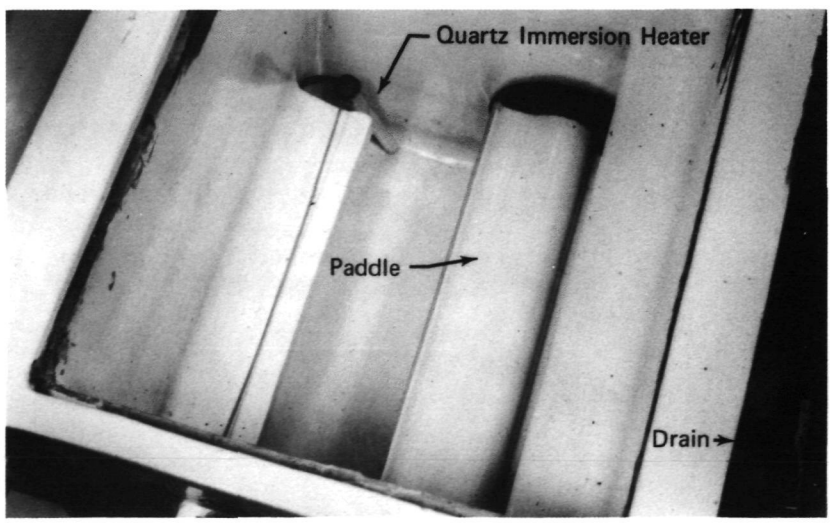

Figure 8. Interior of Bantam Turbinaire Splash Etcher FD 56985

Table IV. Splash Etcher Test Results

Specimen Number	Maskant	Etchant+	Additive	Additive Concentration, ppm	Temperature, °F[1]	Paddle Velocity, rpm	Time, min	Milling Rate mils/min^2	Depth, mils[3]	Passage Width, mils[3] Masked	Passage Width, mils[3] Final	Percent Side Etch	Surface Finish, rms
1	KMER	450g/l $FeCl_3$ 100 ml/l HCl	-	-	80	760	120	0.25	30	30	89	98	160
2	Silver	RCE+100 ml/l HCl	-	-	115	760	45	0.34	16	12	40	90	140
3	Silver	RCE+100 ml/l HCl	-	-	115	760	90	0.28	26	12	58	94	120
4	Silver	RCE	-	-	80	1250	140	0.15	23	12	55	93	130
5	Silver	450g/l $FeCl_3$	Nitric Acid	33.0**	80	760	100	0.15	15	12	41	97	240
6	Silver	↓	Nitric Acid	66.0**	80	760	120	0.17	20	12	40	70	220
7	Silver	↓	Nitric Acid	99.0**	80	760	90	0.22	20	12	49	93	140
8	Silver	↓	Nitric Acid	165.0**	80	760	120	0.15	18	12	40	78	140
9	Silver	450g/l $FeCl_3$ 100 ml/l HCl	DMG	0.13	80	760	60	0.18	11	12	34	100	400
10	Silver	↓	DMG***	0.13	80	760	90	0.18	16	12	43	97	180
11	Silver	↓	DMG***	0.26	80	760	60	0.16	10	12	30	95	170
12	Silver	↓	DMG***	0.26	80	760	90	0.16	14	12	40	97	200
13	Silver	↓	DMG***	0.53	80	760	65	0.24	15	22	44	73	220
14	Silver	↓	DMG***	0.53	80	760	120	0.17	20	12	40	68	200
15	Silver	↓	DMG***	1.05	80	760	60	0.24	14	12	36	83	240
16	Silver	↓	DMG***	2.12	80	760	60	0.24	14	12	37	86	220
17	Silver	↓	DMG***	2.12	80	760	120	0.13	16	12	43	97	190
18	Vynatop	Rotogravure	DMG***	1.06	80	1900	120	0.13	16	10	32	67	160
19	Vynatop	Rotogravure	DMG***	1.06	110	1900	120	0.34	41	10	66	69	160
20	KMER	RCE+100 ml/l HCl	Thiourea	0.13	80	760	76	0.17	13	10	31	80	120
21	KMER	↓	Thiourea	0.13	125	760	60	0.25	15	10	38	93	110
22	KMER	↓	Thiourea	0.26	125	760	70	0.22	16	10	36	83	160
23	Vynatop	RCE	Thiourea	0.53	110	1425	90	0.30	28	10	41	57	180
24	Silver	Rotogravure	Thiourea	1.05	110	1900	120	0.24	29	12	44	55	40
25	Silver	↓	Thiourea	1.58	105	1900	120	0.25	30	12	42	50	90
26	Silver	↓	Thiourea	1.58	105	1900	120	0.25	30	12	43	52	80
27	Silver	RCE	Thiourea	0.13	120	1000*	49	0.47	23	12	42	65	100
28	Silver	↓	Thiourea	0.26	120	1000*	49	0.61	30	12	45	55	80
29	Silver	↓	Thiourea	0.53	120	800*	70	0.36	25	12	41	58	90
30	Silver	↓	Thiourea	0.53	120	600*	63	0.43	27	12	45	61	100
31	Silver	↓	Thiourea	0.53	120	400*	105	0.24	25	12	45	66	130
32	Silver	↓	Thiourea	0.53	81	1000*	84	0.23	19	12	31	50	180
33	Silver	↓	Thiourea	0.53	98	1000*	42	0.55	23	12	34	48	140
34	Vynatop	↓	Thiourea	0.53	120	1000*	110	0.18	20	10	39	72	90
35	Silver	↓	Thiourea	0.53	100	1250	120	0.23	28	12	44	57	70
36	Silver	↓	Thiourea	1.05	125	1000*	70	0.36	25	12	36	48	150
37	Silver	↓	Thiourea	1.05	100	1250	120	0.15	18	12	32	56	240
38	Silver	↓	Thiourea	1.05	100	1425	78	0.54	42	12	39	56	310
39	Silver	↓	Thiourea	1.05	100	1000*	90	0.27	24	12	33	44	80
40	Silver	↓	Thiourea	1.58	130	1425	90	0.38	34	12	51	57	120
41	Silver	↓	Thiourea	1.58	120	1425	120	0.33	40	12	54	53	80
42	Silver	↓	Thiourea	2.11	120	1425	120	0.19	23	12	39	59	260
43	Silver	↓	Thiourea	2.64	120	1425	75	0.31	23	12	42	65	360
44	Silver	↓	Thiourea	2.64	100	1425	150	0.19	29	12	49	64	310
45	Silver	Rotogravure	Thiourea	1.05	110	1425	120	0.22	26	12	36	46	60
46	Silver	RCE	Thiourea	0.53	110	1000*	40	0.58	23	12	40	61	90
47	Silver	↓	Thiourea	0.53	120	1000*	30	0.64	19	12	33	55	90
48	Silver	↓	Thiourea	0.53	120	1000*	15	0.42	6	12	20	64	120
								0.50	8	22	32	67	120
49	Silver	↓	Thiourea	0.53	120	1000*	30	0.33	10	12	21	45	100
								0.33	10	22	30	40	
50	Silver	↓	Thiourea	0.53	120	1000*	50	0.30	15	12	31	61	100
								0.32	16	22	41	59	
51	Silver	↓	Thiourea	0.53	120	1000*	60	0.27	16	12	30	56	90
52	Silver	↓	Thiourea	0.53	120	1000*	90	0.24	22	12	38	60	100
								0.28	26	22	51	56	
								0.24	22	32	55	52	
								0.24	22	52	74	50	
53	Silver	RCE+100 ml/l HCl	Thiourea	1.06	120	1000*	15	0.41	6	12	19	58	140
54	Silver	↓	Thiourea	1.06	120	1000*	45	0.46	21	12	38	62	100
55	Silver	↓	Thiourea	1.06	120	1000*	65	0.43	28	12	44	57	110
56	Silver	↓	Thiourea	1.06	120	1000*	80	0.42	34	12	54	62	100
57	Silver	↓	Thiourea	1.06	120	400*	90	0.31	28	12	49	69	140
58	Silver	↓	Thiourea	1.06	120	600*	75	0.35	26	12	46	65	120
59	Silver	↓	Thiourea	1.06	120	800*	60	0.28	19	12	36	63	120
60	Silver	RCE	Potassium Sulfide	1.48	120	1900	60	0.40	24	12	38	54	180
61	Silver	↓	Potassium Sulfide	2.22	120	1900	60	0.36	22	12	35	52	200
62	Silver	↓	Potassium Sulfide	3.70	120	1900	60	0.49	29	12	53	71	180
63	Silver	↓	Potassium Sulfide	3.70	120	1900	60	0.36	22	12	42	68	160
64	Silver	↓	Potassium Sulfide	6.34	120	1900	90	0.27	24	12	49	77	210
65	Silver	↓	HMTA***	0.53	120	1260	100	0.32	32	12	50	59	200
								0.37	22	22	62	54	
66	Silver	↓	HMTA***	1.06	110	1260	60	0.22	13	12	28	62	180
								0.27	16	22	38	50	
67	Silver	↓	HMTA***	1.06	100	1260	90	0.15	14	12	28	57	160
								0.20	18	22	40	50	
68	Vynatop	Rotogravure	Sodium Oxalate	3.30	110	1800	120	0.22	26	10	57	90	230
69	Silver	RCE	Indole	1.06	110	1900	60	0.52	31	22	54	52	200
70	Silver	↓	Indole	2.11	120	1900	60	0.60	36	12	49	51	210
								0.67	40	22	59	46	
71	Silver	↓	Indole	2.11	110	1900	90	0.35	32	12	44	50	180
								0.42	38	22	54	42	
72	KMER	500 g/l $FeCl_3$ 100 ml/l HCl	SCH	0.26	110	760	60	0.09	5	10	-	-	220
73	Silver	RCE	Lead Chloride	2.64	110	1900	120	0.50	60	22	78	47	160
74	Silver	↓	Lead Chloride	5.28	110	1900	60	0.52	31	12	48	58	190
75	Silver	↓	Lead Chloride	5.28	110	1900	60	0.31	19	12	34	58	210
			Thiourea	1.06				0.34	21	22	40	43	
76	Vynatop		PMC 9325***	132.0**	110	1900	120	0.02	2	10	-	-	450
77	Vynatop	Rotogravure	PMC 9325***	1.32**	110	1900	110	0.27	30	10	47	62	170
78	Silver	↓	PMC 9325***	2.64**	100	1900	80	0.29	24	12	38	58	300
79	Silver	↓	PMC 9325***	3.96**	110	1900	120	0.21	25	12	46	68	180
80	Silver	RCE	PMC 9323***	2.64**	120	1900	60	0.36	22	12	40	64	210
81	Silver	↓	PMC 9323***	9.25**	100	1900	120	0.30	36	12	59	65	310
82	Silver	↓	PMC 9323***	2.64**	120	720	90	0.21	19	12	36	63	380
83	Silver	↓	PMC 9323***	2.64**	100	720	240	0.12	29	12	52	68	350
								0.18	43	22	76	63	
84	Silver	↓	Peri 13a***	0.53	80	760	60	0.22	13	12	36	92	250
85	Silver	↓	Peri 13a***	0.53	80	760	120	0.14	17	12	39	72	230
86	KMER	↓	Thiourea	0.26	115	760	60	0.27	16	10	40	93	160
			EDTA	2.6									
87	Silver	500 g/l $FeCl_3$ 100 g/l Hcl	SCH	0.26	90	760	40	0.48	19	12	40	74	90
			Nitric Acid	33**									
88	KMER	RCE	Thiourea	0.13	100	1000*	60	0.30	18	10	62	137	400
			Copper	0.26									
89	Silver	RCE	Thiourea	0.13	100	1000*	90	0.27	24	12	58	100	210
			Copper	0.26									
90	Silver	↓	Thiourea	0.13	100	1000*	120	0.20	24	12	58	100	380
			Copper	0.26									
91	KMER	↓	Thiourea	0.13	100	1000*	120	0.25	30	10	91	150	320
			Copper	0.26									
92	Silver	↓	Thiourea	0.13	100	1000*	180	0.13	23	12	37	54	90
			Copper	0.26									
93	Silver	↓	Thiourea	0.53	100	1000*	240	0.13	31	12	49	60	80
			Copper	0.26									
94	Silver	↓	Thiourea	0.53	80	1000*	300	0.05	15	12	26	46	110
			Copper	0.26				0.07	20	22	40	45	
95	Silver	↓	Thiourea	0.53	120	1000*	120	0.16	20	12	26	35	160
			Copper	0.26									
96	Silver	↓	Thiourea	0.53	100	1000*	120	0.24	29	12	41	50	160
			Copper	0.26									
97	Silver	↓	Thiourea	2.64	110	1425	100	0.25	25	12	41	58	230
			Phosphoric Acid	10.0**									
98	Silver	↓	Thiourea	2.64	125	1425	66	0.39	26	12	50	73	150
			Phosphoric Acid	10.0*									
			Zinc Chloride	2.64									
99	Silver	↓	Thiourea	5.28	120	1425	120	0.15	18	12	40	78	530
			Phosphoric Acid	10.0**									
			Zinc Chloride	5.28									
100	Silver	↓	Thiourea	5.28	110	1425	187	0.13	25	12	50	76	600
			Phosphoric Acid	10.0**									
			Zinc Chloride	5.28									
			Glass Bead***	26.4									
101	Silver	Rotogravure	Thiourea	1.58	110	1900	77	0.23	18	12	30	50	100
			DMG***	0.26									
102	Silver	↓	Thiourea	1.05	110	2000	120	0.26	31	12	49	60	90
			DMG***	.53									
103	Silver	↓	PMC 9325***	3.96**	110	1900	120	0.18	21	12	42	71	230
			DMG***	1.06				0.20	24	22	52	63	
104	Silver	RCE	Thiourea	1.06	120	1900	150	0.15	23	12	33	44	200
			Sulfuric Acid	2.64**									
105	Silver	↓	Thiourea	1.32	120	1900	90	0.28	26	12	43	60	200
			Sulfuric Acid	3.30**				0.33			51	48	
106	Silver	↓	Thiourea	1.32	120	1900	120	0.17	20	12	36	60	220
			Sulfuric Acid	3.30**				0.25	30	22	52	50	
107	Silver	↓	Thiourea	2.64	100	1900	120	0.18	22	12	46	77	230
			Sulfuric Acid	6.61**									
108	Silver	↓	Potassium Sulfide	6.34	100	1900	60	0.38	23	12	38	56	170
			Nitric Acid	6.61**				0.43	26	22	49	52	
109	Vynatop	↓	Potassium Sulfide	6.34	100	1900	60	0.38	22	10	44	77	170
			Nitric Acid	6.61**				0.42	26	20	58	73	
110	Silver	↓	Potassium Sulfide	6.34	100	1900	60	0.41	24	12	39	56	150
			Nitric Acid	19.82**				0.47	28	22	49	48	
111	Vynatop	↓	Potassium Sulfide	6.34	100	1900	60	0.40	24	10	45	73	150
			Nitric Acid	19.82**				0.43	26	20	57	71	

*Specimens etched in Master Etcher Model PC-32HS
**Concentration units ml/l rather than g/l
+RCE: 42° Be ferric chloride, Rapid Circuit Etch, Hunt Chemical Corp.
Rotogravure: 48° Be ferric chloride, Hunt Chemical Corp.
***DMG: Dimethylglyoxime disodium salt octahydrate
HMTA: Hexamethylenetetramine
SCH: Semicarbazidehydrochloride
Peri 13a: 40% Formamidine disulfide dihydrochloride, 49% ethylene thiourea, 9% diaminophenol dihydrochloride
PMC 9323: HoCut-237, E. F. Houghton Company
PMC 9235: Shell Soluble Oil W, Code-62103, Emulsion 155B, Shell Oil Company
Glass Bead: Glass beads 0.0005-0.0021 in., Florida Silica Sand Company

[1] $K = (5/9)(F + 459.67)$
[2] $cm/min = (mil/min)(2.54 \times 10^{-3})$
[3] $cm = (mil)(2.54 \times 10^{-3})$

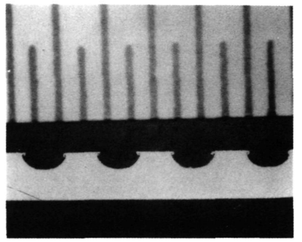

Figure 9. Cross Section of Chemically Machined Nickel-200 Using no Side Etch Inhibitors FD 59679

A significant reduction of side etch was observed by using thiourea as a side etch inhibitor. Figure 10 illustrates the effect of concentration on side etch for specimens tested with thiourea at temperatures from 80-130° (300-328°K), passage depths from 0.020-0.050 in. (0.051-0.127 cm) and paddle tip velocities above 1745 fpm (8.86 m/sec). Using 48° Be' ferric chloride solution with the thiourea additive generally resulted in smoother surfaces but had little effect on side etch. Dissolved copper in the etchant was also investigated but with no noticeable effect on side etch.

The expected concentration dependence on side etch was established with the additives disodium salt of dimethyglyoxime, octahydrate (DMG) and thiourea. The optimum concentration of thiourea was about 1.0 g/l. Figure 11 shows typical cross sections of passages machined in etchants containing thiourea.

The disodium salt of dimethylglyoxime, octahydrate showed some reduction of side etch at concentrations ranging from 0.25 to 2.0 g/l (figure 12). The expected concentration relationship with side etch was shown and minimum side etch was observed at 0.5 g/l. Increasing the etchant im-

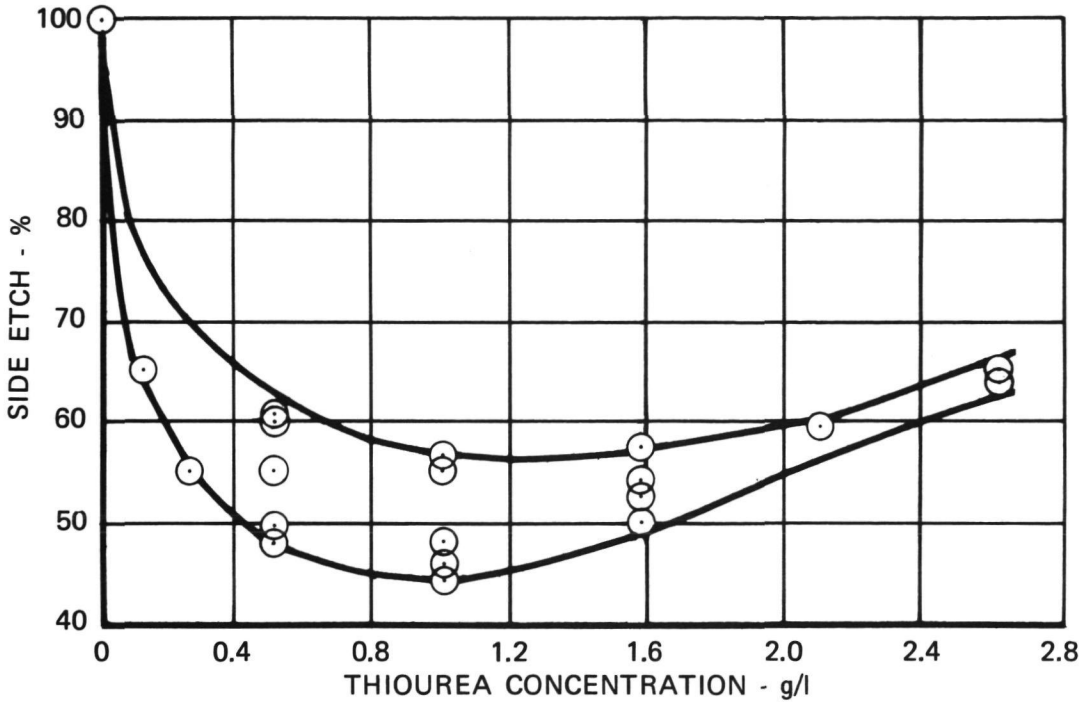

Figure 10. Effect of Thiourea Concentration on Side Etch FD 59680

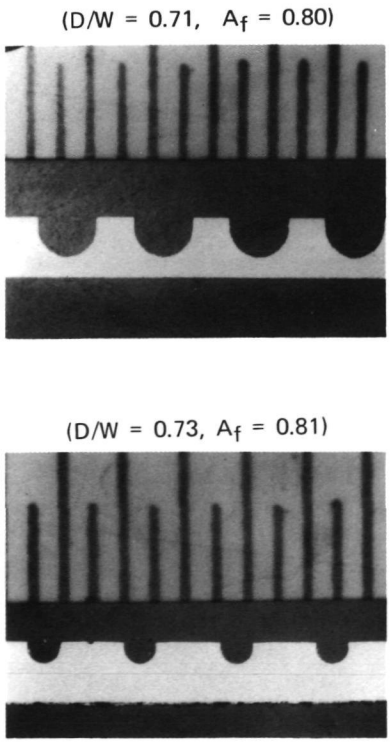

Figure 11. Cross Sections of Chemically Machined Nickel-200 Using Thiourea Additive FD 59681

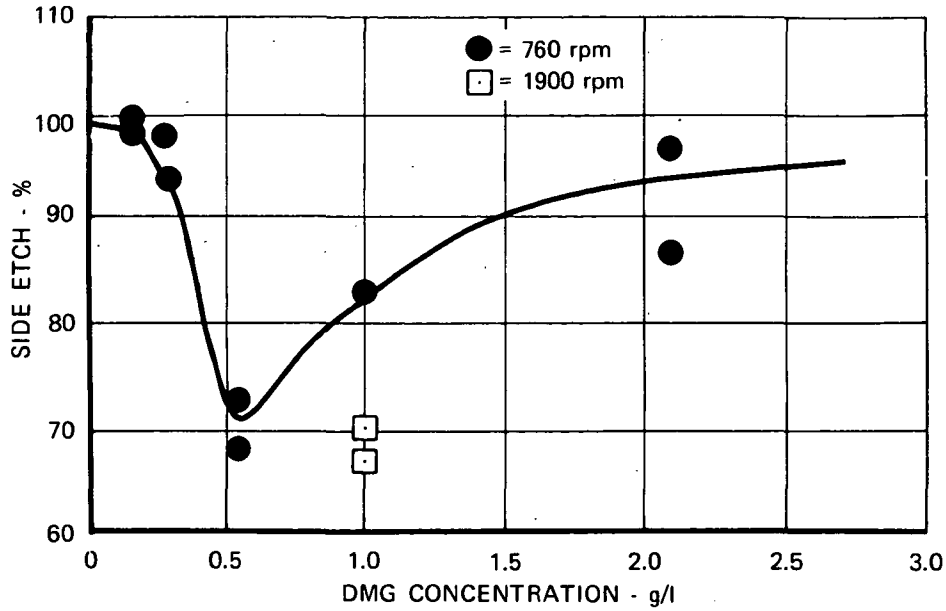

Figure 12. Effect of Dimethylglyoxime Concentration on Side Etch FD 59682

pingement velocity by increasing the paddle speed from 760 rpm to 1900 rpm was observed to further reduce the side etch at 1.0 g/l concentration.

Lead chloride reduced undercutting equivalent to thiourea or potassium sulfide. Solutions containing lead chloride are more stable than those with thiourea, but offer no advantage over potassium sulfide. Lead chloride is also extremely toxic and must be used with caution. The addition of thiourea to etchants containing lead chloride did not further reduce undercutting.

Figure 13 compares the results of the thiourea splash etching with other inhibitors; potassium sulfide, hexamethylenetetramine, indole, and sodium oxalate. Potassium sulfide results fell within the ranges of side etch observed with etchants containing thiourea, supporting the hypothesis of the formation of a nickel sulfide compound. Potassium sulfide increases the stability of etchants since, being an inorganic compound, it is not as readily hydrolyzed as the thiourea in ferric chloride solutions.

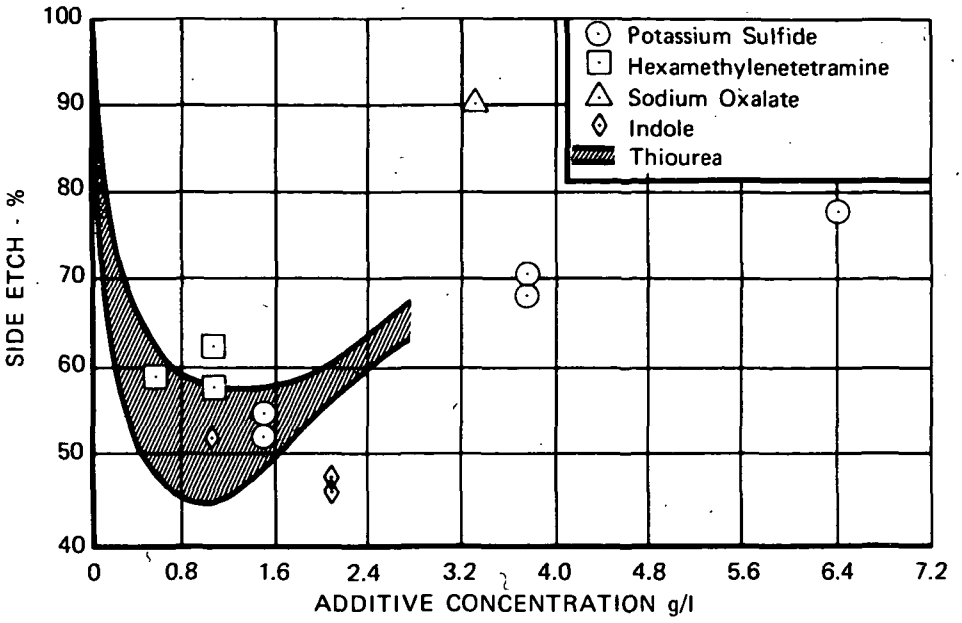

Figure 13. Comparison of Side Etch Inhibitors FD 59683

Hexamethylenetetramine did not show as much side etch inhibition as did thiourea. Sodium oxalate showed only slight etch reduction. Indole was a good side etch inhibitor, but etchants containing indole were unstable and after a few hours, a black gummy substance formed and floated on the surface. When this material contacted the nickel plate being etched, it adhered to the surface and completely stopped local etching. An extremely non-uniform etch resulted.

Semicarbizide hydrochloride was investigated but was found to be such an efficient inhibitor that concentrations as low as 0.26 g/l reduced the milling rate threefold, and also gave an extremely rough, pitted etched surface. The addition of nitric acid to the etching solutions increased the milling rate but did not result in reduced side etch.

Passages etched using suspensions of HoCut-237 (PMC 9323) and Shell Soluble Oil W, Code 62103, Emulsion 155B (PMC 9325) oils were extremely

rough with excessive overhang of the land over the passage (figure 14).

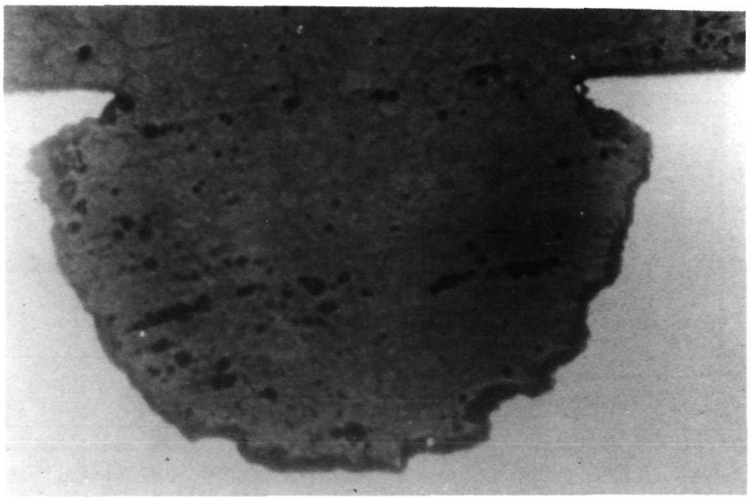

Figure 14. Corss Section of Chemically Machined Nickel-200 Using HoCut-237 Oil Additive FD 59684

Various combinations and additions were evaluated with the above mentioned inhibitors. No significant advantage was observed.

Both the U. S. Stoneware Bantam Turbinaire splash etcher and a Master Etcher Model PC-32HS were used to determine the effects of velocity on side etch. These two etchers have essentially the same features; however, the Master Etcher (figures 15 and 16) is a production-size etcher whereas the U.S. Stoneware Bantam Turbinaire etcher is a laboratory-size etcher. Because the Master Etcher had a paddle with a larger diameter and because no direct measurement of etchant velocity was available, paddle tip speed was used to compare etchant impingement velocity (figure 17). The data show that an appreciable reduction of side etch was obtained with a change in paddle tip speed from 0 to about 2000 fpm (10.16 m/sec) whereas higher velocities did not have an effect. These results are consistent with results presented in Reference 5.

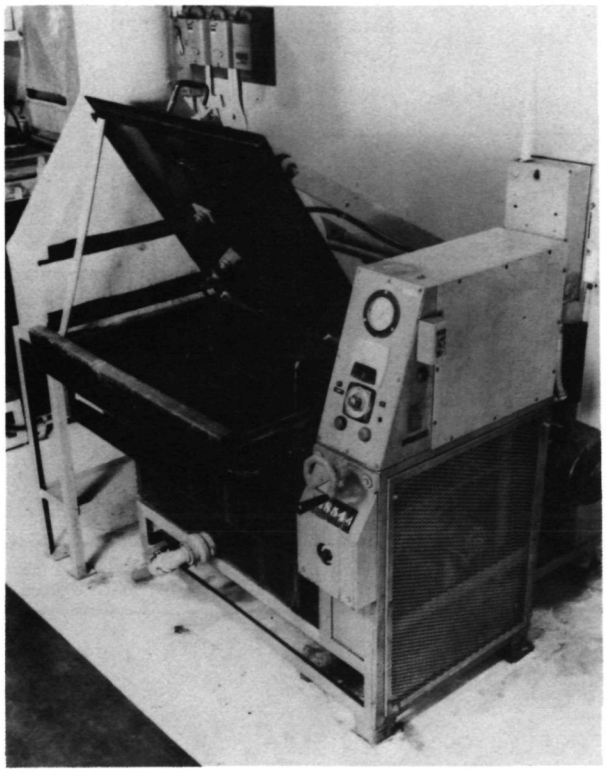

Figure 15. Master Etcher Model PC-32HS GS 10291

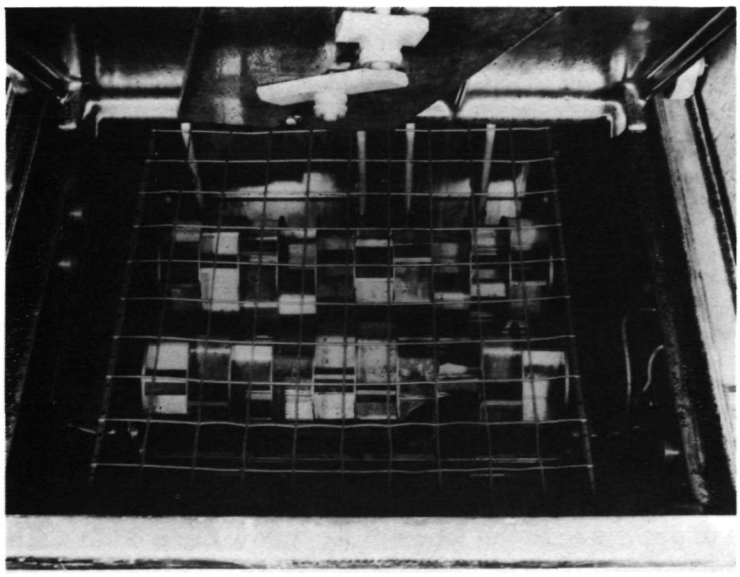

Figure 16. Interior View of Master Etcher Model PC-32HS GD 10292

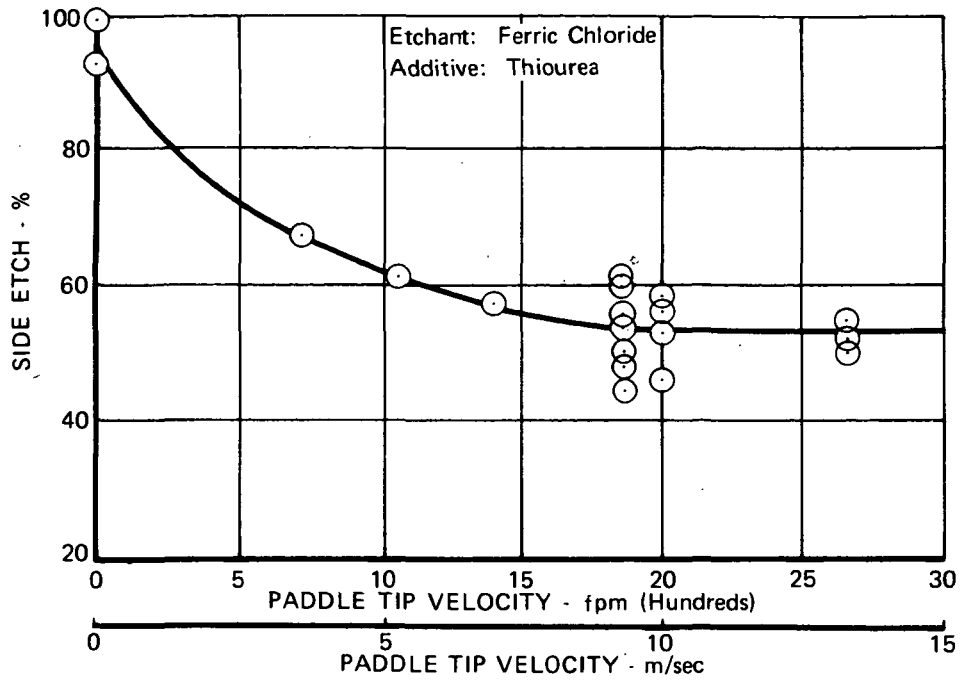

Figure 17. Effect of Velocity on Side Etch FD 59685

The effect of temperature on side etch was determined by comparing specimens run in the laboratory-size and production-size etchers at paddle velocities of 1745 fpm (8.86 m/sec) or greater in a 42 to 48° Be' ferric chloride solution containing 0.50 to 1.60 g/l thiourea and machined to depths of 0.019 in (0.048 cm) or greater at temperatures from 80 to 130°F (300 to 328°K). Over the range investigated, only etching rate varied with temperature; no effect of temperature on the degree of side etch was observed (Figure 18) and all side etch values were 53 $\pm$8%. No etchant temperature dependent relationship between side etch and depth of etch or age of solution was readily apparent (Table V). Temperatures for milling nickel, therefore, would be chosen to provide a suitable milling rate.

Passage dimensions ranging from 0.012 to 0.052 in (0.030 cm to 0.132 cm) were used on a single nickel specimen to determine the effect of

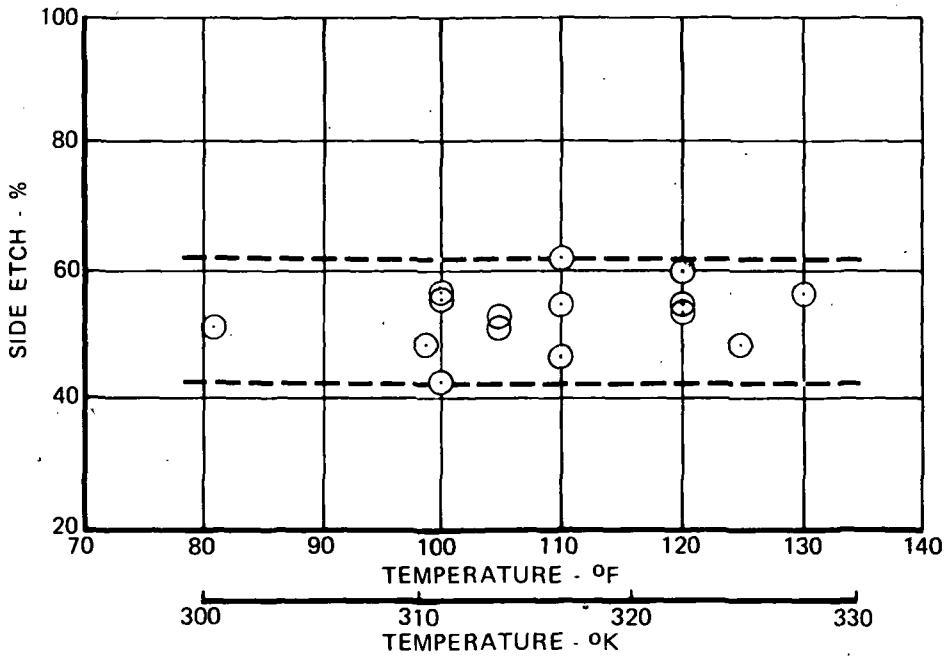

Figure 18. Effect of Temperature on Side Etch FD 59686

starting passage width on side etch. Figure 19 shows the results of this study. Increasing the starting width up to 0.030 in (0.076 cm) reduced undercutting appreciably. Above 0.030 in (0.076 cm), changes were not significant.

Variations in surface finish were generally small with different solutions. Values from 100-300 rms were obtained in most cases (see Table IV).

The etching solutions investigated in this program did not cause any measurable intergranular attack of Nickel 200. A typical cross section of a machined passage at 500X magnification is shown in Figure 20.

Tests were made in the splash etcher using modified etching procedures to reduce side etch. One variation investigated was to cycle the etcher on and off periodically during the etching process. The purpose of doing

Table V. Effect of Etchant Temperature on Side Etch

Specimen Number	Passage Depth in. (cm)	Age of Solution Hours	Temperature ^{o}F (^{o}K)	Side Etch, %
35	0.028 (0.071)	31	100 (311)	57
39	0.024 (0.061)	7	100 (311)	44
36	0.025 (0.064)	7	125 (325)	48
45	0.026 (0.066)	10	110 (317)	46
32	0.019 (0.048)	168	81 (300)	50
33	0.023 (0.058)	173	98 (310)	48
46	0.023 (0.058)	12	110 (317)	61
47	0.019 (0.048)	14	120 (322)	55
24	0.029 (0.074)	29	110 (317)	55
38	0.042 (0.107)	14	100 (311)	56
52	0.022 (0.056)	5	120 (322)	60
40	0.034 (0.086)	29	130 (328)	57
41	0.040 (0.102)	70	120 (322)	53
25	0.030 (0.076)	53	105 (314)	50
26	0.030 (0.076)	67	105 (314)	52

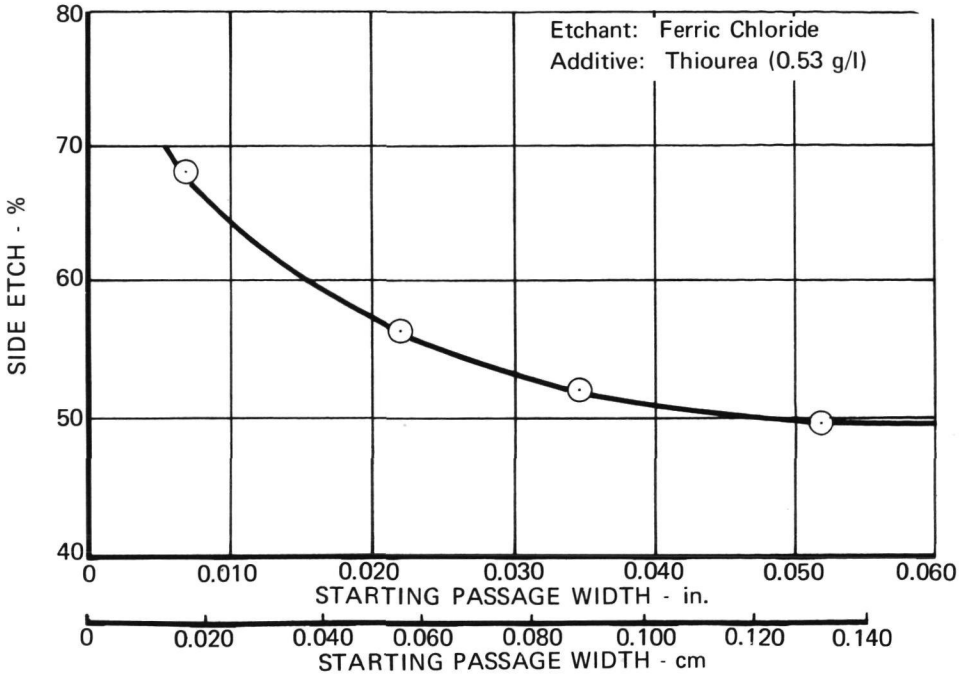

Figure 19. Effect of Passage Width on Side Etch FD 59687

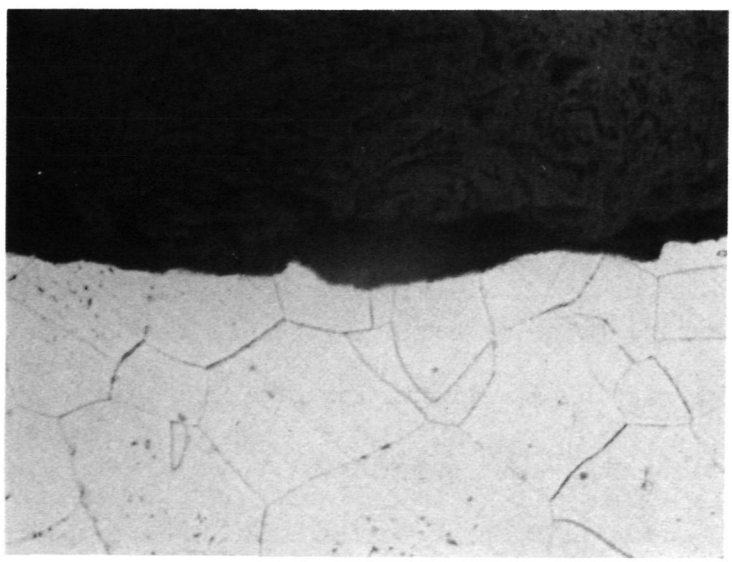

Figure 20. Photomicrograph of Chemically Machined Nickel-200 FD 59688

this was to allow time for a layer of side wall protection to build up. This technique did not produce less undercutting than did continuous etching; results are presented in Table VI.

A form of depth stepping, called photoresist banking, was investigated. It involved the same principles as powder banking (that of protecting the sidewalls with a maskant after each cut is made) but appeared to be more adaptable to production use. In photoresist banking the entire plate was coated with a positive photoresist and re-exposed after partial etching. Photographic developing theoretically resulted in removal of the resist on the bottom of the passage while the resist on the sidewalls, not exposed to light, remained. Two commercially available positive photoresists, Shipley AZ 340 and Kodak KAR, were evaluated using this technique and depth-to-width ratios greater than 1.0 were achieved (Figure 21). Shipley AZ 340 provided the most consistent results and was used for most of the tests. When coating the test panels with resist, they were coated and then turned over with the etched portion facing down to allow excess maskant to drain off. (If the resist coating was too thick, longer light exposures were required; if too thin, complete removal of the resist coating occurred during developing). The best line definition was produced by exposing the coated plate with a MacBeth Mark 50 Constantarc Printing Lamp (Figure 22) 3.50 ft (1.067 m) distant for 20 sec, followed by developing for 60 sec. Results of the photoresist banking tests are presented in Table VII and the recommended procedure for preparing panels using photoresist banking is detailed in Appendix C.

Table VI. Modified Splash Etcher Test Results

Specimen Number	Maskant	Etchant **	Additive **	Additive Concentration g/l	Temperature, °F	Temperature, (°K)[1]	Paddle Velocity, rpm	Time, min	Milling Rate, mil/min[2]	Depth, mils[3]	Passage Width mils[2] Masked	Passage Width mils[2] Final	Depth/ Width Ratio	Percent Side Etch	Surface Finish, rms	Etching Procedure Comments
A	Silver	RCE	Thiourea + Copper	0.26 0.26	100	(311)	1000*	120	0.24	30	12	45	0.61	55	110	Silver bent over after reaching depth of 15 mils.
B	Silver	↓	Thiourea + Copper	0.53 0.26	100	(311)	1000*	180	0.22	39	12	54	0.72	54	150	
C	Silver	↓	Thiourea	1.05	100	(317)	1000*	150	0.21	32	12	41	0.73	45	65	
D	Silver	Rotogravure	Thiourea + DMG+	1.58 0.26	110	(317)	2000	116	0.16	19	12	34	0.56	63	80	Cycled 10 min on and 2 min off
E	Silver	↓	Thiourea + DMG	1.59 0.53	110	(317)	2000	120	0.18	21	12	34	0.62	52	70	Cycled 5 min on and 2 min off
F	Silver	↓	Thiourea + DMG	1.58 0.53	110	(317)	2000	75	0.15	11	12	23	0.47	50	70	Cycled 0.5 min on and 0.25 min off
G	Silver	↓	Thiourea + DMG	1.58	90	(305)	2000	166	0.08	14	12	26	0.59	50	130	Cycled 0.75 min on and 1.33 min off
H	Silver	RCE	Potassium Sulfide	1.48	120	(322)	1900	60	0.3[illegible]	21	12	36	0.58	57	190	20 volt cathodic potential applied to nickel
I	Silver	↓	Potassium Sulfide	2.22	120	(322)	1900	60	0.44 0.50	26 30	12 22	50 62	0.52 0.48	73 67	220	138 volt cathodic potential applied to nickel
J	Silver	↓	Potassium Sulfide	2.22	120	(322)	1900	60	0.53	32	12	55	0.58	67	220	138 volt anodic potential applied to nickel

*Machined in Master Etcher Model PC-32HS.
**RCE: 42° Be $FeCl_3$
Rotogravure: 48° Be $FeCl_3$
+DMG: Dimethylglyoxime disodium salt, octahydrate
RCE: 42° $FeCl_3$ - Hunt Chemical Corp.
Rotogravure: 48° $FeCl_3$ - Hunt Chemical Corp.

[1] $K = (5/9)(F + 459.67)$
[2] $cm/min = (mils/min)(2.54 \times 10^{-3})$
[3] $cm = (mil)(2.54 \times 10^{-3})$

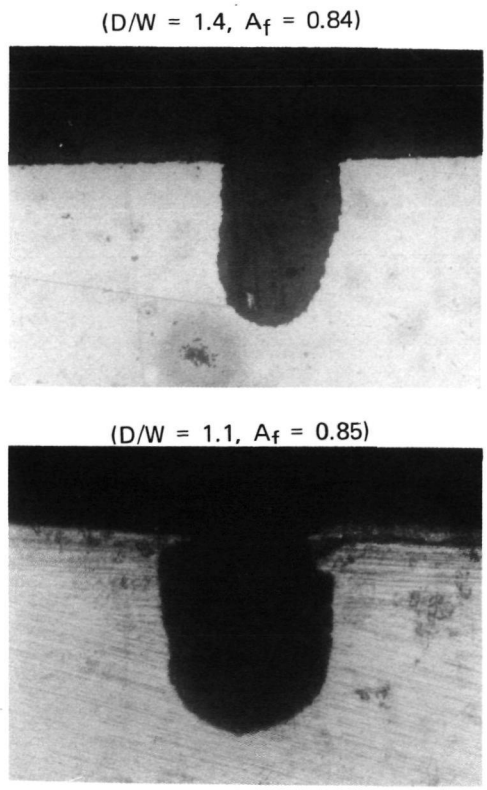

Figure 21. Photoresist Banked Passaged in Nickel-200 FD 59690

Figure 22. Printing Lamp and Vacuum Contact Printing Frame FE 81930

Table VII. Photoresist Banking Results

Specimen Number	Etchant	Initial Maskant	Banking Maskant	Time Cycle, min/No. of cycles	Total Time, min	Paddle Velocity, rpm	Temperature, °F	Temperature, (°K)[1]	Depth, mils[2]	Milling Rate,[3] mils/min	Passage Width, mils Before	Passage Width, mils After	Depth/ Width Ratio	Surface Finish, rms	Percent Side Etch
1B	48° Be $FeCl_3$ + 1.06 g/l thiourea	Silver	AZ340	15/9	135	1900	110	(317)	16	0.12	12	19	0.84	240	22
									22	0.17	22	29	2.70		16
2B		Silver	AZ340	15/13	195	1900	110	(317)	18	0.09	12	27	0.66	250	42
									24	0.12	22	38	0.63		33
3B		Silver	AZ340	15/7	105	1900	110	(317)	21	0.20	12	26	0.31	220	33
4B		Silver	AZ340	30/2	60	1900	110	(317)	20	0.33	12	30	0.67	180	45
									25	0.41	20	44	0.56		44
5B		Silver	AZ340	30/3	90	1900	110	(317)	22	0.25	12	30	0.73	190	41
									28	0.31	22	44	0.67		39
6B		Silver	AZ340	30/4	120	1900	110	(317)	26	0.22	12	31	0.84	210	37
									30	0.25	22	46	0.65		40
7B		Silver	AZ340	20/7	140	1900	110	(317)	29	0.26	12	21	1.38	160	16
									31	0.28	22	28	1.11		10
8B		Silver	AZ340	30/6	180	1900	120	(322)	26	0.14	12	28	0.93	210	31
									36	0.20	22	37	0.19		21
9B		Silver	AZ340	30/5	150	1900	120	(322)	19	0.12	12	16	1.19	200	11
									23	0.15	22	29	0.74		16
10B		Silver	AZ340	45/3	135	1900	120	(322)	22	0.17	12	29	0.76	220	40
11B		Silver	AZ340	50/3	150	1900	120	(322)	24	0.16	12	25	0.96	200	27
12B	42° Be $FeCl_3$ + 1.06 g/l thiourea	Silver	AZ340	30/4	120	1000*	120	(322)	20	0.17	12	19	1.05	120	18
13B		Silver	KAR	20/4	80	1000*	120	(322)	25	0.30	22	43	0.58	190	42
14B		Silver	AZ340	20/5	100	1000*	120	(322)	27	0.31	22	26	1.04	180	7

*Machined in Master Etcher Model PC-32HS.

[1] $K = (5/9)(F + 459.67)$

[2] $cm = (mil)(2.54 \times 10^{-3})$

[3] $cm/min + (mil/min)(2.54 \times 10^{-3})$

5. Spray Etching of Nickel 200

The experimental spray etcher shown in Figure 23 was assembled to investigate the spray etching technique. Spray nozzles provided jet streams impinging on the work piece while it revolved slowly. This system did not provide the uniform passages desired and the passage depth varied across the panel, but it was useful to compare side etch with splash etching results. Results from the experimental etcher are presented in Table VIII as samples No. 14 and 15. Comparison of these results with the splash etcher results showed little difference in side etch. The spray system did provide faster milling rates because of the increased velocity of the impinging etchant.

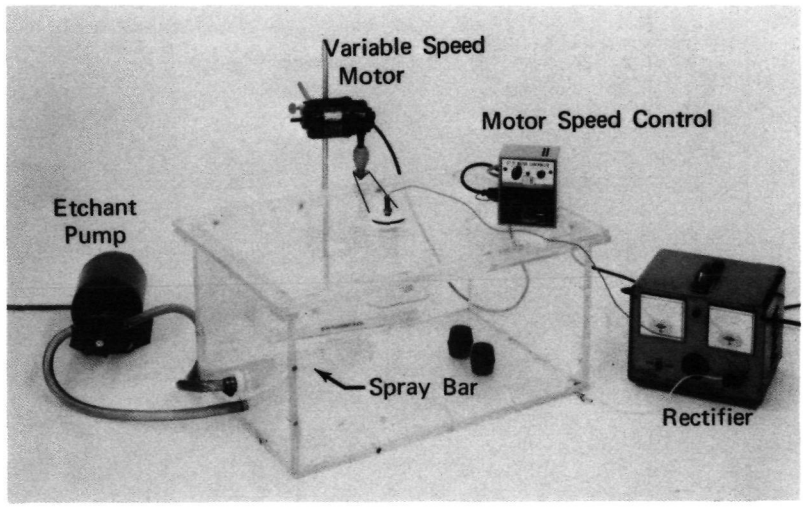

Figure 23. Experimental Spray Etcher FD 59681

Chem-Cut Corporation of State College, Pennsylvania, etched six samples with their Model 568 Spray Etcher. Two samples were etched by the Eastman Kodak Company of Rochester, New York, using a custom-built spray etcher. Results are presented in Table VIII as samples No. 1 to 8.

Table VIII. Spray Etching Results

Sample Number	Etched By	Maskant	Etchant **	Additive**	Concentration, g/l	Etchant Supply Pressure, psig[1]	Etchant Temperature, °F	Etchant Temperature, (°K) [2]	Etch Depth, mils[3]	Etch Rate,* mil/min[4]	Passage Width mils[2] Masked	Passage Width mils[2] Final	Depth/ Width Ratio	Percent Side Etch
1	Chemcut	Waycoat	RCE	-	-	37	120	(322)	28	1.00	10	51	0.74	72
2	Chemcut	Waycoat	RCE	Thiourea	1.06	37	120	(322)	29	0.90	10	49	0.59	68
3	Chemcut	Waycoat	RCE	Thiourea	2.12	37	120	(322)	23	0.50	10	50	0.46	87
4	Chemcut	Silver	RCE	-	-	37	120	(322)	28	0.98	10	51	0.74	74
5	Chemcut	Silver	RCE	Thiourea	1.06	37	120	(322)	24	0.74	10	43	0.56	65
6	Chemcut	Silver	RCE	Thiourea	2.12	37	120	(322)	21	0.44	10	40	0.53	71
7	Kodak	Silver	RCE	Thiourea	1.06	17	120	(322)	27	0.50	10	44	0.61	64
									31	0.57	20	55	0.56	57
8	Kodak	Silver	RCE	Thiourea	1.06	17	120	(322)	26	0.50	20	49	0.53	56
9	Peri	Dynachem	48° Be $FeCl_3$	-	-	***	75	(298)	29	0.31	20	54	0.54	59
10	Peri	Dynachem	48° Be $FeCl_3$	ETU	3.0	***	85	(303)	18	0.30	20	35	0.51	43
11	Peri	Dynachem	48° Be $FeCl_3$	ETU	3.0	***	85	(303)	20	0.29	20	38	0.53	45
				PF-76	2.2									
12	Peri	Dynachem	48° Be $FeCl_3$	ETU	3.0	***	75-85	(297-303)	30	0.23	20	58	0.52	63
				PF-76	2.2									
13	Peri	Dynachem	48° Be $FeCl_3$	ETU	3.0	***	85	(303)	32	0.143	20	58	0.55	59
				PF-76	2.2									
14	FRDC	Vynatop	Rotogravure	Thiourea	0.53	NA	80	(300)	47	0.79	10	58	0.81	51
15	FRDC	Vynatop	Rotogravure	Thiourea	0.53	NA	100	(311)	8	0.12	10	18	0.44	50

*Approximate

** Rotogravure: 48° $FeCl_3$ - Hunt Chemical Corp.
ETU: Ethylene Thiourea
PF-76: Monochloroacetic Acid

***See Appendix D

[1] $N/cm^2 = (psig + 14.7)\ (0.6895)$

[2] $K = (5/9)\ (F + 459.67)$

[3] $cm = (mil)\ (2.54 \times 10^{-3})$

[4] $cm/min = (mil/min)\ (2.54 \times 10^{-3})$

Side etch was calculated from passage dimensions measured by FRDC and varied from 87% to 56%.

The data indicate high etchant velocities such as provided by the spray etcher resulted in less undercutting than with splash etcher when no thiourea was added to the etchant. With thiourea concentration at optimum levels (based on the splash etcher results), the side etch was approximately the same as that attained in the splash etcher.

Commercially available spray etchers have the advantages of: (1) ability to make wide variations in etchant spray quality, (2) interchangeability of the pressure atomizing nozzles, and (3) ability to etch very large panels (limited only by width). The spray etching system also provides faster milling rates because of the greater velocity of the impinging etchant.

6. Platemakers Eductional and Research Institute (PERI)

The success of thiourea as a side etch inhibitor additive for nickel encouraged further investigation of copper techniques. Thiourea and thiourea derivatives are prime ingredients in some commercially available copper powderless etching solutions. The Platemakers Educational and Research Institute (PERI) etched several samples with thiourea derivatives; results are presented in Table VIII as samples 9 through 13. A letter report covering the work performed by PERI is presented in Appendix D. The additives investigated showed similar results as achieved at FRDC with either thiourea or potassium sulfide.

7. Electrochemical Machining

An experimental electrochemical machining etcher was constructed at FRDC to investigate the feasibility of the technique (Figure 24). It consisted of a titanium container with three spray nozzles on a spraybar. The work piece was placed in a face-down position and rotated slowly while

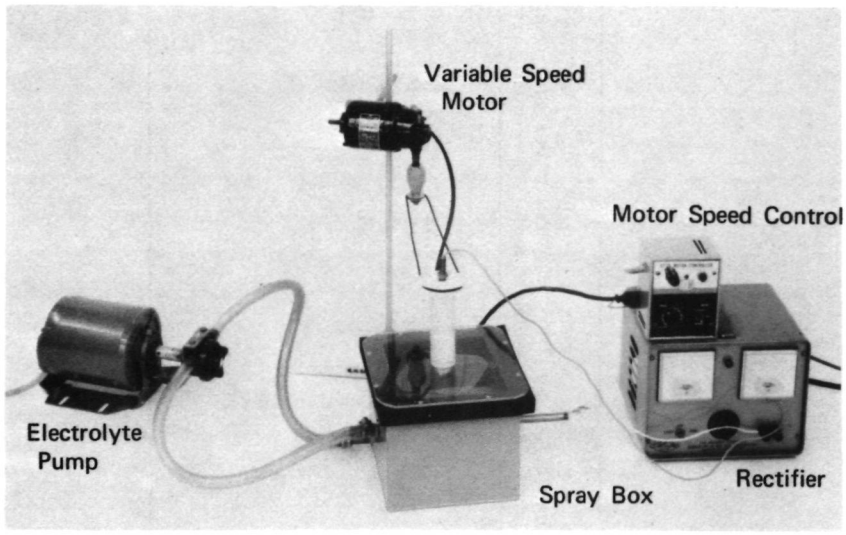

Figure 24. Experimental Electrochemical Machining Etcher FD 59692

the spray impinged upward on the plate. Electric current was supplied by 15 and 120 v rectifiers.

Three Nickel 200 samples were electrochemically machined with less than complete success; test data are listed in Table IX. The first two samples tested were quickly coated with an insoluble material and a precipitate formed in the sodium chloride electrolyte. As machining proceeded, the solution became more alkaline since:

$$Ni \longrightarrow Ni^{++} + 2e^{-} \qquad \text{(Anode reaction)}$$

and

$$2H_2O + 2e^{-} \longrightarrow 2OH^{-} + H_2 \qquad \text{(Cathode reaction)}$$

$$Ni^{++} + 2OH \longrightarrow Ni\ (OH)_2$$

The result was dissolution of nickel at the anode and production of hydroxide at the cathode. The nickel and hydroxide reacted forming insoluble nickel hydroxide in the passages being machined.

Boric acid was added to the electrolyte to control the pH by reacting with the nickel hydroxide to form water:

$$Ni(OH)_2 + 2HBO_3 \longrightarrow Ni(BO_3)_2 + 2H_2O$$

Table IX. Electrochemical Machining Results

Specimen Number	Electrolyte	Concentration g/l	Current Density[1] amps/in.[2]	Maskant	Temperature, °F	(°K)	Time, min	Depth, mil[3]	Milling Rate mil/min[4]	Passage Width mils[2] Masked	Final	Depth/ Width Ratio	Percent Side Etch	Surface Finish, rms
1	Sodium Chloride	300	10	Vynatop	80	(300)	60	9	0.15	10	29	0.31	106	500
								11	0.18	20	41	0.27	95	
2	Sodium Chloride	360	10	Vynatop	80	(300)	60	6	0.10	10	19	0.32	75	600
3	Sodium Chloride Boric Acid	120 25	10	KMER	100	(311)	10	3	0.30	10	16	0.19	100	110
4*	Hydrochloric Acid	50% by volume	10	Silver	100	(311)	15	5	0.33	10	18	0.28	80	20

*Number 4 was Inconel 625 rather than Ni 200

[1] A/cm^2 = (amps/$in.^2$) (0.1550)

[2] K = (5/9) (F + 459.67)

[3] cm = (mil) (2.54×10^{-3})

[4] cm/min = (mil/min) (2.54×10^{-3})

A much smoother surface was produced since the insoluble hydroxide did not interfere with etching.

An Inconel 625 sample was electrochemically etched in a hydrochloric acid electrolyte (Table IX, sample 4) giving a very smooth finish with 80% side etch. Inconel 625 is essentially insoluble in the ferric chloride etchant used for nickel.

Electrochemical machining with photoengraving techniques appears feasible, but more sohpisticated equipment is needed; etching was irregular and maskant failure persisted.

8. Chemical Machining of Nickel Alloys

The most promising alloy based on relative chamber weight (paragraph 1) was Inconel 706; therefore, its machinability in the same etchant used for nickel was evaluated. Results are presented in Table X. Problems were encountered in getting electroplated silver or a photoresist to adhere to the Inconel 706 surface. When adherence was achieved the Inconel 706 milled unevenly and produced an extremely rough and nonuniform surface.

The second alloy selected based on relative chamber weight was Inconel 718. Similar problems encountered with Inconel 706 were found with Inconel 718; the etched passages were rough and nonuniform, although the addition of sulfuric acid to the etchant appeared to reduce the roughness.

Both Inconel X-750 and WASPALOY were successfully etched using the techniques and solutions developed for Nickel 200. The milling rates were slightly less than for Nickel 200, and undercutting was approximately 60%, just slightly greater than for Nickel 200. Typical cross sections of the alloys are shown in Figure 25.

Table X. Nickel Alloy Etching Results

Specimen Number	Alloy	Maskant	Etchant***	Additive	Concentration, g/l	Temperature, °F	(°K)[1]	Velocity, rpm	Time, min	Depth, mils[2]	Milling Rate mils/min[3]	Passage Width, mils[2] Masked	Final	Depth/ Width Ratio	Percent Side Etch	Surface Finish, rms	Intergranular Attack
706A	Inco 706	Silver	RCE	Thiourea	1.05	120	(322)	1000*	120	12	0.12	12	27	0.44	62	320	None
706B	Inco 706	Vynatop	RCE	Thiourea	1.05	120	(322)	1000*	60	Maskant Failed							
706C	Inco 706	Silver	RCE	Thiourea	1.05	120	(322)	1000*	60	Maskant Failed							
X-1	Inco X-750	Silver	RCE	Thiourea	1.05	120	(322)	1900	210	19	0.09	10	30	0.63	55	180	None
										20	0.09	20	33	0.61	42		
X-2	Inco X-750	Silver	RCE	Thiourea	1.05	120	(322)	1000*	120	18	0.15	12	34	0.53	61	160	None
										20	0.16	22	42	7.48	50		
X-3	Inco X-750	Silver	RCE	Thiourea	1.05	120	(322)	1000*	90	29	0.32	12	57	0.51	78	120	None
										34	0.38	22	68	0.50	68		
X-4	Inco X-750	Silver	RCE	Thiourea	1.05	120	(322)	1000*	90	16	0.18	9	30	0.13	66	140	None
W-1	Waspaloy	Silver	RCE	Thiourea	1.05	120	(322)	1900	150	27	0.18	10	38	0.71	51	150	None
										29	0.18	20	50	0.58	52		
W-2	Waspaloy	Silver	RCE	Thiourea	1.05	120	(322)	1000*	120	15	0.12	12	29	0.52			
W-3	Waspaloy	Silver	RCE	Thiourea	1.05	120	(322)	1000*	90	18	0.20	14	38	0.17	66	160	None
W-4	Waspaloy	Silver	RCE	Thiourea	1.05	120	(322)	1000*	90	23	0.25	10	35	0.66	55	130	None
										26	0.28	20	45	0.58	49		
W-5	Waspaloy	Silver	RCE	Thiourea	1.05	120	(322)	1000*	90	23	0.25	10	36	0.64	57	110	None
										26	0.27	20	45	0.58	48		
N-1	Nickel 201	Silver	Rotogravure	Thiourea	1.05	110	(317)	1425	120	25	0.21	12	36	0.69	48	80	None
N-2	Nickel 270	Silver	Rotogravure	Thiourea	1.05	110	(317)	1425	120	28	0.23	12	48	0.70	50	60	None
I-1	Inco 600	Silver	Rotogravure	Thiourea	1.05	110	(317)	1425	120	29	0.24	12	41	0.59	50	90	None
I-2	Inco 625	Silver	Rotogravure	Thiourea	1.05	110	(317)	1425	120	0	0.00	-	-	-	-	-	
I-3	Inco 718	Silver	Rotogravure	Thiourea	1.05	110	(317)	1425	120	12	0.10	-	-	-	-	1000	
I-4	Inco 718	Silver	RCE	Thiourea	1.05	120	(317)	1900	120	25	0.21	12	52	0.98	75	880	

*Machined in master etcher model PC-32HS
**Concentration units ml/l.
***RCE: 42° Be ferric chloride, Rapid Circuit Etch, Hunt Chemical Corp.
Rotogravure: 48° Be ferric chloride, Hunt Chemical Corp.

[1] $K = (5/9)(F + 459.67)$
[2] $cm = (mil)(2.54 \times 10^{-3})$
[3] $cm/min = (mils/min)(2.54 \times 10^{-3})$

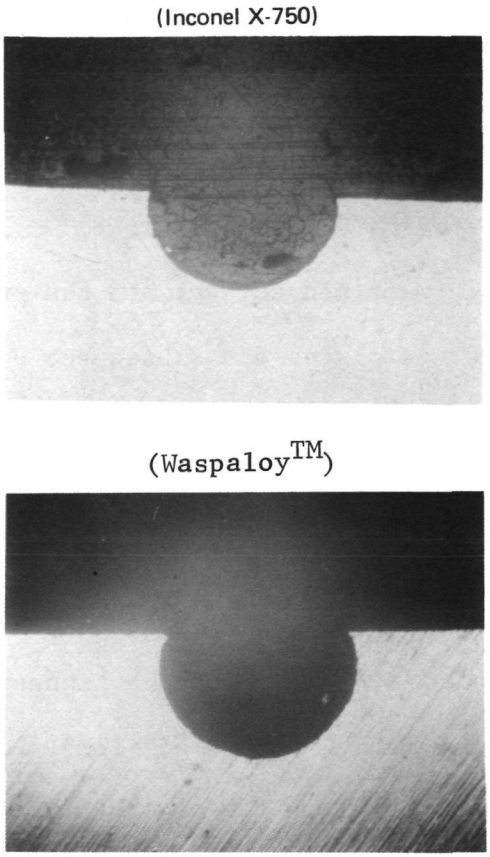

Figure 25. Section Views of Chemically Machined Inconel X-750 and Waspalloy FD 59693

Inconel 600 was chemically machined with good results using the procedures outlined for Nickel 200. Inconel 625 was not noticeably etched by the ferric chloride etchant and the pure nickels, Nickel 201 and Nickel 270, were machined with essentially the same results as for Nickel 200.

All the chemically machined alloys were inspected for intergranular attack by metallurgical examination of cross sections at 500X. No measurable intergranular attack was detected.

COOLANT PASSAGE EVALUATION

A. GENERAL

Under this phase of the program 6 in. x 6 in. (15.2 cm x 15.2 cm) plates were chemically machined to evaluate the process discussed in Section IV and to provide plates for subsequent bonding and structural testing. Several combinations of passage width, passage depth, and land width were etched in Nickel-200 plates and Inconel X-750 plates. Improvements in the chemical machining process were made throughout the manufacture of the plates.

Inconel X-750 and WASPALOY™ were the highest strength alloys that etched in a manner comparable to that of Nickel 200 during the Task I studies. Although use of either alloy would provide the same relative chamber weight, Inconel X-750 was selected for additional investigations because of its lower cost and greater availability.

Selected plates were brazed together to form four sample Thermal Skin panels. These panels served to verify the bonding procedure and were used to perform bend tests to determine passage deformation caused by forming Thermal Skin panels. The bend testing gave an early indication of the bond integrity and the results are discussed in this section.

The remaining plates were used to make sample panels for additional structural testing discussed in Section VI. Plate fabrication, bonding, and bend testing are discussed below.

B. PLATE FABRICATION

A total of 51 plates were manufactured, 30 of Nickel 200 and 21 of Inconel X-750. Inspection data for the plates are given in Tables XI and XII. The values listed in the tables are the mean values of nine

Table XI. Dimensional Data for Chemically Machined Nickel-200 Plates

Part No. DKJ	Serial No.	Design Dimensions: Land Width, in.	Design Dimensions: Passage Width, in.	Design Dimensions: Passage Depth, in.	Design Dimensions: Plate Thickness, in.	Measured Dimensions: Land Width, * in.	Measured Dimensions: Passage Width, ** in.	Measured Dimensions: Passage Depth, ** in.	Measured Dimensions: Plate Thickness, in.	Measured Dimensions: Surface Finish, rms	Calculated Data: Side Etch, %	Calculated Data: Area Factor, Area/DXW	Photoresist Used***	Planned Test Use, Task No.	Comments
5659	1	0.020	0.030	0.030	0.050	0.010 +0.005 -0.009	0.040 +0.009 -0.005	0.027 +0.002 -0.002	0.050 - 0.054		36.1 +17.7 - 7.2	0.81 +0.05 -0.16	Waycoat PF	-	Banked using Shipley's AZ 340 positive photoresist, 4 cycles.
5659	2	0.020	0.030	0.030	0.050	0.006 +0.002 -0.003	0.044 +0.003 -0.002	0.023 +0.000 -0.002	0.050 - 0.052	-	53.6 + 4.4 - 4.1	0.77 +0.07 -0.00	Waycoat PF	-	
5660	1	0.030	0.030	0.030	0.050	0.019 +0.007 -0.007	0.041 +0.007 -0.007	0.032 +0.005 -0.002	0.062 - 0.063	-	33.3 + 2.6 -11.0	0.71 +0.11 -0.01	Shipley's AZ-340	III-2	Positive photoresist banking technique employed.
5660	2	0.030	0.030	0.030	0.050	0.016 +0.006 -0.006	0.044 +0.006 -0.006	0.033 +0.002 -0.002	0.060 - 0.061	-	36.2 + 8.9 - 7.6	0.83 +0.01 -0.09	Waycoat PF	-	Positive photoresist banking technique employed.
5660	3	0.030	0.030	0.030	0.050	0.021 +0.005 -0.001	0.039 +0.001 -0.005	0.028 +0.003 -0.002	0.061	-	33.0 + 1.7 - 5.0	0.57 +0.25 -0.08	Waycoat PF	-	Positive photoresist banking technique employed.
5661	1	0.030	0.060	0.030	0.050	0.021 +0.004 -0.002	0.069 +0.002 -0.004	0.030 +0.002 -0.002	0.047 - 0.048	-	63.8 + 1.1 - 3.9	0.87 +0.00 -0.10	Shipley's AZ-340	-	Land defects resulting from resist failure, excessive resist touch-up required during etching.
5661	2	0.030	0.060	0.030	0.050	0.022 +0.005 -0.003	0.068 +0.003 -0.005	0.029 +0.003 -0.002	0.044 - 0.048	200	65.4 + 0.7 - 5.0	0.80 +0.09 -0.05	Shipley's AZ-340	II-2	Same as DKJ-5661 Serial No. 1.
5661	3	0.030	0.060	0.030	0.050	0.021 +0.003 -0.004	0.069 +0.004 -0.003	0.031 +0.001 -0.002	0.046 - 0.048	200	63.7 + 4.3 - 3.0	0.84 +0.03 -0.03	Shipley's AZ-340	II-2	Same as DKJ-5661 Serial No. 1.
5661	4	0.030	0.060	0.030	0.050	0.021 +0.003 -0.003	0.069 +0.003 -0.003	0.030 +0.002 -0.001	0.047 - 0.048	-	63.9 + 2.2 - 1.8	0.81 +0.01 -0.05	Shipley's AZ-340	III-2	Resist touch-up required but minimum number of land defects occurred.
5661	5	0.030	0.060	0.030	0.050	0.024 +0.004 -0.008	0.066 +0.008 -0.004	0.033 +0.006 -0.005	0.060 - 0.061		54.8 - 7.7 - 0.6	0.70 +0.19 -0.00	Waycoat PF	III-4	No resist touch-up required.
5661	6	0.030	0.060	0.030	0.050	0.020 +0.006 -0.003	0.070 +0.003 -0.006	0.034 +0.006 -0.006	0.062 - 0.063	180	59.2 - 1.9 - 5.3	0.66 +0.20 -0.00	Waycoat PF	III-4	No resist touch-up required.
5661	7	0.030	0.060	0.030	0.050	0.024 +0.002 -0.001	0.066 +0.001 -0.002	0.034 +0.002 -0.005	0.060 - 0.062	220	52.8 - 6.8 - 2.8	0.77 +0.03 -0.06	Waycoat PF	III-4	No resist touch-up required.
5662	1	0.030	0.090	0.030	0.050	0.024 +0.002 -0.003	0.096 -0.003 -0.002	0.028 +0.008 -0.004	0.045 - 0.048	200	63.2 - 5.8 - 9.5	0.77 +0.09 -0.00	Shipley's AZ-340	III-5	Resist touch-up required.
5662	2	0.030	0.090	0.030	0.050	0.028 +0.002 -0.003	0.092 -0.003 -0.002	0.030 +0.004 -0.002	0.045 - 0.046	200	53.1 + 2.7 - 3.0	0.84 +0.02 -0.05	Shipley's AZ-340	III-2	Resist touch-up required.
5662	3	0.030	0.090	0.030	0.050	0.022 +0.003 -0.004	0.098 +0.004 -0.003	0.029 +0.003 -0.002	0.044 - 0.046	150	66.5 + 3.2 - 4.2	0.87 +0.00 -0.05	Shipley's AZ-340	III-5	Resist touch-up required.
5662	4	0.030	0.090	0.030	0.050	0.039 +0.001 -0.001	0.081 +0.001 -0.001	0.024 +0.002 -0.001	0.046 - 0.047	160	42.4 + 3.3 -10.2	0.85 +0.03 -0.07	Shipley's AZ-340	-	Resist touch-up required.
5662	5	0.030	0.090	0.030	0.050	0.028 +0.002 -0.002	0.092 +0.002 -0.002	0.031 +0.001 -0.003	0.060 - 0.061	190	52.0 + 2.4 - 1.5	0.76 +0.12 -0.06	Waycoat PF	-	No resist touch-up required.
5662	6	0.030	0.090	0.030	0.050	0.036 +0.001 -0.003	0.084 +0.003 -0.001	0.027 +0.003 -0.001	0.060 - 0.061	200	44.7 + 1.4 - 0.7	0.86 +0.02 -0.10	Waycoat PF	-	No resist touch-up required.
5662	7	0.030	0.090	0.030	0.050	0.033 +0.003 -0.005	0.087 +0.005 -0.003	0.034 -0.004 -0.005	0.060 - 0.061	170	39.8 - 5.6 - 0.0	0.82 -0.17 -0.01	Waycoat PF	-	No resist touch-up required.
5663	1	0.030	0.060	0.040	0.050	0.034 +0.008 -0.005	0.056 +0.005 -0.008	0.036 -0.003 -0.006	0.062 - 0.063	150	49.8 - 3.9 - 3.1	0.83 -0.05 -0.05	Waycoat PF	II-2	No resist touch-up required.
5663	2	0.030	0.060	0.040	0.050	0.029 +0.005 -0.008	0.061 +0.008 -0.005	0.036 -0.009 -0.003	0.060 - 0.062	130	58.1 - 5.0 - 4.7	0.77 +0.04 -0.03	Waycoat PF	-	No resist touch-up required.
5663	3	0.030	0.060	0.040	0.050	0.035 -0.004 -0.007	0.055 +0.007 -0.004	0.033 +0.007 -0.002	0.060 - 0.061	-	52.9 - 4.2 - 3.1	0.81 +0.04 -0.01	Waycoat PF	-	No resist touch-up required.
5663	4	0.030	0.060	0.040	0.050	0.032 +0.002 -0.010	0.058 -0.010 -0.002	0.033 +0.011 -0.001	0.060 - 0.061	150	57.3 - 0.0 - 6.5	0.81 +0.03 -0.02	Waycoat PF	II-2	No resist touch-up required.
5664	1	0.030	0.060	0.020	0.035	0.027 +0.003 -0.003	0.063 -0.003 -0.003	0.018 +0.002 -0.000	0.037 - 0.039	180	63.6 - 4.5 - 7.0	0.84 +0.08 -0.02	Shipley's AZ-340	-	Resist touch-up required.
6427	1	0.010	0.030	0.010	0.060	0.012 +0.002 -0.001	0.028 -0.001 -0.002	0.009 +0.001 -0.000	0.062 - 0.063	260	40.0 +10.0 - 4.3	0.81 +0.02 -0.12	Waycoat PF	III-3	No resist touch-up required.
6428	1	0.020	0.030	0.010	0.060	0.021 -0.001 -0.001	0.029 +0.001 -0.001	0.011 +0.001 -0.001	0.061 - 0.062	310	40.0 -10.0 - 1.0	0.91 +0.06 -0.16	Waycoat PF	III-3	No resist touch-up required.
6429	1	0.030	0.030	0.010	0.060	0.030 +0.001 -0.001	0.030 +0.001 -0.001	0.011 +0.001 -0.000	0.061 - 0.062	260	44.4 - 5.6 - 5.5	0.85 +0.02 -0.42	Waycoat PF	III-3	No resist touch-up required.
6477	1	0.030	0.060	0.020	0.050	0.033 +0.006 -0.002	0.057 -0.002 -0.006	0.019 +0.002 -0.001	0.061 - 0.062	210	43.5 - 5.0 -14.1	0.66 +0.17 -0.00	Waycoat PF	II-2	Banked using Shipley's AZ 340 positive photoresist, 1 cycle after 0.010-in. depth.
6477	2	0.030	0.060	0.020	0.050	0.018 +0.004 -0.001	0.072 -0.001 -0.004	0.023 +0.000 -0.002	0.060 - 0.061	-	70.8 - 1.9 - 5.6	0.77 -0.05 -0.06	Waycoat PF	-	
6477	3	0.030	0.060	0.020	0.050	0.027 +0.006 -0.001	0.063 +0.001 -0.006	0.021 +0.000 -0.001	0.047 - 0.049	160	53.6 - 5.4 -11.1	0.80 -0.02 -0.01	Waycoat PF	II-2	

*Calculated based on "master" dimensions and measured passage width.
**Dimensions determined from RTV photo-inspection technique.
***All plates were silver plated before applying the photoresist. Nitric acid was used to print the silver plate when Shipley's AZ-340 resist was used; for Waycoat resist, phosphoric acid de-plating was used.

1 cm = (in) (2.540)

Table XII. Dimensional Data for Chemically Machined Inconel X-750 Plates

Part No. DKJ	Serial No.	Design Dimensions: Land Width, in.	Design Dimensions: Passage Width, in.	Design Dimensions: Passage Depth, in.	Design Dimensions: Plate Thickness, in.	Measured Dimensions*: Land Width, * in.	Measured Dimensions*: Passage Width, ** in.	Measured Dimensions*: Passage Depth, ** in.	Measured Dimensions*: Plate Thickness, in.	Calculated Data: Surface Finish, rms	Calculated Data: Side Etch, %	Calculated Data: Area Factor, Area/DXW	Photoresist Used ***	Planned Test Use, Task No.	Comments
6478	1	0.030	0.060	0.030	0.060	0.022 +0.000 -0.003	0.068 +0.003 -0.000	0.032 +0.002 -0.003	0.057 - 0.058	-	60.0 + 5.9 - 0.0	0.79 +0.002 -0.05	Waycoat PF	II-2	Banked using Shipley's AZ 340 positive photoresist, 2 cycles.
6478	2	0.030	0.060	0.030	0.060	0.020 +0.006 -0.005	0.070 +0.005 -0.006	0.032 +0.001 -0.002	0.057 - 0.058	-	62.4 + 4.5 - 5.8	0.76 +0.06 -0.01	Waycoat PF	II-2	Banked using Shipley's AZ 340 positive photoresist, 2 cycles.
6479	1	0.030	0.090	0.030	0.060	0.018 +0.003 -0.003	0.102 +0.003 -0.003	0.034 +0.001 -0.003	0.056 - 0.058	170	61.7 + 4.5 - 0.8	0.77 +0.04 -0.001	Waycoat PF	-	Not banked.
6479	2	0.030	0.090	0.030	0.060	0.039 +0.005 -0.001	0.081 +0.001 -0.005	0.029 +0.001 -0.007	0.056 - 0.057	230	37.2 +10.5 - 5.6	0.76 +0.07 -0.03	Waycoat PF	III-5	Positive photoresist banked after etching 0.010-in. deep to compensate for slightly increased percent side etch. Base of passage exposed by scraping with a sharp tool.
6479	3	0.030	0.090	0.030	0.060	0.040 +0.006 -0.002	0.080 +0.002 -0.006	0.027 +0.005 -0.004	0.057 - 0.058	180	37.1 + 5.2 -11.2	0.81 +0.08 -0.05	Waycoat PF	III-5	Same as Serial No. 2
6479	4	0.030	0.090	0.030	0.060	0.011 +0.003 -0.003	0.109 +0.003 -0.003	0.031 +0.001 -0.001	0.056 - 0.058	200	79.0 + 2.4 - 1.5	0.82 +0.05 -0.04	Waycoat PF	-	Not banked.
6479	5	0.030	0.090	0.030	0.060	0.036 +0.002 -0.006	0.084 +0.006 -0.002	0.031 +0.003 -0.002	0.057 - 0.058	-	38.9 + 0.5 - 6.6	0.81 +0.06 -0.15	Waycoat PF	-	Banked using Shipley's AZ 340 positive photoresist, 2 cycles.
6480	1	0.030	0.060	0.040	0.060	0.028 +0.006 -0.005	0.062 +0.005 -0.006	0.043 +0.006 -0.005	0.057 - 0.058	-	48.8 +12.2 -10.3	0.86 +0.07 -0.15	Waycoat PF	III-4	Positive photoresist banked after etching 0.010-in. deep to compensate for slightly increased percent side etch. Base of passages exposed by scraping with a sharp tool.
6480	2	0.030	0.060	0.040	0.060	0.014 +0.003 -0.004	0.076 +0.004 -0.003	0.035 +0.002 -0.003	0.057 - 0.058	230	75.5 + 8.8 - 0.0	0.79 +0.07 -0.04	Waycoat PF	II-2	Excess undercutting believed to be a result of spent etchant.
6480	3	0.030	0.060	0.040	0.060	0.010 +0.005 -0.013	0.080 +0.013 -0.005	0.041 +0.002 -0.002	0.057 - 0.058	-	72.5 + 4.6 - 6.2	0.78 +0.01 -0.05	Waycoat PF	-	Banked using Shipley's AZ 340 positive photoresist, 3 cycles, land quality decreased appreciably from 0.030 to 0.040-in. depth.
6480	4	0.030	0.060	0.040	0.060	0.018 +0.011 -0.002	0.072 +0.002 -0.011	0.040 +0.004 -0.005	0.057 - 0.058	-	65.1 + 0.7 -11.4	0.78 +0.11 -0.03	Waycoat PF	-	
6480	5	0.030	0.060	0.040	0.060	0.009 +0.007 -0.009	0.081 +0.009 -0.007	0.037 +0.004 -0.003	0.057 - 0.058	-	82.2 + 2.7 - 2.4	0.77 +0.03 -0.07	Waycoat PF	-	
6480	6	0.030	0.060	0.040	0.060	0.026 +0.009 -0.004	0.064 +0.004 -0.004	0.034 +0.002 -0.002	0.057 - 0.058	200	64.4 + 2.8 - 8.2	0.74 +0.03 -0.00	Waycoat PF	II-2	
6481	1	0.030	0.060	0.020	0.060	0.025 +0.005 -0.003	0.065 +0.003 -0.005	0.021 +0.003 -0.001	0.057 - 0.058	150	58.3 +16.0 - 8.3	0.76 +0.03 -0.00	Waycoat PF	III-4	Not banked.
6481	2	0.030	0.060	0.020	0.060	0.026 +0.003 -0.003	0.064 +0.003 -0.003	0.019 +0.002 -0.000	0.057 - 0.058	210	61.3 + 8.7 - 8.0	0.78 +0.10 -0.05	Waycoat PF	II-2	Banked using Shipley AZ 340 positive photoresist, 1 cycle after 0.010-in. deep.
6481	3	0.030	0.060	0.020	0.060	0.030 +0.007 -0.003	0.060 +0.003 -0.007	0.021 +0.000 -0.001	0.057 - 0.058	260	39.0 +17.1 - 0.6	0.69 +0.18 -0.00	Waycoat PF	II-2	
6482	1	0.030	0.030	0.010	0.060	0.029 +0.002 -0.006	0.031 +0.006 -0.002	0.011 +0.002 -0.001	0.056 - 0.058	210	50.0 +18.8 - 4.5	0.79 +0.06 -0.12	Waycoat PF	III-3	Not banked.
6483	1	0.020	0.030	0.010	0.060	0.013 +0.002 -0.001	0.037 +0.001 -0.002	0.014 +0.000 -0.000	0.056 - 0.057	190	58.9 + 4.1 - 3.3	0.84 +0.04 -0.24	Waycoat PF	III-3	Banked using Nicrocoat Binder **** after etching 0.003-in. deep to compensate for slightly increased percent side etch. Base of passages exposed by scraping with a sharp tool.
6484	1	0.010	0.030	0.010	0.060	0.014 +0.001 -0.003	0.026 +0.003 -0.001	0.009 +0.003 -0.001	0.056 - 0.058	-	33.3 +11.1 - 5.5	0.81 +0.08 -0.09	Waycoat PF	-	Same as DKJ-6483 Serial No. 1.
6484	2	0.010	0.030	0.010	0.060	0.008 +0.001 -0.002	0.032 +0.002 -0.001	0.010 +0.002 -0.000	0.057 - 0.058	280	60.0 + 5.0 -10.0	0.81 +0.13 -0.14	Waycoat PF	III-3	Not banked.
6484	3	0.010	0.030	0.010	0.060	0.007 +0.002 -0.001	0.033 +0.001 -0.002	0.011 +0.000 -0.001	0.057 - 0.058	-	61.6 + 4.0 - 8.5	0.85 +0.09 -0.16	Waycoat PF	-	Not banked.
6485	1	Flat Plate			0.060				0.057 - 0.058	20				III-2	
6485	2	Flat Plate			0.060				0.057 - 0.058	20				III-2	
6485	3	Flat Plate			0.060				0.057 - 0.058	20				III-4	
6485	4	Flat Plate			0.060				0.057 - 0.058	20				III-2	

*Calculated based on "master" dimensions and measured passage width.
**Dimensions determined from RTV photo-inspection technique.
***All etched plates were silver plated before applying the photoresist; phosphoric acid deplating was used to print the silver plate.
****Nicrocoat Binder (available from Wall Calmonoy Corp., Detroit, Michigan) is similar in behavior to shelac except very fast drying.

1 cm = (in) (2.540)

measurements from a given plate, (Figure 26), with the tolerance for each based on the maximum and minimum of the nine values. Plates were inspected by making an impression of the cooling passages with nonadhering room temperature vulcanizing (RTV) rubber. After curing, the RTV molding was peeled from the etched plate and sectioned. The molding cross-sections were then photographed at approximately 20X enlargement, and dimensions taken from the 20X photograph. The photographs showed an exact replica of the plate cross-section and therefore any undercutting could readily be evaluated.

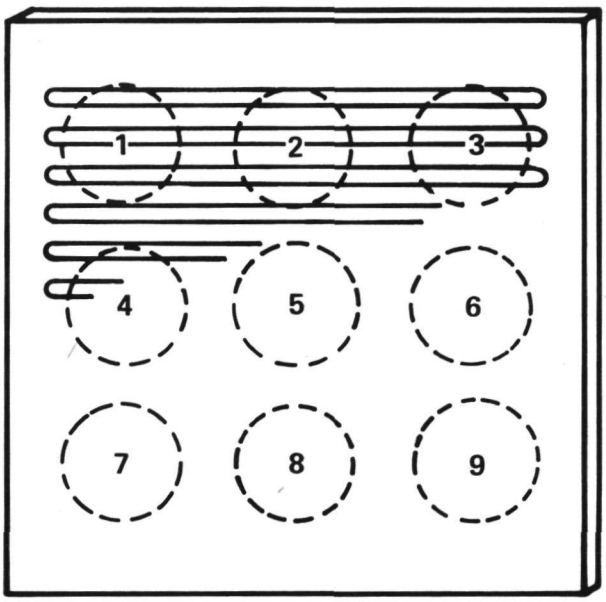

Figure 26. Plate Inspection Locations FD 40053

A basic objective was to characterize the passages obtained by etching and little effort was given to attaining exact design dimensions. The results are most meaningful in terms of tolerances or dimensional variations from passage to passage.

C. CHEMICAL MACHINING PROCEDURES

The initial chemical machining procedure used was to electroplate 0.001 in. (0.00254 cm) thick silver onto the surface to be etched. The etch pattern was then printed on the plate using Shipley's AZ 340 photoresist and the silver etched using nitric acid. Hunt's RCE ferric chloride etchant with 1.0 g/l thiourea added to reduce side etch was then used to etch the nickel. Defects occurred along the lands and excessive hand touch-up of the pattern before etching the nickel was required. It was recognized that the photoresist was deteriorating during the long etch cycle and that pin holes in the silver would result in a pitted lands.

A more durable resist, Waycoat PF photoresist, was found to withstand the long etch cycles and to virtually eliminate the pitting problem.

The need for using silver plate as a resist was reconsidered. Representative cross-sectional sketches of etched passages using Vyna-Top resist, a very sturdy resist, with and without silver are depicted in Figure 27. The use of silver resist produced 10% to 20% less side etch than when the resist alone was used. Also, the passage edges were more uniform when silver was used because often the undercut resist would break off during etching. The advantage of the silver increased with greater depths.

Passage dimensions were found to vary with the local thickness of the silver resist. The silver tended to be thicker at the four corners of the plate which is characteristic of electroplated metals. When the patterns were etched in the plating using nitric acid, greater undercutting of the electroplated silver occurred in the center (i.e., silver undercutting would progress in the center of the plate while excess

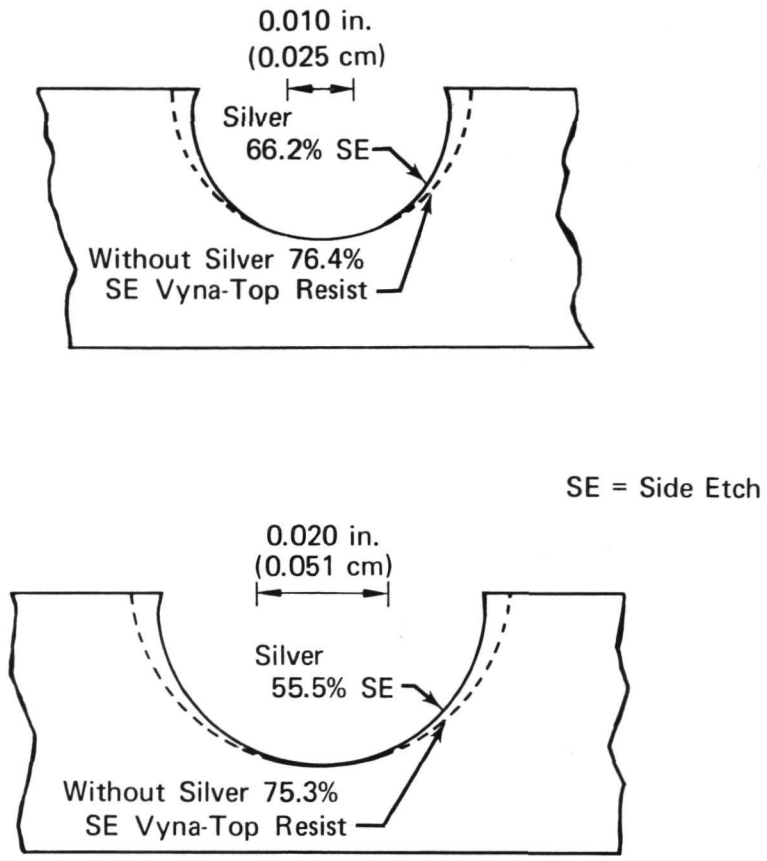

Figure 27. Comparison Between Silverplate and Conventional Resist FD 38703A

silver was being removed at the four corners). This problem was reduced by developing special shielding during plating to obtain uniform silver thickness.

Various methods of removing the silver were investigated. A phosphoric acid plating bath eventually proved to be the fastest, most reliable method while not damaging the resist coating or nickel surfaces. The silver was deplated from the exposed areas by using reverse current in the plating bath. An important advantage of the deplating procedure was that the nickel was not attacked after the silver was removed; therefore, the plate could be stripped and reused any time before actually going into the etcher.

Wide dimensional variations in the etched plates were found to be related to a patterning characteristic of the splash etcher, which produced greater etching near the center of rotation of the work piece holder. Rotating the plates 90 degrees (1.47 rad.) at the same holder radius after each 15 minute etching period was found to minimize variations. This technique was applied when etching the Inconel plates and resulted in reduced tolerances as compared to those for the nickel plates. The powderless etching technique incorporating the advances established during the program is detailed in Appendix B.

Attempts to reduce undercutting by positive photoresist banking resulted in wide variations in dimensions. This was believed to be related to nonuniform removal of the resist and no solution was found to eliminate the large tolerances. The procedure used for positive photoresist banking chemical machining is presented in Appendix C.

D. PLATE BONDING AND BEND TESTS

Four pairs of mating Nickel 200 and Inconel X-750 plates were silver brazed in a vacuum retort to form Thermal Skin® panels. For brazing, the Inconel plate was electroplated with 0.0002 to 0.0005 in. (0.0005 to 0.0013 cm) thick nickel and then 0.0002 to 0.0004 in. (0.0005 to 0.0010 cm) thick silver. The electroplated silver became the braze filler. The retort was equipped with a thin, stainless steel cover so that atmospheric pressure provided plate loading. A vacuum of 100 to 400 microns (0.0001 to 0.0004 cm) Hg was maintained throughout the braze cycle, and a braze temperature of 1825° to 1850°F (1269 to 1283°K) for 10 to 12 minutes was used. A typical temperature vs time plot for the braze cycle is shown in Figure 28.

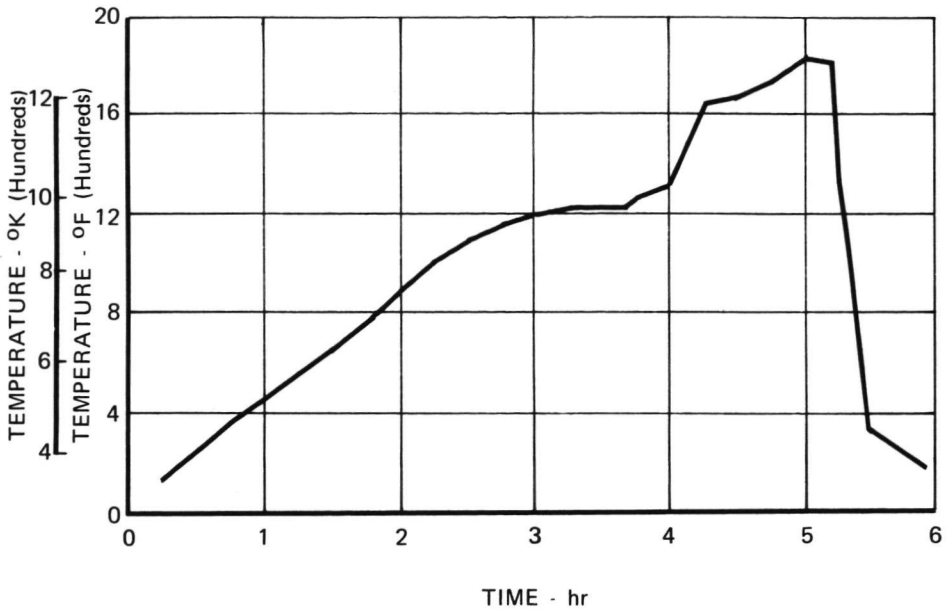

Figure 28. Typical Braze Temperature Cycle FD 59696

Three of the brazed panels were sectioned to evaluate the bonds attained and to yield nine bend test specimens with the sectioning planes parallel to the coolant passages. The fourth panel was sectioned to yield three bend test specimens with the sectioning planes perpendicular to the coolant passages. Figure 29 illustrates the two types of bend specimens.

The bend tests were performed to further test the braze bond and to determine passage deformation during forming. The test equipment used (Figure 30) met the guided bend testing requirements of the ASTM "Standard Method for Guided Bend Test for Ductility of Welds" (Standard EL90-64). Three dies were used during bending to provide three different bend radii (0.328, 0.828, and 1.328 in.) (0.833, 2.103, and 3.373 cm).

Results of the bend tests are presented in Table XIII. Passage area measurements from representative unbent samples were compared to those from the bent samples to determine bent-to-unbent area reduction factors.

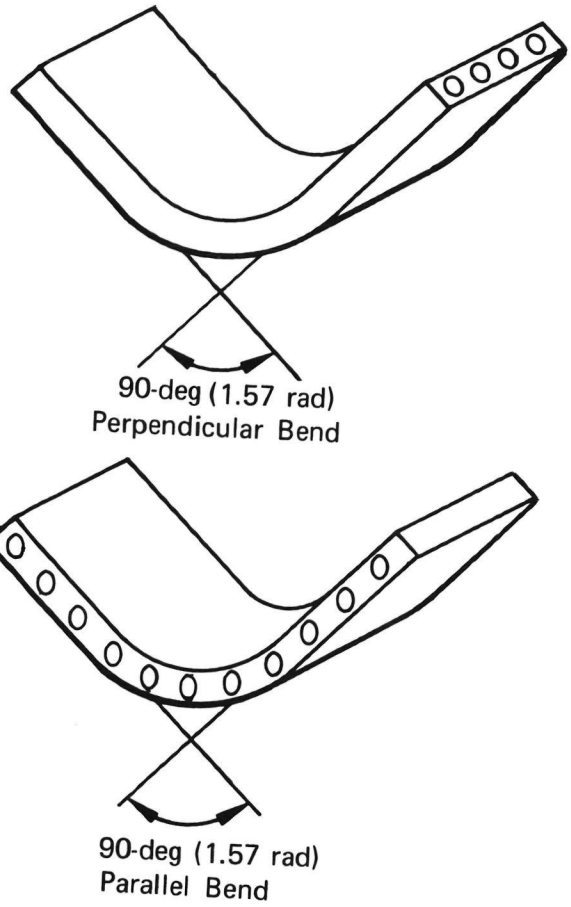

Figure 29. Schematic of Perpendicular and Parallel Bend Specimens FD 43803A

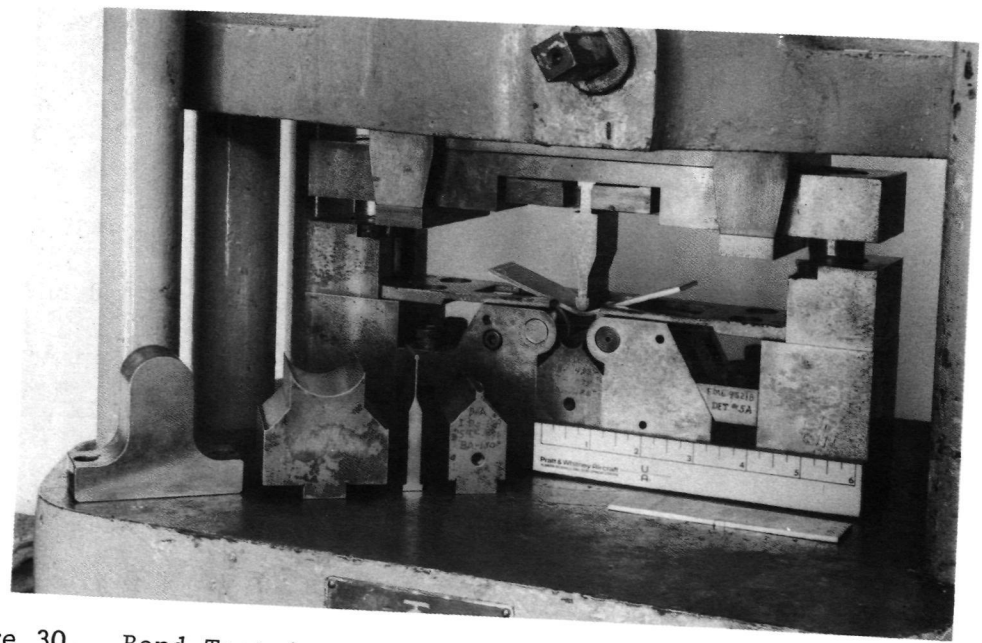

Figure 30. Bend Test Apparatus FC 18070

Table XIII. Bend Test Results

Test No.	Part No.		Type Bend	Bend Radius*	Nickel Plate Contact	Bent-to-Unbent Passage Area,%
	Nickel Plate	Inconel X-750 Plate				
1				A	Die	82.6
2	DKJ-5661-2	DKJ-6478-1	Perpendicular	B	Die	100.8
3				C	Die	98.8
4				A	Punch	90.3
5	DKJ-5663-1	DKJ-6480-2	Parallel	B	Punch	102.2
6				A	Punch	84.5
7	DKJ-5661-3	DKJ-6480-2	Parallel	B	Punch	102.0
8				C		95.5
9	DKJ-5663-4	DKJ-6480-6	Parallel	A	Punch	87.1

* Bend Radii:

Sample	Punch, in. (cm)	Die, in. (cm)
A	0.328 (0.833)	0.500 (1.270)
B	0.828 (2.103)	1.000 (2.540)
C	1.328 (3.373)	1.500 (3.810)

The perpendicular type bend samples showed little passage distortion (Figure 31), but noticeable passage distortion occurred in the parallel bend samples at 0.328 in (0.833 cm) bend radius (see Figure 32). Deformation of the passages was detectable in some of the 0.828 and 1.328 in (2.103 and 3.373 cm) radius bends, but little or no change in area occurred. No bond damage caused by forming was observed.

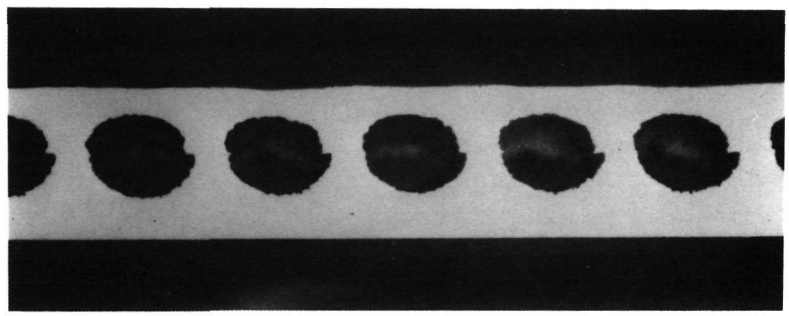

a. Test No. 1, Bend Radius = 0.328 in. (0.833 cm)

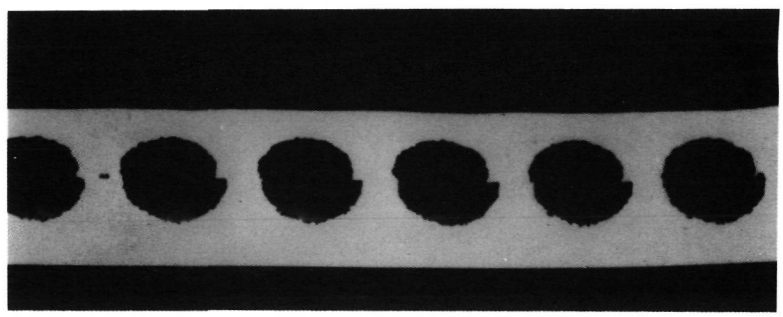

b. Test No. 2, Bend Radius - 0.828 in. (2.103 cm)

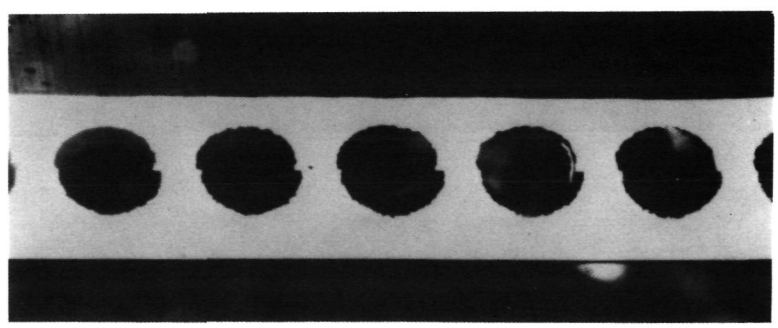

c. Test No. 3, Bend Radius = 1.328 in. (3.373 cm)

Figure 31. Perpendicular Bend Test Samples FD 43815

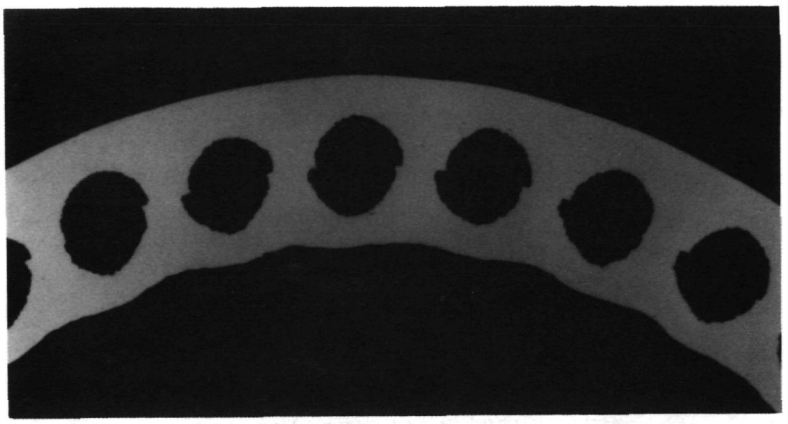

a. Test No. 10, Bend Radius = 0.328 in. (0.833 cm)

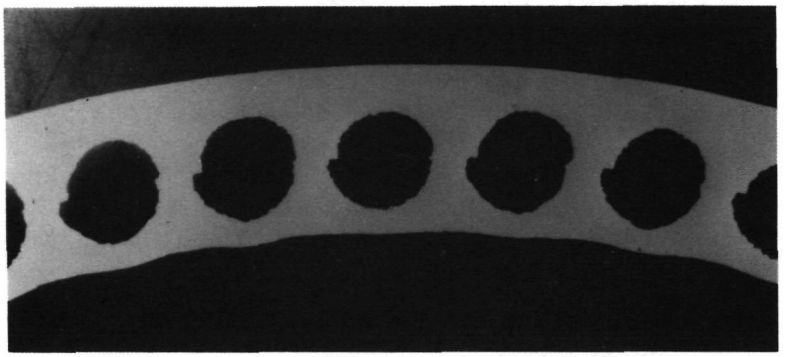

b. Test No. 11, Bend Radius - 0.828 in. (2.103 cm)

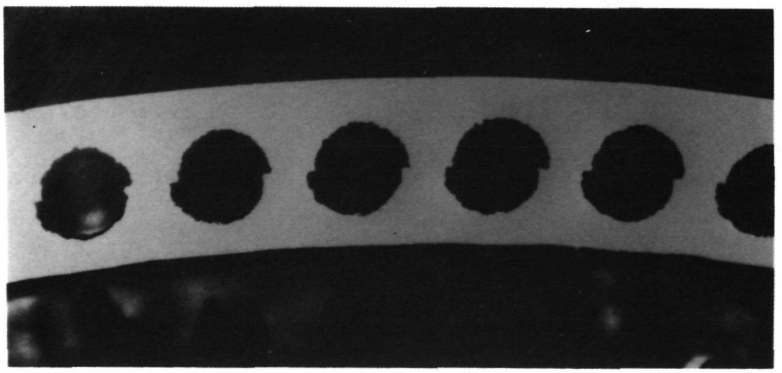

c. Test No. 12, Bend Radius = 1.328 in. (3.373 cm)

Figure 32. Parallel Bend Test Samples FD 43804

THERMAL SKIN® STRENGTH EVALUATIONS

A. GENERAL

Thermal Skin samples were prepared using etched plates described in Section V, Tables XI and XII by silver brazing. The brazed samples were used to perform coolant passage hoop strength tests, braze bond strength tests. Thermal cycle life testing was also performed but the results were inconsistent. The structural test results are presented on the following pages.

B. COOLANT PASSAGE HOOP STRENGTH TESTS

Thin hot wall thickness is desirable in Thermal Skin chambers for best heat transfer characteristics. Minimum wall thickness is limited by individual coolant passage hoop strength. To investigate passage hoop strength of Thermal Skin structures manufactured by the chemical machining process nine test samples were prepared from three 6 in. x 6 in. (15.24 cm x 15.24 cm) silver brazed panels having three variations in passage geometry.

Samples from each panel were hydrostatically pressurized at 80°F (300°K) (ambient), 500°F, (533°K) and 1000°F (811°K). For the 500°F (533°K) and 1000°F (811°K) tests a thermocouple was attached to the Inconel plate for recording test temperature and the specimen was heated in an open-ended cylindrical oven. The ends of the oven were filled with ceramic fiber insulating material, which has the consistency of cotton, so that when failure occurred it would easily be blown free, relieving pressure within the oven.

Failure of each specimen unfortunately occurred in the braze joint rather than the hot wall and therefore maximum hot wall strengths were not identified. The pressures attained are presented in Table XIV; a photograph of a typical test specimen after failure is shown in Figure 33. Burst pressures ranged from 1,700 psig (1,182 n/cm^2) at 1000^{o}F (811^{o}K) to 10,000 psig (13,110 n/cm^2) at room temperature.

The braze failures initiated adjacent to the weld that attached the pressure supply fitting, indicating that the heat from the welding operation weakened the braze joint. Photomicrographs (figure 34) confirmed that the braze joint was affected by the welding operation Figure 34a shows an area where the braze is undisturbed, figure 34b shows an unfailed area that was subjected to heating during welding, and figure 34c shows an area where failure occurred; a lack of a layer of silver braze filler was noted in the heated areas while the electroplated nickel layer remained intact.

C. BRAZE BOND STRENGTH TESTS

Selected for the braze bond strength tests were test panels having geometries such that during pressurization the braze bond would be stressed to its limit before the hot wall failed. These tests were performed by hydrostatically pressurizing the coolant passages in the same manner as for the coolant passage hoop strength tests, but because of the panel geometries and the predicted mode of failure they were distinguished as bond tests.

Nine samples were cut from three 6 in. x 6 in. (15.24 cm x 15.24 cm) panels. Samples from each panel were tested at 80^{o}F (300^{o}K) (ambient), 500^{o}F (533^{o}K), and 1000^{o}F (811^{o}K). The results of the testing are presented in Table XV. The strength of the silver braze joint was

Table XIV. Coolant Passage Hoop Strength Test Results

Item	Nickel Plate Part No.	Nominal Nickel Plate Dimensions: Land Width, in. (cm.)	Nominal Nickel Plate Dimensions: Passage Width, in. (cm.)	Nominal Nickel Plate Dimensions: Hot Wall Thickness, in. (cm).	Inconel Plate* Part No.	Sample	Test Temperature, ^{o}F (^{o}K)	Pressure at Failure, **psig (n/cm^2)
1	DKJ-5660-1	0.019 (0.048)	0.041 (0.104)	0.030 (0.076)	DKJ-6475-1	A	80 Amb (300)	19,000 (13,100)
2						B	500 (533)	8,000 (5,516)
3						C	1,000 (811)	5,000 (3,447)
4	DKJ-5661-4	0.021 (0.053)	0.069 (0.046)	0.018 (0.046)	DKJ-6485-2	A	80 (300)	5,000 (3,447)
5						B	500 (533)	3,100 (2,137)
6						C	1,000 (811)	1,700 (1,272)
7	DKJ-5662-2	0.028 (0.071)	0.092 (0.234)	0.016 (0.041)	DKJ-6485-4	A	80 (300)	4,000 (2,758)
8						B	500 (533)	3,600 (2,482)
9						C	1,000 (811)	2,300 (1,586)

* Inconel plates were not etched, nominal thickness of each was 0.058-in. (0.147 cm.)

** Tap water used for pressurant.

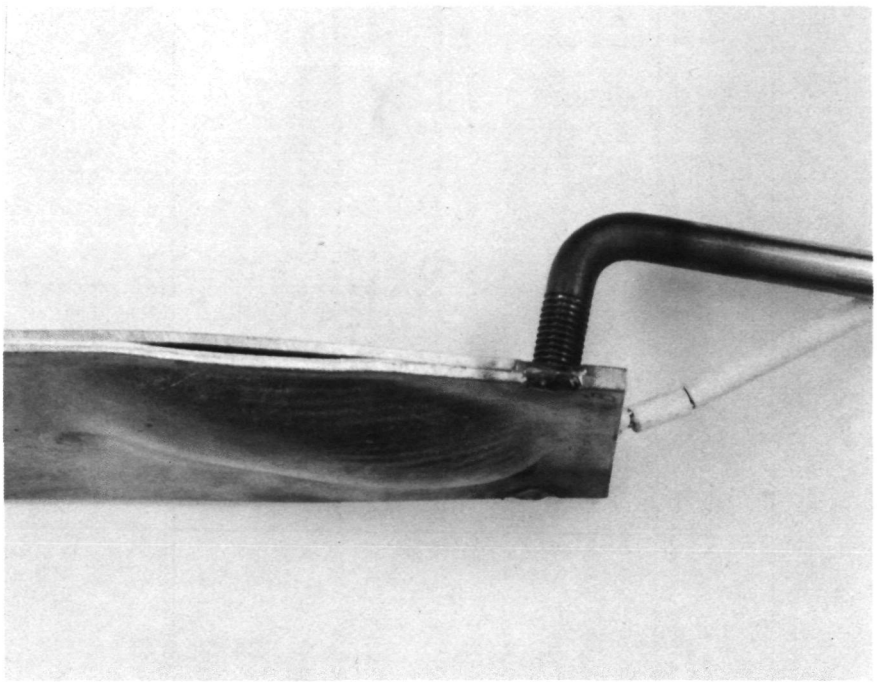

Figure 33. Typical Pressure Failure (Sample No. 2, Table XIII) FL 18547

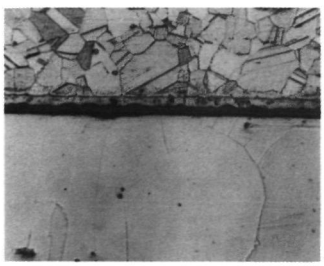

FM 43771

a. Silver-Brazed Bond Line

FM 43769

b. Heat-Affected Bond Line

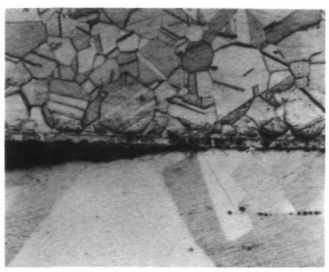

FM 43770

c. Failure at Heat-Affected Bond Line

Figure 34. Photomicrographs of Silver-Brazed Thermal Skin® FD 42174A Test Sample

Table XV. Braze Bond Strength Test Results

Test Item	Nickel Plate Part No.	Nominal Nickel Plate Dimensions: Land Width in. (cm)	Passage Width, in. (cm.)	Hot Wall Thickness, in. (cm)	Inconel Plate*, Part No.	Sample	Test Temperature, °F (°K)	Pressure at Rupture, psig (n/cm^3)	Calculated Braze Strength, psi (n/cm^3)	Comments
1	DKJ-5660-1	0.019 (0.048)	0.041 (0.104)	0.030 (0.076)	DKJ-6485-1	A	500 (533)	19,000 (13,110)	41,000(28,269)	Part first taken to 21,000 psig (14,489 n/cm^2)(pump limit) at 80°F (300°K) without failure.
2						B	500 (533)	19,300 (13,317)	41,000 (28,682)	Braze failed.
3						C	1,000 (811)	9,500 (6,560)	20,500 (14,134)	Braze failed.
4	DKJ-5662-2	0.021 (0.053)	0.069 (0.175)	0.018 (0.046)	DKJ-6485-2	A	80 (300)	9,600 (6,629)	31,600 (21,787)	Braze failed adjacent to welded area.
5						B	500 (533)	9,500 (6,560)	---	Individual passage ruptured in hoop stress.
6						C	1,000 (811)	7,000 (4,836)	23,000 (15,858)	Small defect in braze caused two adjacent passages to rupture together in hoop stress.
7	DKJ-6429-1	0.030 (0.076)	0.030 (0.076)	0.051 (0.130)	DKJ-6482-1	A	80 (300)	12,400 (8,560)	12,400 (8,549)	Braze was damaged prior to test by welding causing premature failure.
8						B	500 (533)	13,400 (9,249)	13,400 (9,239)	Braze was damaged prior to test by welding causing premature failure.
9						C	1,000 (811)	7,600 (5,250)	7,600 (5,240)	Braze was damaged prior to test by welding causing premature failure

*Failure occurred in nickel plate

**Tap water used for pressurant

calculated by multiplying the failure pressure by the ratio of the passage width to land width. Three specimens from the same panel indicated that braze strengths from 20,500 psi (14,134 n/cm^2) at 1000°F (811°K) to 41,600 psi (28,682 n/cm^2) at room temperature could be achieved. One of the test samples exhibiting low braze strength was sectioned (figure 35) to determine if passage misalignment was responsible for the low values. The sectioned sample showed that passage alignment was good, but plate separation had initiated in an area where the braze joint was affected by the heat of welding the pressure inlet fitting to the Inconel plate. The results of tests No. 7, 8, and 9 in Table XV are therefore not representative of a full strength silver braze.

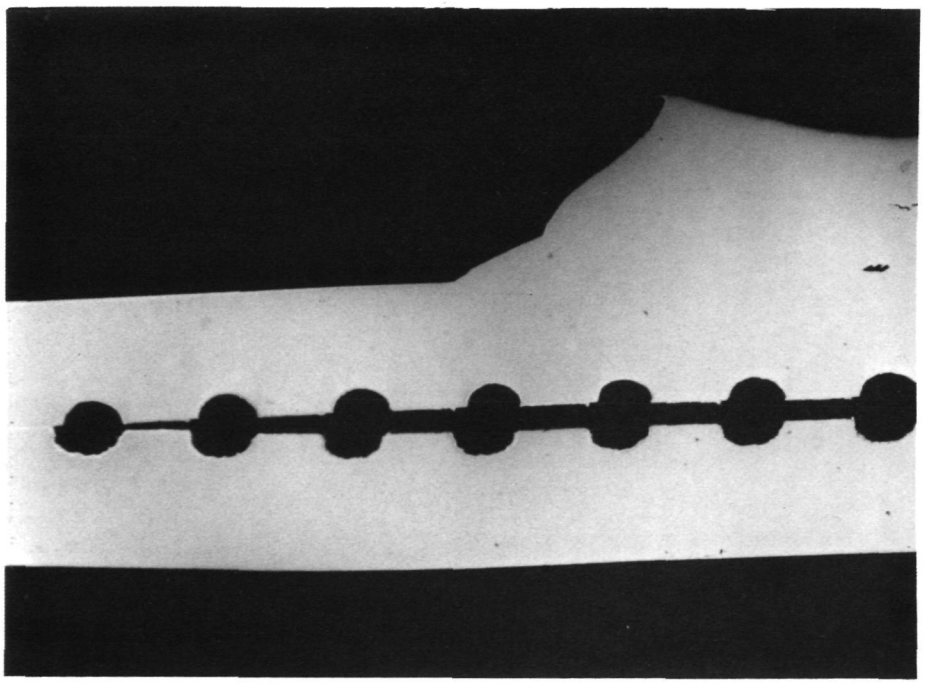

Figure 35. Section View of Braze Bond Test Sample FL 19287

D. OVERALL STRUCTURAL HOOP STRENGTH TESTS

Overall hoop strength tests were performed to establish the chamber pressure load-carrying limits for THERMAL SKIN structures. The testing consisted of performing standard tensile tests with samples cut from Thermal Skin panels in a direction perpendicular to the passages (Figure 36).

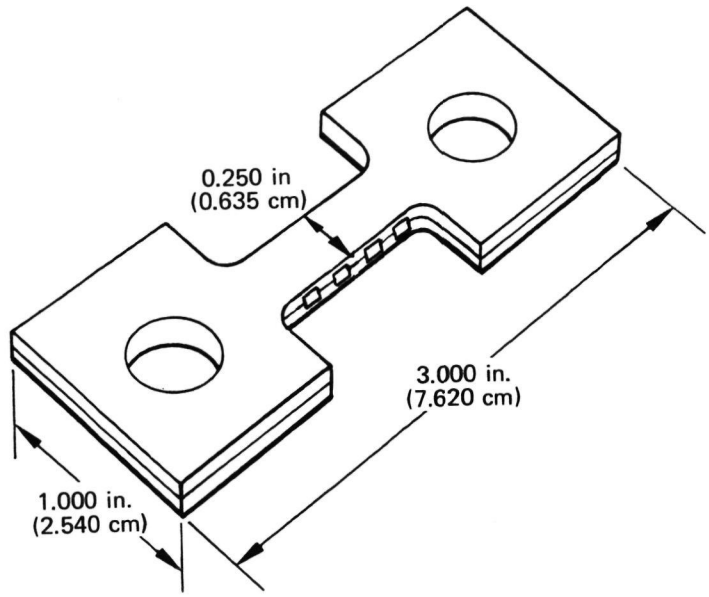

Figure 36. Strucutral Hoop Strength Test Sample FD 59699

Nine samples were obtained from three brazed panels and tested at 80°F (300°K), 500°F (533°K), and 1000°F (811°K). A Young tensile test machine equipped with an open-ended oven for elevated temperature testing was used to perform the tests. Results are presented in Table XVI.

Table XVI. Overall Structural Hoop Strength Test Results

Test No.	Nickel Plate Part No.	Nominal Nickel Plate Dimensions: Land Width, in. (cm.)	Passage Width, in. (cm).	Hot Wall Thickness, in. (cm.)	Inconel Plate Part No.	Nominal Inconel Plate Dimensions: Land Width, in. (cm.)	Passage Width, in. (cm.)	Structural Wall Thickness, in. (cm.)	Test Temp. °F (°K)	Yield Load lb (n)	Ultimate Load, lb (n)	Elongation %	Calculated Inconel Yield Strength,* psi (n/cm²)
1	DKJ-5661-5	0.024 (0.061)	0.066 (0.168)	0.028 (0.071)	DKJ-6185-3	None	None	0.058 (0.147)	80 (300)	2,895 (12,878)	5,550 (24,688)	28.0	93,800 (64,473)
2									500 (533)	2,630 (11,699)	4,880 (21,707)	29.5	83,500 (57,571)
3									1,000 (811)	2,480 (11,032)	4,340 (19,305)	34.0	81,900 (56,468)
4	DKJ-5661-6	0.020 (0.051)	0.070 (0.178)	0.028 (0.071)	DKJ-6481-1	0.025 (0.064)	0.065 (0.165)	0.036 (0.091)	80 (300)	2,085 (9,275)	3,835 (17,059)	18.0	101,500 (69,982)
5									500 (533)	1,820 (8,096)	3,520 (15,658)	17.5	86,200 (59,433)
6									1,000 (811)	1,940 (8,630)	3,120 (13,878)	18.8	98,400 (67,844)
7	DKJ-5661-7	0.024 (0.061)	0.066 (0.168)	0.027 (0.069)	DKJ-6480-1	0.028 (0.071)	0.062 (0.157)	0.014 (0.036)	80 (300)	1,145 (5,093)	1,630 (7,251)	7.0	130,200 (89,770)
8									500 (533)	1,210 (5,382)	1,680 (7,473)	18.5	137,100 (94,527)
9									1,000 (811)	895 (3,981)	1,245 (5,538)	7.5	107,100 (73,843)

* To calculate the Inconel yield strength a tensile test specimen was assumed to have two load carrying members: (1) the nickel hot wall and (2) the Inconel structural wall. The load in the nickel member at the yield point for the speciemns was calculated assuming theoretical yield strength for Nickel 200 material at the testing temperature. The calculated nickel load was subtracted from the test specimen yield load to establish the Inconel load. The Inconel load was then divided by the Inconel structural wall cross-sectional area to give the calculated Inconel yield strength. All specimens were machined to 0.500-in. (1.270-cm.) width before testing.

The tensile strength of the samples were determined by the Inconel X-750 plate and no indication of reduced strength was seen as a result of this plate having grooves. Calculated yield strengths based on minimum cross sectional area ranged from 81,900 psi (56,468 n/cm^2) at 1000^{o}F (811^{o}K) to 93,800 psi (64,673 n/cm^2) at room temperature for the weakest panel. The test results indicated that standard hoop strength calculations based on minimum cross sectional areas would be acceptable without additional factors to account for stress concentration for designing Thermal Skin structural wall thickness.

E. THERMAL CYCLE LIFE TESTS

Thermal-cycle life tests were performed using Thermal Skin test specimens and using the test setup as shown in figures 37 and 38. The samples were heated by an induction coil and then submerged in liquid nitrogen.

A stiffener block was brazed to the Inconel back surface to restrain the panel during testing. This stiffener block also provided a heat sink to maintain a low backplate wall temperature for a sufficient time period to permit a representative temperature gradient in the sample to be attained.

Five samples were tested at simulated combustion-side wall temperatures of 1000^{o}F (811^{o}K), 1500^{o}F (1089^{o}K), or 1700^{o}F (1200^{o}K). For each test, pressure was maintained constant while the nickel wall was cycled between the elevated temperature and -250^{o}F (116^{o}K) (attained by submerging the panel in liquid nitrogen). The temperature cycling was repeated until a drop of internal pressure occurred, which indicated failure. Results are presented in Table XVII.

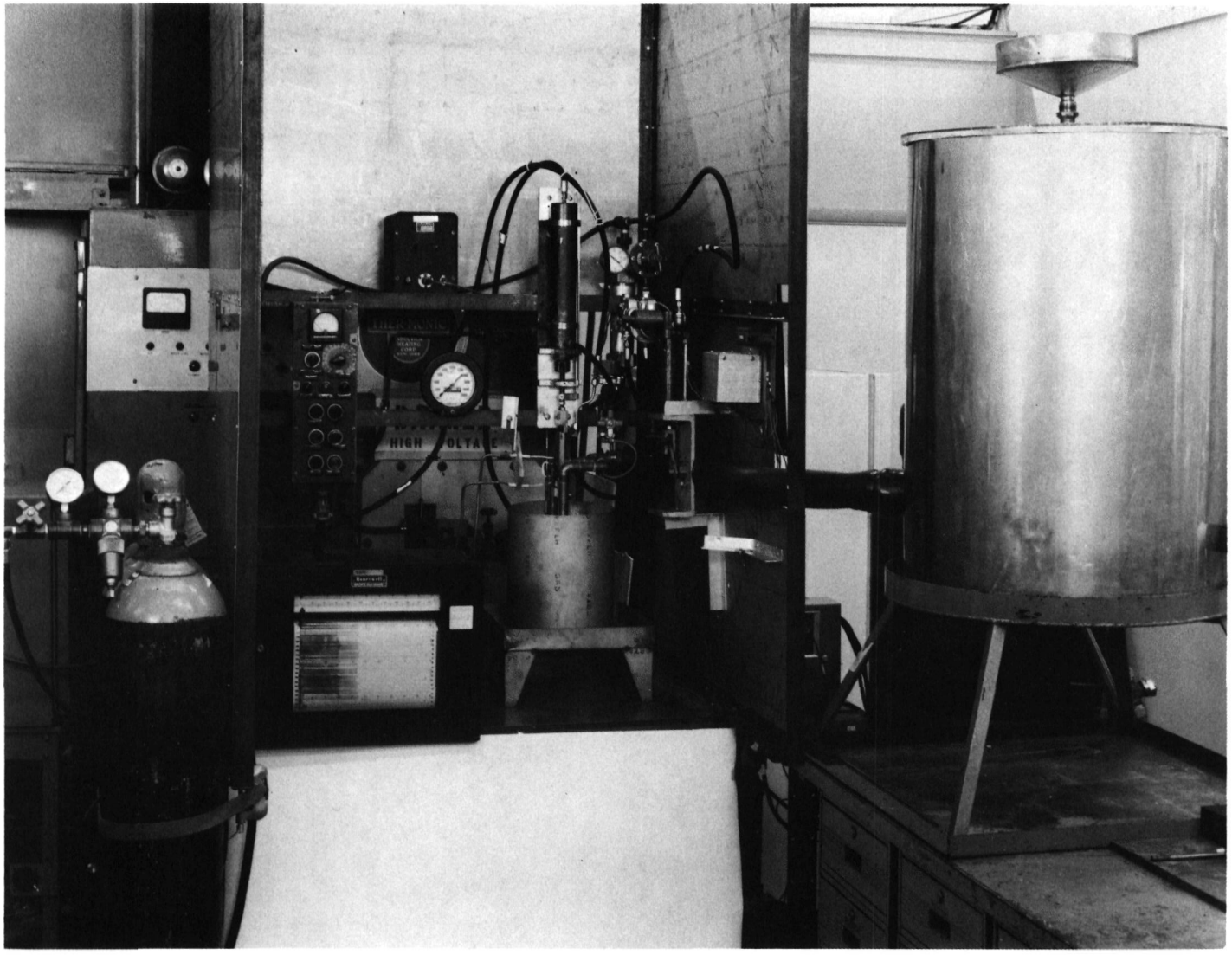

Figure 37. Test Apparatus for Thermal Cycle Testing, Overall View

FC 21872

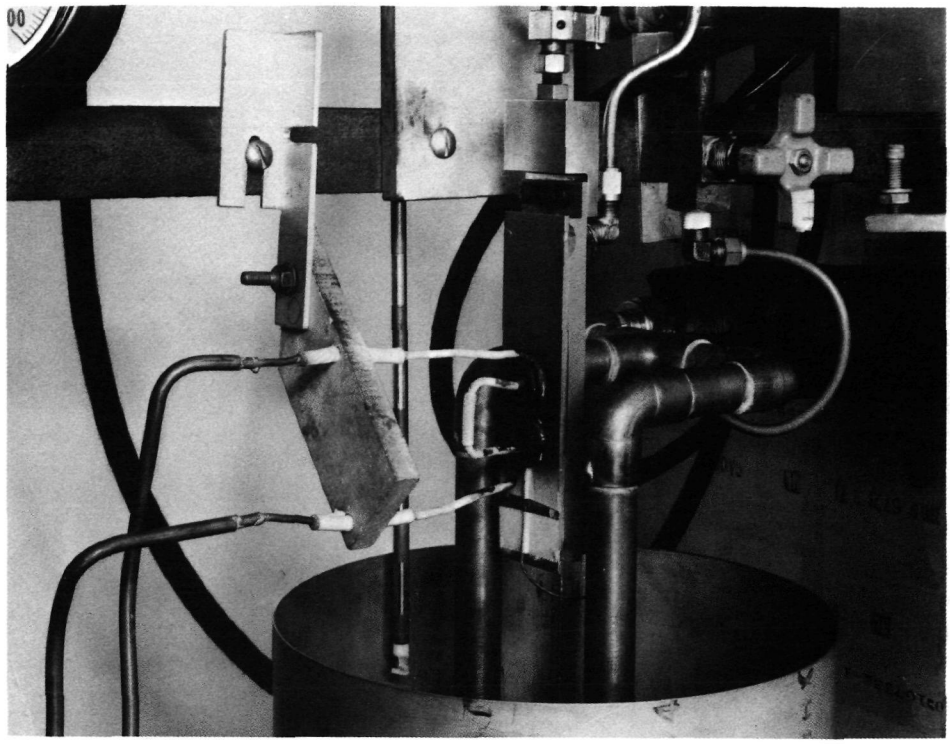

Figure 38. Test Apparatus for Thermal Cycle Testing, Detail View of Test Item FC 21871

Cycle lives ranged from 3 at 1700°F (1200°K) to 201 at 1000°F (811°K) nickel hot wall temperature. A typical thermal cycle failure experienced during the testing is shown in figure 39 and 40 where a surface crack propagated through the nickel wall is illustrated. In Figure 40 silver braze material can be seen along the inside wall of the nickel. The surface of another test sample after testing is shown in Figure 41 and illustrates the effects of the large grain structure of the nickel.

Lower cyclic lives than expected occurred during the testing. The results were also in conflict with those of an independent test of a

Table XVII. Thermal Cycle Test Results

Test No.	Sample Configuration*	Maximum, ^{o}F (^{o}K)	Minimum, ^{o}F (^{o}K)	Inconel Wall Temperature, ^{o}F (^{o}K) (Max)	Stiffener Temperature, ^{o}F (^{o}K) (Max)	Internal Pressure, psig (n/cm^2)	Cycles to Failure
1	A	1700 (1200)	-250 (116)	1100 (866)	Not Recorded	800 (562)	3
2	B	1500 (1089)	-250 (116)	1000 (811)	440 (500)	1000 (700)	36
3	B	1000 (811)	-250 (116)	600 (589)	170 (350)	1000 (700)	201
4	B	1500 (1089)	-250 (116)	1050 (839)	Not Recorded	500 (345)	4
5	A	1000 (811)	-250 (116)	600 (589)	135 (330)	1500 (1034)	146

*Sample Configurations Were:

	A	B
Nickel Plate		
Part No.	DKJ-5662-3	DKJ-5662-1
Land Width, in. (cm.)	0.022 (0.056)	0.024 (0.061)
Passage Width, in. (cm.)	0.098 (0.249)	0.096 (0.244)
Passage Depth, in. (cm.)	0.029 (0.074)	0.028 (0.071)
Hot Wall Thickness, in. (cm).	0.016 (0.041)	0.018 (0.046)
Inconel Plate Part No.	DKJ-6479-3	DKJ-6479-2

Figure 39. Nickel Wall Surface After Test No. 4 FL 19387

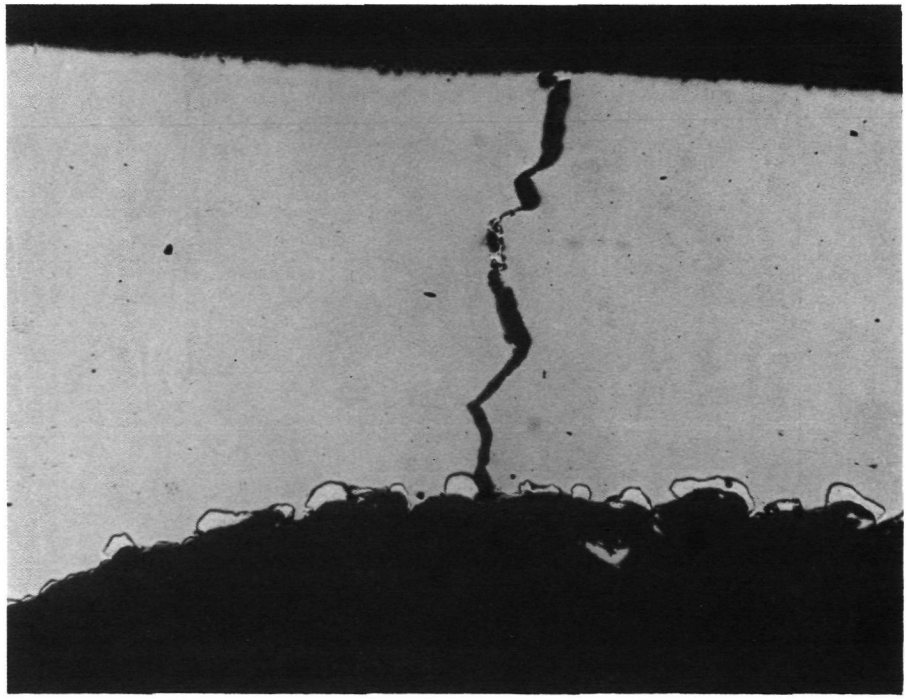

Figure 40. Section View of Nickel Wall After Test No. 4 FM 46332

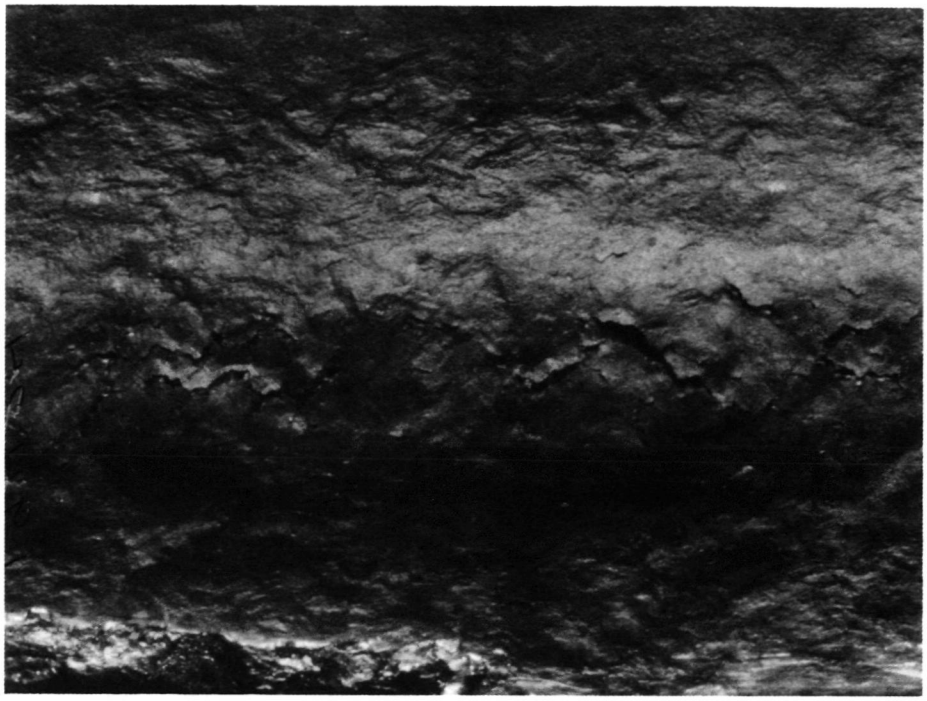

Figure 41. Nickel Wall Surface After Test No. 5 FL 19434

single THERMAL SKIN sample panel made in June 1969. In this test, the sample withstood over 100 cycles with 1000 psig (700 n/cm^2) internal pressure at a nickel wall temperature of 1500^{o}F (1089^{o}K).

Because of the inconsistent results, temperature variations on the surface of an induction coil-heated specimen were investigated using multiple small-wire-gage thermocouples (Figure 42). Temperature differences of up to 35^{o}F (275^{o}K) were observed between adjacent surface thermocouples, one over a passage centerline and one at the midpoint between passages. This differential increased to 140^{o}F (330^{o}K) a short distance from the maximum temperature zone. During tests in which several thermocouples were used on the heated surface, temperature variations of up to 170^{o}F (350^{o}K) were recorded only 0.2 in. (0.5 cm) apart.

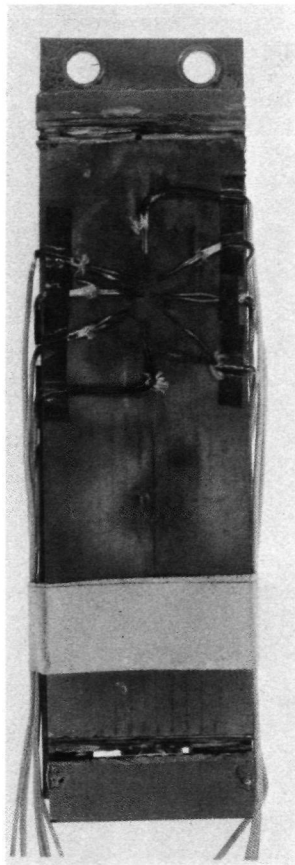

Nickel Face

Access Hole In Stiffner For Attaching Thermocouple to Inconel X-750 Face Of Thermal Skin®

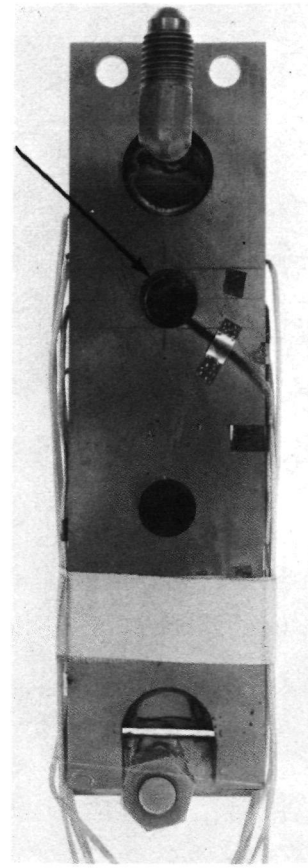

Inconel X-750 Stiffner Face

Figure 42. Mulitple Thermocouple Test Specimen FC 22274

The large surface temperature differences suggest that the temperatures recorded during the testing (which were read from a single thermocouple) were lower than the maximum temperature imposed and therefore any interpretation of the results is questionable.

DIFFUSION BONDING

A. GENERAL

Diffusion bonding is a process of metallurgically joining metals by causing atoms to interdiffuse across mating surfaces. Bonding is accomplished by the application of proper heat and pressure for a predetermined time; the process differs from welding or brazing mainly in that there is no melting. Diffusion bonding was investigated as an alternative process for joining grooved plates to form Thermal Skin® panels because silver brazing forms a relatively low temperature joint that can be weakened by subsequent welding operations. Diffusion bonding would theoretically provide a joint with parent metal strength and melting temperature.

The feasibility of diffusion bonding Thermal Skin plates was demonstrated first in panels joined by the Battelle Memorial Institute (Reference 6), and in samples made at NASA-LeRC. The purpose of the investigation in this program was therefore to determine optimum diffusion bonding conditions and limits, and to evaluate the performance of the optimum diffusion bond.

The diffusion bonding effort was divided into two parts: 1) Determination of Diffusion Bonding Conditions and 2) Diffusion Bonding Evaluation. These parts are discussed on the following pages.

Under the part 1 small samples were bonded using hard tooling. Variations in bonding conditions and diffusion aids were investigated, and bonded panels were structurally tested at room temperature and elevated temperature by hydrostatically pressurizing to failure. The effect of the bonding thermal cycle on the parent metal strength was investigated. The effect on the bond strength of heliarc welding on the structural

wall (Inconel) was also checked. A limited number of electron microprobe analyses were performed on several bond zones to determine the degree of diffusion achieved.

Because of the large area of a typical Thermal Skin® chamber plate (Figure 43) finding a suitable means of applying a large load at elevated temperature was needed. Available methods required a highly specialized hot press or a high pressure autoclave. In either case the available equipment was expensive to use and limited the possible panel size. An effort to develop relatively low cost tooling that could be scaled to meet large size panel requirements was made during the diffusion bonding evaluation part of the investigation.

It was not possible to completely develop the diffusion bonding tool within the scope of the program and alternative bonding techniques were briefly but inconclusively investigated. They were: 1) electroless nickel bonding, a form of transient liquid phase (TLP) bonding and 2) autovac bonding, a diffusion bonding technique found acceptable for iron alloys (Reference 7).

B. DETERMINATION OF DIFFUSION BONDING CONDITIONS

1. General

Establishing minimum cycle time, temperature, and pressure for diffusion bonding Thermal Skin materials was desirable so that excessive grain growth would not occur and so that liberal passage geometry was possible. Grain growth was a function of time and temperature, and a large grain structure was believed to be detrimental to the structural performance of the materials, particularly Nickel 200 thermal cycle life. Establishing the acceptable bonding pressure was important because the unit load at various plate locations was dependent on the local

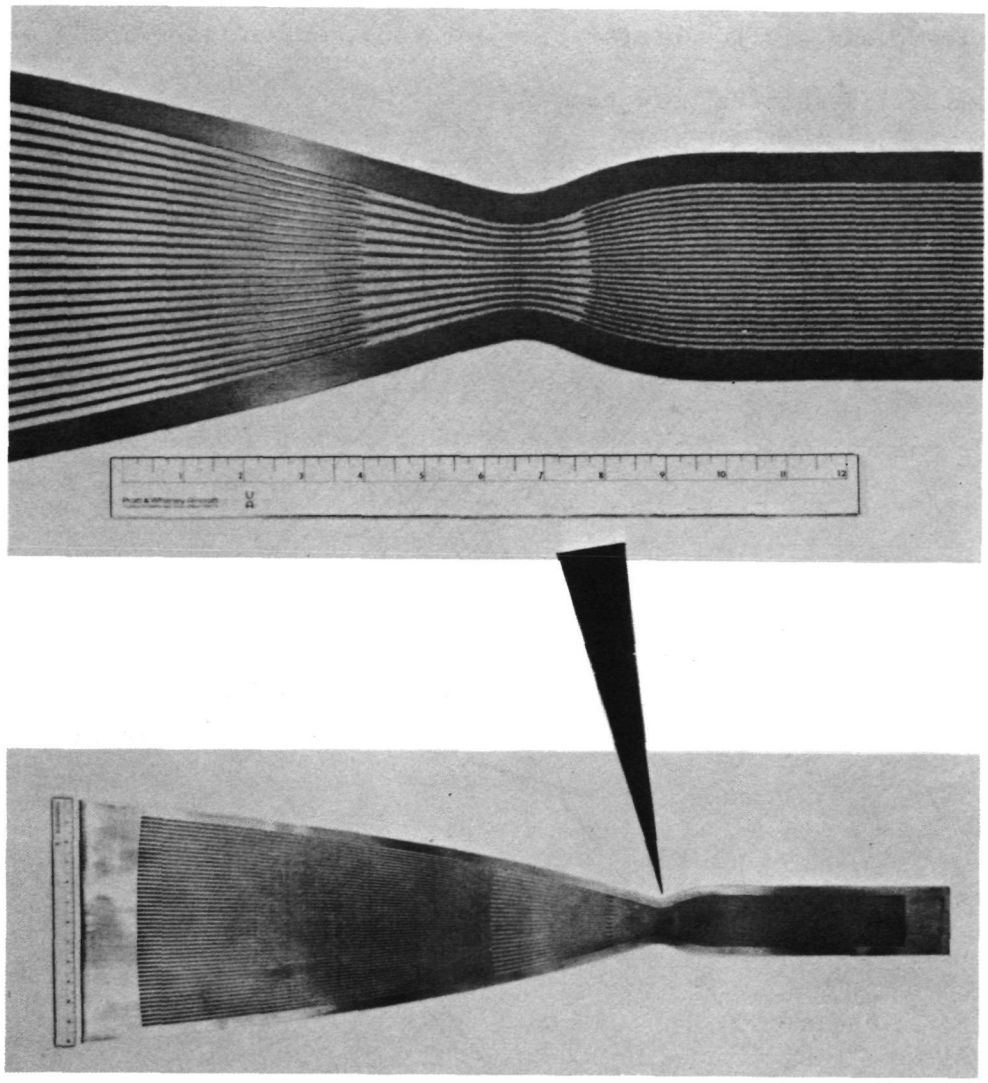

Figure 43. Nickel Plate for 5K Flox/Methane Thrust Chamber FD 27349

passage-to-land width ratio. If one area of a panel was stressed to its yield load then the allowable passage geometry variation at any other location was limited by the minimum acceptable bond pressure. Exceeding the yield load at any location would result in collapsed passages.

2. Experimental Program

Fourteen (14) diffusion bonding runs were performed using small size panels (figure 44) and varying bond conditions (time, temperature,

and load) and surface preparation (as received, polished, and plated). A total of 117 samples were bonded.

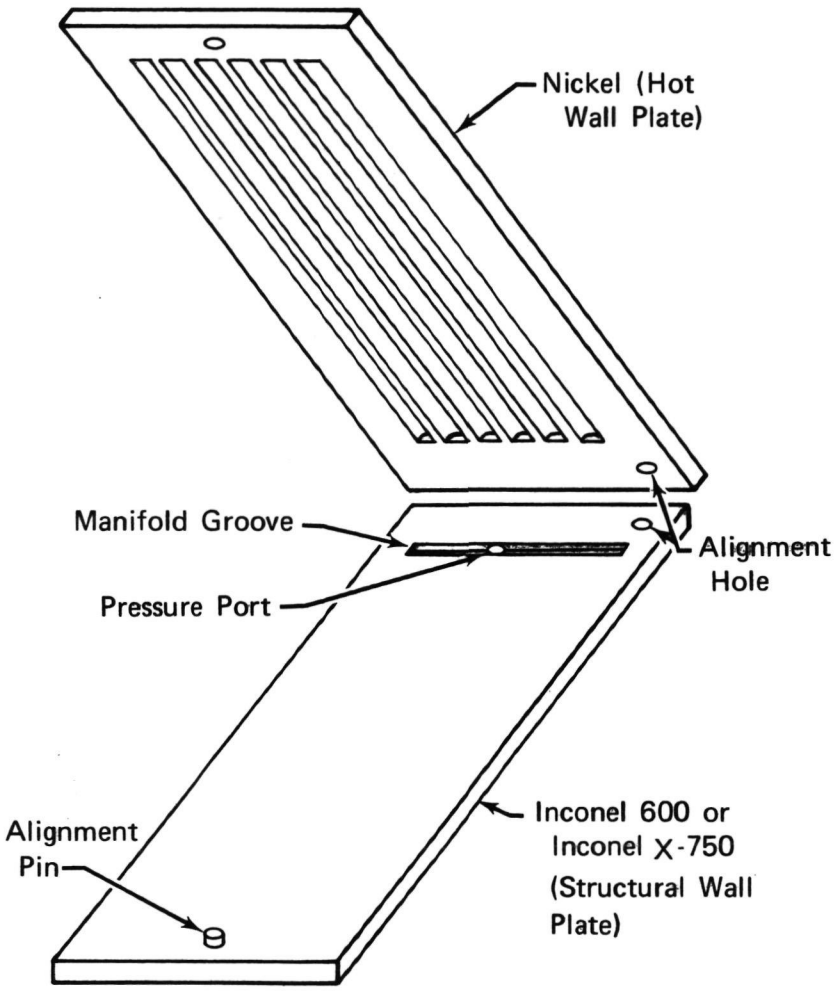

Figure 44. Diffusion Bonding Sample Design FD 59702

Fabrication drawings for the diffusion bonding samples are presented in figures 45 and 46. The Inconel (structural) plate was not grooved in order to eliminate any alignment problems. The nickel (hot wall) plate had a groove pattern with a passage width-to-land width ratio of 2:1 which is typical of that which might be used in a 5000 lb_f (22.241 n) FLOX/methane thrust chamber.

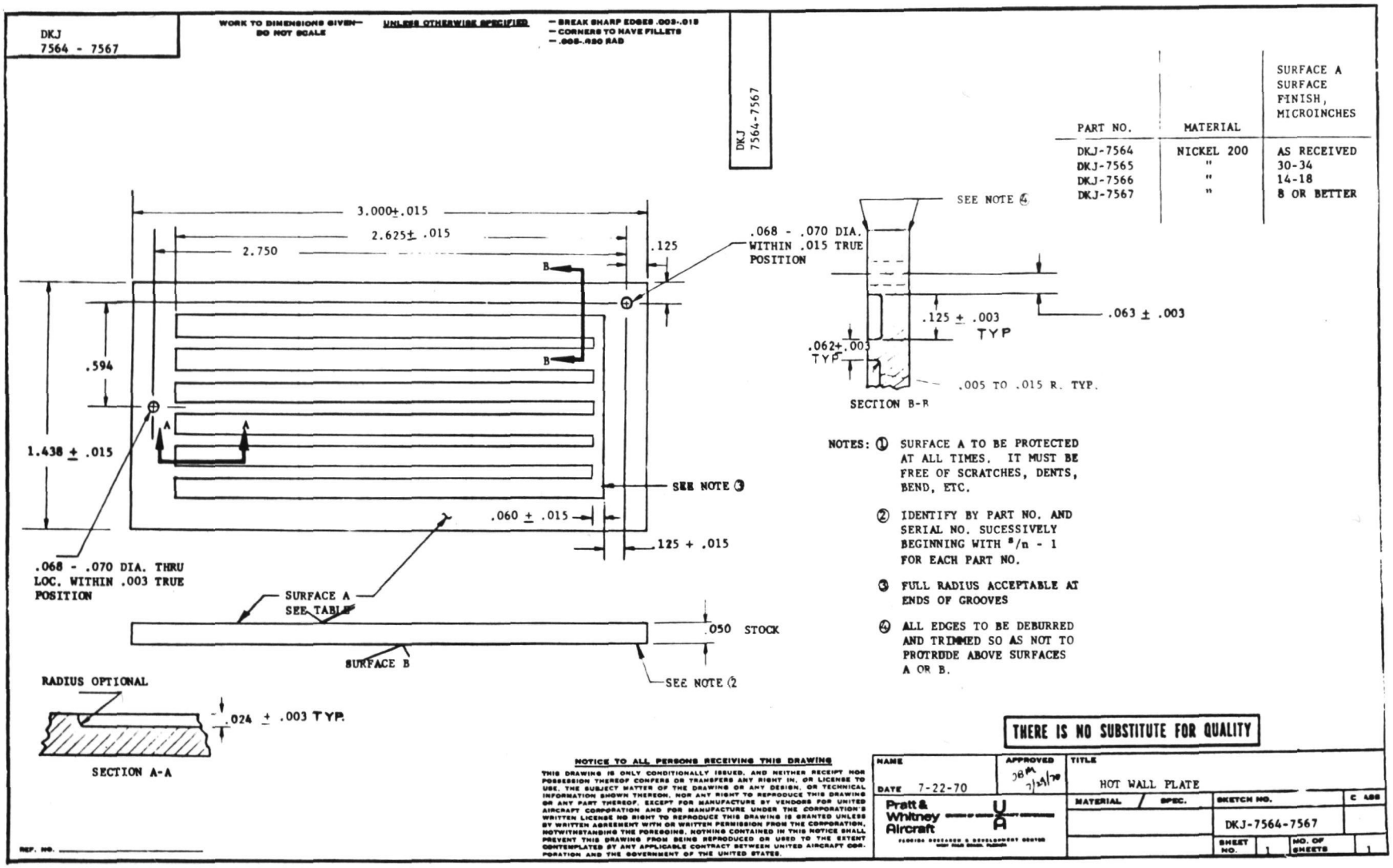

Figure 45. Manufacturing Drawing for Nickel Plate

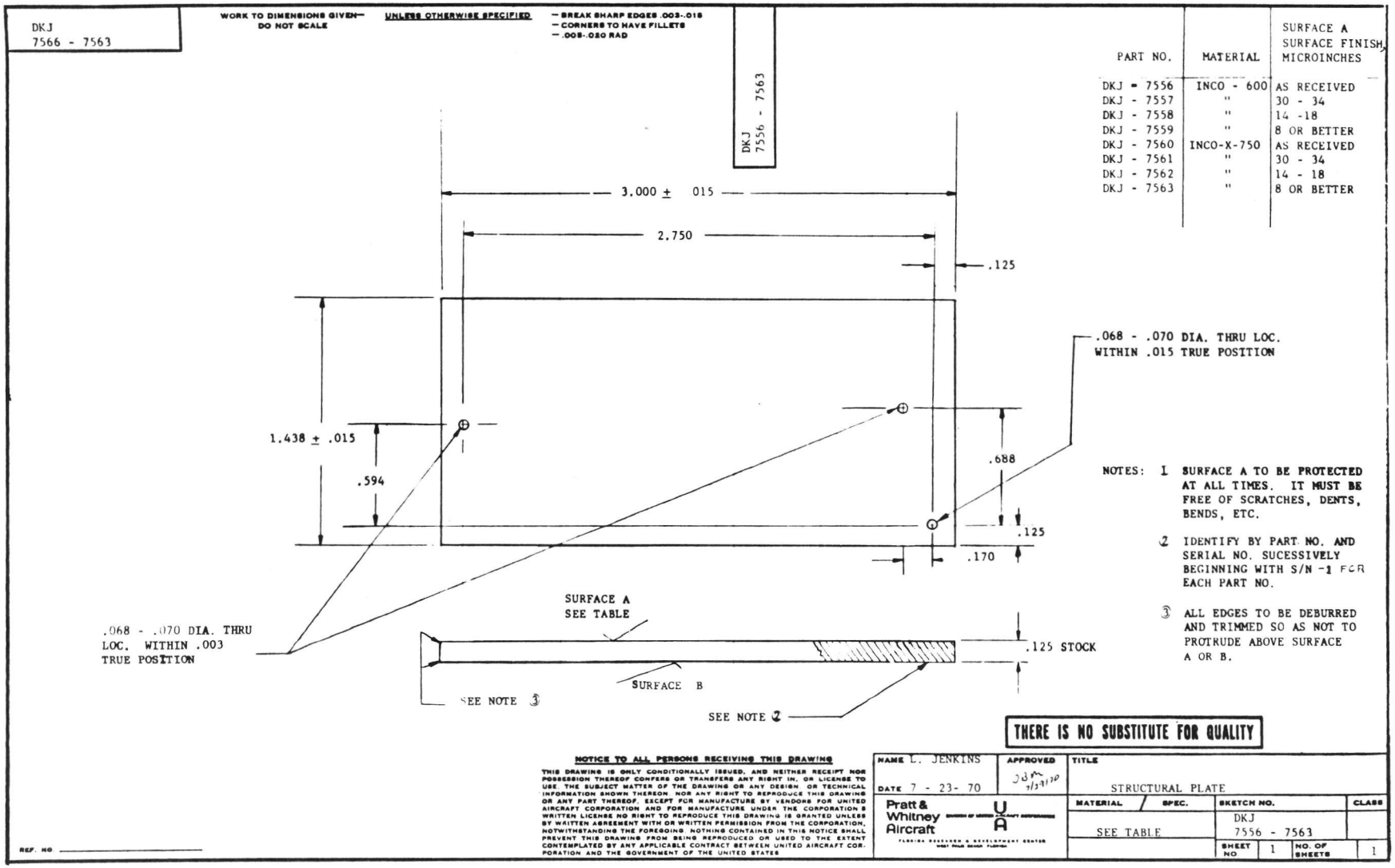

Figure 46. Manufacturing Drawing for Inconel Plate

Sample panels were manufactured from Nickel 200, Inconel 600, and Inconel X-750. The Inconel 600 is representative of the non-age-hardenable nickel alloy group, and the Inconel X-750 of the age-hardenable group. The panels were bonded by a P&WA subcontractor using no internal tooling and using the diffusion bonding facility shown in figure 47. It consisted of a water cooled, hot vacuum press with resistance heaters in intimate contact with the test plates.

The panels were hydrostatically pressure-tested to failure after bonding at either ambient temperature or at 1000°F (811°K) to determine the strength of the bonds achieved. Water was used as the pressurant and all the pressure tests were performed at FRDC. A special test fixture (figure 48) was used to expedite the room temperature testing while for the elevated temperature tests, a high pressure supply tube was welded to the Inconel plate.

The bonding tests performed are summarized in Table XVIII; photographs of the test panels after hydrostatic pressure testing are presented in Appendix E. Failures occurred in either the diffusion bond or in the nickel parent metal in all cases. Because the passage width was twice the land width the tensile load on the bonds was twice the hydrostatic pressure. The results of the hydrostatic pressure tests are discussed below.

a. Ambient Temperature Hydrostatic Pressure Test Results

The bond strength data from the hydrostatic pressure tests performed at ambient temperature are cross plotted in figure 49. In the plots the bond load is presented as the unit load on the Nickel 200 lands expressed in percentage of the respective nickel yield strength at the bonding temperature. The yield strength used for Nickel 200 at elevated temperature is presented in figure 50 for reference.

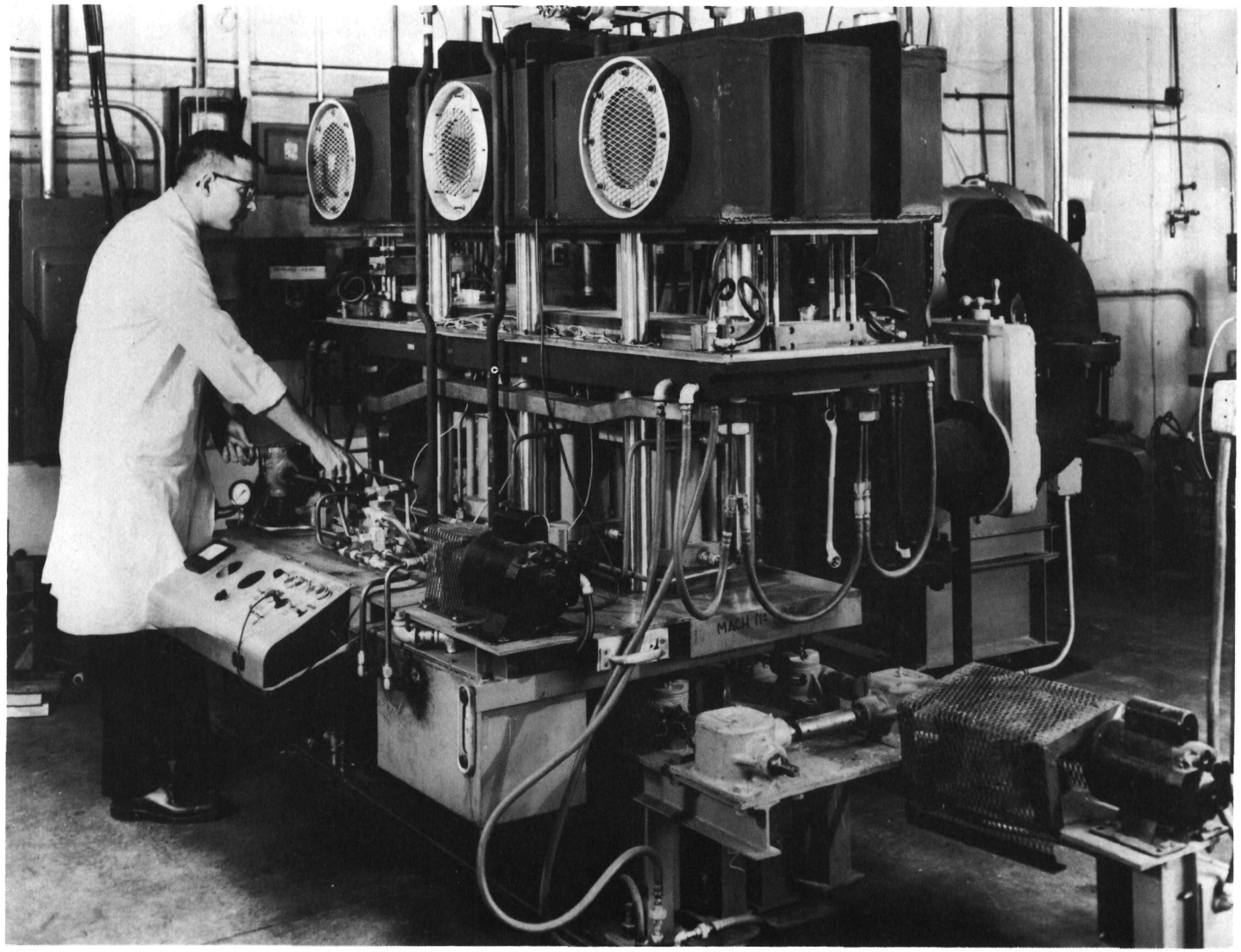

Figure 47. Diffusion Bonding Facility, Hexcel Corporation

FE 110747

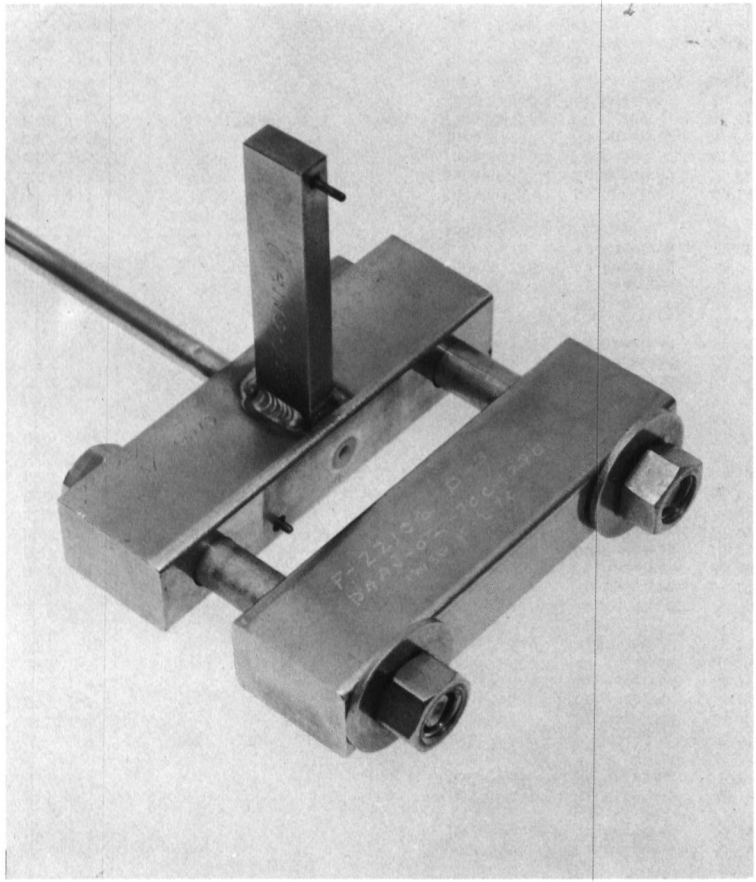

FE 103780

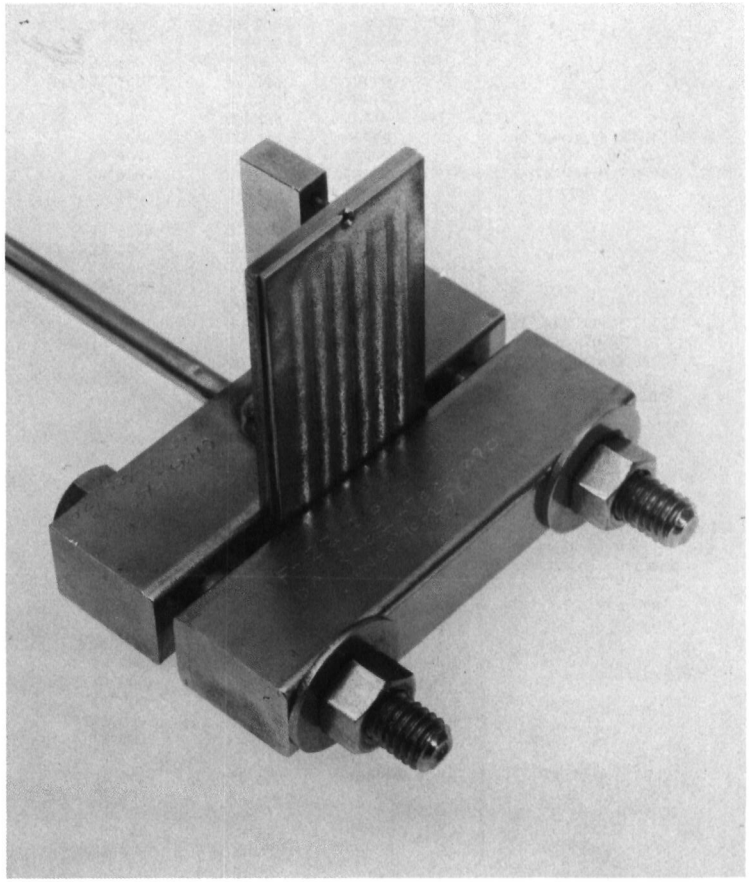

FE 103781

Figure 48. Hydrostatic Pressure Test Tool

Table XVIII. Experimental Diffusion Bonding Results

Sample No.	Bond Conditions: Time, min	Temperature, °F	Temperature, (°K)	Load, psi**	Structural Plate Material	Surface Preparation*: Hot Wall Plate	Surface Preparation*: Structural Plate	Test Temperature, °F	Test Temperature, (°K)	Test Burst Pressure, psi**	Calculated Bond Stress, psi**	Type Failure	Comments
HEX 0-1					Inco X-750	Ni Plated	Ni Plated	RT		20,000	43,300	Parent Mat'l	Sample HEX 0-2 cut in two by HEXCEL to inspect for passage deformation
HEX 0-2					Inco X-750	Mech. Polish	Ni Plated	-		-	-	-	
HEX 0-3	180	1700	(1200)	5050	Inco 600	Mech. Polish	Ni Plated	RT		22,400	48,600	Parent Mat'l	HEXCEL proprietary soft tool used. Ni plating thickness = 0.0001 in. (0.000254 cm)
HEX 0-4					Inco 600	Mech. Polish	As Received	RT		20,200	43,800	Bond	
HEX 1-1					Inco 600	As Received	As Received	RT		23,200	50,300	Bond	Base point test Ni plating thickness = 0.0001 to 0.0002 in. (0.00025 to 0.00051 cm)
HEX 1-2					Inco 600	As Received	Ni Plated	Rt		24,800	53,800	Parent Mat'l	
HEX 1-3					Inco X-750	As Received	As Received	RT		26,400	57,200	Bond	
HEX 1-4					Inco X-750	As Received	Ni Plated	RT		20,400	44,200	Parent Mat'l	
HEX 1-5	180	1700	(1200)	4000	Inco X-750	Ni Plated	Ni Plated	RT		26,000	56,300	Parent Mat'l	
HEX 1-6					Inco 600	As Received	As Received	RT		22,600	49,000	Parent Mat'l	
HEX 1-7					Inco 600	As Received	Ni Plated	RT		24,400	52,900	Parent Mat'l	
HEX 1-8					Inco X-750	As Received	As Received	RT		22,000	47,700	Parent Mat'l	
HEX 1-9					Inco X-750	As Received	Ni Plated	RT		20,400	44,200	Parent Mat'l	
HEX 1-10					Inco X-750	Ni Plated	Ni Plated	RT		24,000	52,000	Bond Mat'l	
HEX 2-1					Inco 600	As Received	As Received	RT		8,500	19,200	Bond	Reduced load test Ni plating thickness = 0.00005 to 0.00009 in. (0.00011 to 0.00023 cm)
HEX 2-2					Inco 600	As Received	Ni Plated	RT		12,100	27,900	Bond	
HEX 2-3					Inco X-750	As Received	As Received	RT		11,950	27,800	Bond	
HEX 2-4					Inco X-750	As Received	Ni Plated	RT		4,000	9,070	Bond	
HEX 2-5	180	1700	(1200)	1000	Inco X-750	Ni Plated	Ni Plated	RT		7,900	17,980	Bond	
HEX 2-6					Inco 600	As Received	As Received	RT		6,475	14,550	Bond	
HEX 2-7					Inco 600	As Received	Ni Plated	RT		10,900	24,300	Bond	
HEX 2-8					Inco X-750	As Received	As Received	RT		5,500	12,600	Bond	
HEX 2-9					Inco X-750	As Received	Ni Plated	RT		11,750	26,700	Bond	
HEX 2-10					Inco X-750	Ni Plated	Ni Plated	RT		24,000	54,600	Bond	
HEX 3-1					Inco 600	As Received	As Received	RT		8,000	18,400	Bond	Reduced time test Ni plating thickness = 0.00006 to 0.00010 in. (0.00015 to 0.00025 cm)
HEX 3-2					Inco 600	As Received	Ni Plated	RT		12,000	27,300	Bond	
HEX 3-3					Inco 600	As Received	Ni Plated	RT		9,000	20,900	Bond	
HEX 3-4					Inco X-750	As Received	Ni Plated	RT		18,000	41,300	Bond	
HEX 3-5	1	1700	(1200)	4000	Inco X-750	Ni Plated	Ni Plated	RT		17,200	39,200	Bond	
HEX 3-6					Inco 600	As Received	As Received	RT		8,800	20,300	Bond	
HEX 3-7					Inco 600	As Received	Ni Plated	RT		12,600	29,300	Bond	
HEX 3-8					Inco X-750	As Received	As Received	RT		7,400	17,050	Bond	
HEX 3-9					Inco X-750	As Received	Ni Plated	RT		11,200	24,600	Bond	
HEX 3-10					Inco X-750	Ni Plated	Ni Plated	RT		14,100	32,100	Bond	
HEX 4-1					Inco 600	As Received	As Received	RT		9,200	18,800	Bond	Ni plating thickness = 0.00007 to 0.00009 in. (0.00018 to 0.00023 cm)
HEX 4-2					Inco 600	As Received	Ni Plated	RT		20,000	41,000	Bond	
HEX 4-3					Inco 600	Ni Plated	Ni Plated	RT		26,000	53,200	Bond	
HEX 4-4					Inco X-750	As Received	Ni Plated	RT		11,000	22,500	Bond	
HEX 4-5	180	1300	(978)	8000	Inco X-750	Ni Plated	Ni Plated	RT		26,000	53,200	Parent Mat'l	
HEX 4-6					Inco X-750	As Received	As Received	RT		10,400	21,300	Bond	
HEX 4-7					Inco 600	As Received	Ni Plated	RT		13,400	27,400	Bond	
HEX 4-8					Inco 600	Ni Plated	Ni Plated	RT		26,000	53,200	Parent Mat'l	
HEX 4-9					Inco X-750	As Received	As Received	RT		9,600	19,650	Bond	
HEX 4-10					Inco X-750	Ni Plated	Ni Plated	RT		24,000	49,200	Parent Mat'l	
HEX 5-1	180	1700	(1200)	4000	Inco X-750	As Received	Ni-Co Plated	RT		23,500	48,200	Parent Mat'l	Ni-Co plating thickness = 0.0002 to 0.0004 in. (0.00051 to 0.00102 cm)

Table XVIII. Experimental Diffusion Bonding Results (Continued)

Sample No.	Bond Conditions: Time, min	Bond Conditions: Temperature, °F	Bond Conditions: Temperature, (°K)	Bond Conditions: Load, psi**	Structural Plate Material	Surface Preparation*: Hot Wall Plate	Surface Preparation*: Structural Plate	Test Temperature, °F	Test Temperature, (°K)	Test Burst Pressure, psi**	Calculated Bond Stress, psi**	Type Failure	Comments
HEX 6-1					Inco 600	As Received	As Received	RT		25,000	57,200	Parent Mat'l	Repeat of base point conditions to provide samples for elevated temperature tests. Samples HEX 6-5 and HEX 6-10 were welded on Inconel side to simulate engine welding. Ni plating thickness = 0.00007 in. (0.00018 cm)
HEX 6-2					Inco 600	As Received	As Received	RT		23,000	52,600	Parent Mat'l	
HEX 6-3					Inco 600	As Received	As Received	1000	(811)	5,800	13,260	Bond	
HEX 6-4					Inco 600	As Received	As Received	1000	(811)	4,800	10,980	Bond	
HEX 6-5	180	1700	(1200)	4000	Inco 600	As Received	As Received	RT		25,000	57,200	Bond	
HEX 6-6					Inco 600	Ni Plated	Ni Plated	RT		25,200	57,600	Parent Mat'l	
HEX 6-7					Inco 600	Ni Plated	Ni Plated	RT		25,000	57,200	Parent Mat'l	
HEX 6-8					Inco 600	Ni Plated	Ni Plated	1000	(811)	5,400	12,340	Bond	
HEX 6-9					Inco 600	Ni Plated	Ni Plated	1000	(811)	6,000	13,710	Bond	
HEX 6-10					Inco 600	Ni Plated	Ni Plated	RT		25,000	57,200	Parent Mat'l	
Repeat Tests													
HEX 6-1	180	1700	(1200)	4000	Inco 600	As Received	As Received	1000	(811)	6,000	13,710	Bond	Parent mat'l failure in hot wall weld repaired and parts retested at elevated temperature.
HEX 6-6					Inco 600	Ni Plated	Ni Plated	1000	(811)	7,200	16,450	Repair Weld	
HEX 7-1					Inco 600	As Received	As Received	RT		5,800	13,260	Bond	Repeat of reduced load test (HEX 2) to provide samples for elevated temperature tests. Samples HEX 7-5 and HEX 7-10 were welded on Inconel side to simulate engine welding. Ni plating thickness = 0.00006 in. (0.00015 cm)
HEX 7-2					Inco 600	As Received	As Received	RT		4,000	9,140	Bond	
HEX 7-3					Inco 600	As Received	As Received	1000	(811)	1,900	4,340	Bond	
HEX 7-4					Inco 600	As Received	As Received	1000	(811)	2,200	5,030	Bond	
HEX 7-5	180	1700	(1200)	1000	Inco 600	As Received	As Received	RT		11,000	25,100	Bond	
HEX 7-6					Inco 600	Ni Plated	Ni Plated	RT		7,000	16,000	Bond	
HEX 7-7					Inco 600	Ni Plated	Ni Plated	RT		5,400	12,340	Bond	
HEX 7-8					Inco 600	Ni Plated	Ni Plated	1000	(811)	3,200	7,310	Bond	
HEX 7-9					Inco 600	Ni Plated	Ni Plated	1000	(811)	2,000	4,570	Bond	
HEX 7-10					Inco 600	Ni Plated	Ni Plated	RT		3,000	6,860	Bond	
HEX 8-1					Inco 600	As Received	As Received	1000	(811)	-	-	Bond	Reduced temperature and load test. Samples HEX 8-4 and HEX 8-7 welded on Inconel side to simulate engine welding. HEX 8-1 would not hold pressure when pressurized. Ni plating thickness = 0.00008 to 0.00009 in. (0.00020 to 0.00023 cm)
HEX 8-2					Inco 600	As Received	As Received	RT		2,000	4,200	Bond	
HEX 8-3					Inco 600	As Received	As Received	1000	(811)	600	1,260	Bond	
HEX 8-4					Inco 600	As Received	As Received	RT		200	420	Bond	
HEX 8-5	180	1300	(978)	2700	Inco 600	As Received	As Received	RT		1,500	3,150	Bond	
HEX 8-6					Inco 600	Ni Plated	Ni Plated	1000	(811)	1,500	3,150	Bond	
HEX 8-7					Inco 600	Ni Plated	Ni Plated	RT		9,800	20,600	Bond	
HEX 8-8					Inco 600	Ni Plated	Ni Plated	RT		4,000	8,400	Bond	
HEX 8-9					Inco 600	Ni Plated	Ni Plated	RT		10,600	22,200	Bond	
HEX 8-10					Inco 600	Ni Plated	Ni Plated	1000	(811)	600	1,260	Bond	
HEX 9-1					Inco 600	As Received	As Received	1000	(811)	4,500	9,210	Bond	Intermediate temperature test. HEX 9-4 and HEX 9-7 welded on Inconel side to simulate engine welding.
HEX 9-2					Inco 600	As Received	As Received	RT		18,500	37,800	Bond	
HEX 9-3					Inco 600	As Received	As Received	1000	(811)	2,400	4,910	Bond	
HEX 9-4					Inco 600	As Received	As Received	RT		23,500	48,100	Bond	
HEX 9-5	180	1500	(1089)	6000	Inco 600	As Received	As Received	RT		20,000	41,000	Bond	
HEX 9-6					Inco 600	Ni Plated	Ni Plated	1000	(811)	4,000	8,190	Bond	
HEX 9-7					Inco 600	Ni Plated	Ni Plated	RT		26,000	53,200	Parent Mat'l	
HEX 9-8					Inco 600	Ni Plated	Ni Plated	RT		27,000	55,300	Parent Mat'l	
HEX 9-9					Inco 600	Ni Plated	Ni Plated	RT		23,500	48,200	Parent Mat'l	
HEX 9-10					Inco 600	Ni Plated	Ni Plated	1000	(811)	5,300	10,870	Bond	

Table XVIII. Experimental Diffusion Bonding Results (Continued)

Sample No.	Bond Conditions: Time, min	Temperature, °F	Temperature, (°K)	Load, psi**	Structural Plate Material	Surface Preparation*: Hot Wall Plate	Structural Plate	Test Temperature, °F	Test Temperature, (°K)	Test Burst Pressure, psi**	Calculated Bond Stress, psi**	Type Failure	Comments
HEX 10-1					Inco 600	Electro Polished	Electro Polished	RT		1,000	2,150	Bond	Ni-Co plating thickness = 0.0002 to 0.0004 in. (0.00051 to 0.00102 cm) All samples except No. -1, -6, and -8 were solution and precipitation heat-treated per AMS 5598 after brazing (i.e., 1800°F for 1 hr, A/C, 1325°F for 8 hr cool 100°F/hr, and 1150°F for 8 hr A/C)
HEX 10-2					Inco 600	Electro Polished	Electro Polished	1000	(811)	3,100	6,350	Bond	
HEX 10-3					Inco X-750	Electro Polished	Ni-Co Plated	1000	(811)	1,500	3,220	Bond	
HEX 10-4					Inco X-750	Electro Polished	Ni-Co Plated	1000	(811)	2,000	4,300	Bond	
HEX 10-5	180	1500	(1089)	2000	Inco X-750	Electro Polished	Ni Plated	1000	(811)	1,825	3,740	Bond	
HEX 10-6					Inco 600	Ni Plated	Ni Plated	RT		200	430	Bond	
HEX 10-7					Inco 600	Ni Plated	Ni Plated	1000	(811)	3,050	6,550	Bond	
HEX 10-8					Inco 600	Ni Plated	Ni Plated	RT		15,000	30,700	Bond	
HEX 10-9					Inco 600	Ni Plated	Ni Plated	1000	(811)	4,000	8,590	Parent Mat'l	
HEX 10-10					Inco 600	Ni Plated	Ni Plated	1000	(811)	4,600	9,880	Bond	
HEX 11-1	480	1500	(1089)	5300	Inco 600	Ni Plated	Ni Plated	1000	(811)	5,600	12,030	Bond	Ni-Co plating thickness = 0.0002 to 0.0004 in. (0.00051 to 0.00102 cm)
HEX 11-2					Inco X-750	Electro Polished	Ni Cobalt Plated	1000	(811)	3,575	7,680	Bond	
HEX 12-1					Inco 600	Ni Plated	Ni Plated	1000	(811)	6,000	14,720	Bond	0.062-in. (0.157 cm) thick nickel-200 hot wall plate having chemically machined grooves used in each HEX 12 sample. Cu plating thickness on structural plates = 0.00007 to 0.00018 in. (0.00018 to 0.00046 cm)
HEX 12-2					Inco 600	Electro Polished	Electro Polished	RT		22,000	66,000	Bond	
HEX 12-3					Inco 600	Electro Polished	Electro Polished	1000	(811)	5,100	13,250	Bond	
HEX 12-4					Inco 600	Ni Plated	Ni Plated	RT		21,200	63,400	Bond	
HEX 12-5	180	1700	(1200)	4600	Inco 600	Ni Plated	Ni Plated	1000	(811)	4,500	11,500	Bond	
HEX 12-6					Inco 600	Cu Plated	Cu Plated	RT		28,000	74,500	Bond	
HEX 12-7					Inco 600	Cu Plated	Cu Plated	1000	(811)	3,600	9,060	Bond	
HEX 12-8					Inco 600	Cu Plated	Cu Plated	-		-	-	Bond	
HEX 12-9					Inco 600	Cu Plated	Cu Plated	RT		30,000	73,000	Bond	
HEX 12-10					Inco 600	Cu Plated	Cu Plated	1000	(811)	5,000	12,880	Bond	
HEX 13-1					Inco 600	Cu Plated	Cu Plated	1000	(811)	4,500	9,670	Bond	0.062-in. (0.157 cm) thick nickel 200 hot wall plate having chemically machined grooves used in HEX 13-2 and HEX 13-4. Plating thickness approximately = 0.0001-in. (0.00025 cm)
HEX 13-2					Inco 600	Cu Plated	Cu Plated	1000	(811)	2,800	8,250	Bond	
HEX 13-3					Inco 600	Ni Plated	Ni Plated	1000	(811)	7,000	15,030	Parent Mat'l	
HEX 13-4					Inco 600	Mech. Polish	As Received	1000	(811)	6,500	20,400	Bond	
HEX 13-5	360	1900	(1311)	2000	Inco 600	Ni Plated	Ni Plated	1000	(811)	5,000	10,750	Bond	
HEX 13-6					Inco 600	Cu Plated	Cu Plated	1000	(811)	4,400	9,450	Bond	
HEX 13-7					Inco 600	Electro Polished	Electro Polished	1000	(811)	7,000	15,030	Parent Mat'l	
HEX 13-8					Inco 600	Mech. Polish	As Received	1000	(811)	7,000	15,030	Parent Mat'l	
HEX 13-9					Inco 600	Ni Plated	Ni Plated	-		-	-	-	
HEX 13-10					Inco 600	Ni Plated	Ni Plated	1000	(811)	6,000	12,890	Parent Mat'l	

*As received material had approximately 16-32AA finish.

**n/cm^2 = (psi) (0.6895)

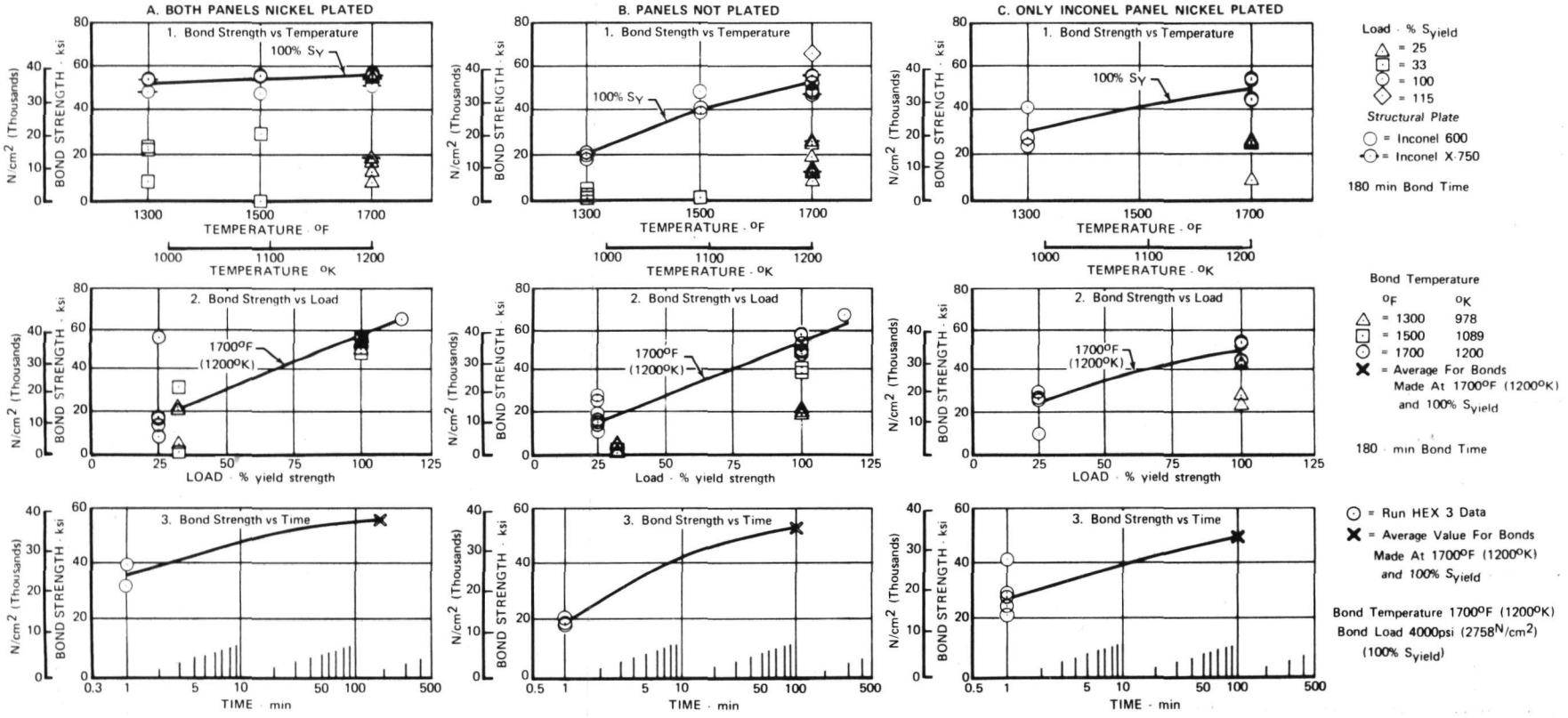

Figure 49. Diffusion Bonding Parameter Correlations for Ambient Temperature Tests

FD 59703

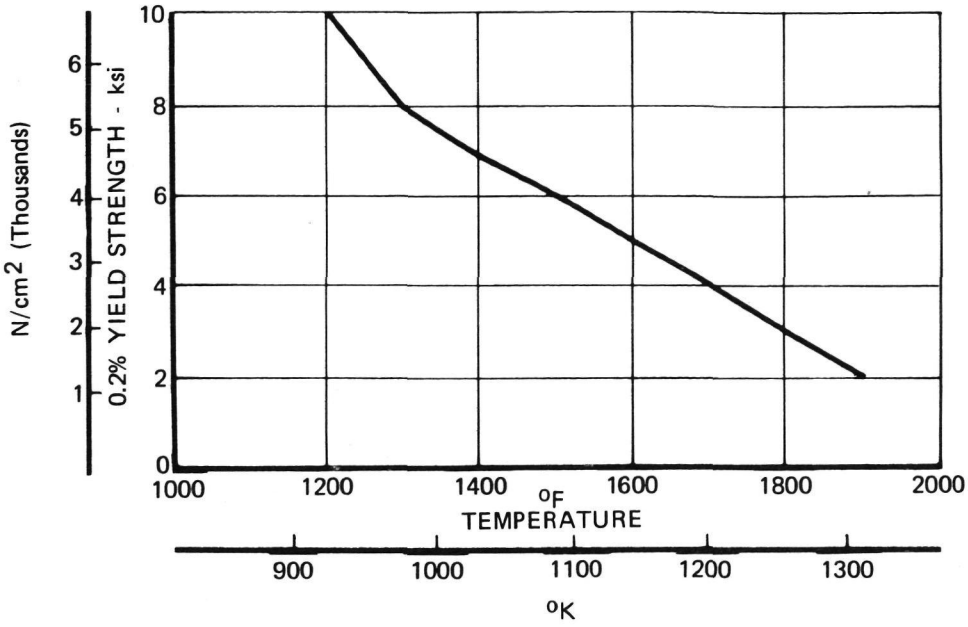

Figure 50. Approximate Yield Strength of Nickel-200 at Elevated Temperatures FD 59704

Highest bond strengths were obtained at the higher values of bonding temperature, time, and load, and when both panels were nickel plated prior to bonding. For both-panels-nickel-plated samples, only a slight degradation in bond strength was indicated when the bonding temperature was reduced from 1700°F (1200°K) to 1300°F (978°K), provided yield load was used during bonding and provided the bond time was 180 min. Reducing the load or reducing the bond time gave reduced strengths. No difference in bond strength between Nickel 200 and Inconel 600 or Nickel 200 and Inconel X-750 was detected.

Panels not plated or plated on only the Inconel side demonstrated significant reduction in bond strength at bond conditions less than 1700°F (1200°K), 100% yield load, or 180 min. duration.

Nickel 200 strength is reported to be dependent on grain size (Reference 8), and Nickel 200 thermal cycle life is suspected to be

dependent on grain size. Figures 51 shows that the surface roughness of hydrostatic pressure test samples was significantly greater for panels bonded at 1700°F (1200°K) compared with panels bonded at 1300°K (978°K). Comparison between nickel grain size for panels bonded at 1300°F (978°K) and 1700°F (1200°K) is illustrated in figure 52.

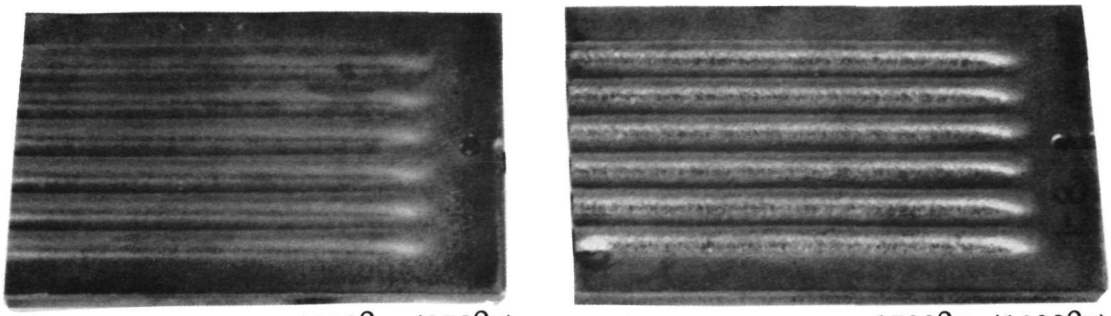

Bond Temperature = 1300°F (978°K) Bond Temperature = 1700°F (1200°K)

Figure 51. Effect of Bonding Temperature on Nickel Surface FD 48596

The 14 diffusion bonded samples from run series No. HEX 0 and HEX 1 were metallographically examined after hydrostatic pressure testing. The bond interfaces were found to have an accumulation of carbides (figure 53), however, no voids were found in any of these bond areas. The accumulated particles at the bond line did not cause poor tensile strengths at room temperature but may be responsible for poor strength at elevated temperatures. Subsequent tests were made at elevated temperatures and are discussed below.

Metallographic examination of the HEX 2 samples (bonded at reduced (load) showed significant voids along the bond line (figure 54) which illustrated the importance of having high bond load to achieve intimate contact at the bond joint.

Section View of Sample No. HEX4-4,
Bond Temperature = 1300°F (978°K)

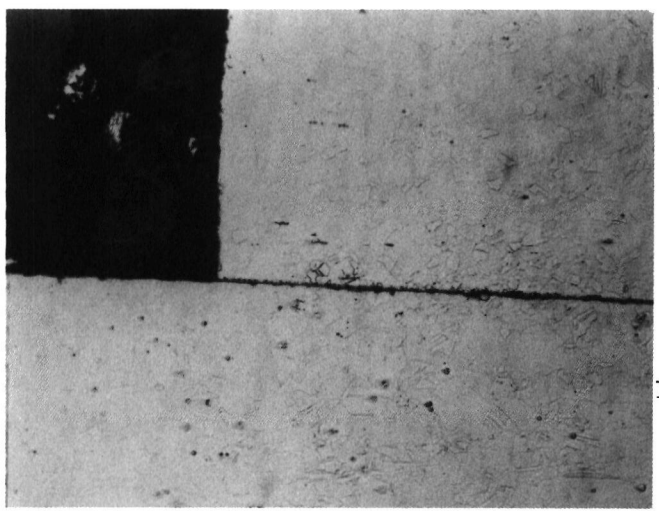

100X

FD 49976A

Section View of Sample No. HEX5-1,
Bond Temperature = 1700°F (1200°K)

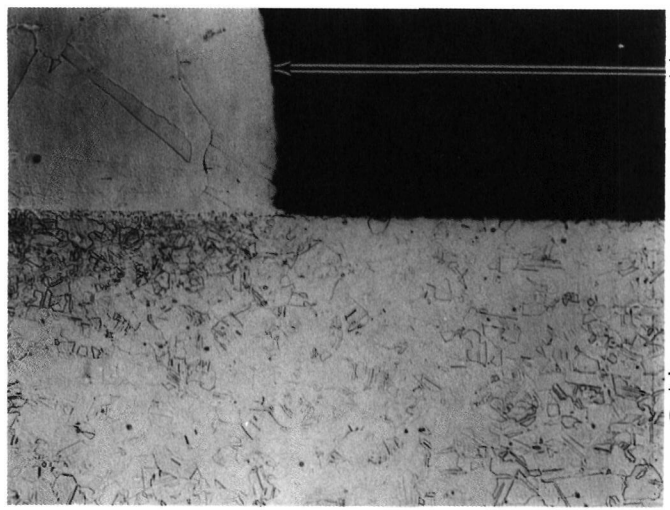

100X

FD 49977A

Figure 52. Photomicrographs Showing Effect of Bonding Temperature on Nickel Grain Size

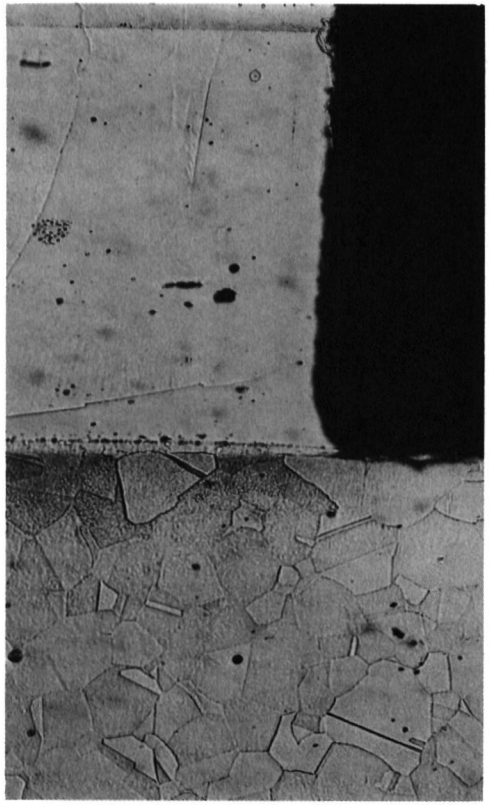

a. Nl-200 to Inconel 600 Diffusion Bond HEXO-4 (Soft Tooling)

FAM 49919

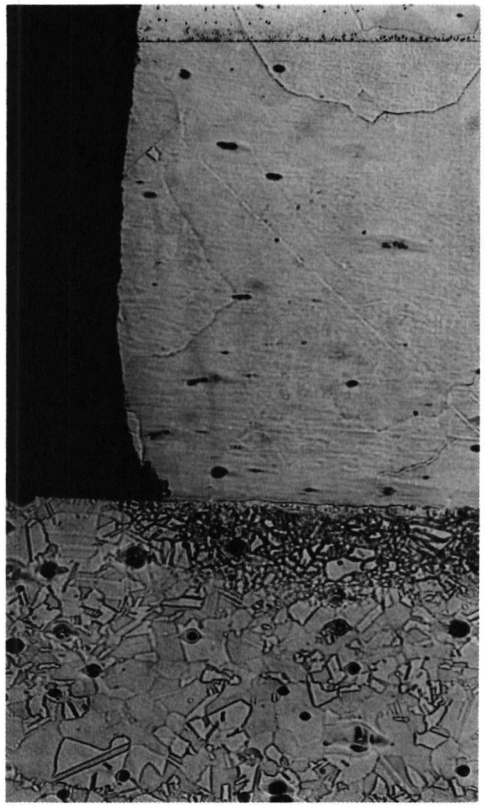

b. Ni-200 to Inconel X-750 (Ni Plated) HEXl-8 (Hard Tooling)

FAM 49918

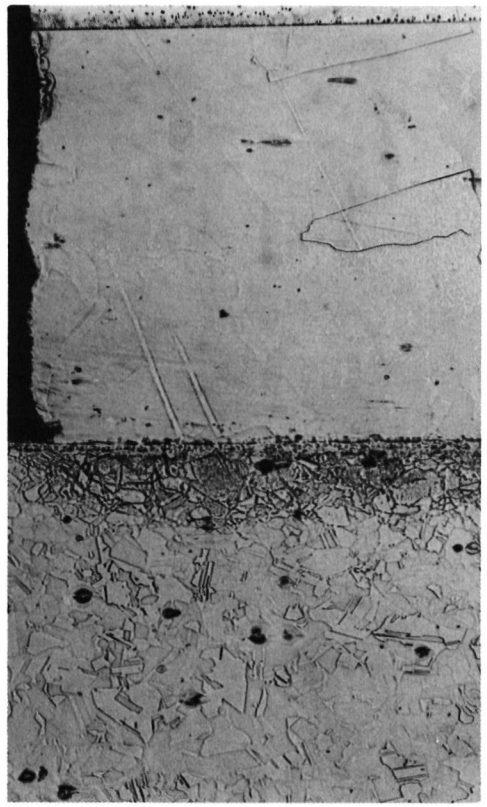

c. Ni-200 to Inconel X-750 (Ni Plated) Diffusion Bond HEXl-9 (Hard Tooling)

FAM 49917

Figure 53. Typical Photomicrographs of Diffusion Bonds

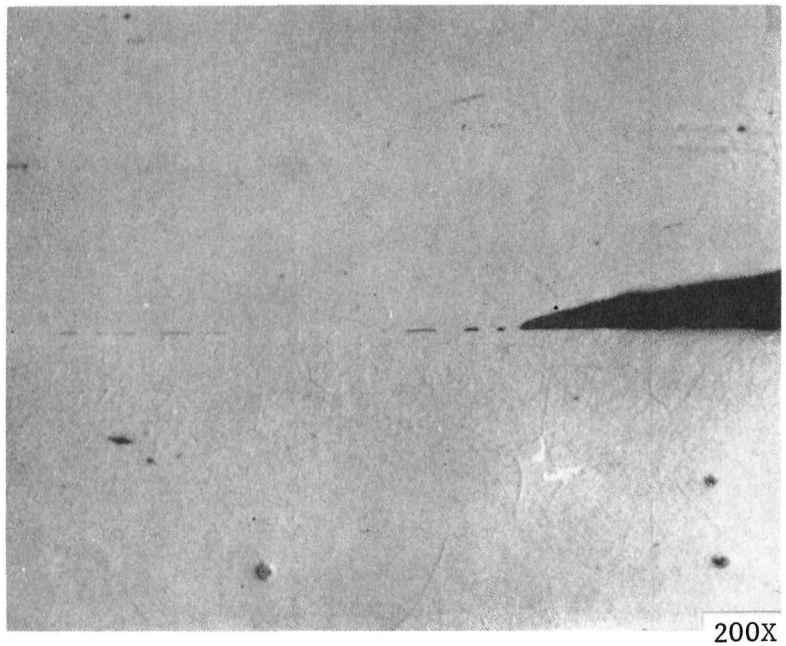

200X

a. As Polished

FAM 51048

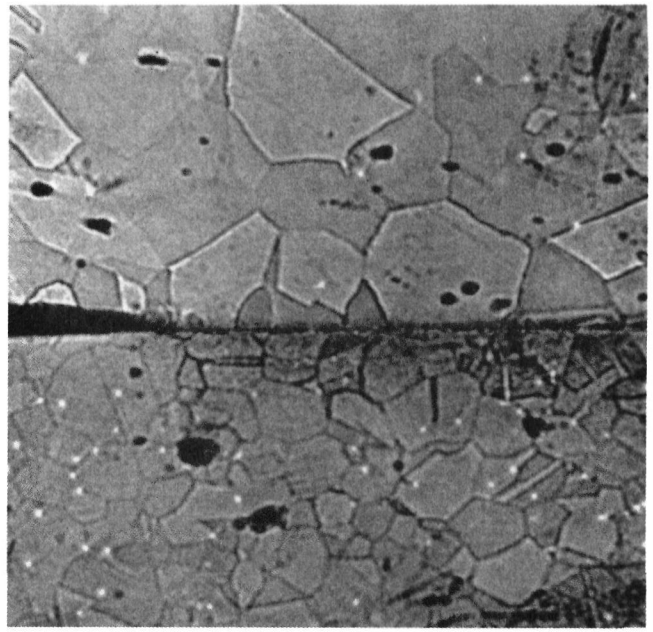

100X

b. Polished and Etched

FAM 50871

Figure 54. Photomicrographs Showing Effect of 25% Yield Strength Bond Load

b. Elevated Temperature Test Results

Results of pressure tests conducted at 1000°F (811°K) are presented in figure 55. In each case, contrary to the room temperature results, less than parent metal bond strength was observed. The nickel-plated samples bonded at 1700°F (1200°K) and 100% nickel yield strength bond load failed at 47 to 63% of parent metal (Nickel 200) strength. Nickel-plated samples bonded at 1500°F (1089°K) and 100% nickel yield strength bond load failed at 31 to 42% of parent metal strength. The unplated samples demonstrated bond strengths still lower than those of the plated samples.

In an attempt to improve the bond strength at elevated temperatures, seven of the ten samples from run HEX 10 were heat-treated after bonding using the solution and precipitation heat-treat cycles for Inconel X-750 (i.e. 1800°F (1255°K) for 1 hr A/C, 1325°F (991°K) and 8 hr cool (100°F/hr (311°K/hr), and 1150°F (894°K) for 8 hr A/C). The heat-treatment apparently did not improve the bond strengths and these samples demonstrated bond strengths below the parent material (Nickel 200) strength. It was noted without conclusion that the surface texture of the heat-treated parts in the failure regions (figure 56) was similar to that observed during thermal cycle life testing discussed in Section VI.

Post-test examination of samples bonded at 1700°F (1200°K) and tested at elevated temperatures revealed incomplete bonding areas along the lands. Representative views presented in figures 57 and 58 show localized areas that were poorly bonded. These localized poorly bonded areas could have initiated premature failure of the sample. The use of hard tooling which cannot compensate for nonuniformities in plate thickness was suspected to be responsible for the weak bonds.

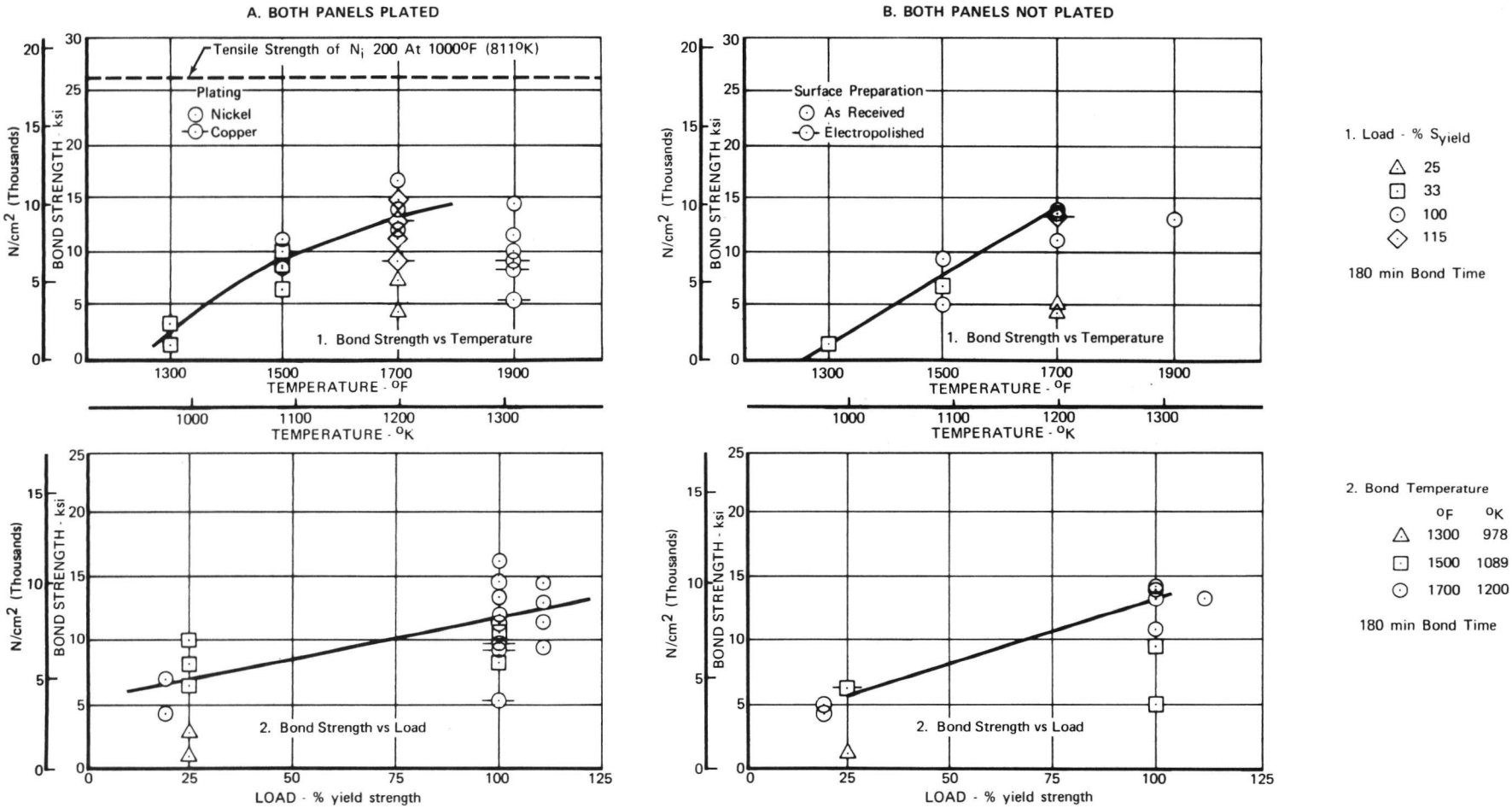

Figure 55. Diffusion Bonding Parameter Correlations for Elevated Temperature Tests

FD 59707

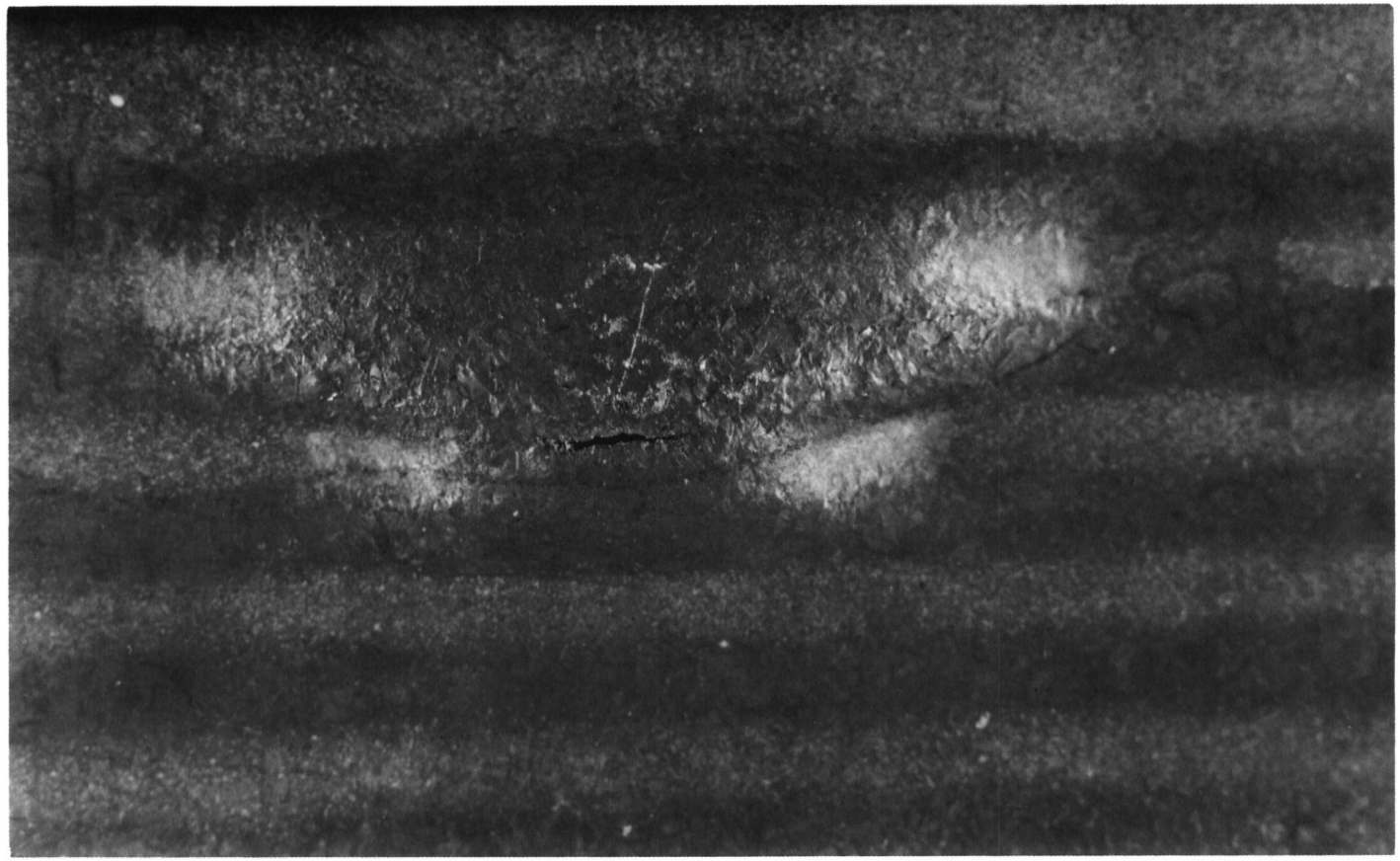

Figure 56. Nickel Surface After HEX10-4 Pressure Test

FE 108102

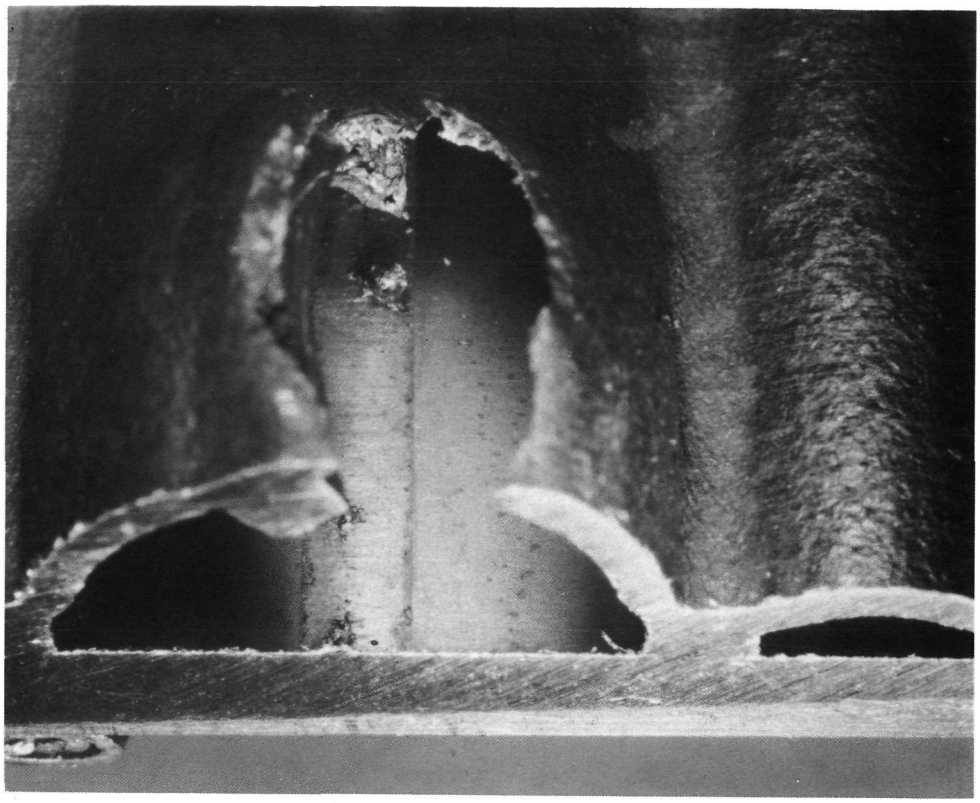

Figure 57. Bond Failure After HEX6-9 1000°F (811°K) Pressure Test FAL 20895

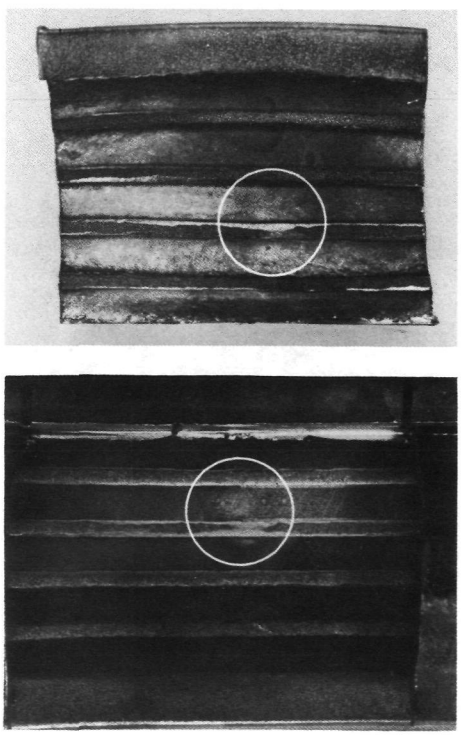

Figure 58. Bond Failure After HEX12-3 1000°F (811°K) Pressure Test FD 51851

Test samples from bond run HEX 13, made at 1900^{0}F (1311^{o}K) bond temperature, demonstrated high bond strengths at 1000^{o}F (811^{o}K), however, hot wall failures occurred preventing attainment of rupture loads on the bond. A typical hot wall failure observed from run HEX 13 tests is shown in figure 59. Stress concentration in the square cornered passage of the hot wall may have been responsible for reduced burst pressures.

Figure 59. Parent Material Failure After HEX13-8 1000^{o}F (811^{o}K) Pressure Test FAL 21860

c. Diffusion Aids

Electroplated nickel, copper, and 60% nickel-40% cobalt were investigated as aids to diffusion; each gave improved bond strengths over non-plated samples. At room temperature, bond strengths at least

as great as Nickel 200 strength were achieved with each type diffusion aid. However, at 1000°F (811°K) bond failures occurred before parent metal failures therefore indicating that less than complete bonding had been achieved.

The series HEX 13 bonds included samples with copper filler, nickel filler, and no filler; typical photomicrographs are shown in figure 60. In each case it appeared that a cloud of precipitate, probably carbides that were concentrated at the surfaces before bonding, had diffused into the Inconel 600 material. Little or no diffusion of the braze fillers into the parent materials was observed.

d. Effect of Welding

To investigate the effect of external welding on diffusion-bonded parts, heliarc welds were made on the Inconel side of two samples from run HEX 6, 7, 8, and 9, using a Hastelloy-W welding rod (figure 61). No bond degradation was found.

e. Electron Microprobe Analysis

Samples HEX 4-8, 4-9, and 6-10 were selected for electron microprobe analysis to determine elemental gradients. This analysis indicated little or no homogenization of the constituents of either Inconel 600 or Inconel X-750 across the bond line and into Nickel 200 plates. The nickel and iron distribution scans from samples HEX 5-1 and 6-10 are shown in figures 62 and 63, respectively. The 0.0025 in. (0.00635 cm) bond filler region is indicated on each scan.

3. Effect of Diffusion Bonding Temperature Cycle on Parent Material Strength

Plate stock samples of Nickel 200, Nickel 201, Inconel 600, and Inconel X-750 were each subjected to a diffusion bonding thermal cycle of 180 minutes to determine the effect of this heat treatment on their

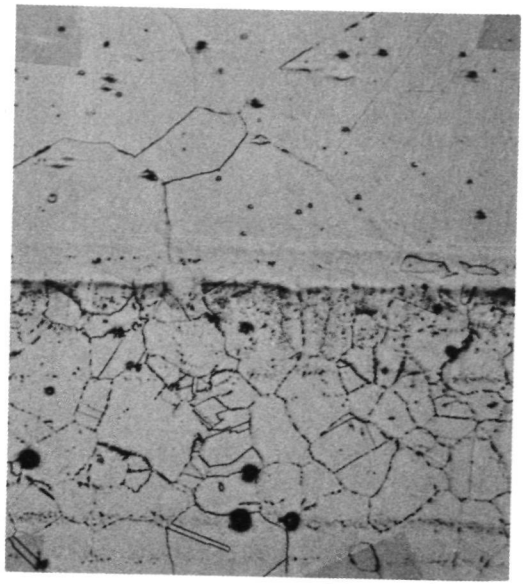

Mag: 100X

FAM 60468

a. Sample HEX13-1
(Copper Diffusion Aid)

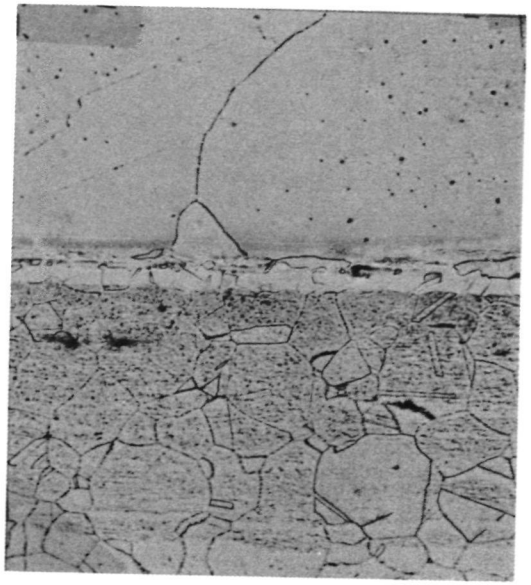

Mag: 100X

FAM 60469

b. Sample HEX13-3
(Nickel Diffusion Aid)

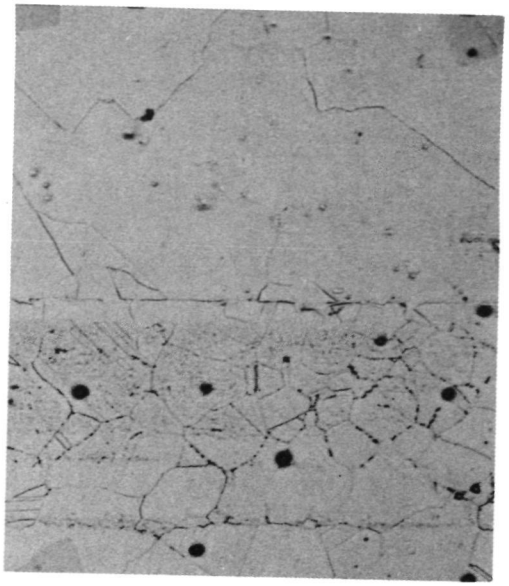

Mag: 100X

FAM 60470

c. Sample HEX13-8
(No Diffusion Aid)

Figure 60. Photomicrographs of Typical Bonds Obtained with Diffusion Aids

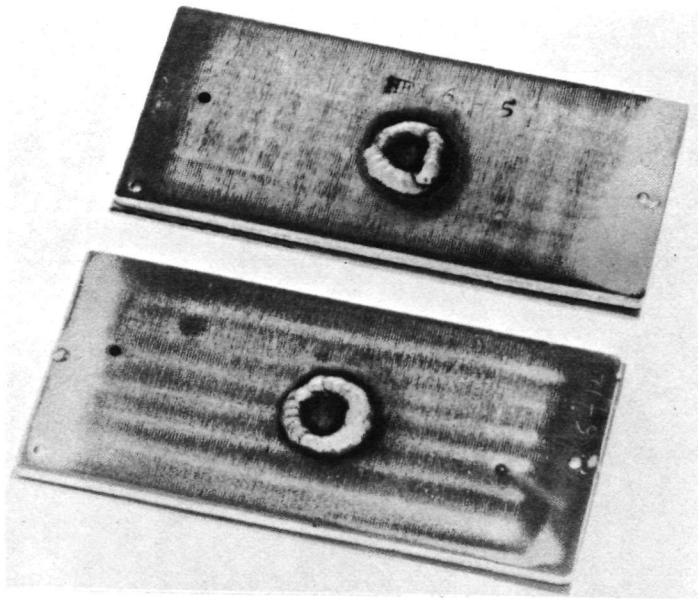

Figure 61. Typical Heliarc Welded Samples FE 105760

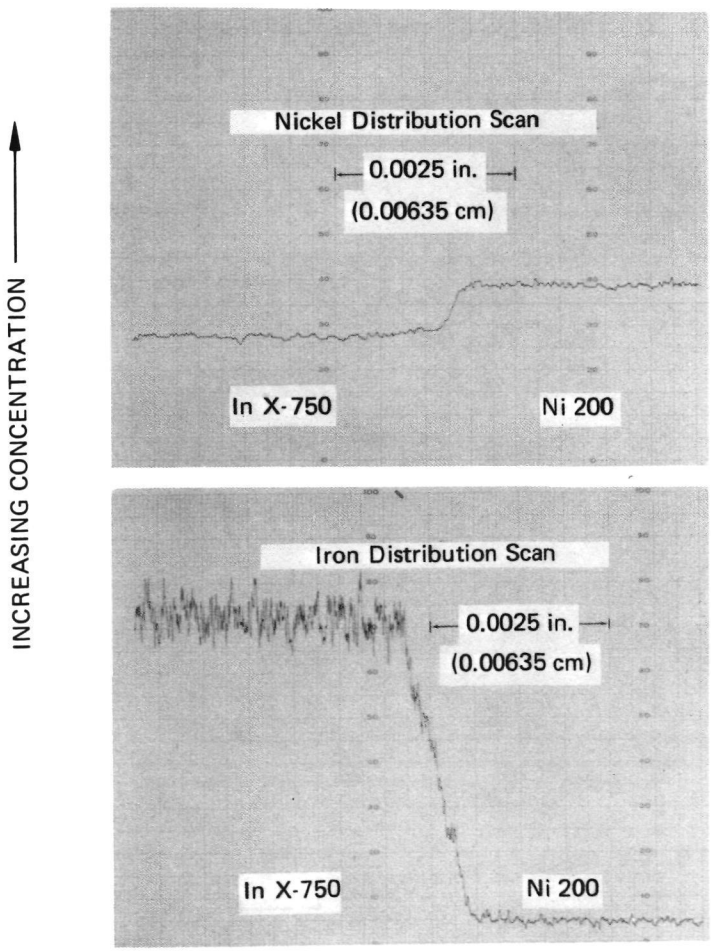

Figure 62. Electron Microprobe Scan for Sample HEX5-1 FD 59709

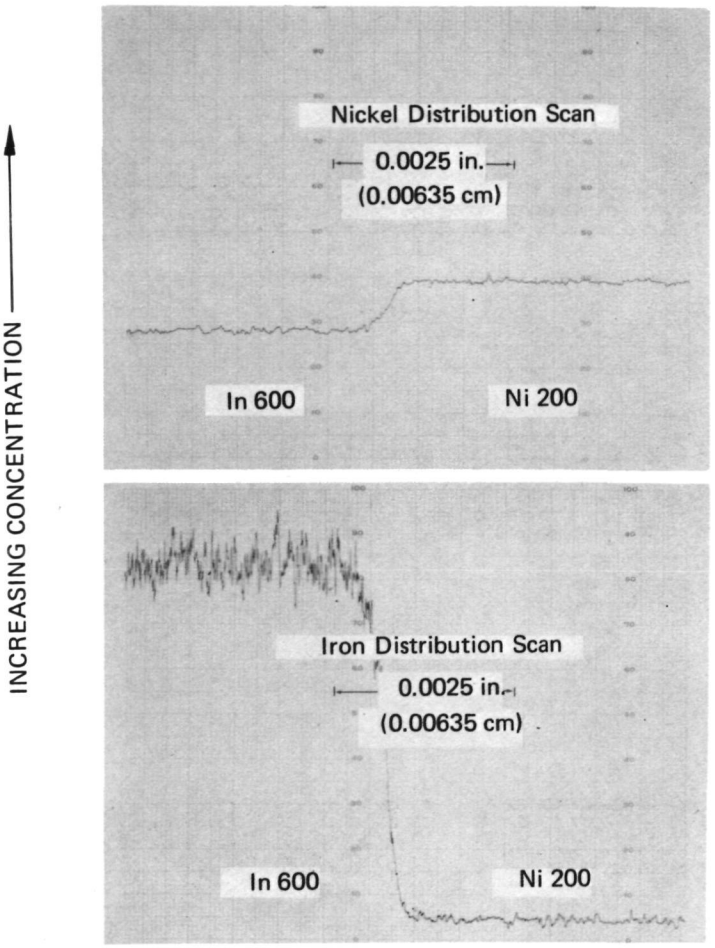

Figure 63. Electron Microprobe Scan for Sample HEX6-10 FD 59708

respective tensile strength. Tensile tests were performed at 1000°F (811°K), a representative engine operating temperature.

The tensile test results are compared with material design strength values in table XIX. Nickel 200 and Nickel 201 material tensile strengths were not affected significantly by the temperature cycle; Inconel 600 yield strength decreased about 7000 psi but was still about 4500 psi above the design value; and the Inconel X-750 yield strength almost doubled after thermal cycling because the material was in the annealed condition as received, and heating it to 1700°F (1200°K) for 3 hr had the effect of partially age-hardening the material. However, the

Table XIX. Effect of Diffusion Bonding Temperature Cycle on Parent Material Strengths

Material	Condition*	Yield Strength 0.2% Offset, psi [1]	Ultimate Tensile Strength, psi [1]	Elongation %
Nickel 200	As received	11,560	32,500	64.5
Nickel 200	As received	13,020	31,300	32.3
Nickel 200	Temperature cycled	9,430	31,770	60.5
Nickel 200	Temperature cycled	9,560	32,200	54.5
Nickel 200	Design value	9,100	26,100	69.0
Nickel 201	As received	9,030	31,200	58.3
Nickel 201	As received	8,730	30,900	32.8
Nickel 201	Temperature cycled	11,500	31,400	30.5
Nickel 201	Temperature cycled	7,950	28,520	28.5
Nickel 201	Design value	NA	NA	NA
Inconel 600	As received	35,500	91,300	39.8
Inconel 600	As received	35,100	89,300	40.3
Inconel 600	Temperature cycled	28,550	83,500	36.0
Inconel 600	Temperature cycled	27,650	80,000	31.8
Inconel 600	Design value	22,400	74,200	46.4
Inconel X-750	As received**	42,300	101,200	45.0
Inconel X-750	As received**	45,800	105,100	58.0
Inconel X-750	Temperature cycled	83,800	144,300	31.0
Inconel X-750	Temperature cycled	83,000	144,600	32.0
Inconel X-750	Design value***	102,400	139,200	18.6
Inconel X-750	Fully heat treated	117,100	158,600	21.8
Inconel X-750	Fully heat treated	117,800	159,200	26.0
Inconel X-750	Temperature cycled	72,100	126,400	36.7
Inconel X-750	Temperature cycled	72,100	126,400	38.5

*All temperature cycled material heated at 1700°F (1200°K) for 180 min.

**Annealed.

***Solution heat treated.

[1] n/cm^2 = (psi)(.6895)

yield strength for Inconel X-750 was still less than the design value for the fully age-hardened condition. Starting with fully heat-treated Inconel X-750 material, the simulated diffusion bonding cycle reduced the yield strength from approximately 117,000 to 72,000 psi (80,669 to 49,642 n/cm^2). This Inconel could have been restored to its full heat-treated strength by a subsequent heat treatment.

C. DIFFUSION BONDING EVALUATION (Task V-2)

1. General

The need for diffusion bonding using soft tooling to provide a uniform pressure load, and therefore accommodate small variations in plate thickness and parallelism, was established during the experimental bonding work discussed in Paragraph B. During this phase of the program a new bonding tool which was hydrostatically pressurized at temperature was investigated. The tool provided uniform pressure loading and the design was scaleable to larger sizes.

Chemically machined plates were prepared for the bonding tests using the diffusion bonding tool, and dimensional evaluations of these plates were made for comparison with earlier chemical machining results.

2. Chemically Machined Plates

Plates for diffusion bonding were manufactured using the optimum etching techniques developed during the program and outlines in Appendix B. Dimensional data for the etched plates (Nickel 200 and Inconel 600) are presented in Tables XX and XXI. The dimensions achieved illustrate the tolerances which can be expected from the chemical machining process and show a significant improvement over earlier results. Although noticeable deviation from design dimensions were accepted,

Table XX. Dimensional Data for Commercially Produced Nickel Plates

		Design Dimensions				Measured Dimensions					Calculated Data				
Part No.* DKJ	Serial No.	Land Width, in. 1	Passage Width, in.	Passage Depth, in.	Plate Thickness, in.	Land Width,** in.	Passage Width,*** in.	Passage Depth,*** in.	Plate Thickness, in.	Surface Finish, rms	Side Etch, %	Area Factor, Area/DXW	Planned Test Use, Task No.	Comments
8408	1	0.050	0.066	0.024	0.125	0.058 +0.000 -0.002	0.058 +0.002 -0.000	0.024 +0.000 -0.001	0.125-0.126		43.8 +4.1 -0.0			Sample PWA-1.
8408	2	0.050	0.066	0.024	0.125	0.057 +0.002 -0.002	0.059 +0.002 -0.002	0.024 +0.001 -0.000	0.125-0.126		45.8 +4.2 -4.1		V-2;VI	Sample PWA-2.
8408	3	0.050	0.066	0.024	0.125	0.056 +0.001 -0.000	0.060 +0.000 -0.001	0.024 +0.000 -0.001	0.125-0.126		46.0 +1.9 -0.2		V-2;VI	
8408	4	0.050	0.066	0.024	0.125	0.058 +0.001 -0.001	0.058 +0.001 -0.001	0.024 +0.001 -0.001	0.125-0.126		43.8 +2.0 -2.1	0.82 +0.05 -0.01	V-2;VI	Sample PWA-5.
8408	5	0.050	0.066	0.024	0.125	0.057 +0.000 -0.001	0.059 +0.001 -0.000	0.023 +0.002 -0.000	0.126		47.8 +0.1 -3.8		V-2;VI	
8408	6	0.050	0.066	0.024	0.125	0.057 +0.001 -0.000	0.059 +0.000 -0.001	0.023 +0.001 -0.000	0.125-0.126	43	47.8 +0.0 -4.0			
8408	7	0.050	0.066	0.024	0.125	0.055 +0.001 -0.000	0.061 +0.000 -0.001	0.025 +0.001 -0.000	0.124-0.126	61	48.0 +0.0 -3.8			
8408	8	0.050	0.066	0.024	0.125	0.055 +0.001 -0.001	0.061 +0.001 -0.001	0.025 +0.001 -0.001	0.124-0.126	59	48.0 +2.0 -2.0			
8409	1	0.050	0.037	0.024	0.125	0.051 +0.000 -0.001	0.036 +0.001 -0.000	0.023 +0.001 -0.000	0.125-0.126		56.5 +2.2 -2.3	0.90 +0.02 -0.04	V-2;VI	
8409	2	0.050	0.037	0.024	0.125	0.049 +0.002 -0.000	0.038 +0.000 -0.002	0.025 +0.000 -0.001	0.123-0.125		56.0 +2.3 -2.0			Sample PWA-6.
8409	3	0.050	0.037	0.024	0.125	0.051 +0.001 -0.001	0.036 +0.001 -0.001	0.022 +0.002 -0.001	0.124-0.126	63#	59.0 +2.9 -4.7			
8409	4	0.050	0.037	0.024	0.125	0.051 +0.001 -0.002	0.036 +0.002 -0.001	0.022 +0.002 -0.001	0.122-0.125	63#	59.0 +0.5 -2.2			
8409	5	0.050	0.037	0.024	0.125	0.049 +0.001 -0.001	0.038 +0.001 -0.001	0.025 +0.000 -0.001	0.124-0.126	63#	56.0 +2.0 -2.0			
8409	6	0.050	0.037	0.024	0.125	0.045 +0.005 -0.002	0.042 +0.002 -0.005	0.025 +0.001 -0.001	0.123-0.125	63#	64.0 +2.0 -8.0			
8409	7	0.050	0.037	0.024	0.125	0.046 +0.002 -0.001	0.041 +0.001 -0.002	0.024 +0.000 -0.001	0.122-0.125	63#	64.6 +2.1 -4.3			
8410	1	0.050	0.108	0.046	0.125	0.067 +0.001 -0.002	0.091 +0.002 -0.001	0.045 +0.001 -0.001	0.126		42.2 +1.3 -1.0		V-2	Sample PWA-3.
8410	2	0.050	0.108	0.046	0.125	0.065 +0.002 -0.001	0.093 +0.001 -0.002	0.046 +0.002 -0.001	0.124-0.126	28	43.5 +1.2 -1.3			
8410	3	0.050	0.108	0.046	0.125	0.066 +0.002 -0.003	0.092 +0.003 -0.002	0.045 +0.001 -0.000	0.121-0.125	33	43.3 +3.4 -3.1			
8410	4	0.050	0.108	0.046	0.125	0.056 +0.001 -0.004	0.102 +0.004 -0.001	0.058 +0.001 -0.002	0.122-0.127	35	42.2 +4.3 -0.9			
8410	5	0.050	0.108	0.046	0.125	0.060 +0.002 -0.002	0.098 +0.002 -0.002	0.046 +0.000 -0.001	0.124-0.126	60	48.9 +3.3 -2.2			
8411	1	0.100	0.197	0.046	0.125	0.117 +0.001 -0.002	0.180 +0.002 -0.001	0.045 +0.000 -0.000	0.124-0.126	19	42.2 +2.2 -1.1	0.94 +0.00 -0.04	V-2	Sample PWA-4.
8412	1	0.100	0.050	0.046	0.125	0.090 +0.003 -0.007	0.060 +0.007 -0.003	0.045 +0.003 -0.001	0.123-0.125		55.6 +4.5 -3.4		V-2;VI	

*Waycoat PF or equvalent photoresist was used on all plates.
**Calculated based on "master" dimensions and measured passage width.
***Dimensions determined from RTV photo-inspection technique.
#Passage is too narrow for inspection tooling. Visually checked with a surface comparator.

1 cm = (in) (2.540)

Table XXI. Dimensional Data for Commercially Produced Inconel-600 Plates

Part No.* DKJ	Serial No.	Design Dimensions: Land Width, in.	Passage Width, in.	Passage Depth, in.	Plate Thickness, in.	Measured Dimensions: Land Width,** in.	Passage Width,*** in.	Passage Depth,*** in.	Plate Thickness, in.	Surface Finish, rms	Calculated Data: Side Etch, %	Area Factor, Area/DXW	Comments
8401	1	0.050	0.066	0.024	0.050	0.056 +0.001 -0.005	0.060 +0.005 -0.001	0.025 +0.001 -0.000	0.051-0.052		46.0 +7.8 -3.7		Sample PWA-1.
8401	2	0.050	0.066	0.024	0.050	0.056 +0.002 -0.002	0.060 +0.002 -0.002	0.025 +0.001 -0.001	0.051-0.0515		46.0 +4.0 -2.0		
8401	3	0.050	0.066	0.024	0.050	0.054 +0.002 -0.003	0.062 +0.003 -0.002	0.026 +0.000 -0.002	0.051-0.052		48.1 +7.9 -2.1	0.79 +0.00 -0.06	Sample PWA-5.
8401	4	0.050	0.066	0.024	0.050	0.054 +0.004 -0.002	0.062 +0.002 -0.004	0.025 +0.000 -0.001	0.051-0.052		50.0 +2.0 -8.0		Sample PWA-2.
8401	5	0.050	0.066	0.024	0.050	0.050 +0.001 -0.000	0.066 +0.000 -0.001	0.022 +0.000 -0.000	0.050-0.051	24	65.9 +0.0 -2.2		
8401	6	0.050	0.066	0.024	0.050	0.047 +0.000 -0.002	0.069 +0.002 -0.000	0.025 +0.001 -0.001	0.050-0.052	60	64.0 +6.8 -2.4		
8401	7	0.050	0.066	0.024	0.050	0.046 +0.000 -0.004	0.070 +0.004 -0.000	0.025 +0.000 -0.001	0.050-0.052	60	66.0 +8.0 -0.0		
8402	1	0.050	0.066	0.024	0.060	0.054 +0.001 -0.002	0.062 +0.002 -0.001	0.024 +0.002 -0.001	0.062-0.063		52.1 +2.2 -4.1		
8403	1	0.050	0.037	0.024	0.050	0.050 +0.001 -0.004	0.037 +0.004 -0.001	0.021 +0.002 -0.000	0.051-0.0515		64.3 +3.0 -5.1	0.80 +0.09 -0.02	
8403	2	0.050	0.037	0.024	0.050	0.050 +0.002 -0.004	0.037 +0.004 -0.002	0.021 +0.002 -0.000	0.051-0.0515		64.3 +3.0 -5.2		Sample PWA-6.
8403	3	0.050	0.037	0.024	0.050	0.044 +0.001 -0.002	0.043 +0.002 -0.001	0.024 +0.001 -0.001	0.050-0.051	63#	68.7 +5.1 -2.0		
8403	4	0.050	0.037	0.024	0.050	0.043 +0.001 -0.002	0.044 +0.002 -0.001	0.025 +0.000 -0.001	0.050	63#	68.0 +7.0 -2.0		
8403	5	0.050	0.037	0.024	0.050	0.042 +0.001 -0.002	0.045 +0.002 -0.001	0.024 +0.002 -0.001	0.050-0.051	63#	72.9 +4.2 -3.7		
8403	6	0.050	0.037	0.024	0.050	0.043 +0.001 -0.001	0.044 +0.001 -0.001	0.025 +0.000 -0.001	0.050-0.052	63#	68.0 +4.9 -0.0		
8403	7	0.050	0.037	0.024	0.050	0.045 +0.001 -0.003	0.042 -0.003 -0.001	0.024 +0.001 -0.001	0.050-0.051	63#	66.7 +7.2 -2.7		
8404	1	0.050	0.108	0.024	0.050	0.053 +0.001 -0.004	0.105 +0.004 -0.001	0.023 +0.001 -0.000	0.051-0.052		56.5 +8.7 -2.3		Sample PWA-3.
8404	2	0.050	0.108	0.024	0.050	0.049 +0.001 -0.001	0.109 +0.001 -0.001	0.023 +0.000 -0.000	0.050-0.052	39	65.2 +2.2 -2.2		
8404	3	0.050	0.108	0.024	0.050	0.044 +0.001 -0.003	0.114 +0.003 -0.001	0.024 +0.001 -0.001	0.050-0.052	70	72.9 +6.3 -4.9		
8404	4	0.050	0.108	0.024	0.050	0.045 +0.000 -0.000	0.113 +0.000 -0.000	0.023 +0.000 -0.000	0.050-0.051	86	73.9 +0.0 -4.3		
8405	1	0.050	0.108	0.024	0.060	0.047 +0.001 -0.002	0.111 +0.002 -0.001	0.023 +0.000 -0.001	0.061-0.063	89	69.6 +4.3 -2.2		
8406	1	0.100	0.197	0.024	0.050	0.099 +0.002 -0.005	0.198 +0.005 -0.002	0.025 +0.000 -0.001	0.051-0.0515	115	60.0 +10.0 -8.0	0.87 +0.06 -0.00	Sample PWA-4.
8407	1	0.100	0.050	0.024	0.050	0.100 +0.003 -0.002	0.050 +0.002 -0.003	0.022 +0.001 -0.001	0.051-0.0515		65.9 +5.5 -4.0		

*Waycoat PF or equivalent photoresist was used on all plates.
**Calculated based on "master" dimensions and measured passage width.
***Dimensions determined from RTV photo-inspection technique.
#Passage too narrow for inspection tooling. Visually checked with a surface comparator.

1 cm = (in) (2.540)

dimensional variations within a given plate were small indicating that by iteration of the etching master, precise design dimensions can be achieved. The passage shape of two typical plates are shown in figures 64 and 65.

3. Diffusion Bonding Tool

An experimental bonding tool which could take plates up to 6 in x 6 in (15.24 cm x 15.24 cm) was designed and built (figure 66). The tool consisted of a structural box which housed a pressuring diaphragm block, and a block for holding the panel to be bonded while providing a controlled atmosphere. A thin metal diaphragm was seam welded over the experimental bond panel so that fluid pressure load could be transmitted uniformly to the panel. A thin metal diaphragm was seam welded in place on the pressure block. The tool was constructed completely of Waspalloy^{TM} and is shown in figure 67 prepared for assembly.

To use the tool, a panel to be bonded is placed in the panel block beneath a thin metal cover which is coated with stop-off solution to prevent bonding to the panel. The metal cover is seam welded in place so that a vacuum atmosphere can be achieved. The panel block and pressurizing block are placed in the structural housing and fifteen preloading bolts are tightened against the pressure block. The assembly is placed inside a standard brazing furnace having an inert or reducing atmosphere. After reaching the bond temperature water pressure is applied to the pressure diaphragm using a hand operated positive displacement pump. A small diameter heavy-wall stainless steel tube was used between the pump (located outside of the oven) and the tool pressure block. Although steam existed in the pressure block and part of the supply pressure tubing, the volume was small and the system reacted as if a completely incompressible fluid was used.

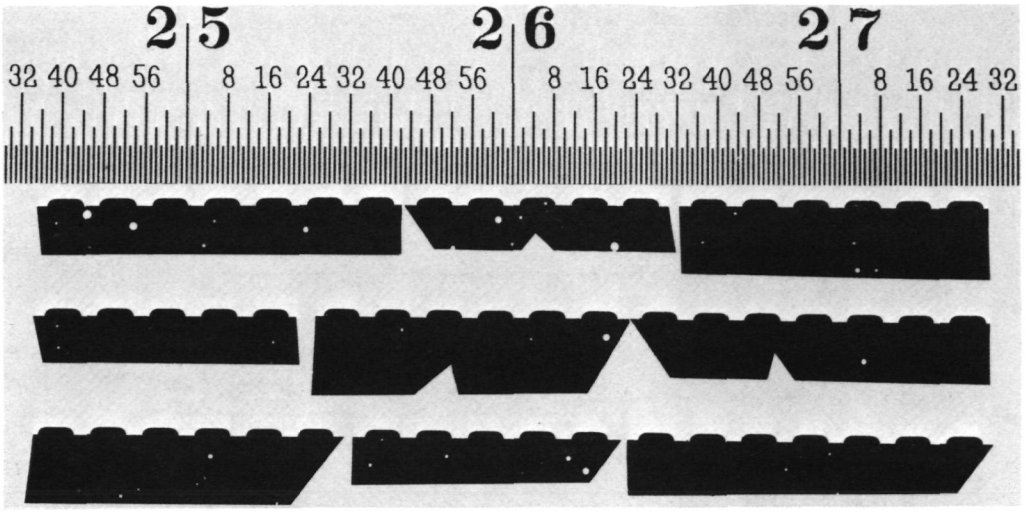

Figure 64. Section Views of Etched Plate Showing Typical Wide Passage Shape FAC 25240

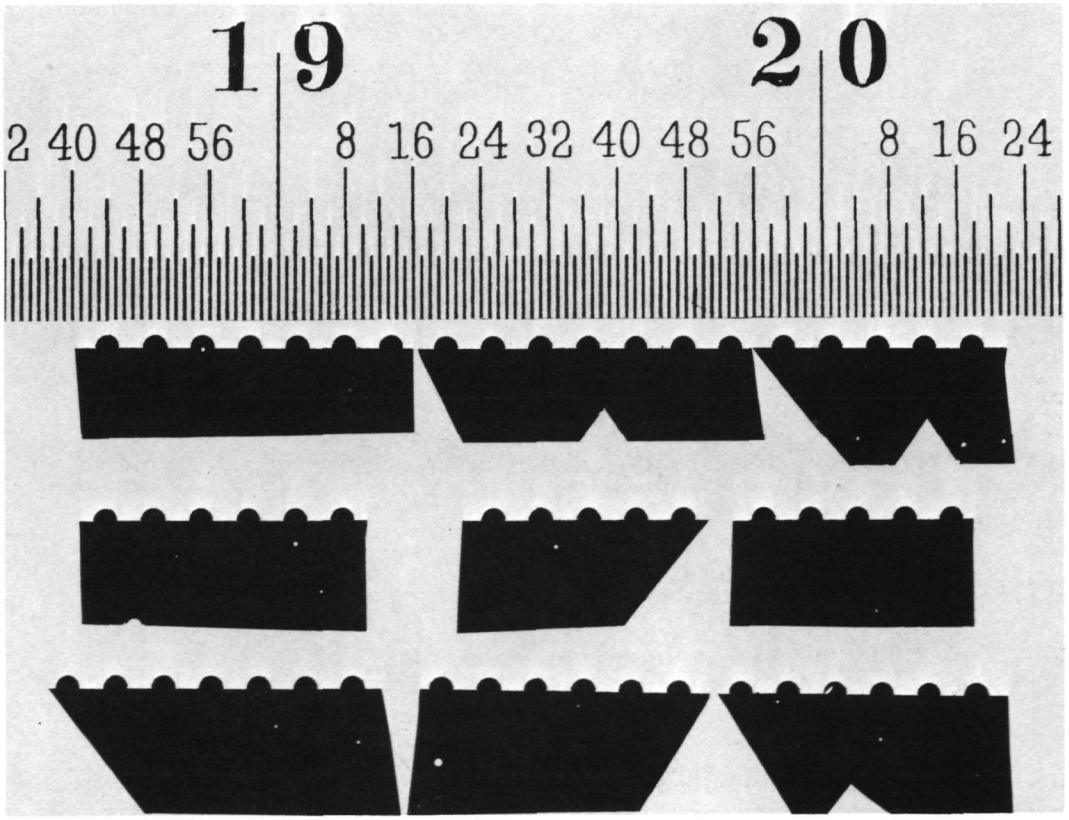

Figure 65. Section Views of Etched Plate Showing Typical Narrow Passage Shape FAC 25235

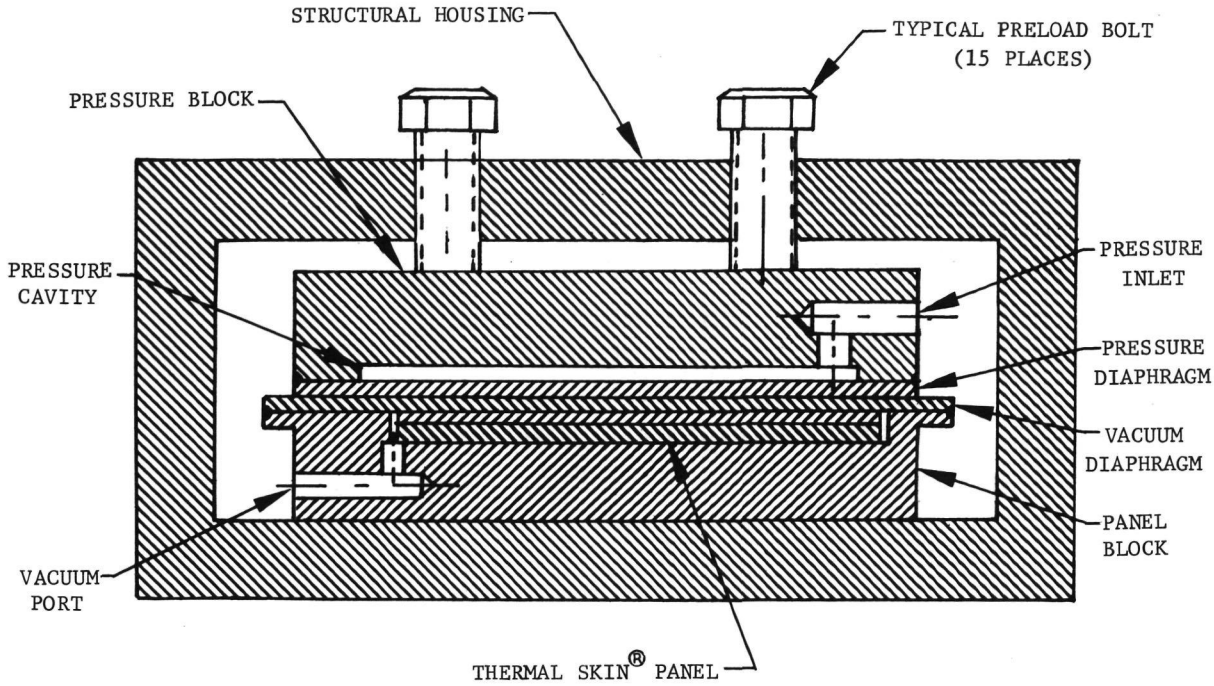

Figure 66. Diffusion Bonding Tool Schematic

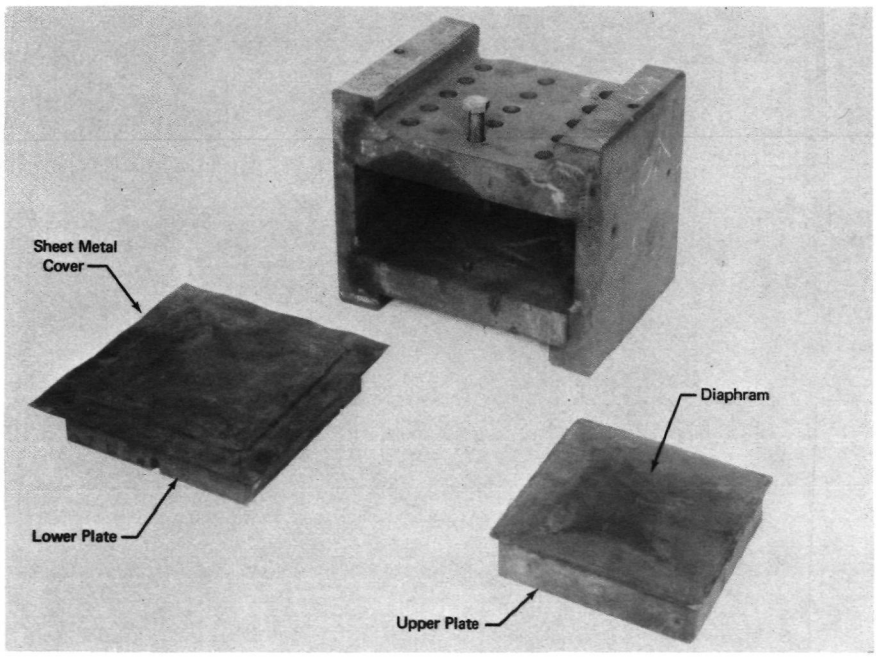

Figure 67. Diffusion Bonding Tool Photograph FE 110089A

4. Diffusion Bonding Runs

Good bonds were attained at 1700°F (1200°K), 100% Nickel 200 yield strength load, and a 180 min. duration during the effort described in Section B, and nickel plating both plates before bonding improved the reliability of attaining a good bond. These conditions were used as a starting point for use with the diffusion bonding tool.

The runs performed with the diffusion bonding tool are outlined in Table XXII. During each bonding run the welded pressure diaphragm leaked at temperature. Several modifications to the diaphragm geometry were made including use of Waspalloy, Inconel 600, and a specially designed diaphragm having a thick periphery for welding and a thin center for flexibility (Figure 68). However, the diaphragm welds persisted in cracking during operation and a major redesign of the tool was beyond the scope of the program.

The feasibility of the type tooling investigated was best demonstrated during the third run where a pressure of 1900 psig was maintained for 20 min. at 1500°F (1089°K). Pressure tests of the panel bonded during this run indicated that about 50% parent metal strength was achieved in the bond (Table XXIII).

5. Alternative Bonding Methods

Two alternative methods of bonding Thermal Skin panels were briefly investigated: (1) electroless nickel brazing, and (2) "auto-vac" bonding. The results of these investigations are discussed in the following paragraphs.

a. Electroless Nickel Brazing

In the electroless nickel brazing method both panels were electroless nickel plated, the nickel plating containing 8 to 10% phosphorus

Table XXII. Summary of PWA Diffusion Bonding Tests

Bond No.	Ni-200 Plate P/N	Inco-600 Plate P/N	Temp. ^{o}F (^{o}K)	Time* min.	Tool Pressure psi (n/cm^2)	Comments
PWA-1	DKJ-8401-1	DKJ-8408-1	1500 (1089)	10/75	2000 (1379)	Weld leak at pressurizing diaphragm.
PWA-2	DKJ-8401-4	DKJ-8408-2	1700 (1200)	3/180	1725 (1189)	Seam weld design modified before test did not prevent weld leak at pressure.
PWA-3	DKJ-8404-1	DKJ-8410-1	1500 (1089)	20/180	1900 (1310)	Inconel 600 pressurizing diaphragm used (was Wapaloy™) - did not prevent a weld leak at pressure. Pressure test result of bond samples presented in Monthly No. 28.
PWA-4	DKJ-8406-1	DKJ-8411-1	1500 (1089)	6/180	2020 (1393)	Weld leaks at Inconel 600 pressurizing diaphragm.
PWA-5	DKJ-8401-3	DKJ-8408-4	1700 (1200)	28/180	1725 (1189)	Improved diaphram design-electron beam welded - did not prevent seam weld leak.
PWA-6	DKJ-8403-2	DKJ-8409-2	1700 (1200)	1/180	2300 (1586)	Repaired PWA-5 diaphram-still leaked at pressure.
PWA-7	DKJ-8403-1	DKJ-8409-1	1700 (1200)	5/180	2300 (1586)	Had unusualy pressure spike to 3500 psi (2413 n/cm^2) at start-weld leak occured 5 min later.

*First number is time at pressure, second is time at temperature.

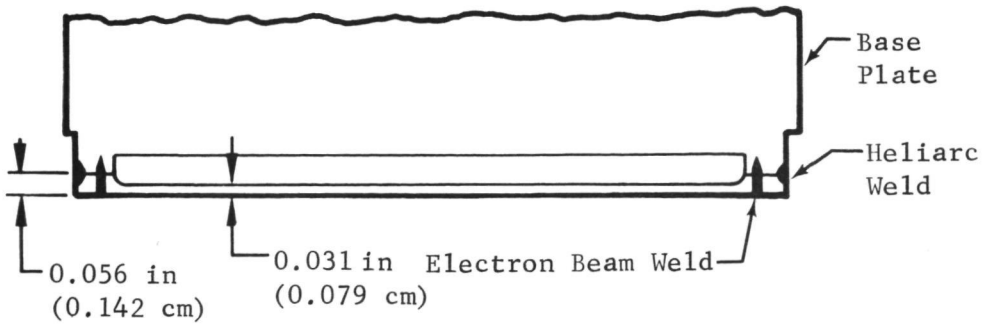

Figure 68. Modified Pressure Diaphragm Design FD 56619

and being between 0.0002 to 0.0003 in. thick (0.00051 to 0.00076 cm). The phosphorus in the plating depresses the melting point to about 1635°F (1164°K) and when subjected to temperatures greater than 1635°F (1164°K) melts and forms a conventional braze bond. If conditions are held, the phosphorus diffuses into the parent material and the melting temperature of the plating increases. In theory, the plating resolidifies at constant temperature as the phosphorus diffuses. In sufficient time, enough phosphorus diffuses into the parent material to give a near-nickel material-strength bond.

A summary of the electroless nickel bond results is presented in Table XXIV. Three 6 in x 6 in (15.24 cm x 15.24 cm) panels were bonded in a vacuum type retort at 1700°F (1200°K) and then cut into smaller samples for structural testing. The results of hydrostatic pressure tests performed with the electroless nickel bond samples are presented in Table XXV. Bond strengths achieved were well below the parent metal strength indicating additional development necessary. However, composition analysis and precise melting temperature determination of the electroless nickel should be performed before future bonding attempts are made.

Table XXIII. Diffusion Bonding Pressure Test Results

Sample No.*	Part No. and S/N	Bond Conditions			Test Temperature, °F	Hydrostatic Burst Pressure, psig (n/cm^2)	Calculated Bond Stress, psig (n/cm^2)	Type Failure
		Temperature, °F** (°K)	Time at Load, min	Load, psig (n/cm^2)				
PWA-3-A	8416-1	1500 (1089)	20	1900 (1320)	RT	9,200 (6353)	19,900 (13,731)	Bond***
PWA-3-B	8416-1	1500 (1089)	20	1900 (1320)	RT	11,600 (8008)	25,100 (17,316)	Bond
PWA-3-C	8416-1	1500 (1089)	20	1900 (1320)	RT	12,200 (8422)	26,400 (18,212)	Bond in edge margin

*Part was nickel plated 0.0001 in. (0.00025 cm.) maximum before diffusion bonding.
**Temperature was held for 3 hr.
***Failure may have started near weld along edge.

Table XXIV. Summary of Electroless Nickel Bonding Tests

Sample No.	Nickel Plate P/N	Inconel Plate P/N	Tests	Comments
ENB-1	DKJ-8401-2	DKJ-8408-3	1 EBW & tensile 3 Pressure	Bond retort malfunction may have prevented uniform pressure loading during bonding.
ENB-2	DKJ-8402-1	DKJ-8408-5	1 EBW & bend 3 Pressure	Bonded concurrently with ENB-3.
ENB-3	DKJ-8407-1	CKJ-8412-1	1 EBW & bend 3 Pressure	Bonded concurrently with ENB-2.

NOTE: Each plate was plated 0.0002 to 0.0003 in. (0.00051 to 0.00076 cm.) thick with 8% to 10% phosphorus nickel (1635°F (1164°K) melting temperature) by the electroless nickel plating process and brazed at 1700°F (1200°K) for 10 min. in a vacuum-type retort for plate loading.

Table XXV. Pressure Test Results for Electroless Nickel Bonds

Sample No.	Passage Width in. (cm.)	Land Width in. (cm.)	Failure Pressure psig (n/cm^2)	Calculated Bond Strength psi (n/cm^2)
ENB-1a			3000 (2079)	3200 (2206)
ENB-1b	0.060 (0.152)	0.056 (0.142)	3000 (2079)	3200 (2206)
ENB-1c			2900 (2010)	3100 (2137)
ENB-2a			Bond failed immediately	
ENB-2b	0.062 (0.157)	0.054 (0.137)	on pressurizing (50 psi)(.34 n/cm^2)	
ENB-2c				
ENB-3a			2000 (1389)	1360 (938)
ENB-3b	0.060 (0.152)	0.090 (0.229)	2000 (1389)	1360 (938)
ENB-3c			2000 (1389)	1360 (938)

NOTE: Each test performed at room temperature using water pressurant.

b. Auto-Vac Bonding

The second alternative bonding method investigated was the "auto-vac" cleaning technique examined by Moore and Holko at the NASA Lewis Research Center (Reference 7).

Moore and Holko found that in a steel assembly of two parts seal-welded at the periphery of the faying surfaces and heated to 2000°F (1367°K) for 30 minutes surface cleaning is self-generated. After an initial pressure increase due to the elevated temperature, a vacuum is formed within the sealed gap. This process has been explained as an absorption of the oxygen within the closed space. Further diffusion of metal ions to the surface enriches the surface with metal atoms. Moore called this process "auto-vac" cleaning because cleaning of the surfaces is autogenous (self-generated), and a vacuum is theoretically produced in the gap.

The panels that were to be bonded using the auto-vac technique were electron-beam welded around the periphery to enhance the auto-vac cleaning effect rather than heliarc welded. Electron beam welding was made in a vacuum therefore the Thermal Skin® passages were evacuated prior to the bonding process.

Three 6 in x 6 in (15.24 cm x 15.24 cm) panels were bonded using the auto-vac cleaning process. Temperatures were 1800°F (1255°K), 2000°F (1367°K), and 2200°F (1477°K) respectively for a run duration of 180 min. each. The auto-vac bonds are itemized in Table XXVI. The better of the three panels, sample AV-3, was bonded at the highest temperature, 2200°F (1477°K). It was later used for an electron beam weld tensile test specimen, which is discussed in the Electron Beam Welding Section.

Table XXVI. Summary of "Auto-Vac" Bonding Tests

Sample No.	Nickel Plate P/N	Inconel Plate P/N	Bond Temp. ^{o}F (^{o}K)	Bond Time min.	Tests	Comments
AV-1	DKJ-8403-7	DKJ-8409-7	1800 (1255)	180	None	No bond.
AV-2	DKJ-840-6	DKJ-8409-6	2000 (1367)	180	None	Bond failed during test sample preparation.
AV-3	DKJ-8403-3	DKJ-9409-3	2200 (1477)	180	EBW & tensile	Bond failed during test sample preparation.

NOTE: Each plate sandwich was clamped and electron beam seal welded in a vacuum to enhance the bonding process.

Although poor bonds resulted in each case it is believed that the general procedure has merit. The concept of electron beam seal welding a leak tight assembly and then bonding in an inert atmosphere at elevated temperature eliminates the need for expensive tooling and allows many panels to be bonded concurrently. Using a diffusion aid such as electroplated copper or electroless nickel appears attractive, but investigation in this direction was beyond the scope of this program.

ELECTRON BEAM WELDING

A. SUMMARY

Electron beam seam welding was investigated for joining individual Thermal Skin® panels. The investigation was made in four series of tests. In the first series, basic electron beam welding parameters (accelerating voltage, beam current, and weld speed) were investigated. The second series was conducted to investigate the effects of varying beam rotation, gun-to-work distance, beam focus, and beam-to-work angle. Various seam designs were investigated in the third series. The fourth series involved structural tests of samples welded using the optimum welding schedule established in the first three series of tests.

B. DESCRIPTION OF ELECTRON BEAM WELDING

Electron beam welding is attractive for joining Thermal Skin staves (figure 69) because it permits a very narrow fusion zone as well as a small heat-affected zone. Both features are desirable so that coolant passages can be located close to the seams for good cooling capability and will not be damaged during the stave-joining operation.

The electron beam produces such intense local heating that it almost instantly vaporizes a hole in the work piece. The walls of this hole are molten, and, as the beam moves along the work piece, the metal on the advancing side of the hole melts and flows around the advancing vapor core and solidifies along the rear side to make the weld.

An electron-beam gun is shown schematically in figure 70. Electrons are emitted from a cathode and accelerated toward an anode in a hard vacuum atmosphere. They pass through a small hole in the center of the anode and continue toward the work piece. An electromagnetic lens

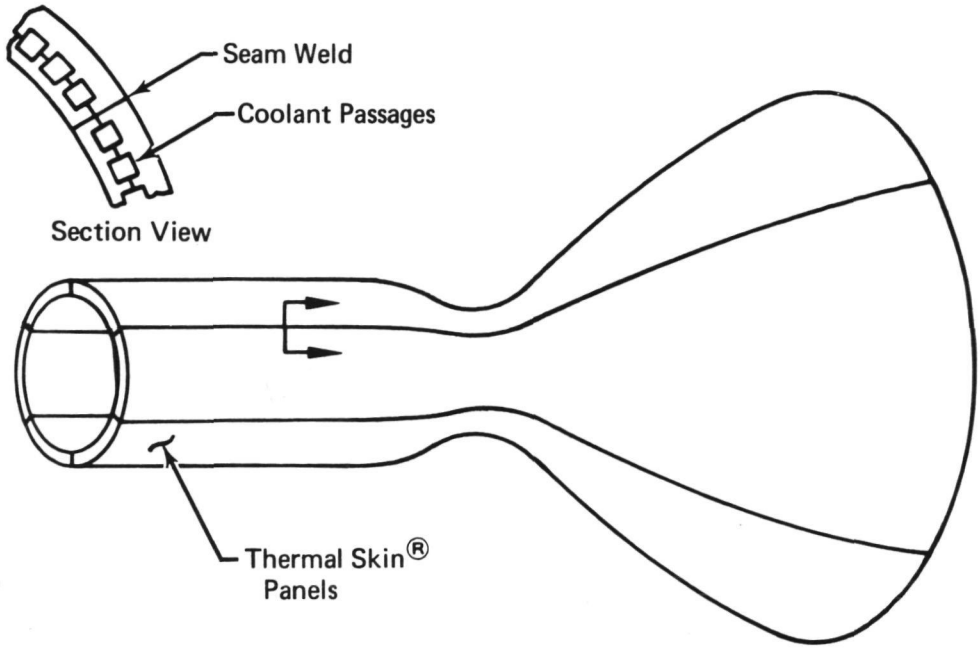

Figure 69. Thermal Skin® Chamber Schematic FD 47893A

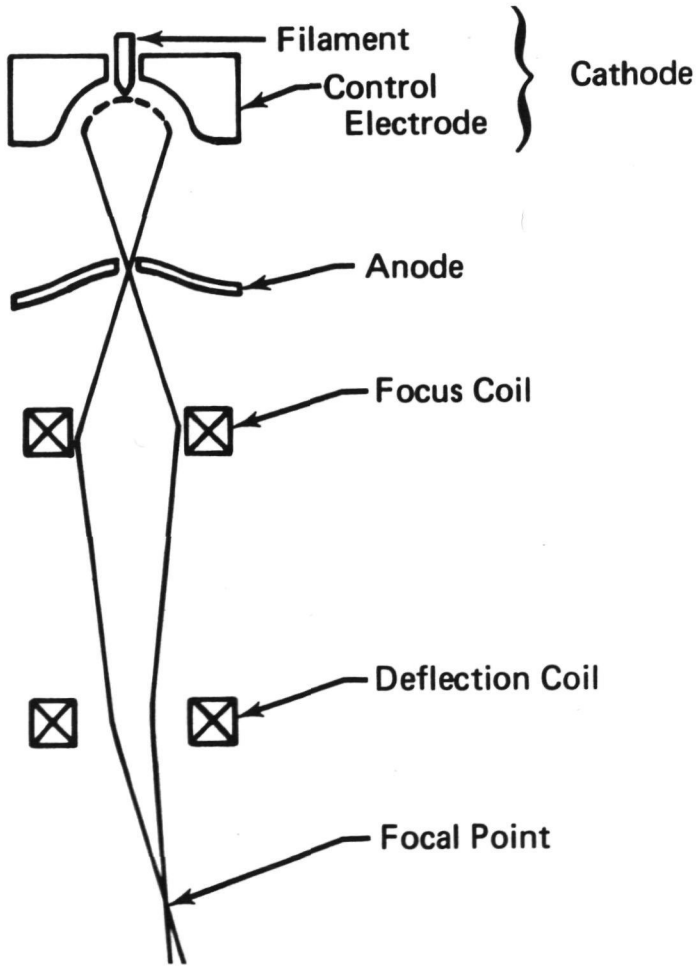

Figure 70. Electron Beam Gun Schematic FD 47894A

system (focus coil) placed downstream of the anode is used to converge the beam and to control the beam focal spot at the work piece.

A beam deflection coil just below the focus coil is sometimes used to deflect the beam from the gun centerline, either to follow a desired weld pattern or to create a cyclic beam pattern during welding. A rotating magnetic field can be created by the deflection coil so that the beam will be deflected in a circular pattern; this results in a "prolate cycloid" weld pattern on the work piece (figure 71) and in effect increases the beam diameter. Beam rotation was investigated during the program as a means of welding adjacent staves when there are relatively large gaps between them.

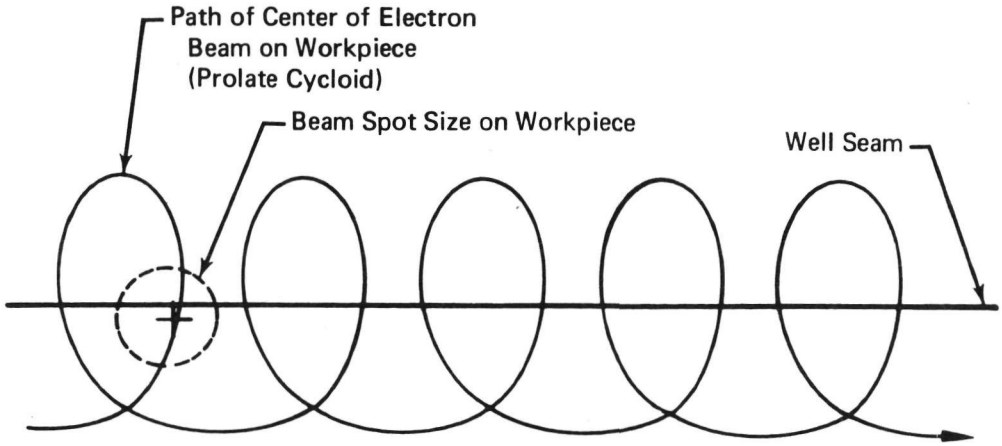

Figure 71. Electron Beam Weld Pattern Using Beam Deflection Coil FD 47895A

The two types of electron beam welders available are classified as either high or low voltage. Low voltage welders operate at levels up to 60 kv whereas high voltage equipment operates above 60 kv, usually up to 150 kv. Equivalent beam energies are obtained by using proportionately higher amperage levels in the low voltage welder. An important dif-

ference between the two types of equipment is that in the low voltage welder both the gun and the work piece are movable. In the high voltage machine, only the work piece moves. At present, high voltage equipment is not equipped with a movable gun because of the large size and bulk of the gun and the required amount of electrical insulation. Both types of equipment were investigated during the program to determine which would be best for welding Thermal Skin staves.

C. EXPERIMENTAL PROGRAM

1. Preliminary Welds

Exploratory welds were made using a high-voltage electron beam welder at FRDC to establish ranges to be investigated and to identify the most important variables. These welds were made using clamped Inconel 600 and Nickel 200 plates. All welds were made from the Inconel 600 side. The test samples after sectioning, polishing, and etching are shown in figure 72. Various combinations of voltage, current, and speed at several energy rates were investigated to determine their effects on the weld nugget shape and penetration. The results of photographic analysis of the welds are shown in table XXVII. Depth, width, and area recorded in table XXVII are illustrated in figure 73. Although the results indicate that all parameters (voltage, current, energy level, and speed) are important, the deepest penetrations and narrowest welds were obtained with high speeds and high energy levels.

2. Basic Parameter Tests

The basic electron beam welding parameters, (accelerating voltage, beam current, and weld speed) were investigated during Series I. These three variables determine the energy rate input to the work piece and

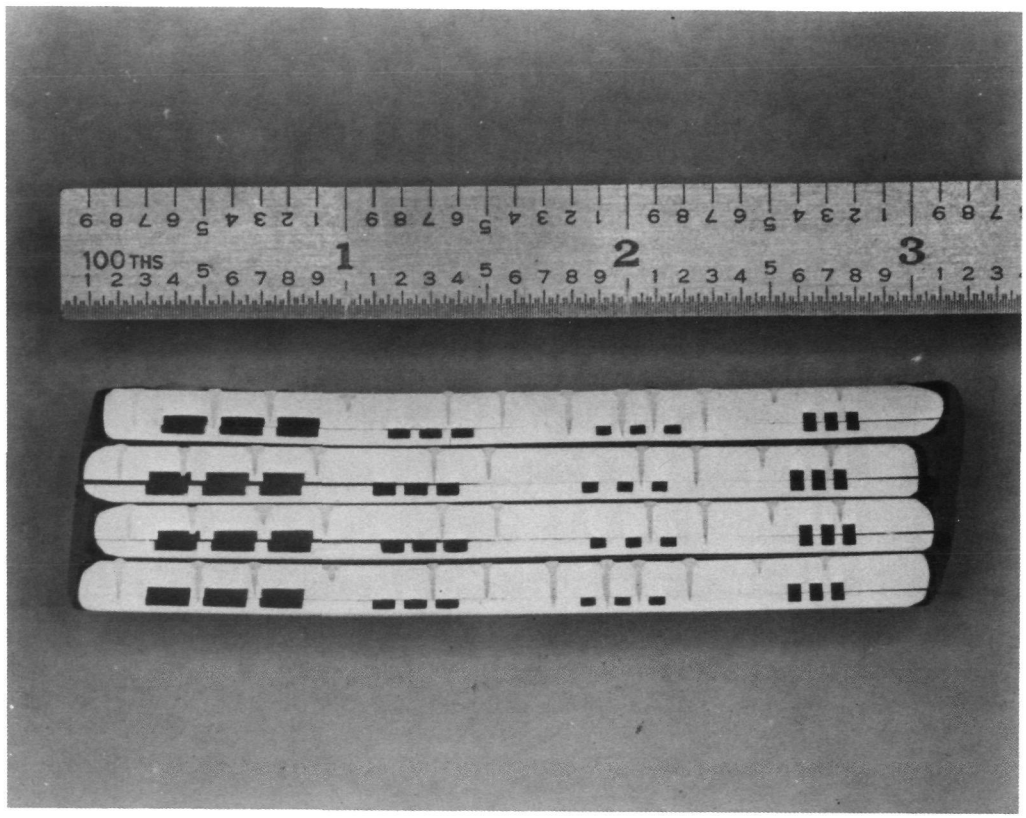

Figure 72. Preliminary Electron Beam Welds FAL 21169

have a significant effect on weld quality. Thirty welds were performed using low and high voltage equipment. The tests were performed using flat plates of Inconel 600 and Nickel 200 material machined to simulate a Thermal Skin chamber weld seam. The test sample design is shown in figure 74. The weld samples were constructed so that three magnitudes of seam gap were welded during each test. The mating edges of the samples were stepped so that distinct gap dimensions were achieved and maintained during welding. The test sample design called for zero-gap regions between 0.005 and 0.010 in (0.013 and 0.025 cm) gap regions to prevent the weld from drawing the plates together and closing the gap. Actual gap dimensions were measured prior to welding and deviated somewhat from the design dimensions.

Table XXVII. Results of Preliminary Electron Beam Welds

Weld No.	Voltage, kv	Current, ma	Speed, ipm[1]	Energy Rate, joules/in.[2]	Depth, in.[3]	Width, in.[3]	Area, in.[2,4]	Depth/ Width
1	140	5.7	30	1600	0.147	0.025	0.035	5.88
2	140	5.7	40	1200	0.135	0.022	0.030	6.15
3	140	5.7	60	800	0.120	0.018	0.022	6.65
4	140	2.86	40	600	0.050	0.024	0.026	2.08
5	140	8.57	40	1800	0.156	0.026	0.042	6.0
6	100	5.7	40	855	0.080	0.019	0.018	4.2
7	120	5.7	40	1026	0.119	0.019	0.023	6.27
8	140	2.86	20	1200	0.109	0.027	0.023	4.04
9	100	5.7	28.5	1200	0.102	0.024	0.028	4.24
10	120	5.7	34.2	1200	0.116	0.019	0.028	6.11
11	140	8.57	60	1200	0.142	0.018	0.028	7.9

FB gun to work-piece distance = 6 in.[3]

[1] m/sec = (ipm)(.0423)

[2] joules/cm = (joules/in) ÷ (2.540)

[3] cm = (in)(2.540)

[4] $cm^2 = (in^2)(6.452)$

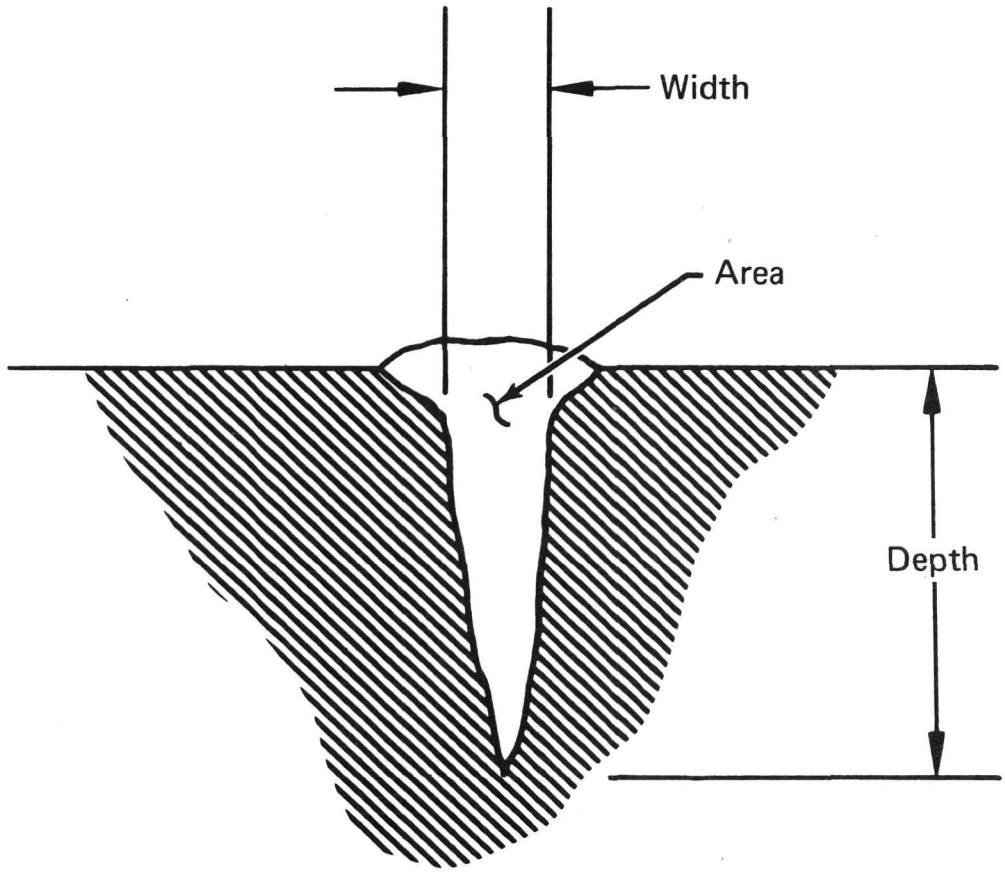

Figure 73. Electron Beam Welding Terminology FD 49372A

To expedite the testing the Inconel and nickel plates rather than being brazed or bonded were held in place by tack-welding the edges and by clamping rigidly in a fixture (figure 75).

The welding conditions used and comments on resulting welds are given in table XXVIII for the high voltage welder and in table XXIX for the low voltage welder. Preliminary welds made at FRDC indicated that the best welds would be achieved at the highest voltages. The first 13 welds in each welder were therefore made near the voltage limit for the welder. The last two welds on each welder were made at reduced voltages to verify the effects of reduced voltage.

A photograph of three sections of high voltage weld No. 4 (Table XXVIII) after being etched is shown in figure 76. The three sections show the

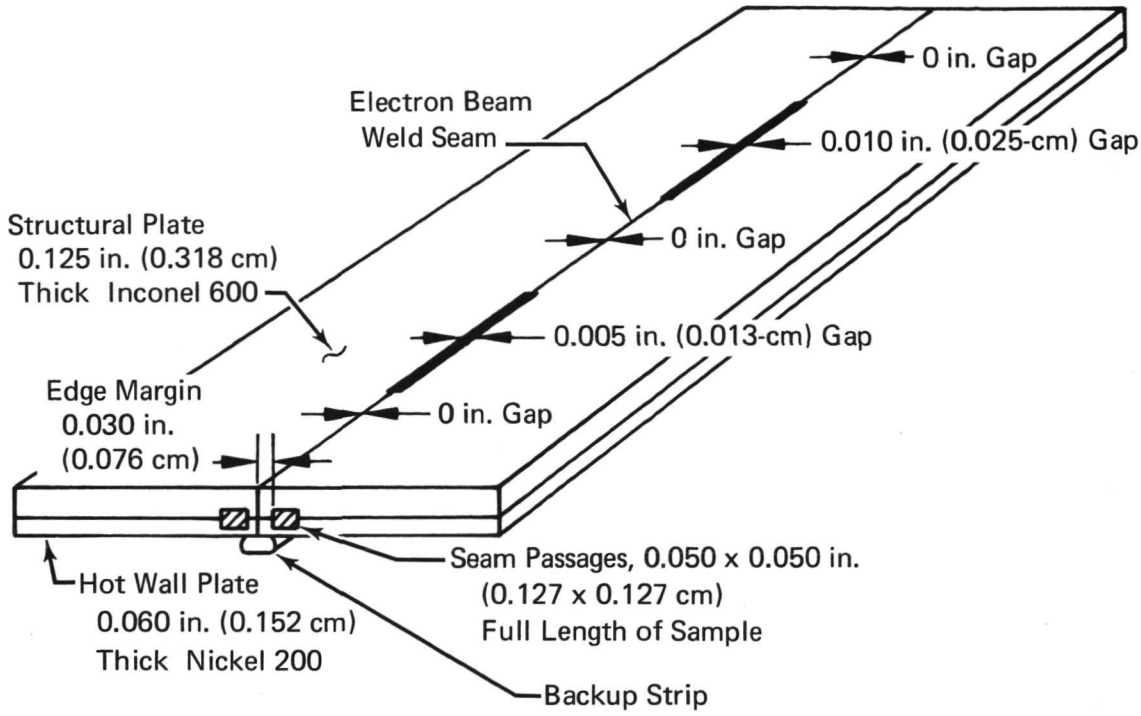

Figure 74. Electron Beam Welding Test Sample FD 51070A

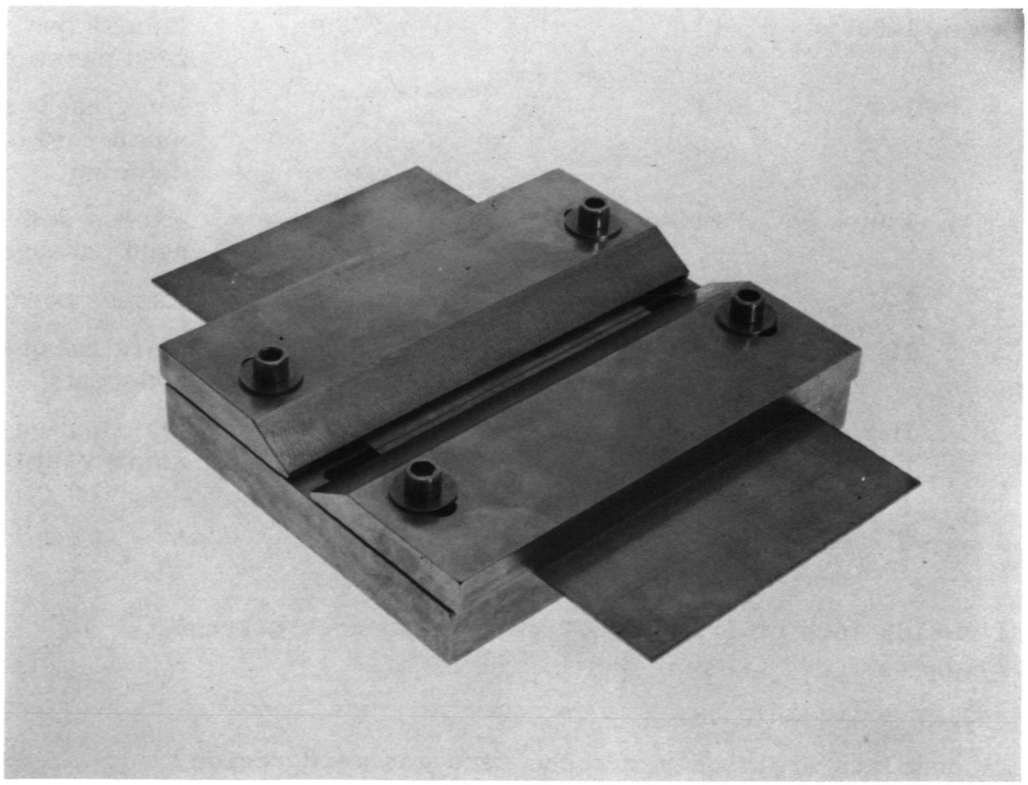

Figure 75. Electron Beam Welding Fixture FC 22432

Table XXVIII. Series I High Voltage Welds

Weld No.[1]	Voltage, kv	Current, ma	Speed ipm[2]	Energy Rate, joules/in.[3]	Comments[4]
1	140	10	50	1680	Insufficient Penetration
2	140	10	40	2100	Acceptable Weld
3	140	10	30	2800	Excess power, slight undercut
4	140	11	40	2310	Acceptable Weld
5	140	12	50	2020	Acceptable Weld
6	140	12	45	2240	Acceptable Weld
7	140	12	40	2520	Sample manufactured incorrectly, does not apply
8	140	12	35	2880	Excess power, damaged passage
9	140	12	30	3360	Excess power, damaged passage
10	140	13	40	2730	Excess power, damaged passage
11	140	14	50	2360	Marginal quality, small void in weld detected
12	140	14	40	2940	Excess power, damaged passage
13	140	14	30	3920	Excess power
14	120	14	40	2520	Marginal quality, undercut
15	100	14	40	2100	Marginal quality, small void in weld detected

[1] All welds made at 6 in. (15.2 cm) gun-to-work distance.

[2] cm/sec = (ipm)(.0423)

[3] joules/cm = (joules/in.) ÷ (2.540)

[4] All comments apply only for the zero gap weld region.

Table XXIX. Series I Low Voltage Welds

Weld No.[1]	Voltage, kv	Current, ma	Speed, ipm[2]	Energy Rate, joules/in.[3]	Comments[4]
1	50	40	50	2400	Insufficient penetration, damaged passage
2	50	35	40	2620	Damaged by vendor error
3	50	25	30	2500	Insufficient penetration, damaged passage
4	50	35	40	2620	Insufficient penetration, damaged passage
5	50	40	50	2400	Insufficient penetration
6	50	36	45	2400	Insufficient penetration, undercut.
7	50	36	40	2700	Lost sample
8	50	36	35	3090	Almost full penetration, damaged passage
9	50	36	30	3600	Undercut and voids
10	50	36.4	40	3730	Undercut and voids
11	50	39.2	50	2360	Undercut and voids
12	50	39.2	40	2940	Undercut
13	50	39.2	30	3920	Excess energy, damaged passages
14	42.9	39.2	40	2520	Undercut and voids
15	35.75	39.2	40	2100	Damaged passages and voids

[1] All welds made at 6 in. (15.2 cm) gun-to-work distance.

[2] cm/sec = (ipm)(.0423)

[3] joules/cm = (joules/in.) ÷ (2.540)

[4] All comments apply only for the zero gap weld region

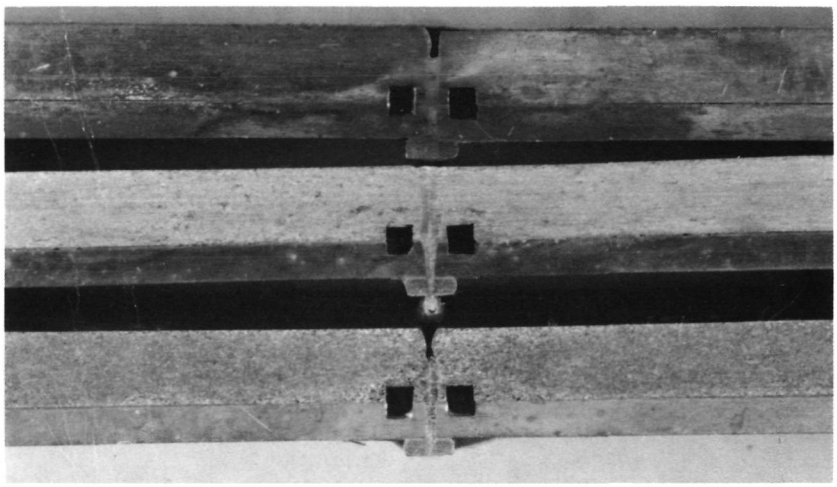

Figure 76. Section Views of Series I High Voltage Weld Sample No. 4. FAL 23472

weld at 0.006-in. (0.015 cm) gap, a 0.000-in. gap, and 0.006-in (0.015 cm) gap (as measured prior to welding); an acceptable weld was made at zero gap, but voids occurred in the welds at 0.006-in. (0.015 cm) gap.

Comparison of the high voltage and low voltage welds showed that at equal power levels the high voltage welds consistently had greater penetration and a narrower melt zone than did the low voltage welds. In each low voltage test, the weld broke into an adjacent passage or did not fully penetrate the seam. Section views of comparable welds are presented in figure 77.

The high voltage welder was selected for use in subsequent welding investigations based on these results. Also, high voltage welds No. 14 and 15 were of marginal quality, verifying that the best welds would be achieved at a 140 kv accelerating voltage. Acceptable welds were achieved at energy rates of 2020 to 2310 joules/in (795 to 909 joules/cm) with an accelerating voltage of 140 kv. Therefore an energy rate of 2310 joules/in

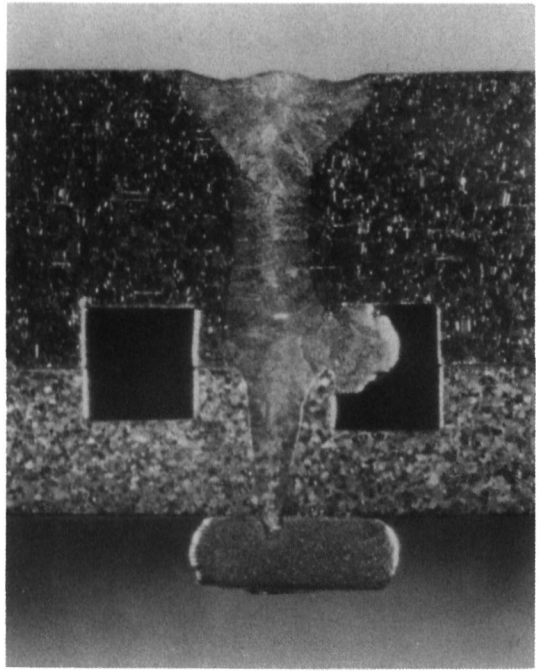

MAG: 12X

Low Voltage Weld No. 3
50 Kv, 25 ma, 30 imp (1.27 cm/sec),
2500 Joules/in. (984 joules/cm)

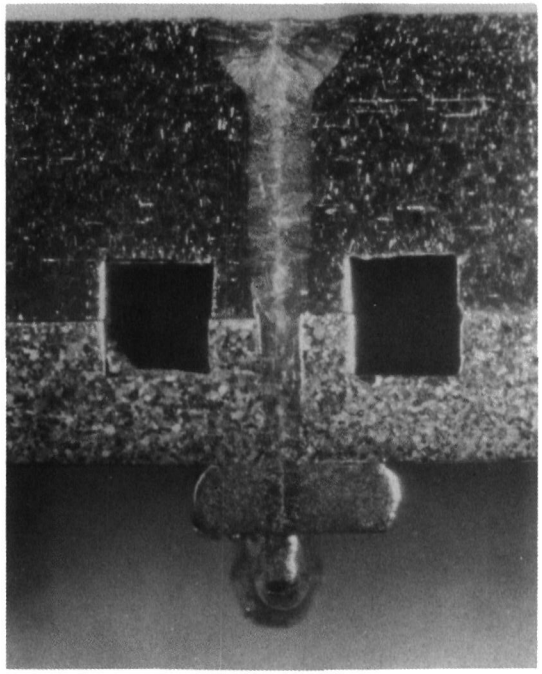

MAG: 12X

High Voltage Weld No. 3
150 Kv, 10 ma, 30 ipm (1.27 cm/sec),
2800 Joules/in. (1102 joules/cm)

Figure 77. Comparison Between Low and High Voltage Welds

FD 53388A

(909 joules/cm) was selected as the base point for additional testing.

3. Parameter Variation Tests

During this series of tests, beam rotation, gun-to-work distance, beam focus, and beam-to-work angle were investigated. Beam rotation increased the effective weld width and was investigated as a possible means of welding large gaps. Gun-to-work distance, beam focus, and beam-to-work angle were investigated to determine how the weld would be affected if these parameters varied in the process of welding a contoured rocket chamber.

Electron beam gun-to-work distance was investigated at 12 in. (30.48 cm) and 24 in. (60.96 cm) distances. The tolerable beam focus band was investigated with the beam focused approximately 2 in (5.08 cm) above and 2 in. (5.08 cm) below the part. Weld angles were varied from 15 to 30 deg (0.262 to 0.524 rad.) to simulate welding along a chamber contour.

The Series II tests were performed on samples of the same design used in the Series I tests (figure 74). Welds were evaluated by sectioning the samples and examining the weld in the cross section. The welding schedule followed is given in table XXX and the evaluation of the welds is presented in Table XXXI. Figure 78 shows the degree of fill that was obtained at 0.004 in (0.010 cm) and 0.009 (0.023 cm) gaps with 0.0025 in. (0.00635 cm) radius beam rotation. Insufficient filling occurred and the weld broke into one of the passages at zero gap indicating that greater edge margin would be required for welds made with a rotating beam. In another sample 0.005 in. (0.0127 cm) radius beam rotation was used and resulted in incomplete penetration and passage blockage indicating 0.005 in. (0.0127 cm) beam rotation was excessive.

Table XXX. Series II Welds

Weld No. *	Test Type	
1	Beam rotation	0.0025 in. (0.0064 cm.) radius
2	Beam rotation	0.005 in. (0.013 cm.) radius
3	Gun-to-work distance	12 in. (30 cm.)
4	Gun-to-work distance	24 in. (61 cm.)
5	Focus	2 in. (5 cm) above seam
6	Focus	2 in. (5 cm.) below seam
7	Angle (side to side)	15 deg (0.262 rad)
8	Angle (side to side)	30 deg (0.524 rad)
9	Angle (end to end)	15 deg (0.262 rad)
10	Angle (end to end)	30 deg (0.524 rad)

*All welds made with a beam voltage of 140 kv, a beam current of 11 ma, and a speed of 40 ipm (1.69 cm/sec).

Table XXXI. Evaluation of Series II Welds

Weld No.	Test[1] Type	Minimum Width of Weld in Inconel Plate, in.	Description of Weld[2]	Evaluation
1	0.0025 in.[5] radius beam rotation, 500 cps	0.033	Nearly complete fill at 0.004 in. gap	0.0025-in. radius beam rotation improved weld at 0.004 in gap but passage blockage occurred at zero gap.
2	0.005-in. radius beam rotation, 500 cps	0.033	Lack of penetration at zero gap	0.005-in. radius beam rotation is too great.
3	12-in. gun-to-work distance	0.034	Reduced penetration	Greater power required for greater gun-to-work distance. Weld is much wider than for 6-in. gun-to-work distance.
4	24-in. gun-to-work distance	0.038	Passage blockage. Lack of penetration	
5	Focus 2 in. above seam	0.030	Passage blockage and voids.	Inconsistent
6	Focus 2 in. below seam	0.029	Weld looked the same as for sharp focus	
7	15-deg[6] side-to-side angle	0.023	Weld broke into one passage	Side-to-side angles greater than 5 deg produce unacceptable joints.
8	30-deg side-to-side angle	0.025	Weld broke into both passages	
9	15-deg end-to-end angle[3]	0.026	Weld unaffected by angle	15 deg and 30 deg angles do not affect the weld in a 6-in. section.
10	30-deg end-to-end angle[3]	0.024[4]	Slight undercut in weld above plane of focus	

[1] For all welds, except as noted, weld energy was 2310 Joules/in., gun-to-work distance was 6 in., focus was on the part; and the electron beam was 90 deg to the part.

[2] Unless noted otherwise, each weld had the following characteristics: (1) full penetration; (2) underfill at sections where gap existed; and (3) complete fill at zero gap sections.

[3] Beam focused at height of center of sample.

[4] Width of weld in nickel plate. This sample was welded from the nickel side.

[5] cm = (in)(2.540)

[6] rad = (deg)(0.01745)

[7] joules/cm = (joules/in) ÷ (2.540)

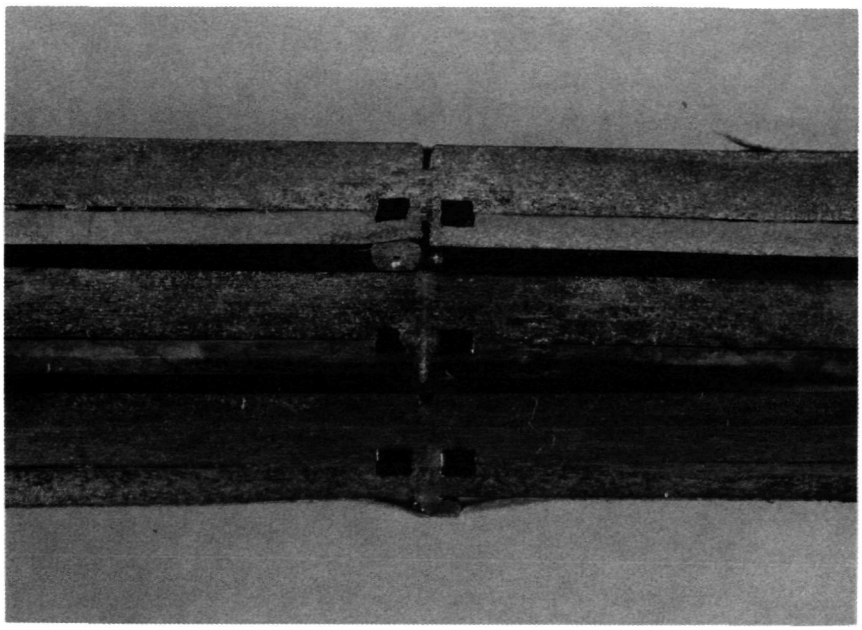

EB Series II, Sample No. 1

Figure 78. Effect of 0.0025-in. (0.00635 cm) Beam Rotation FAL 23465

Increasing the gun-to-work distance caused a widening of the weld, particularly in the crown. Figure 79 shows a weld made at 24-in. (60.96 cm) gun-to-work distance. Incomplete penetration and passage blockage occurred.

Defocusing the beam resulted in passage blockage and voids in the weld zone, as indicated in figure 80.

Varying the beam-to-work angle appeared to have little effect. The weld nugget was no wider than for the base point weld and good penetration was obtained.

4. Modified Seam Design and Minimum Edge Margin Tests

Minimum practical edge margins for the conventional seam design were investigated and two modified seam designs, biased and split (figure 81), that could provide added cooling at the weld seams of Thermal Skin chambers, were evaluated. Both modified seam designs had the weld passing through

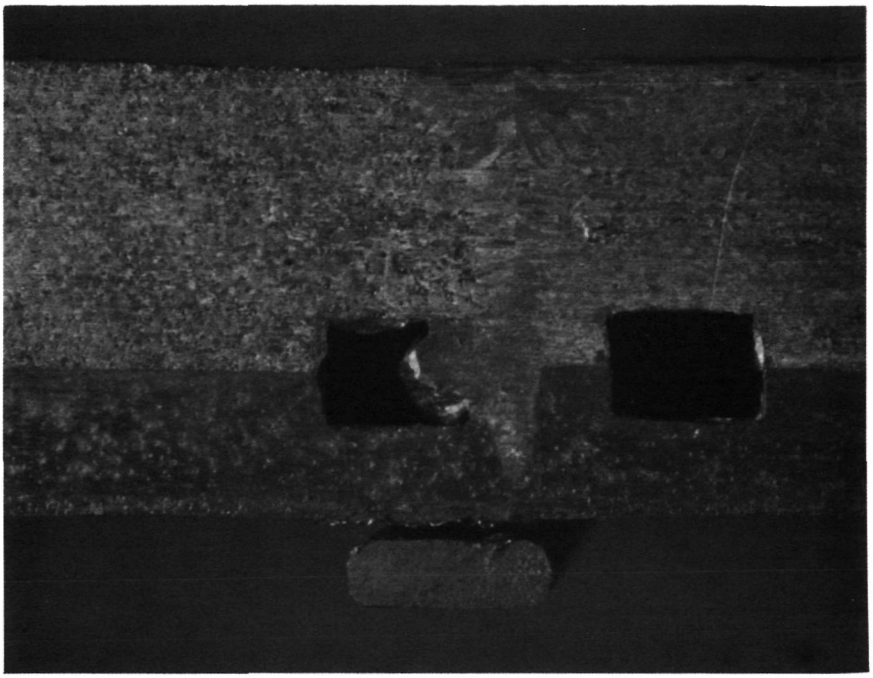

12X

EB Series II, Sample No. 4

Figure 79. Effect of 24-in. (60.96 cm) Gun-to-Work Distance FAL 23467

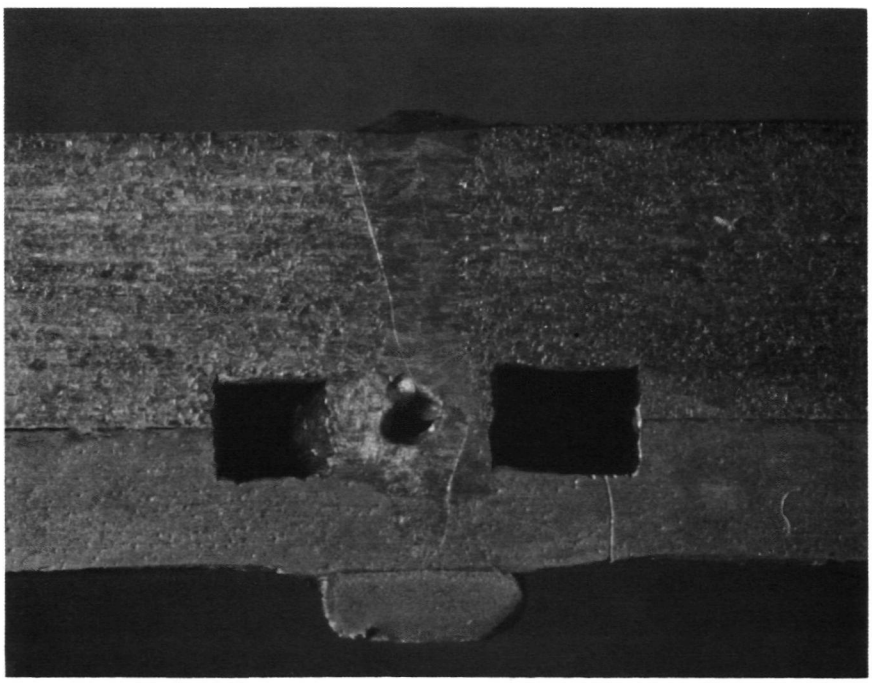

12X

EB Series II, Sample No. 5

Figure 80. Effect of Beam Focus 2-in. (5.08 cm) Above Seam FAL 23468

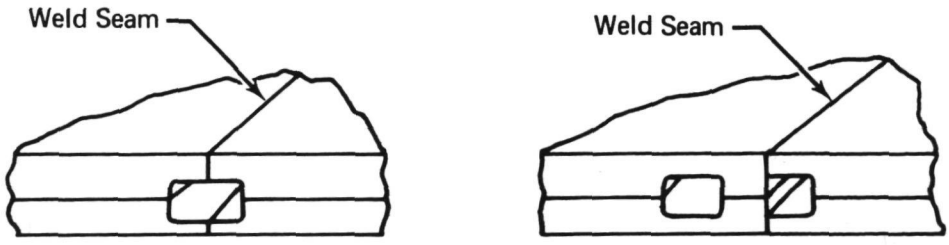

A. Split Passage at Seam

B. Biased Passage at Seam

Figure 81. Modified Seam Configurations FD 46626B

a coolant passage so that seam cooling would be a maximum.

The welding schedule is given in table XXXII and the evaluation of the welds in table XXXIII. In the first three welds, minimum edge margin was investigated using samples that had an edge margin varying from 0.050 (0.127 cm) to 0.010 in. (0.0254 cm). X-ray inspection was used to determine where the welds had broken into the passages, which occurred at passage separations of 0.047 in (0.1092 cm) to 0.051 in. (0.1293 cm). A single panel minimum edge margin of 0.026 in. (0.066 cm) was therefore indicated.

Partial passage blockage was encountered with both of the modified seam designs investigated. The weld flowed into the biased passage causing some blockage of the passage (figure 82). Weld splatter occurred inside the split passage sample causing varying amounts of blockage (figure 83).

Table XXXII. Series III Welds

Weld No.	Test Type	Voltage, kv	Current, ma	Speed, ipm [1]	Energy Rate, Joules/in. [2]
1	Edge margin	140	11.0	40	2310
2	Edge margin	140	10.5	40	2205
3	Edge Margin	140	10.0	40	2100
4	Biased passage	140	8.0	40	1680
5	Biased passage	140	7.0	40	1470
6	Biased passage	140	7.5	40	1575
7	Split passage	140	7.0	40	1470
8	Split passage	140	7.5	40	1575
9	Split passage	140	8.0	40	1680

[1] cm/sec = (imp ÷ 12)(.508)

[2] joules/cm = (joules/in) ÷ (2.540)

Table XXXIII. Evaluation of Series III Welds

Weld No.	Test Type	Width of Weld in Inconel Plate, in. [2]	Description of Weld	Evaluation
1	Edge margin 2310 Joules/in.[1]	0.025	Underfill. Weld broke into passage at 0.047 in. passage separation	A minimum passage separation of 0.050 to 0.060 in. is required to avoid breaking into passages. If bulging of the weld at the nickel-Inconel interface could be eliminated, a passage separation of 0.030 to 0.035 in. would be sufficient.
2	Edge margin 2205 Joules/in.	0.022	Underfill. Weld broke into passage at 0.047 in. passage separation	
3	Edge margin 2100 Joules/in.	0.027	Underfill. Weld broke into passage at 0.051 in. passage separation	
4	Biased passage 1680 Joules/in.	0.024	Lack of penetration at zero gap. Approximately 20% blockage of biased passage by weld	Greater power required. Increasing speed may reduce flow of weld into passage.
5	Biased passage 1470 Joules/in.	0.021		
6	Biased passage 1575 Joules/in.	0.023		
7	Split passage 1470 Joules/in.	0.022		
8	Split passage 1575 Joules/in.	0.022	Splatter in passage caused some blockage	Difficult to attain a smooth passage with this type of weld because of splatter.
9	Split passage 1680 Joules/in.	0.022		

[1] joules/cm = (joules/in.) ÷ (2.540)

[2] cm. = (in.)(2.540)

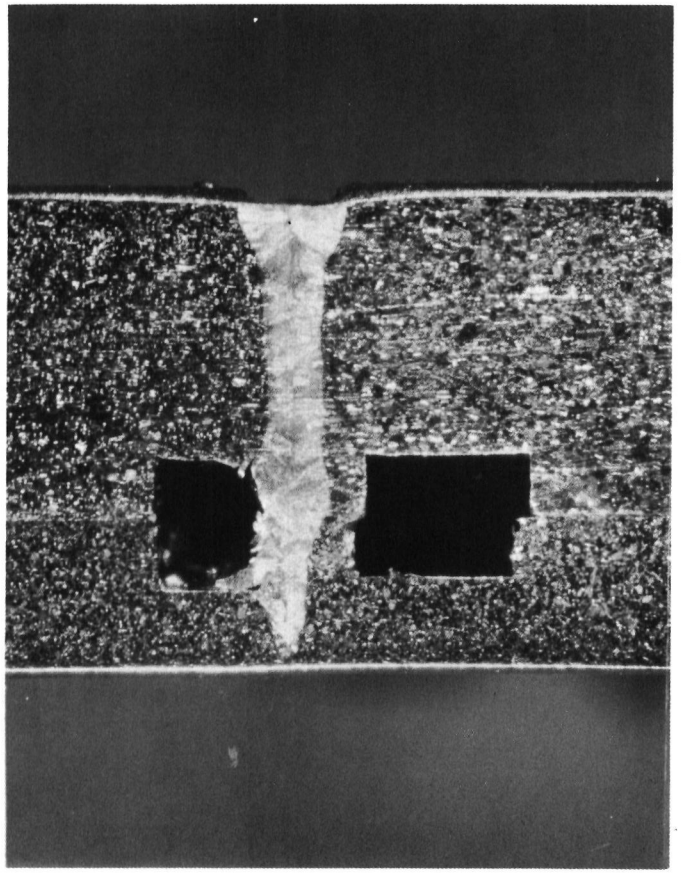

EB SERIES III, SAMPLE NO. 6

Figure 82. Biased Passage Weld FL 22460

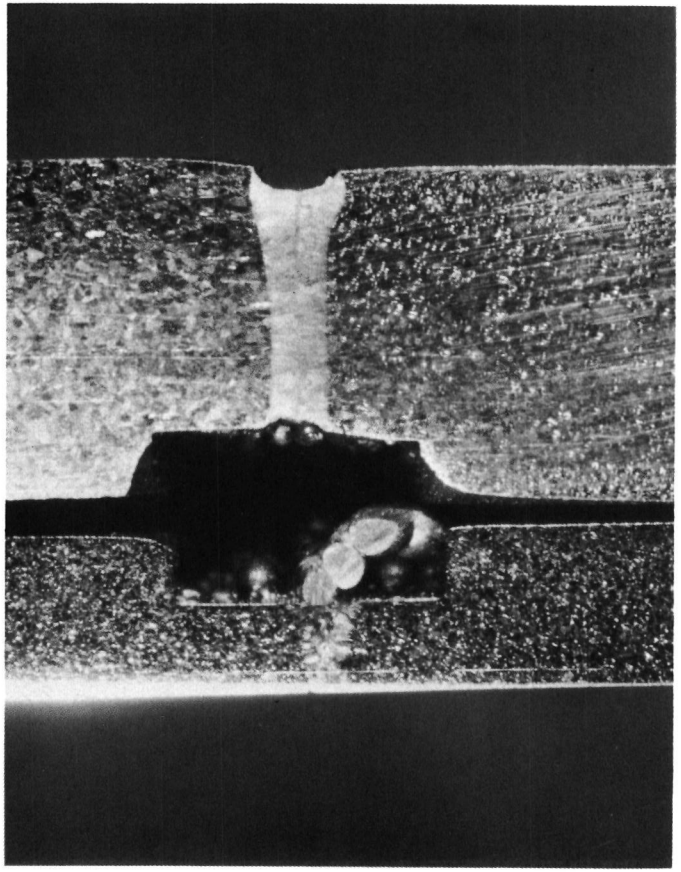

EB SERIES III, SAMPLE NO. 7

Figure 83. Split Passage Weld FL 22461

5. Structural Tests

Thermal Skin panels manufactured under the diffusion bonding study (Section VII) were electron beam welded using the best welding conditions established during the earlier series of experimental welds. These welds are summarized in table XXXIV.

Bend and tensile tests were performed on the welded samples. The bend test samples are shown in figures 84, 85 and 86; no damage to the welds due to bending was detectible and passage area change was small. It was noted, however, that the welds had unexpectedly broken into adjacent coolant passages. The welding parameters used had given no passage deformation during earlier tests and apparently were not duplicated. The non-repeatability of weld behavior was contributed to equipment drift and therefore test welds immediately before chamber welding would be recommended.

Tensile test results for electron beam welded seams are presented in table XXXV and indicated that a good structural joint approaching parent metal strength (Inconel 600) was achieved. The ductility of the joint was less than that of the parent material and rupture of each sample occurred at the weld (figure 87). Also noted from the tensile tests was the differences in material ductility due to different heat treating cycles occurring during bonding of the panels. Sample AV-3 was bonded at 2200°F (1477°K) giving a highly annealed structure while sample ENB-1, bonded at 1700°F (1200°K) was significantly less ductile.

Table XXXIV. Summary of Electron Beam Welds Using Bonded Samples

Sample No.	Subsequent Tests	Comments on Weld Quality
ENB-1	Tensile	Not evaluated.
ENB-2	Bend	Fusion zone penetrated into passage resulting in passage blockage.
ENB-3	Bend	Fusion zone penetrated into passage resulting in passage blockage.
AV-3	Tensile	Full penetration not achieved, no passage deformation observed.
PWA-5	Bend	Fusion zone penetrated into passage resulting in passage blockage.

NOTE: Each sample was welded at 140 KV, 11 ma, 40 ipm (1.69 cm/sec) and 6 in. (15.2 cm) gun-to-work distance.

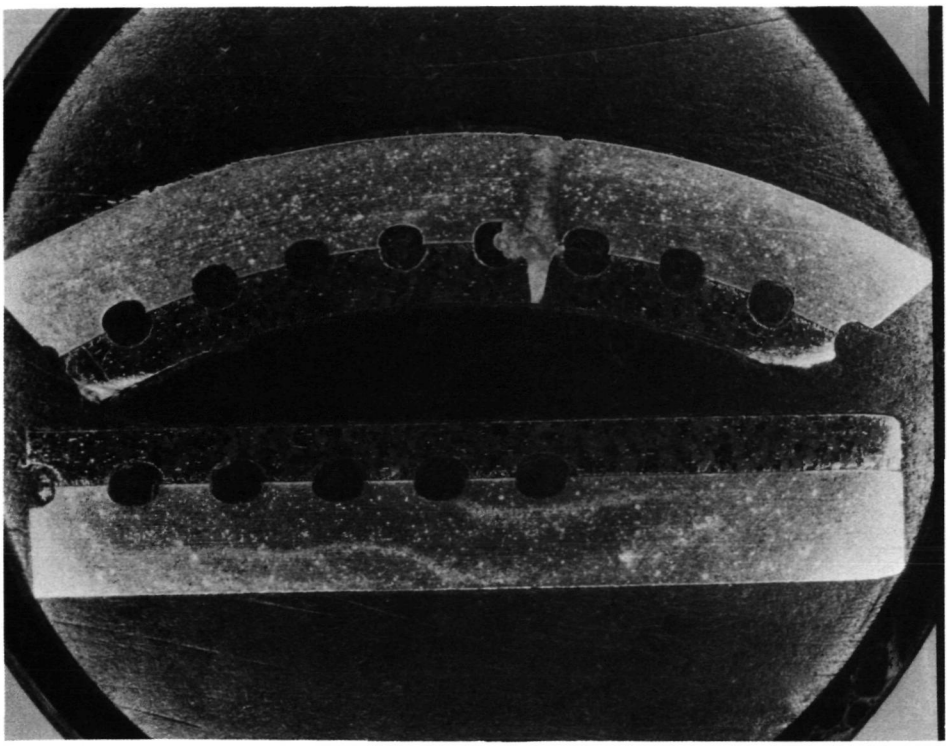

Figure 84. Electron Beam Welded Bend Test Sample ENB-2 FL 23941

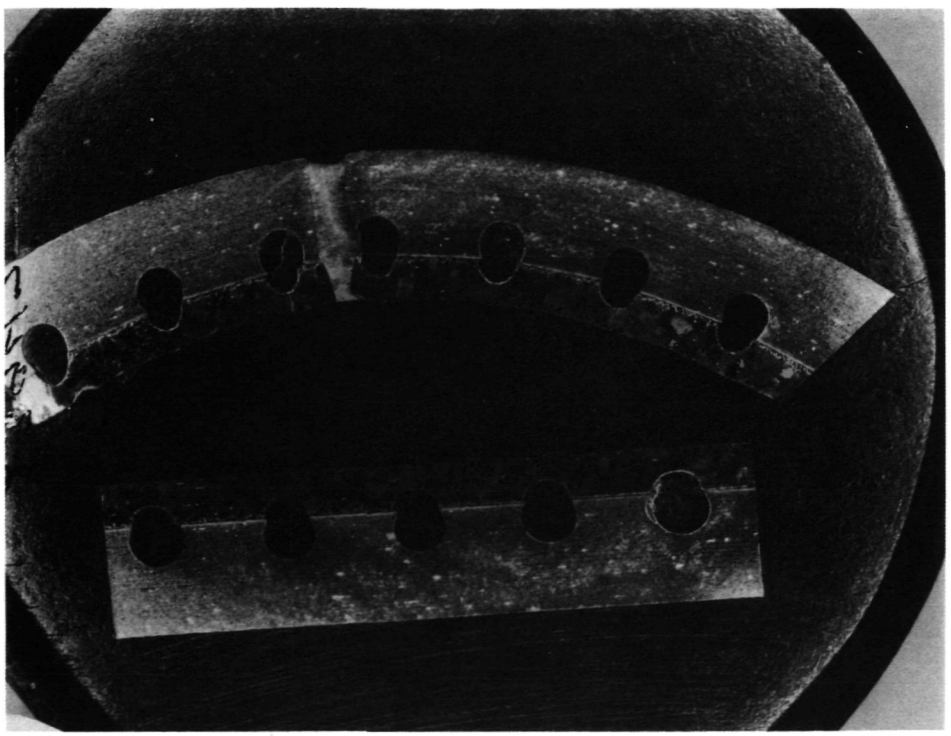

Figure 85. Electron Beam Welded Bend Test SAMPLE ENB-3 FL 23942

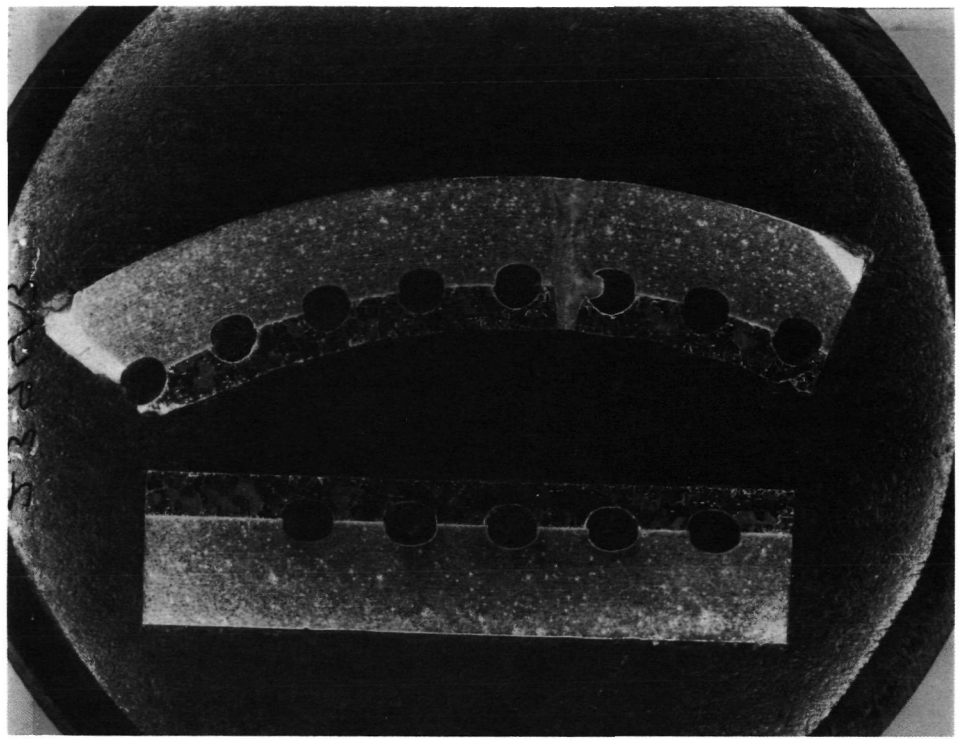

Figure 86. Electron Beam Welded Bend Test Sample PWA-5 FL 23943

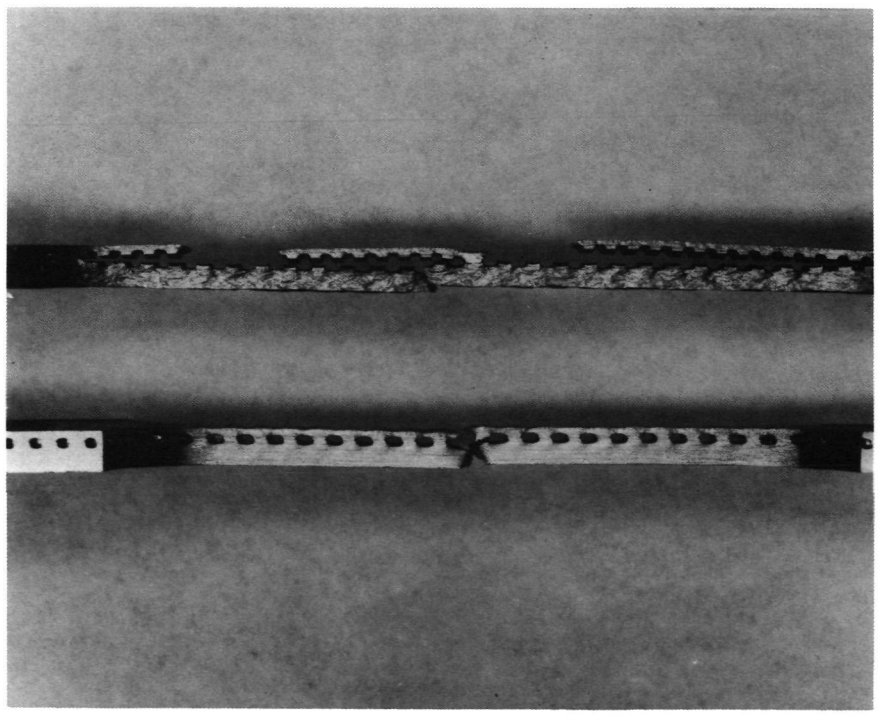

Figure 87. Electron Beam Welded Tensile Test Specimens FAL 23701

Table XXXV. Tensile Tests Results for Electron Beam Welded Samples

Sample No.	Plate	Land Width in.[1]	Passage Depth in.	Passage Depth in.	Plate Thickness in.	Panel Thickness in.	Stress Depth in.	Sample Width in.	Yield Load lb_f [2]	Tensile Load lb_f	Stress Area $in.^2$ [3]	Calculated INCO Strength* Yield/Tensile psi[4]
ENB-1	Ni-200	0.056	0.060	0.025	0.051	0.176	0.026	0.303	1390	3300	0.007878	
	INCO-600	0.056	0.060	0.024	0.125	0.176	0.101	0.303	1390	3300	0.03063	45,500/108,000
AV-3	Ni-200	0.044	0.043	0.024	0.050	0.175	0.026	0.303	910	2600	0.007878	
	INCO-500	0.051	0.036	0.022	0.125	0.175	0.103	0.303	910	2600	0.031209	29,200/83,300

* Assumes No Strength in Ni; Inconel-600 design strength: Yield = 30,000 psi, tensile = 80,000 psi; nickel-200 design strength: Yield = 15,000 psi, tensile = 55,000 psi.

[1] cm = (in)(2.540)

[2] n = $(lb_f)(4.448)$

[3] $cm^2 = (in^2)(6.452)$

[4] n/cm^2 = (psi)(.689476)

Table XXXVI. Chemical Machining Patents

PATENT	MATERIALS	OBJECT OF PATENT	ETCHING SOLUTION	ETCHING METHOD	COMMENT
2,746,848, 5/22/56, Etching, Jones, PERI, Inc.	Copper; Brass	1. Elimination of side etch 2. Provide etching composition to eliminate powder banking	1. 30 to 42° Be' (preferably 40 to 42° Be') ferric chloride 2. 0.4 to 10 gm/liter (preferably 0.8 to 2.0 gm/liter) thiourea.	1. Splash (1530 to 2000 rpm) 2. Spray (ΔP = 20-psi nozzle 3 inches from plate) 3. Brush 4. Jet stream (0.035 to 0.070 inch streams 1/2 to 1 inch from plate).	1. Age of thiourea-ferric chloride solution must not be over 120 hours 2. Best etch factors were obtained with jet stream (nonatomizing) system.
3,033,725, 5/8/62, Powderless Etching of Copper Plates, Daugherty and Vaughan, PERI, Inc.	Copper; Copper Alloys	Provide a new powderless etching solution that doesn't require aging	1. 30 to 42° Be' (test made with 40° Be') ferric chloride 2. Passivating agent is formamidine disulfide salts (e.g., formamidine disulfide hydrochloride) 0.6 to 1.3 gm/l of etching solution (1.0 gm/l was used in tests).	1. Splash (20 to 30°C, 900 ft/min) 2. Jet stream (900 ft/min).	States that formamidine disulfide as a passivating agent has advantage over thiourea because etching solution does not have to be aged. An aging time of 36 hours for thiourea solution is mentioned as desirable.
3,136,670, 6/9/64, Powderless Etching Rogers and Borth, PERI, Inc.	Copper; Brass	Provide better sidewall protection than thiourea.	1. 26 to 46 Be' (preferably 30° Be') ferric chloride 2. 0.1 to 25 gm/l (preferably 0.2 to 5 gm/l) of copper thiourea chloride 3. Formamidine disulfide dihydrochloride (0.15 to 4.0 parts by weight of copper thiourea chloride).	Splash (550 rpm, 80°F).	Gives qualitative results in examples 2 through 6 that show, for a 30° Be' ferric chloride solution, best side wall protection was obtained for depth of 0.020 inch with 0.8 gm/l copper thiourea chloride and 0.4 gm/l formamidine disulfide dihydrochloride.
3,144,368, 8/11/64, Powderless Etching, Daugherty and Vaughan, PERI, Inc.	Copper; Brass	Provide procedure for adding "makeup" aged thiourea etching solution	Makeup Solution 1. 26 to 46° Be' (preferably 30 to 35° Be') ferric chloride 2. 20 to 50 gm/l (preferably 30 to 40 gm/l) of thiourea.		Ageing of thiourea-ferric chloride before use should be at least 1 hour (1 to 2 hours is recommended).
3,161,552, 12/15/64, Composition and Process for Powderless Etching, Bradley and Borth, PERI, Inc.	Copper; Brass	Provide control of the character of protective film formed by ethylene thiourea by use of modifying agent	1. 26 to 46° Be' (preferably 30° Be') ferric chloride 2. Passivating agent is 0.5 to 10 gm/l (preferably 0.5 to 5 gm/l) of ethylene thiourea and formamidine disulfide. Proportion of ethylene thiourea to formamidine disulfide is 0.15 to 4 (preferably 1.0 to 1.75). 3. Modifying agent to be 1.25% (preferably about 10%) by weight of passivating agent. Thirteen modifying agents are listed in patent. Preferred modifying agents are: (1) pyrogallol, (2) 2,4- diaminophenol, and (3) tannic acid. (2) is amidol (p 334, Merck 7th Ed).	Splash (8 inch paddle wheel; 600 rpm; 80°F ± 1°F).	States that ethylene thiourea provides a strongly adherent film. It states that the film is so strong that it would be unsuitable for some work if used alone.

Table XXXVI. Chemical Machining Patents (Continued)

PATENT	MATERIALS	OBJECT OF PATENT	ETCHING SOLUTION	ETCHING METHOD	COMMENT
3,271,282, 9/6/66, Process for Etching Photo-Engraving Copper, Borth, PERI, Inc.	Copper	Provides a means for improving effectiveness of etching by impressing a voltage across etchant	1. Ferric chloride 200 to 460 gm/l of both 2. Passivating agents: a. Formamidine disulfide compound 0.6 to 3 gm/l (Patent 3,033,725) b. Alkylamine and alkanolamine compounds in combination with formamidine disulfide compounds 0.005 to 10 ml/l (preferably 3 to 6 ml/l) of the amine compound (Patent 3,033,793).	Splash etcher with ac or dc power; ac voltage 3 to 50 v (preferably 6 to 12 v), 1 to 5 amps (preferably 2 to 3 amps); dc power 3 to 50 v (especially 6 v), 1 to 5 amps.	Cites example wherein a 30° Be' ferric, chloride solution containing 2 gm/l of ammonium persulfate, 2.4 gm/l of formamidine disulfide and 5 cc/l of mixed isoproponal amines. Using 6 v dc across bath, side wall protection was maintained for 5-1/2 hours. Without voltage potential, side wall protection diminished in same time period.
3,287,191, 11/22/66, Etching of Printed Circuit Components, Borth, PERI, Inc.	Printed circuits involving copper or silver-plated onto copper.	Provides a specific formulation for etching printed circuits.	1. 20 to 48° Be' (200 to 460 gm/l) of ferric chloride 2. Passivating agent ethylene thiourea 1 to 8 gm/l (preferably 1.5 to 3 gm/l) 3. 0.10 to 10 gm/l of modifier, like amidol (0.1 to 0.8 gm/l).	Splash etcher (paddle 8 inch diameter, 600 rpm; 80°F).	States that although ethylene thiourea is preferred, methyethypropyl, isoprophylphenol, diphenol, or acetylbutyrol can be used.
3,340,195, 9/5/67, Process of Etching, Borth and McKeone, PERI, Inc.	Copper; Brass; beryllium copper and nickel alloys (Kovar)	Provides two-phase etching solution. Implies that patented solution would be preferred for depths over 0.025 in.	1. 20 to 48° Be' (preferably 30° Be') ferric chloride 2. Thiourea derivatives of 1 to 4 gm/l (preferably 2.4 gm/l) 3. Nonionic surfactant is polyethylene glycol esters 0.5 to 2% (preferably 1%) 4. Oils (kerosene, cotton-seed oil) or emulsified silicone oil 10 to 30 cc/l.	Spray etcher 1/2 hp, 12 to 13-psi nozzle pressure.	States that ammonium persulfate or chromic acid can be used for etching in lieu of ferric chloride.
3,458,371, 7/29/69, Composition and Process for Powderless Etching, Borth and McKeone, PERI, Inc.	Copper alloys, Kovar	Provides means of reducing undercutting in the powderless etching process.	1. 20 to 48° Be' (preferably 30° Be') ferric chloride 2. 0.4 to 4 (preferably 3.5 gm/l) thiourea derivative 3. 0.01 to 1 gm/l (preferably 0.02 to 0.1 gm/l) ascorbic acid 4. Modifying agent per patent 3,161,552.	Splash etcher	States that when copper ion concentration reaches about 4.5 oz/gallon (3.4 gm/l) one losses side wall slope control and wall become perpendicular to plate surface without ascorbic acid.

APPENDIX B
PROCEDURE FOR POWDERLESS CHEMICAL MACHINING PROCESS

1. Silver Plate Per Specification AMS 2410

   1.1 Thickness of silver to be 0.0007 ± 0.0002 in. (0.00178 ± 0.00051 cm.)

   1.2 Uniformity of silver in area to be printed to be ± 0.0001 in. (± 0.00025 cm.)

2. Coat With Waycoat PF Photoresist or Equivalent

   2.1 Immerse silver-plated panel in 10% HCl for 2 ± 1 min. Water rinse and dry.

   2.2 Spin coat panel with Waycoat PF photoresist at 80 rpm for 15 min at medium heat (approximately 170°F (350°K))*. Other means, e.g., spray, dip, etc., may be used if acceptable results can be demonstrated.

   2.3 Apply second coat as in item 2.2.

   2.4 Dry at 160°F (344°K) to 180°F (356°K) for 1 hour.

3. Expose Photoresist

   3.1 Place negative over plate to be exposed on special vacuum table.**

   3.2 Close lid and pull vacuum over system.

   3.3 Place light source*** 3-½ ft (1.07 m) from plate.

   3.4 Expose for 15 ± 2 minutes.

   3.5 Release vacuum and remove plate.

4. Develop Photoresist

   4.1 Immerse plate in Waycoat developer or equivalent for 1 minute.

   4.2 Water rinse for 4 ± 1 minute.

      4.2.1 Plate to be completely submerged for time period.

   4.3 Dry at 160°F (344°K) to 180°F (356°K) for 1 hour.

5. Touch Up

   5.1 Use Waycoat photoresist to touch up as required.

   5.2 Dry at 160° (344°K) to 180°F (356°K) for 30 minutes.

---

*Using Douthitt Litho Plate Whirler or equivalent
**Using Douthitt Model "D" Vacuum Printing Frame or equivalent.
***Using Macbeth Mark 50 Constantarc Printing Lamp or equivalent.

6. Strip Silver

6.1 Place in a phosphoric acid plating bath and deplate silver using reverse current.

6.1.1 Masking tape* should be applied to back of plate so silver is not removed.

6.2 Remove plate when all silver is removed from areas not masked with photoresist.

7. Touch Up

7.1 Use Waycoat PF or equivalent to touch up as required.

7.2 If any touch up is done, dry at 160°F (344°K) to 180°F (356°K) for 30 minutes.

8. Chemically Machine Panel

8.1 Etching solution to be 42° Baumé $FeCl_3$ (Hunt's RCE or equivalent) containing 1.06 g/l thiourea in Master Etcher Model PC-32HS or equivalent.

8.1.1 Check Baumé at 4 hour intervals and maintain at 42° Baumé by addition of water.

8.1.2 Check thiourea content after 100 hours by etching scrap nickel for 10 minutes. If nickel turns black, solution is satisfactory; if shiny metal is showing, add 0.8 g/l thiourea. This procedure should be repeated every 48 hours after the 100-hour age of solution is reached.

8.1.3 To prepare a new solution for use, check milling rate with scrap panel; if rate is greater than 0.0003-in (0.00076-cm) etch scrap nickel until rate drops to 0.0003-in (0.00076-cm).

8.2 Temperature of solution to be 120° $\pm$ 2°F (322 $\pm$ 1.1°K).

8.3 Paddle speed to be 1000 rpm.

8.4 The solution level in etcher to be maintained so that paddle dips 3/16 $\pm$ 1/16 in. (0.476 $\pm$ 0.159 cm) in the solution.

8.5 Rotate panel 90 deg at the same holder radius after every 15 minutes of etching.

8.6 The approximate etching time necessary to obtain the desired passage depth can be computed based on 0.00034 in (0.00085 cm)/min. Check the depth 1/2 hour before reaching the time computed and return to etcher for a time calculated from:

---

*Use Scotch Brand No. 470 or equivalent.

$$T = \frac{(D)\ t}{d} - t$$

where T = time required to finish etching panel
D = required depth (total)
t = time panel has been etched
d = measured depth after time, t

8.7 Check etch depth after etching for calculated time, T. If satisfactory, continue with next step; of not, repeat calculation in item 8.5 and return to etching step.

8.8 Rinse in water.

9. Clean Up

9.1 Remove tape.

9.2 Rinse in water.

9.3 Remove Waycoat resist with cold trichloroethylene or Waycoat stripper.

9.4 Remove silver as in item 6.1 (omit item 6.1.1.).

APPENDIX C
PROCEDURE FOR RESIST BANKING CHEMICAL MACHINING PROCESS

1. Silver Plate Per Specification AMS 2410

   1.1 Thickness of silver to be 0.0007 ± 0.0002 in. (0.00178 ± 0.00051 cm).

   1.2 Uniformity of silver in area to be printed to be ±0.0001 in. (±0.00025 cm).

2. Coat With Waycoat PF Photoresist or equivalent

   2.1 Immerse silver-plated panel in 10% HCl for 2 ± 1 minute. Water rinse and dry.

   2.2 Spin coat panel with Waycoat PF photoresist at 80 rpm for 15 minutes at medium heat (approximately 170°F (350°K))*. Other means, e.g., spray, dip, etc., may be used if acceptable results can be demonstrated.

   2.3 Apply second coat as in item 2.2.

   2.4 Dry at 160° (344°K) to 180°F (356°K) for 1 hour.

3. Expose Photoresist

   3.1 Place art work negative over plate to be exposed on special vacuum table.**

   3.2 Close lid and pull vacuum over system.

   3.3 Place light source*** 3-1/2 ft (1.07 cm) from plate.

   3.4 Expose for 15 ± 2 minutes.

   3.5 Release vacuum and remove plate.

4. Develop Photoresist

   4.1 Immerse plate in Waycoat developer or equivalent for 1 minute.

   4.2 Water rinse for 4 ± 1 minute.

      4.2.1 Plate to be completely submerged for time period.

   4.3 Dry at 160° (344°K) to 180°F (356°K) for 1 hour.

5. Touch Up

   5.1 Use Waycoat photoresist to touch up as required.

   5.2 Dry at 160° (344°K) to 180°F (356°K) for 30 minutes.

---

*Using Douthitt Litho Plate Whirler or equivalent.
**Using Douthitt Model "D" Vacuum Printing Frame or equivalent.
***Using Macbeth Mark 50 Constantarc Printing Lamp or equivalent.

6. Strip Silver

6.1 Place in a phosphoric acid plating bath and deplate silver using reverse current.

6.1.1. Masking tape* should be on back of plate so silver is not removed.

6.2 Remove plate when all silver is removed from areas not masked with photoresist.

7. Touch Up

7.1 Use Waycoat PF or equivalent to touch up as required.

7.2 If any touch up is done, dry at 160° (344°K) to 180°F (356°K) for 30 minutes.

8. Chemically Machine Panel

8.1 Etching solution to be 42° Baumé $FeCl_3$ (Hunt's RCE or equivalent) containing 1.06 g/l thiourea in Master Etcher Model PC-32HS or equivalent.

8.1.1 Check Baumé at 4 hour intervals and maintain at 42° Baumé by additions of water.

8.1.2 Check thiourea content after 100 hours by etching scrap nickel for 10 minutes. If nickel turns black, solution is satisfactory; if shiny metal is showing, add 0.8 g/l thiourea. This procedure should be repeated every 48 hours after the 100-hour age of solution is reached.

8.1.3 To prepare a new solution, check milling rate with scrap panel; if rate is greater than 0.0003 in (0.00076 cm)/min, etch scrap nickel until rate drops to 0.0003 in (0.00076cm).

8.2 Temperature of solution to be 120° $\pm$ 2°F, (322 $\pm$ 1.1°K).

8.3 Paddle speed to be 1000 rpm.

8.4 The solution level in etcher to be maintained so that paddle dips 3/16 $\pm$ 1/16 in (0.476 $\pm$ 0.159 cm) in the solution.

8.5 Etch panel for 20 minutes; check depth; rotate panel 15 deg. before each additional etching period.

8.5.1 Back of panel should be masked with tape as in item 6.1.1.

8.5.2 When desired depth is reached, go to item 13.

8.5 Rinse in water.

8.6 Remove tape.

---

*Use Scotch Brand No. 470 or equivalent.

8.7 Rinse in acetone.

8.8 Dry at 150° (338°K) to 160°F (344°K) for 15 minutes.

9. Apply Positive Photoresist

9.1 Coat etched side of plate with Shipley's AZ340 positive photoresist by brushing so that all etched surfaces are coated with a thin layer of resist.

9.2 Excess resist may be removed by placing face of plate down on absorbent material, such as a paper towel.

9.3 Dry at 150° to 160°F (338 to 344°K) for 90 minutes with face of plate down.

10. Expose Resist

10.1 Align reverse image (positive) of the previously used negative art work using index marks or other suitable means for maximum accuracy.

10.2 Expose to light source 3-1/2 ft (1.07 cm) from panel for 45 $\pm$ 2 seconds.

11. Develop Resist

11.1 Develop in AZ303 developer diluted 1:4 with deionized water for 25 to 40 seconds.

11.1.1 Do not allow air bubbles to be trapped in passages preventing contact with developer. Light scrubbing with a soft brush can be used to remove entrapped air.

11.2 Water rinse thoroughly.

11.3 Replace protective masking tape on back of panels.

12. Chemical Machining

12.1 Return to item 8.

13. Clean Up

13.1 Remove tape.

13.2 Rinse in water and acetone.

13.3 Remove Waycoat with cold trichloroethylene or Waycoat stripper.

13.4 Remove silver as in item 6.1 (omit item 6.1.1).

APPENDIX D

PERI ®
PLATEMAKERS
EDUCATIONAL & RESEARCH
INSTITUTE
2447 WESTERN AVENUE / PARK FOREST, ILLINOIS 60466 / 312-748-6262

March 12, 1970

TO: PRATT & WHITNEY AIRCRAFT

FROM: PLATEMAKERS EDUCATIONAL & RESEARCH INSTITUTE

RE: REPORT ON NICKEL ETCHING STUDIES - P.O. F196296

Objective of the study covered by this report was to determine the effect on etch factor (ratio of depth to side etch), of the use of various bath compositions for etching of nickel. Etched depth of .030" was desired.

Material furnished by Pratt & Whitney included 6 x 6 lapped NI200 plates and positive and negative film (.020" passages, .040" lands) of the required line pattern.

Results of the work are described below:

Photoresist Preparation - Dynachem 500 CMR photoresist, diluted 70:30 with Dynachem Resist Thinner, was whirler-coated on the cleaned, phosphate-treated nickel plates. Plates were prebaked, exposed, developed and post-baked, following directions of the resist manufacturers.

Etching Studies - The first 6 plates tested (9087A-9092A) were etched in the Master PC-32HS paddle etching machine. All other plates were etched in the Dynamil 50 Spray Etcher.

Experiments in Paddle Machine - The ferric chloride used in the machine was 30° Baume. The first two plates (9087A and 9088A) were etched without any additives. The top etched away before the depth reached .030" of an inch. The addition of GT-1 (2.8 gm/liter) resulted in a slower etch rate and an etch factor of .238. Plate 9090A was etched after the addition of PF-152 (2 gm/liter) and there was little change from plate 9089A. The addition of triethanolamine (4 cc/l) resulted in little change for plate 9091A (etch factor .295). The addition of 67.5 grams of monochloroacetic acid resulted in an etch factor of .263 for plate 9092A.

Experiments in Spray Machine - Experimentation continued in the Dynamil 50 Spray Etcher using 48° Baume ferric chloride. Plates 9093S-9097S were run in the first bath. Plate 9093S showed an improvement in etch factor (1.245). The addition of 2.8 g/qt of ETU and 2 g/qt. of monochloroacetic acid on succeeding trials resulted in etch factors of 1.285 (plate 9094S) and 1.46 (plate 9095S). Plates 9096S and 9097S were run at a later date.

A new bath of (1) 48° Be $FeCl_3$, (2) 2.8 gm/qt ETU and (3) 2.0 gm/qt. PF-152 was prepared. Plate 9098S, which was a silver plated sheet which had been exposed to a nitric-sulfuric de-silvering treatment, etched very slowly, (.000011"/min.). Nitric acid, in proportion of 30 cc/qt was added to the bath, and plate 9099SA, of regular nickel composition, was etched. Etch rate for this plate was no different from that noted with similar plates in baths to which no nitric acid had been added. Plate 9098S was returned to the bath -- no increase in etch rate was noted in the nitric acid-modified bath. Bath was discarded.

A new bath of (1) 48° Be $FeCl_3$, (2) 2.8 g/qt ETU, (3) 2.0 g/qt. monochloroacetic acid. Plates 9099SB and 9100S resulted in etch factors of 1.50 and 1.55 respectively. The bath was dumped as this phase ended and also due to the excessive etching time needed to reach the required depth.

In order to compare spray-etcher results with 30° Be ferric chloride to results from the paddle machine, plate 9101S was etched in a bath of 30° Be $FeCl_3$ and 2.3 g/qt. of GT-1. Sideward etch was excessive and the top was lost before the required depth was reached.

Plate 9102S was etched in a 30° Be $FeCl_3$ and 2.5 g/qt. 13a. Again sideward etch was excessive and the top would have been gone before the required depth was reached.

Plates 9103S and 9104S were etched in (1) 30° Be $FeCl_3$, (2) 2.5 g/qt. 13b. Plate 9103S had an etch factor .540. I g/qt. of monochloroacetic acid was added and plate 9104S had an etch factor of .580. The bath was dumped due to no improvement with the additives used.

Plates 9105S and 9106S were etched in (1) 48° Be $FeCl_3$, (2) 2.5 g/qt 13b. Plate 9106S was run the same length of time as 9103S and 9104S. Plate 9106S had an etch factor 1f 2.66 compared to .540 and .580 for 9103S and 9104S. Apparently the use of 48° Be $FeCl_3$ rather than 30° Be $FeCl_3$ results in a better etch factor.

Summary - Conclusions from this study may be summarized as follows:

Best results were obtained with:

(a) Spray etcher
(b) 48° Be $FeCl_3$ as compared to 30° Be
(c) ETU performed better as a banking agent
(d) Monochloroacetic acid appears to improve the etch factor
(e) Dynachem 5000 CMR was the better resist as compared to K.T.F.R.

Note: GT-1 = Formamidine Disulfide Dihydrochloride
ETU = Ethylene Thiourea
PERI 13a = 40% GT-1, 49% ETU, 9% Diaminophenol Dihydrochloride
PERI 13b = 47% GT-1, 53% ETU
PF-152 = Ammonium Bifluoride
TEA = Triethanol Amine
PF-76 = Monochloroacetic Acid

Table XXXVII Etching Data

Following were etched in Master PC-32HS Paddle Etching Machine (750 rpm)

Sample #	Etching Time	Depth	Etch rate (in. x10^{-3})	Etch Factor	Temp. ^{o}F	$FeCl_3$ ^{o}Be	Additives*	Comments
9087A	60 min	.031"	.51	--	78°	30°	None	Maskant lost
9088A	40 "	.019"	.475	--	78°	30°	"	" "
9089A	40 "	.0051	.127	.238	78°	30°	GT-1	Shallow, rough
9090A	40 "	.0049	.123	.272	78°	30°	GT-1 & PF-152	" "
9091A	40 "	.0056	.140	.295	78°	30°	GT-1, PF-150, TEA	" "
9092A	40 "	.0050	.125	.263	78°	30°	GT-1, PF-152, TEA, PF-76	" "

Table XXXVII Etching Data (Continued)

Due to consistantly slow etch rates and rough etching encountered in paddle machine, balance of experimental etching was conducted in Dynamil 50 Spray Etcher (nozzle pressure approx. 11 in.Hg)

Sample #	Etching Time	Depth	Etch Rate (in.x10^{-3})	Etch Factor	Temp.°F	$FeCl_3$ (°Be)	Additives*	Comments
9093S	90 min.	.028	.31	1.245	75°	48°	None	
9094S	60 "	.018	.30	1.285	85°	48°	ETU	
9095S	65 "	.019	.292	1.46	85°	48°	ETU, PF-76	
9096S	135 "	.031	.233	1.19	75-85°	48°	" "	
9097S	210 "	.030	.143	1.18	85°	48°	" "	
9098S	210 "	.015	.005	--	85°	48°	" "	Ag plated
9099SA	120 "	.031	.258	--	90°	48°	" "	Maskant etched away
9099SB	100 "	.033	.333	1.50	90°	48°	" "	
9100S	120 "	.019	.155	1.55	83°	48°	" "	
9101S	60 "	.0096	.147	--	78°	30°	GT-1	Maskant etched away
9102S	45 "	.018	.290	--	78°	30°	PERI 13a	" "
9103S	15 "	.0088	.433	.540	82°	30°	PERI 13b	
9104S	15 "	.0058	.386	.580	77°	30°	PERI 13b, PF-77	
9105S	60 "	.011	.184	1.36	80°	48°	" " "	
9106S	15	.0040	.266	2.66	81-86°	48°	PERI 13b, PF-152	

*Bath composition given in written report.

APPENDIX E

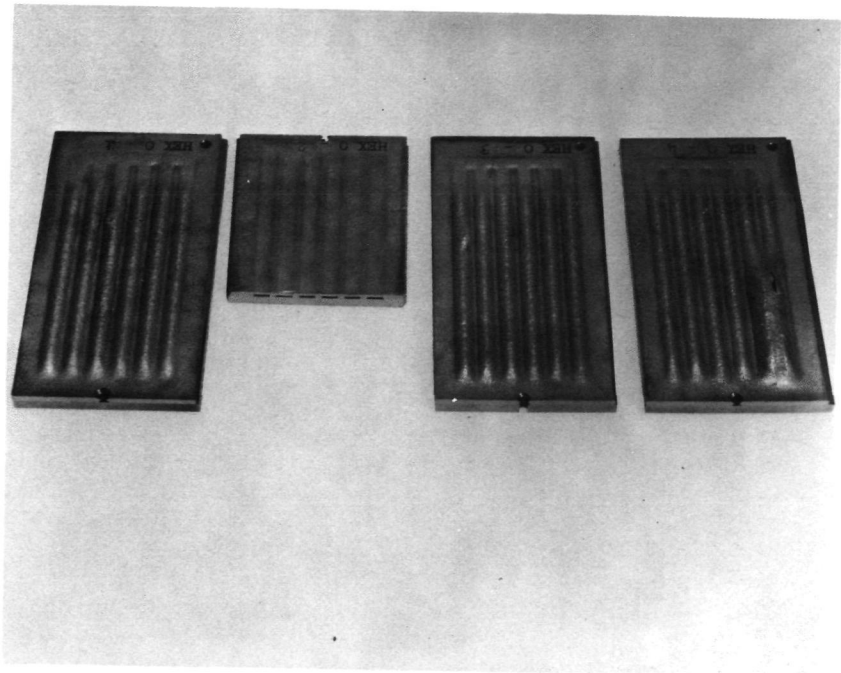

Figure 88. Run HEXO Samples (Soft Tooling)

FE 103779

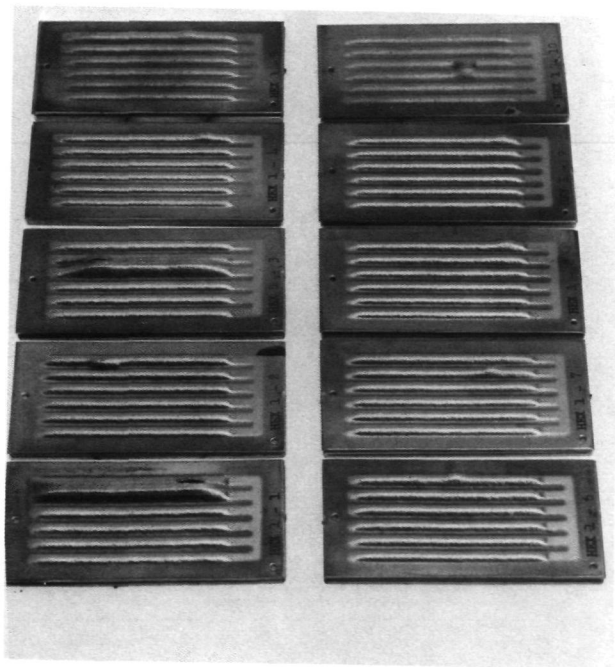

Figure 89. Run HEX1 Samples

FE 103778

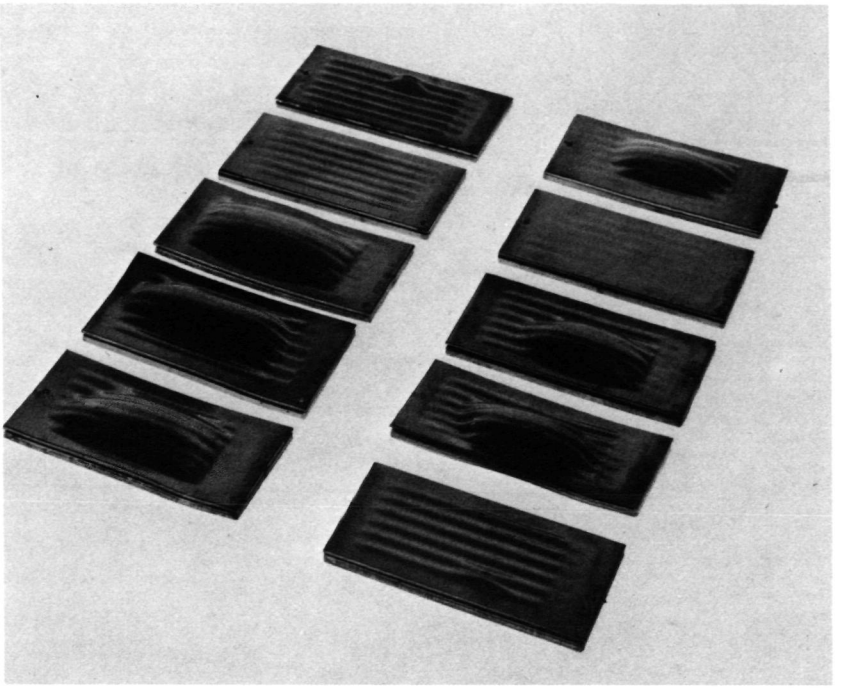

Figure 90. Run HEX2 Samples FC 22839A

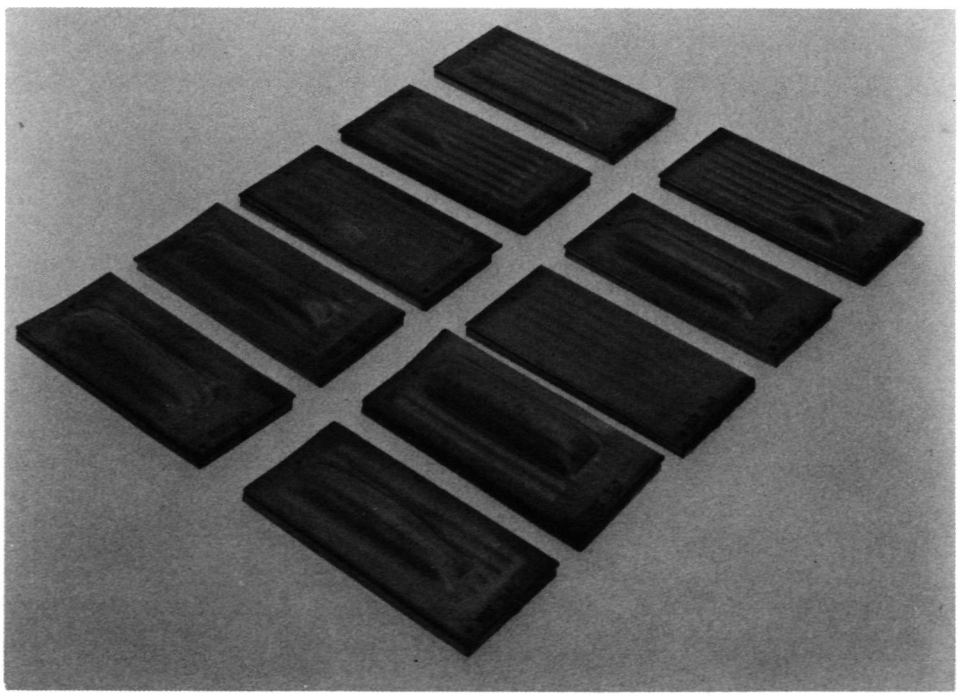

Figure 91. Run HEX3 Samples FE 104309

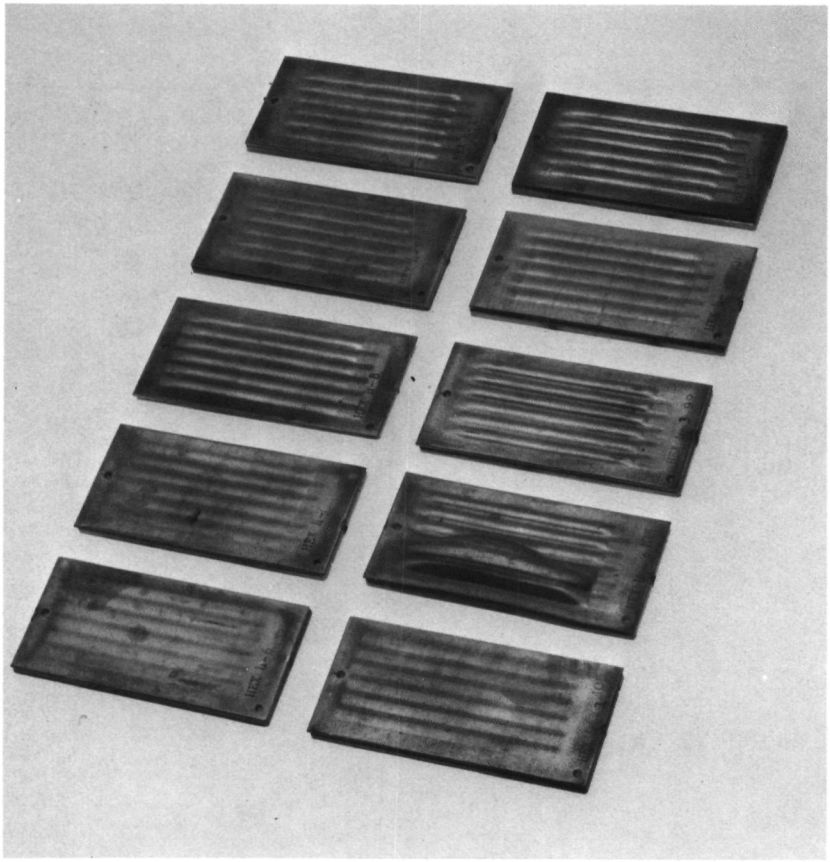

Figure 92. Run HEX4 Samples FE 105049

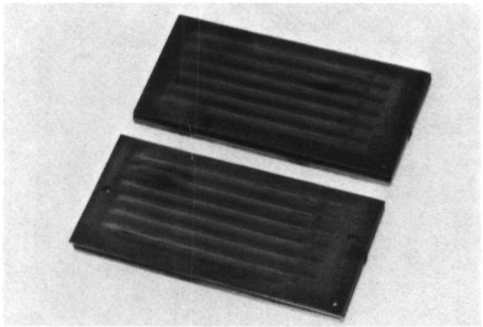

Figure 93. HEX4-3 and HEX4-5 Samples FAE 105764

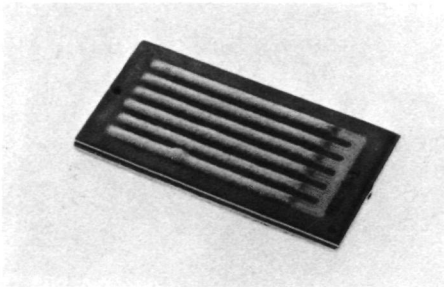

Figure 94. Run HEX5 Samples FD 49972

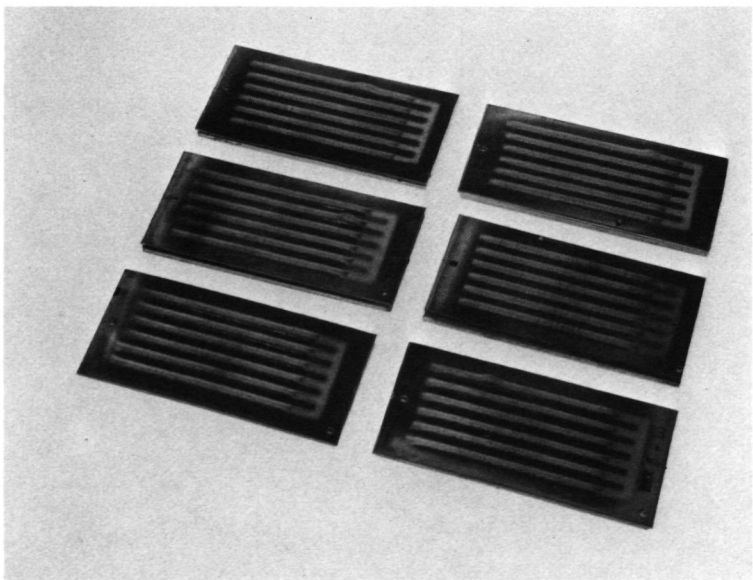

Figure 95. Run HEX6 Samples, Room Temperature Tests FE 105763

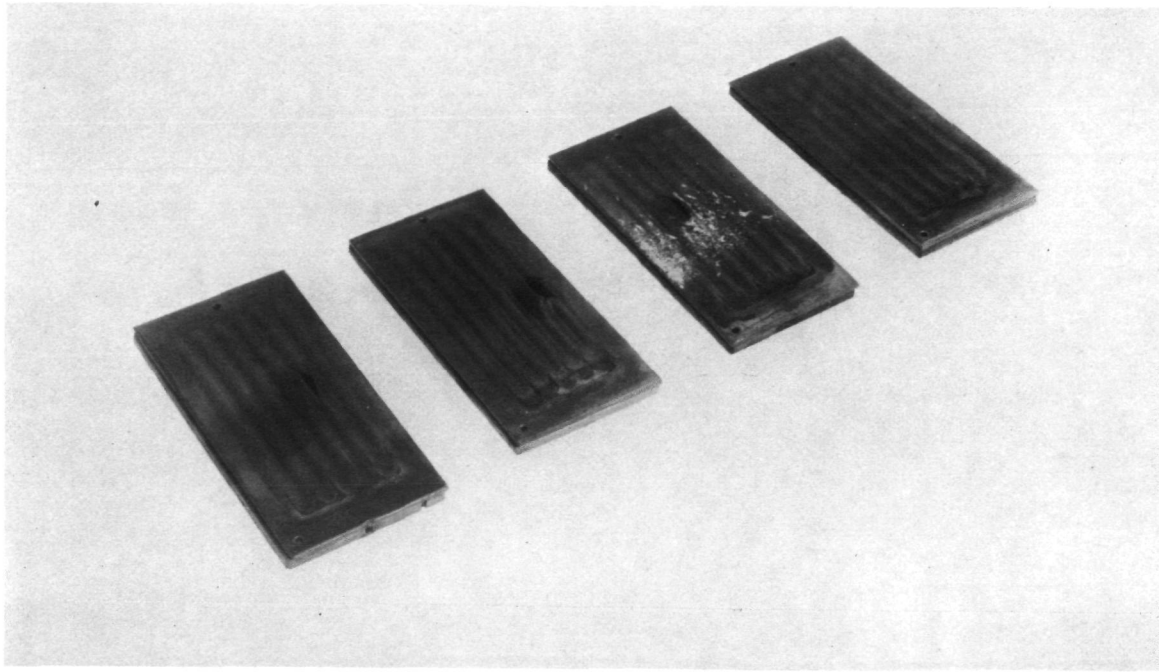

Figure 96. Run HEX6 Samples, 1000°F (811°K) Tests FD 49973

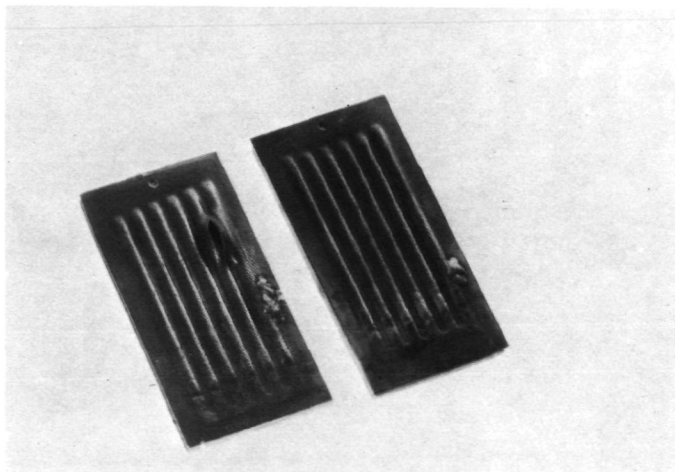

Figure 97. HEX6-1 and HEX6-6 Samples, Repaired and Retested at 1000°F (811°K) FE 107399

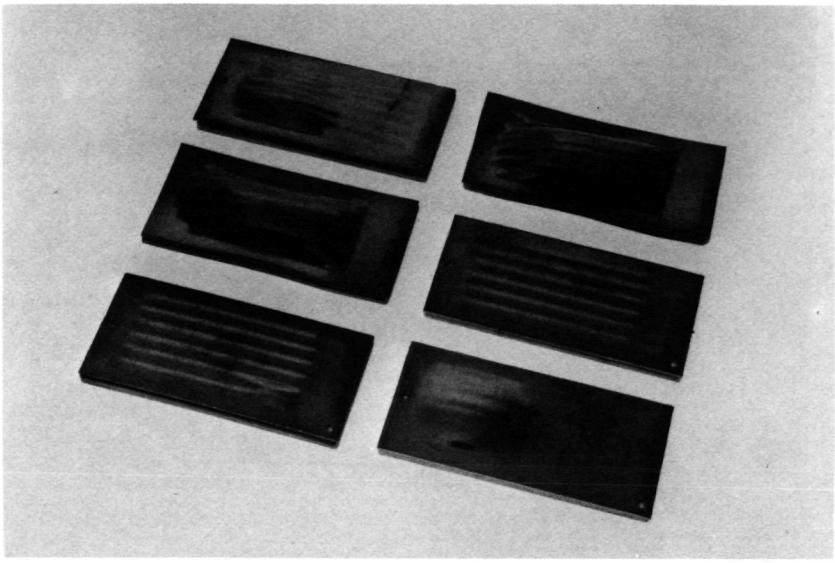

Figure 98. Run HEX7 Samples, Room Temperature Tests FE 105762

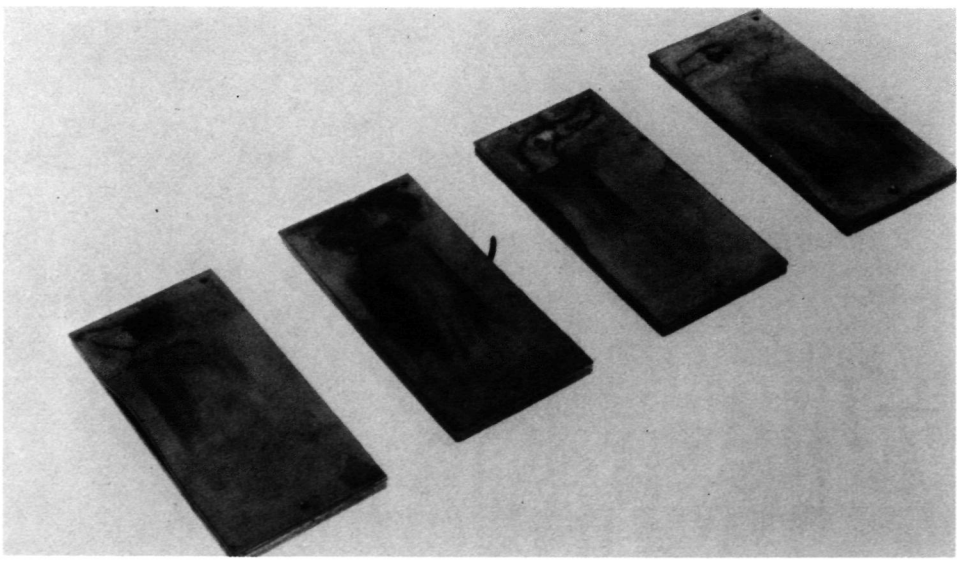

Figure 99. Run HEX7 Samples, 1000°F (811°K) Tests FE 49974

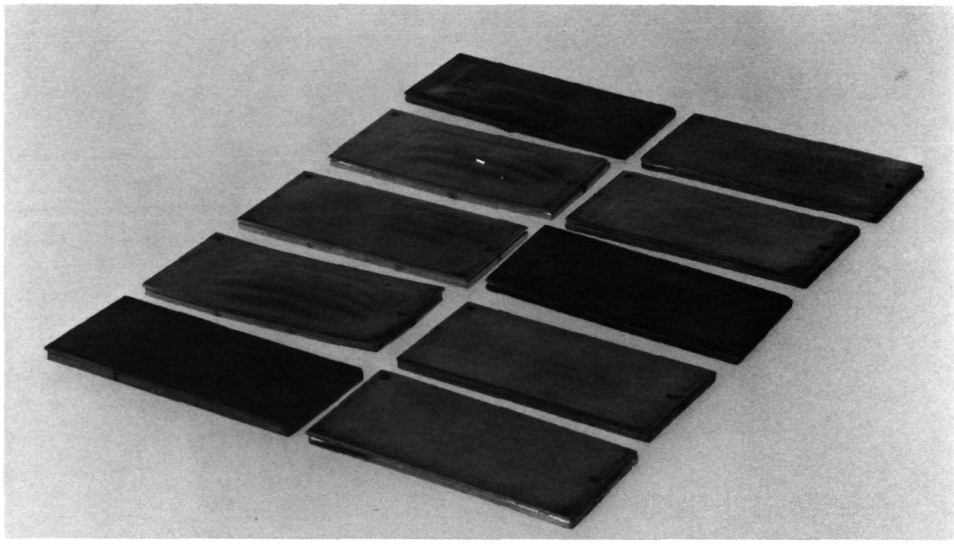

Figure 100. Run HEX8 Samples FE 106615

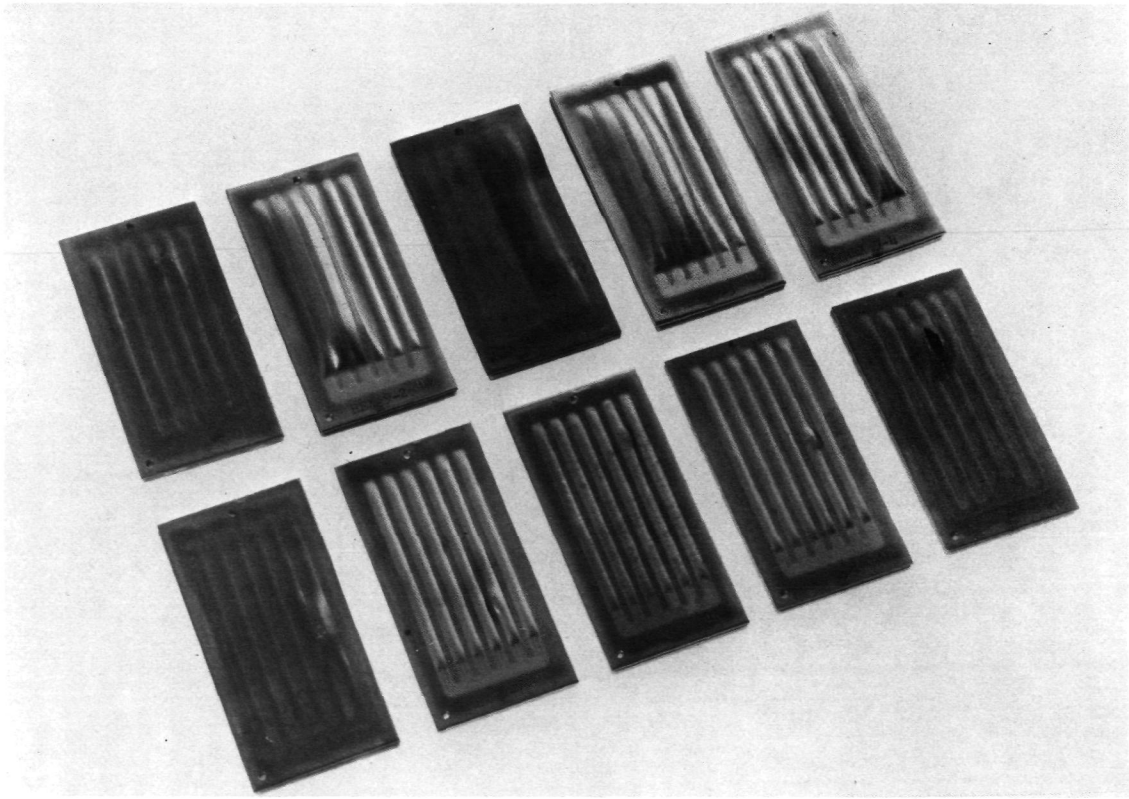

Figure 101. Run HEX9 Samples FE 107400

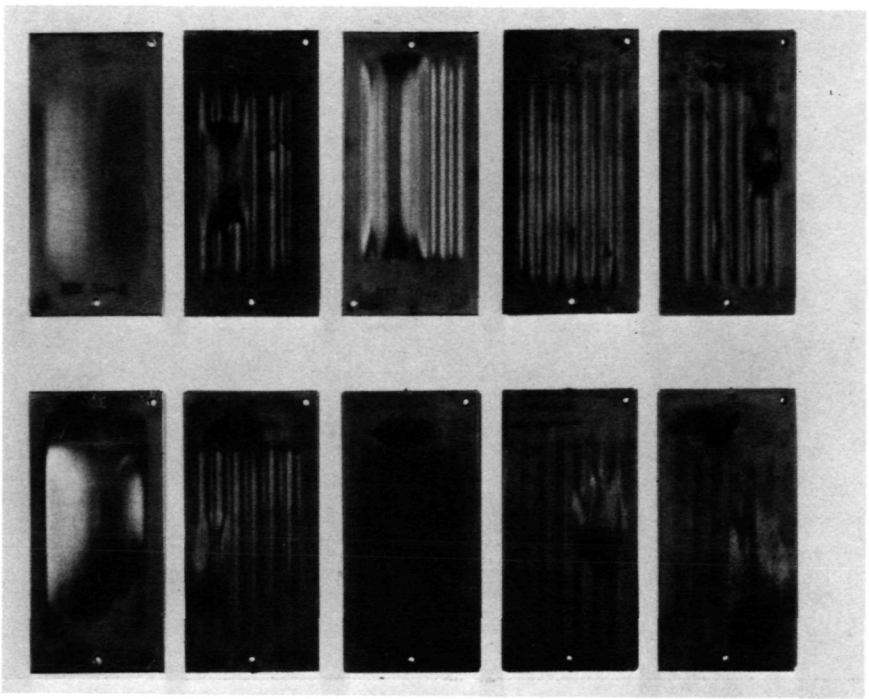

Figure 102. Run HEX10 Samples FE 108030

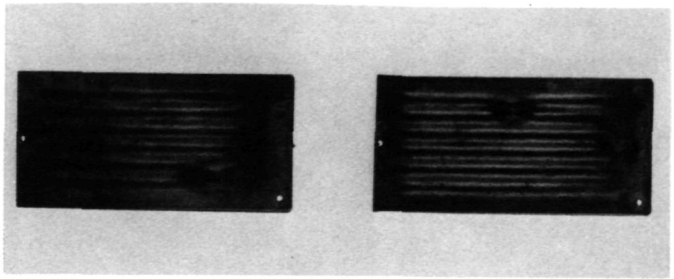

Figure 103. Run HEX11 Samples FE 108031

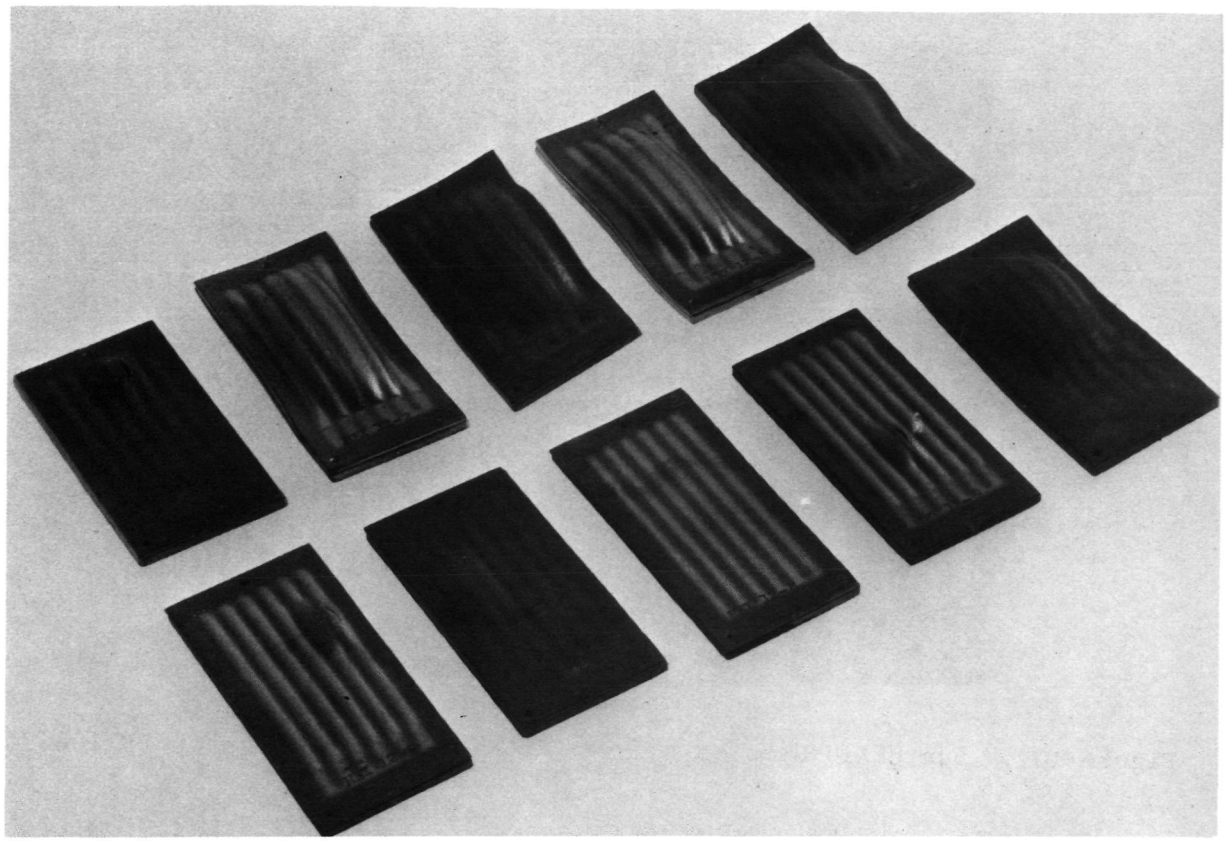

Figure 104. Run HEX12 Samples FE 108222

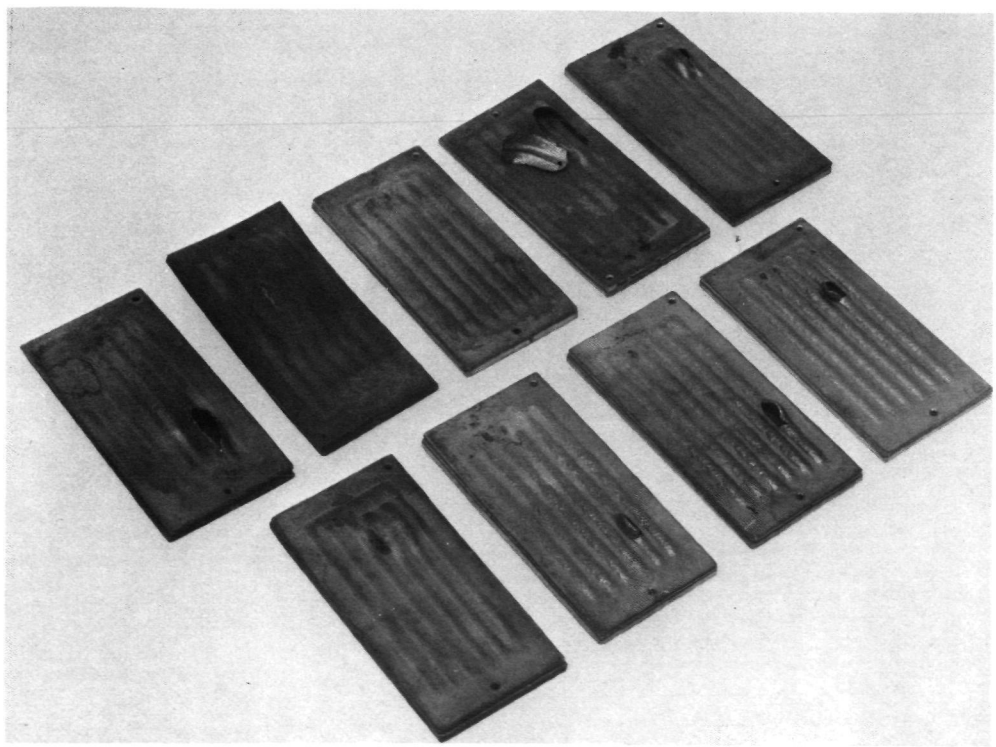

Figure 105. Run HEX13 Samples FE 108891

APPENDIX F

REFERENCES

1. Olafsen, Gurklis, and Boulger, Machining and Grinding of Nickel and Cobalt Base Alloys, NASA TMC-53446, A.D. 634075 (1966).
2. Glenski, Chemical Milling High-Temperature Alloys and Steels, General Dynamics/Convair, A.D. 829 039 (1961).
3. Borth and Rogers, Powderless Etching of Copper, Technical Association of the Grphic Arts, Thirteenth Annual Meeting, June 12-14, 1961.
4. Easley, TAGA Proceeding, 76-84 (1954).
5. Benton and Dunkelberger, J. Photochem. Etching 2, No. 3, 4 (1967).
6. J. P. Mitchell, Space Storable Regenerative Cooling Investigation, Final Report NASA CR-72704, PWA FR-4000, Pratt & Whitney Aircraft, Florida Research and Development Center, October 8, 1971. (Unclassified).
7. Moore and Holko, Practical Method for Diffusion Welding of Steel Plate in Air, NASA Technical Note D-6409, National Aeronautics and Space Administration, Lewis Research Center, July 1971.
8. Huntington Nickel Alloys Bulletin, Huntington Alloy Products Division, The International Nickel Company, Inc., Huntington, West Virginia 25720.

APPENDIX G

DISTRIBUTION LIST FOR FINAL REPORT

NAS3-13312 P&W CR 120988

Instructions:

Final reports are being sent directly to the "Recipient" and the "Designee" per the quantities specified in the respective columns, R and D. When no copies are specified in column D, a carbon copy of the letter of transmittal is being sent to the person named as the "Designee".

REPORT COPIES R	D	RECIPIENT	DESIGNEE
		National Aeronautics & Space Administration Lewis Research Center 21000 Brookpark Road Cleveland, Ohio 44135	
1		Attn: Contracting Officer, MS 500-313	
5		E. A. Bourke, MS 500-203	
1		Technical Report Control Office, MS 5-5	
1		Technology Utilization Office, MS 3-16	
2		AFSC Liaison Office, 501-3	
2		Library	
1		Office of Reliability & Quality Assurance, MS 500-III	
1		J. W. Gregory Chief, MS 500-203	
13		R. A. Duscha Project Manager, MS 500-209	
1		T. J. Moore, MS 105-1	
1		K. H. Holko, MS 105-1	
1		Director, Shuttle Technology Office, RS Office of Aeronautics & Space Technology NASA Headquarters Washington, D. C. 20546	
2		Director Space Prop. and Power, RP Office of Aeronautics & Space Technology NASA Headquarters Washington, D. C. 20546	
1		Director, Launch Vehicles & Propulsion, SV Office of Space Science & NASA Headquarters Washington, D. C. 20546	

REPORT COPIES R D	RECIPIENT	DESIGNEE
1	Director, Materials & Structures Div, RW Office of Aeronautics & Space Technology NASA Headquarters Washington, D.C. 20546	
1	Director, Advanced Manned Missions, MT Office of Manned Space Flight NASA Headquarters Washington, D. C. 20546	
20	National Technical Information Service Springfield, Virginia 22151	
1	National Aeronautics & Space Administration Ames Research Center Moffett Field, California 94035 Attn.: Library	Hans M. Mark Mission Analysis Division
1	National Aeronautics & Space Administration Flight Research Center P. O. Box 273 Edwards, California 93523 Attn: Library	
1	Director, Technology Utilization Division Office of Technology Utilization NASA Headquarters Washington, D. C. 20546	
1	Office of the Director of Defense Research & Engineering Washington, D. C. 20301 Attn: Office of Asst. Dir. (Chem Technology)	
2	NASA Scientific and Technical Information Facility P. O. Box 33 College Park, Maryland 20740 Attn: NASA Representative	
1	Nation Aeronautics & Space Administration Goddard Space Flight Center Greenbelt, Maryland 20771 Attn: Library	Merland L. Moseson, Code 620
1	National Aeronautics & Space Administration John F. Kennedy Space Center Cocoa Beach, Florida 32931 Attn: Library	Dr. Kurt H. Debus

REPORT COPIES R D	RECIPIENT	DESIGNEE
1	National Aeronautics & Space Administration Langley Research Center Langley Station Hampton, Virginia 23365 Attn: Library	E. Cortwright Director John Allred
1	National Aeronautics & Space Administration Manned Spacecraft Center Houston, Texas 77001 Attn: Library	J. G. Thiobodaux, Jr. Chief, Propulsion & Power Division
1	National Aeronautics & Space Administration George C. Marshall Space Flight Center Huntsville, Alabama 35912 Attn: Library	Hans G. Paul James Thomas
1	Jet Propulsion Laboratory 4800 Oak Grove Drive Pasadena, California 91103 Attn: Library	Henry Burlage, Jr. Duane Dipprey
1	Defense Documentation Center Cameron Station Building 5 5010 Duke Street Alexandria, Virginia 22314 Attn: TISIA	
1	RTD (RTNP) Bolling Air Force Base Washington, D. C. 20332	
1	Arnold Engineering Development Center Air Force Systems Command Tullahoma, Tennessee 37389 Attn: Library	Dr. H. K. Doetsch
1	Advanced Research Projects Agency Washington, D. C. 20525 Attn: Library	
1	Aeronautical Systems Division Air Force Systems Command Wright-Patterson Air Force Base, Dayton, Ohio Attn: Library	D. L. Schmidt Code ARSCNC-2

REPORT COPIES R D	RECIPIENT	DESIGNEE
1	Air Force Missile Test Center Patrick Air Force Base, Florida Attn: Library	L. J. Ullian
1	Air Force Systems Command Andrews Air Force Base Washington, D. C. 20332 Attn: Library	Capt. S. W. Bowen SCLT
1	Air Force Rocket Propulsion Laboratory (RPR) Edwards, California 93523 Attn: Library	Donald Penn Robert Wiswell
1	Air Force Rocket Propulsion Laboratory (RPM) Edwards, California 93523 Attn: Library	
1	Air Force FTC (FTAT-2) Edwards Air Force Base, California 93523 Attn: Library	Donald Ross
1	Air Force Office of Scientific Research Washington, D. C. 20333 Attn: Library	SREP, Dr. J. F. Masi
1	Space & Missile Systems Organization Air Force Unit Post Office Los Angeles, California 90045 Attn: Technical Data Center	
1	Office of Research Analyses (OAR) Holloman Air Force Base, New Mexico 88330 Attn: Library	
1	U. S. Air Force Washington, D. C. Attn: Library	Col. C. K. Stambaugh, Code AFRST
1	Commanding Officer U. S. Army Research Office (Durham) Box CM, Duke Station Durham, North Carolina 27706 Attn: Library	
1	U. S. Army Missile Command Redstone Scientific Information Center Redstone Arsenal, Alabama 35808 Attn: Document Section	Dr. W. Wharton

REPORT COPIES R D	RECIPIENT	DESIGNEE
1	Bureau of Naval Weapons Department of the Navy Washington, D. C. Attn: Library	J. Kay, Code RTMS-41
1	Commander U. S. Naval Missile Center Point Mugu, California 93041 Attn: Technical Library	
1	Commander U. S. Naval Weapons Center China Lake, California 93557 Attn: Library	
1	Commanding Officer Naval Research Branch Office 1030 E. Green Street Pasadena, California 91101 Attn: Library	
1	Director (Code 6180) U. S. Naval Research Laboratory Washington, D. C. 20390 Attn: Library	H. W. Carhart J. M. Krafft
1	Picatinny Arsenal Dover, New Jersey 07801 Attn: Library	I. Forsten
1	Air Force Aero Propulsion Laboratory Research & Technology Division Air Force Systems Command United States Air Force Wright-Patterson AFB, Ohio 45433 Attn: APRP (Library)	R. Quigley C. M. Donaldson
1	Electronics Division Aerojet-General Corporation P. O. Box 296 Azusa, California 91703 Attn: Library	
1	Space Division Aerojet-General Corporation 9200 East Flair Drive El Monte, California 91734 Attn: Library	

REPORT COPIES R D	RECIPIENT	DESIGNEE
1	Aerojet Ordance and Manufacturing Aerojet-General Corporation 11711 South Woodruff Avenue Fullerton, California 90241 Attn: Library	
1	Aerojet Liquid Rocket Company P. O. Box 15847 Sacramento, California 95813 Attn: Technical Library 2484-2015A	
1	Aeronutronic Division of Philco Ford Corp. Ford Road Newport Beach, California 92663 Attn: Technical Information Department	Dr. L. H. Linder
1	Aerospace Corporation 2400 E. El Segundo Blvd. Los Angeles, California 90045 Attn: Library-Documents	J. G. Wilder
1	Arthur D. Little, Inc. 20 Acorn Park Cambridge, Massachusetts 02140 Attn: Library	A. C. Tobey
1	Astropower Laboratory McDonnell-Douglas Aircraft Company 2121 Paularino Newport Beach, California 92163 Attn: Library	
1	DCIC, Battelle Memorial Institute Columbus Lab. Room 11-9021 505 King Ave. Columbus, Ohio 43201 Attn: Library	J. F. Lynch
1	ARO, Incorporated Arnold Engineering Development Center Arnold AF Station, Tennessee 37389 Attn: Library	
1	Susquehanna Corporation Atlantic Research Division Shirley Highway & Edsall Road Alexandria, Virginia 22314 Attn: Library	

REPORT COPIES R	D	RECIPIENT	DESIGNEE
1	1	Battelle Memorial Institute 505 King Ave. Columbus, Ohio 43201 Attn: Report Library, Room 6a	Ken Meiners
1		Beech Aircraft Corporation Boulder Facility Box 631 Boulder, Colorado Attn: Library	Douglas Pope
1	1	Bell Aerosystems, Inc. Box 1 Buffalo, New York 14240 Attn: Library	A. E. Leach
1		Instruments & Life Support Division Bendix Corporation P. O. Box 4508 Davenport, Iowa 52808 Attn: Library	John M. Brueger
1		Bellcomm 955 L'Enfant Plaza, S. W. Washington, D. C. Attn: Library	H. S. London
1		Boeing Company Space Division P. O. Box 868 Seattle, Washington 98124 Attn: Library	J. D. Alexander C. F. Tiffany
1		Boeing Company 1625 K Street, N. W. Washington, D. C. 20006	
1		Boeing Company P. O. Box 1680 Huntsville, Alabama 35801	Ted Snow
1		Chemical Propulsion Information Agency Applied Physics Laboratory 8621 Georgia Avenue Silver Spring, Maryland 20910	Tom Reedy
1		Chrysler Corporation Missile Division P. O. Box 2628 Detroit, Michigan Attn: Library	John Gates
168			

REPORT COPIES R D	RECIPIENT	DESIGNEE
1	Chyrsler Corporation Space Division P. O. Box 29200 New Orleans, Louisiana 70129 Attn: Librarian	
1	Grumman Aircraft Engineering Corporation Bethpage, Long Island, New York Attn: Library	Joseph Gavin
1	Hercules Powder Company Allegheny Ballistics Laboratory P. O. Box 210 Cumberland, Maryland 21501 Attn: Library	
1	Honeywell Inc. Aerospace Division 2600 Ridgeway Road Minneapolis, Minnesota Attn: Library	
1	IIT Research Institute Technology Center Chicago, Illinois 60616 Attn: Library	C. K. Hersh
1	Kidde Aer-Space Division Walter Kidde & Company, Inc. 567 Main Street	R. J. Hanville
1	Ling-Temco-Vought Corporation P. O. Box 5907 Dallas, Texas 75222 Attn: Library	
1	Lockheed Missiles and Space Company P. O. Box 504 Sunnyvale, California 94087 Attn: Library	
1	Lockheed Propulsion Company P. O. Box 111 Redlands, California 92374 Attn: Library, Thackwell	H. L. Thackwell
1	Marquardt Corporation 16555 Saticoy Street Box 2013 - South Annex Van Nuys, California 91409	L. R. Bell, Jr.

REPORT COPIES R D	RECIPIENT	DESIGNEE
1	Martin-Marietta Corporation (Baltimore Division) Baltimore, Maryland 21203 Attn: Library	
1	Denver Division Martin-Marietta Corporation P. O. Box 179 Denver, Colorado 80201 Attn: Library	Dr. Morgenthaler F. R. Schwartzberg
1	Orlando Division Martin-Marietta Corporation Box 5827 Orlando, Florida Attn: Library	J. Fern
1	Western Division McDonnell Douglas Astronautics 5301 Bolsa Ave. Huntington Beach, California 92647 Attention: Library	R. W. Hallet G. W. Burge P. Klevatt
1	McDonnell Douglas Aircraft Corporation P. O. Box 516 Lambert Field, Missouri 63166 Attn: Library	R. A. Herzmark
1 1	Rocketdyne Division North American Rockwell, Inc. 6633 Canoga Avenue Canoga Park, California 91304 Attn: Library, Department 596-306	Donald Fulton
1	Space & Information Systems Division North American Rockwell 12214 Lakewood Blvd. Downey, California Attn: Library	
1	Northrop Space Laboratories 3401 West Broadway Hawthorne, California Attn: Library	Dr. William Howard
1	Purdue University Lafayette, Indiana 47907 Attn: Library (Technical)	Dr. Bruce Reese

REPORT COPIES R	D	RECIPIENT	DESIGNEE
1		Radio Corporation of America Astro-Electronics Products Princeton, New Jersey Attn: Library	
1		Rocket Research Corporation Willow Road at 116th Street Redmond, Washington 98052 Attn: Library	F. McCullough, Jr.
1		Stanford Research Institute 333 Ravenswood Avenue Menlo Park, California 94025 Attn: Library	Dr. Gerald Marksman
1		Thiokol Chemical Corporation Redstone Division Huntsville, Alabama Attn: Library	John Goodloe
1	1	TRW Systems Inc. 1 Space Park Redondo Beach, California 90278 Attn: Tech. Lib. Doc. Acquisitions	Curtis Watts
1		TRW TAPCO Division 23555 Euclid Avenue Cleveland, Ohio 44117	P. T. Angell
1		United Aircraft Corporation Corporation Library 400 Main Street East Hartford, Connecticut 06108 Attn: Library	Dr. David Rix Erle Martin Frank Owen Wm. E. Taylor
1	1	United Aircraft Corporation Pratt & Whitney Division Florida Research & Development Center P. O. Box 2691 West Palm Beach, Florida 33402 Attn: Library	Dr. Schmidtke
1		United Aircraft Corporation United Technology Center P. O. Box 358 Sunnyvale, California 94038 Attn: Library	Dr. David Altman

REPORT COPIES R	D	RECIPIENT	DESIGNEE
1		Vickers Incorporated Box 302 Troy, Michigan	
1		Vought Astronautics Box 5907 Dallas, Texas Attn: Library	

PO 060117 MDA 26464 SE 19705 200 10-72